

Copyright  
by  
Talal Eid Alotaibi  
2012

**The Thesis Committee for Talal Eid Alotaibi  
Certifies that this is the approved version of the following thesis:**

**Examination of Focal Adhesion Kinase's FAT Domain Structural  
Response to Applied Mechanical Load**

**APPROVED BY**

**SUPERVISING COMMITTEE:**

---

**Tess J. Moon, Supervisor**

---

**Pengyu Ren**

**Examination of Focal Adhesion Kinase's FAT Domain Structural  
Response to Applied Mechanical Load**

**by**

**Talal Eid Alotaibi, B.E**

**Thesis**

Presented to the Faculty of the Graduate School of

The University of Texas at Austin

in Partial Fulfillment

of the Requirements

for the Degree of

**Master of Science in Engineering**

**The University of Texas at Austin**

**May 2012**

## **Dedication**

Dedicated to my mother Modhi

## **Acknowledgements**

I would like to thank my supervisor, Dr. Tess J. Moon, for her guidance and support; it has been a privilege to work with her. My sincere gratitude is also goes to Steven Kreuzer for the technical support he provided. My gratitude also extended to Dr. Pengyu Ren for serving on my committee. I am also thankful to Dr. Michael Schaller for his recommended references for the thesis.

I like also to thank Kuwait Embassy for giving me the opportunity to pursue my graduate study at the University of Texas at Austin. I am also thankful to National Science Foundation (NSF) for their support (Grant CBET1133351 to IMPACT Laboratory at The University of Texas at Austin) as well as to Texas Advanced Computing Center (TACC). I am most thankful to my family for their support and patience.

## **Abstract**

### **Examination of Focal Adhesion Kinase's FAT Domain Structural Response to Applied Mechanical Load**

Talal Eid Alotaibi, M.S.E

The University of Texas at Austin, 2012

Supervisor: Tess J. Moon

Focal adhesion kinase (FAK) is a non-receptor tyrosine kinase. Activated FAK is crucial to many biological processes, such as cell proliferation, migration, and survival, all of which have been implicated in the progression and development of cancer. Tyrosine 925 is a Src-phosphorylation site that is located within the FAT domain in the C-terminal of FAK. It has been suggested that the helix containing Y925 (Helix 1) has to come out of the FAT bundle and the region flanking Y925 has to adopt  $\beta$ -strand conformation. In order to phosphorylate, the mechanisms promoting the required structural changes are unclear. So, Molecular Dynamics (MD) and Constant Force Molecular Dynamics (CFMD) simulations were used to study what makes Y925 accessible for phosphorylation.

Under thermal fluctuation only and in the presence or the absence of LD motifs, MD simulations suggest that H1 does not appear to have a propensity to leave the bundle adopt  $\beta$ -strand conformation. Then, two different load scenarios were used; axial and perpendicular with 100 pN constant load applied to H1 N-terminus with the two paxillin

LD motifs constrained. For both load scenarios, H1 has two different behaviors: typical and atypical. In the axial load scenario, the first two residues at the N-terminal of H1 (besides Y925) have low propensity to unfold. However, H1 does not show any proclivity to leave the bundle. For the perpendicular load scenario with the absence of P2 (LD motif binds to H1/H4 hydrophobic patch), one simulation out of 21 showed that H1 undergoes the required structural rearrangement. In general, CFMD simulations show that the FAT domain has a very low propensity (3%) to undergo the structural changes needed for Y925 phosphorylation. This has two implications: either mechanical load is insufficient to make Y925 available for phosphorylation and/or this kind of process (structural changes needed for Y925 phosphorylation) is slow process that needs a long time to occur.

## Table of Contents

Table of Contents .....	viii
List of Tables .....	xiii
List of Figures .....	xvi
<b>CHAPTER 1. INTRODUCTION .....</b>	<b>1</b>
1.1 Focal Adhesion Kinase (FAK).....	1
1.2 Focal Adhesion Targeting Domain (FAT).....	2
1.3 Y925 Phosphorylation Requirements .....	4
1.4 Understanding Pre-Phosphorylation Process .....	4
<b>CHAPTER 2. LITERATURE REVIEW .....</b>	<b>8</b>
2.1 Focal Adhesion Kinase (FAK).....	8
2.2 Focal Adhesion Targeting (FAT) Domain.....	8
2.2.1 FAT Structure .....	8
2.3 Paxillin .....	9
2.4 Paxillin Association with FAT .....	10
2.5 Phosphorylation of Y925 .....	11
2.5.1 H1 Position.....	11
2.5.2 H1 Unfolding .....	13



2.6 Salt Bridges between H1 Tail and H4.....	14
2.7 Methionine Zipper between H1, H2, H3 and H4.....	14
2.8 Interactions between Paxillin LD Motifs and FAT Domain.....	15
<b>CHAPTER 3. METHODOLOGY .....</b>	<b>17</b>
3.1 Structures .....	17
3.1.1 FAT/Paxillin Complex without H4 Tail and P1/P2 Unconstrained.....	17
3.1.2 Augmented FAT/Paxillin Complex with H4 Tail and P1/P2 Constrained .....	19
3.1.2.1 H4 Tail Addition .....	20
3.1.2.2 LD Motifs Extension-Loop Addition.....	22
3.1.1 Initial Structures for Mechanically Loaded Simulations .....	23
3.1.1.1 H1/H4 Tail Interactions .....	24
3.1.1.2 H1/H4 Tail Positions.....	25
3.1.1.3 Selected Seeds for Axial Load Simulation .....	26
3.1.1.3.1 H1/H4 Tail Interaction .....	26
3.1.1.3.2 H1/H4 Tail Position .....	27
3.1.1.3.3 Initial Structures Used for Axial Load Simulations.....	28
3.1.1.4 Selected Seeds for Perpendicular Load Simulation .....	29
3.1.1.4.1 H1/H4 Tail Interactions .....	29
3.1.1.4.2 H1/H4 Tail Position .....	30
3.1.1.4.3 Initial Structures Used for Perpendicular Load Simulations .....	31
3.2 Simulations .....	33
3.2.1 Pre-Equilibration.....	34
3.2.2 Energy Minimization and Equilibration .....	34
3.2.3 Equilibrium Simulations .....	36
3.2.3.1 FAT/Paxillin Complex without H4 Tail and P1/P2 Unconstrained .....	36
3.2.3.2 FAT/Paxillin Complex with H4 Tail and P1/P2 Constrained..	36

3.2.3.3 H1 Isolation.....	37
3.2.3.4 Paxillin LD Motif Isolation.....	37
3.2.4 Mechanically Loaded Simulations.....	37
3.2.4.1 Axial Load Simulations .....	38
3.2.4.2 Perpendicular Load Simulation.....	40
3.2.5 Simulation Times.....	42
3.3 Analysis.....	44
3.3.1 Energy Landscape Analysis.....	44
3.3.2 H1 Behavior .....	45
3.3.2.1 H1 Position.....	45
3.3.2.2 H1 Unfolding .....	46
3.3.2.2.1 Backbone Dihedral Angle $\psi$ .....	46
3.3.2.2.2 Hydrogen Bonds via Donor-Acceptor Pairs .....	47
3.3.3 Salt Bridges between H1 Tail and H4.....	50
3.3.4 H1/H4 Tail Interaction.....	50
3.3.5 Final State of FAT's Structure under Applied Load.....	51
<b>CHAPTER 4. RESULTS.....</b>	<b>55</b>
4.1 Equilibrium Results .....	55
4.1.1 FAT/Paxillin Complex without H4 Tail and P1/P2 Unconstrained.....	55
4.1.1.1 H1 Position.....	56
4.1.1.2 H1 Unfolding .....	58
4.1.1.2.1 Backbone Dihedral Angle $\psi$ .....	58
4.1.1.2.1 Hydrogen Donor-Acceptor Pairs.....	60
4.1.1.3 Salt Bridges between H1 Tail and H4.....	61
4.1.2 Augmented FAT/Paxillin Complex with H4 Tail and P1/P2 Constrained .....	65
4.1.2.1 H1 Position.....	66
4.1.2.2 H1 Unfolding .....	68
4.1.2.2.1 Backbone Dihedral Angle $\psi$ .....	68

4.1.2.2.1 Hydrogen Donor-Acceptor Pairs.....	69
4.1.2.3 Salt Bridges between H1 Tail and H4.....	70
4.1.3 H1 Isolation.....	72
4.1.4 Paxillin LD Motif Isolation.....	73
4.1.5 Equilibrium Result Summary .....	75
4.2 Loaded Scenario Results.....	77
4.2.1 Axial Load Scenario Results.....	77
4.2.1.1 H1 Typical Behavior.....	79
4.2.1.1.1 H1 Position.....	79
4.2.1.1.2 H1 Unfolding .....	81
4.2.1.1.3 Salt Bridges between H1 Tail and H4.....	85
4.2.1.1.4 H1/H4 Tail Interaction.....	89
4.2.1.1.5 FAT Structure in its Final States.....	90
4.2.1.2 H1 Atypical Behavior .....	92
4.2.1.3 Axial Load Scenario Result Summary.....	95
4.2.2 Perpendicular Load Scenario Results .....	97
4.2.2.1 H1 Typical Behavior.....	97
4.2.2.1.1 H1 Position.....	98
4.2.2.1.2 H1 Unfolding .....	100
4.2.2.1.3 Salt Bridges between H1 Tail and H4.....	104
4.2.2.1.4 H1/H4 Tail Interaction.....	108
4.2.2.1.5 FAT Structure in its Final States.....	109
4.2.2.2 H1 Atypical Behavior .....	111
4.2.2.3 Repeatability of H1 Atypical Behavior.....	114
4.2.2.3.1 H1 Position.....	115
4.2.2.3.2 H1 Unfolding .....	117
4.2.2.3.3 Salt Bridges between H1 Tail and H4.....	121
4.2.2.3.4 H1/H4 Tail Interaction.....	123
4.2.2.3.5 FAT Structure in its Final States.....	123

4.2.2.4 Perpendicular Load Scenario Result Summary .....	126
<b>CHAPTER 5. CONCLUSIONS .....</b>	<b>127</b>
5.1 Under Equilibrium, Y925 Phosphorylation Conditions Not Met .....	127
5.2 Under Axial Load, Y925 Phosphorylation Conditions Not Met .....	129
5.3 Under Perpendicular Load, Y925 Phosphorylation Conditions Not Met .....	129
5.4 Mechanical Load is Insufficient Over the Examined Timescales .....	130
<b>CHAPTER 6. FUTURE WORK .....</b>	<b>131</b>
<b>APPENDIX A. PDB FILES.....</b>	<b>133</b>
<b>APPENDIX B. MDP SIMULATION FILES .....</b>	<b>224</b>
<b>APPENDIX C. MATLAB CODES .....</b>	<b>229</b>
<b>APPENDIX D. H1/H4 TAIL INTERACTION TABLES .....</b>	<b>248</b>
<b>REFERENCES.....</b>	<b>258</b>

## List of Tables

Table 2-1: A summary of the reported interactions of the FAT/paxillin complex. Salt bridges are shown in red, methionine zipper is in green and electrostatic interactions are in blue .....	16
Table 3-1: Equilibruim and mechanically loaded simulations. ....	43
Table 3-2: Classification of different FAT structures in the final states that were observed during the simulations. Each symbol describes a different structure a portion of the FAT domain would adopt. Those states are illustrated in Figure 3-24 .....	52
Table 4-1: H1 typical and atypical behaviors under axial load, applied to the N-terminus of H1 tail and P1/P2 constrained. Eight out of ten simulations have typical behavior, while two have atypical behavior. (Table 3-1, AX.WT. P1P2).....	78
Table 4-2: Final state of the structure of the region flanking Y925 for H1 typical behavior under constant force applied axially to the N-terminus of H1 tail. (Table 3-1, AX.WT.P1P2).....	90
Table 4-3: Final state of the structure of the region flanking Y925 for H1 typical and atypical behaviors under constant force applied axially to the N-terminus of H1 tail. (Table 3-1, AX.WT.P1P2).....	96
Table 4-4: H1 typical and atypical behaviors under perpendicular load, applied to the N-terminus of H1 tail and P1 constrained. Nine out of twelve simulations have typical behavior, while three have atypical behavior. (Table 3-1, PR.WT. P1P2).....	97

Table 4-5: Final state of the structure of the region flanking Y925 for H1 typical behavior under constant force applied perpendicularly to the N-terminus of H1 tail. (Table 3-1, PR.WT.P1).....	109
Table 4-6: Final state of the structure of the region flanking Y925 for H1 typical and atypical behaviors under constant force applied perpendicularly to the N-terminus of H1 tail. (Table 3-1, PR.WT.P1). ....	126
Table D-1: Electrostatic interactions found between H1/H4 tail that have a probability greater than 10% of 20 ns simulation time long. These runs belong to the equilibration simulation of the FAT/paxillin complex (with H4 tail and P1/P2 constrained). ....	248
Table D-2: Electrostatic interactions found between H1/H4 tail that have a probability greater than 10% of 20 ns simulation time long. These runs belong to the equilibration simulation of the augmented FAT/paxillin complex (with H4 tail and P1 constrained).....	249
Table D-3: Electrostatic interactions found between H1/H4 tail that have a probability greater than 10% of 20 ns simulation time long. These runs belong to the axial load simulations of the augmented FAT/paxillin complex (with H4 tail and P1 constrained). They represent the typical behavior of H1.....	250
Table D-4: Electrostatic interactions found between H1/H4 tail that have a probability greater than 10% of 20 ns simulation time long. These runs belong to the axial load simulations of the augmented FAT/paxillin complex (with H4 tail and P1 constrained). They represent the atypical behavior of H1.....	252
Table D-5: Electrostatic interactions found between H1/H4 tail that have a probability greater than 10% of 20 ns simulation time long. These runs belong to the	

perpendicular load simulations of the augmented FAT/paxillin complex (with H4 tail and P1 constrained). They represent the typical behavior of H1.....	253
--	-----

Table D-6: Electrostatic interactions found between H1/H4 tail that have a probability greater than 10% of 20 ns simulation time long. These runs belong to the perpendicular load simulations of the augmented FAT/paxillin complex (with H4 tail and P1 constrained). They represent the atypical behavior of H1. ....	255
--	-----

Table D-7: Electrostatic interactions found between H1/H4 tail that have a probability greater than 10% of 20 ns simulation time long. These runs belong to the perpendicular load simulations of the augmented FAT/paxillin complex (with H4 tail and P1 constrained). They represent the repeatability of atypical behavior of H1.....	256
--	-----

## List of Figures

- Figure 1-1: The organization of FAK, which starts with a non-catalytic FERM domain located at the N-terminal; a catalytic kinase domain in the mid section; and a non-catalytic FRNK domain at the C-terminal. The FRNK domain consists of two domains: the unstructured region and FAT domain (modified [1])..... 1
- Figure 1-2: The structure and location of Focal Adhesion Targeting (FAT) domain.  
 A) Cartoon representation of the FAT/paxillin complex. The construction of this complex is described in detail in chapter 3 (Methodology, Structures, Figure 3-1). The first helix (H1) of this complex is shown in magenta, the second helix (H2) in orange, the third helix (H3) in blue, and the last helix (H4) in yellow. The paxillin LD motifs are represented as follows: LD4, that binds to the first hydrophobic patch HP1, is shown in black (named P1), LD2, that binds to the second hydrophobic patch HP2, is in white (named P2). P1 and P2 will be used in this thesis. B) Illustration of the location of the FAT domain relative to the Kinase and FERM domains. .... 3
- Figure 1-3: The hypothesized structure of the FAT domain that is required for Y925 phosphorylation. H1 comes out of the bundle as well as the region flanking Y925 adopts a  $\beta$ -strand conformation. .... 4
- Figure 1-4: The hypothesized mechanism of the activation of the FAK. A) The N-terminal of the FAK (FERM domain) acts as a tether while the C-terminal (FAT domain) acts as an opposite tether. When loaded at both terminals, FAK is presumably mechanically activated. B) The



hypothesized activation mechanism of FAT domain where the load comes from the rest of FAK through H1 tail and LD motifs (P1, P2) act as reactions.....	6
Figure 2-1: An organization of the different domains of paxillin, including the two LD motifs that bind to the FAT domain (LD4 ‘P1’ at HP1 and LD2 ‘P2’ at HP2) (modified [17]). .....	10
Figure 2-2: Illustration of an observed swapped dimer created in vitro after six months in solution. A) Two different FAT domains in a four-helix bundle form. B) The swapped dimer structure is formed when two FAT domains exchange their first helix (modified [21]). .....	12
Figure 2-3: FAT domain, including two structural homologues apolipoprotein E (apoE) and the Vinculin tail (Vt) ( modified [13]). .....	13
Figure 2-4: Two salt bridges that are located in the region near the N-terminal of H1 (near Y925). Those salt bridges are between H1 tail and H4 (SB1: R919-D1039 and SB2: D922-R1042).....	14
Figure 2-5: Methionine zipper is formed by four methionine residues, one each from the four helices. The view shown is roughly along the bundle’s central axis near region of the C-terminal of H1 where those methionine residues located.....	15
Figure 2-6: Electrostatic interactions between paxillin and the FAT sub-domain. The left figure shows the interactions between P1 and H2, while the right figure illustrates the interaction between P2 with H4.....	16
Figure 3-1: FAT/paxillin complex without H4 tail and P1/P2 unconstrained. A) Three different FAT domains (green, magenta and cyan) that bind to the LD	

motifs (yellow, grey and dark pink) from either side. B) Selected FAT domains (FAT domain binds to LD motif at HP2 and FAT domain binds to LD motif at HP1) from pdb entry 1ow7 and the overlapped structure. C) FAT/paxillin complex. This structure was used for equilibrium (EQ) without H4 tail (WOT) simulation (Table 3-1).	19
Figure 3-2: FAT sequence for different species. Here, the mouse FAK sequence was used to identify the last five missing residues (QTRPH) of the FAK sequence (modified [13]).	21
Figure 3-3: Illustration of the paxillin sequence in chicken. The sequence of LD4 is shown in black. The sequence of extensional loop added to the N-terminal of LD4 motif is SASSA (in blue). The sequence of LD4 motif is TRELDELMASLS. The sequence of the extensional loop added to the C-terminal of LD4 motif is DFKFM (modified [28]).	22
Figure 3-4: Augmented FAT/paxillin complex with H4 tail and P1/P2 constrained.	
A) The FAT/paxillin complex without H4 tail and P1/P2 unconstrained (constructed from 1ow7.pdb, Figure 3-1. C). B) FAT/paxillin complex after adding missing residues (QTRPH) as a random coil using Pymol for H4 helix. This is referred to as the “H4 tail” throughout. C) FAT/paxillin complex after adding five residues to the LD4 motif (N-terminal, SASSA; C-terminal, DFKFM). This structure was used in the mechanically loaded (AX,PR) with H4 tail (WT) simulations (Table 3-1).	23

Figure 3-5: Illustration of H1/H4 tail interactions (here are three hydrogen bonds) that were observed during one simulation. The H1 tail is shown in cyan and the H4 tail in magenta. ....	24
Figure 3-6: Reference system for defining the position of H1/H4 tail with respect to each other. The angle $\alpha$ (a-b-c-d) illustrates the rotation of H1 tail with respect the reference frame formed by (b-c-d-e). The angle $\gamma$ (f-e-d-c) illustrates the rotation of H4 tail with respect the reference frame formed by (b-c-d-e). The angle $\eta$ (b-c-d-e) illustrates the twisting of reference frame (H1/H4 axes). The sign of these angles follow the right hand rule where the dash line between the points “e” and “b” is the reference. If $\alpha$ and $\gamma$ have the same sign, they are separated. However, if they have different sign, they cross each other. When they are equal to zero, it means they are above each other. ....	26
Figure 3-7: H1/H4 tail electrostatic interactions over time. This figure illustrates the different behaviors of the H1/H4 tail. Run #2 is different for each case while all the other runs show a high probability for H1/H4 tail to interact. Seeds were selected to sample these scenarios. Each bar represents a total time 20 ns. (Table 3-1, EQ.WT.P1P2).....	27
Figure 3-8: Position of H1/H4 tail with respect to each other. This figure shows the different behavior of the H1/H4 tail. The reference angle $\eta$ is reasonably stable and taken to be a fixed reference. In Run 2, H1/H4 tail is separated while in other simulation they are cross each other. Seeds 1, 2, 3 and 4 were obtained from Run3 while Seed 5 was selected from Run2. (Table 3-1, EQ.WT.P1P2). ....	28

Figure 3-9: Five selected seeds for the axial load simulations (Table 3-1, AX.WT.P1P2). A view from H1's N-terminal in a direction normally parallel to the axis of H1 taken from two different simulation runs (Seed 5 from Run 2, Seeds 1-4 from Run 3) of the equilibrium simulations of augmented FAT/paxillin complex (Table 3-1, EQ.WT.P1P2). .....	29
Figure 3-10: H1/H4 tail electrostatic interactions over time. This figure illustrates the diverse behavior of the H1/H4 tail. In Run 2 and Run 3, H1/H4 tail have fewer interactions while in all the other runs they show a high probability for H1/H4 tail to interact. Seeds "initial conditions" were selected to elucidate this wide range of behavior. Each bar represents a total time 20 ns. (Table 3-1, EQ.WT.P1).....	30
Figure 3-11: Position of H1/H4 tail with respect to each other. This figure shows the different behavior of the H1/H4 tail. The reference angle $\eta$ is reasonably stable and taken to be a fixed reference. In Run 2, H1/H4 tail is separated while in other simulation they are cross each other. Seeds 1, 2, 3, 4 and 5 were obtained from Run3 while Seed 6 was selected from Run2. (Table 3-1, EQ.WT.P1).....	31
Figure 3-12: Six selected seeds for the perpendicular load simulations (Table 3-1, PR.WT.P1). Views from H1's N-terminal in a direction normally parallel and perpendicular to the axis of H1 taken from two different simulation runs (Seed 6 from Run 2, Seeds 1-5 from Run 3) of the equilibrium simulations of augmented FAT/paxillin complex (Table 3-1, EQ.WT.P1). .....	32

Figure 3-13: Four types of FAT/paxillin without H4 tail used in the equilibrium simulations. The symbol “+” means that the LD motif is present, and “-” means that LD motif is absent from the FAT/paxillin complex. The first + or - indicates the presence or the absence of P1, while the second indicates the presence or the absence of P2. .... 33

Figure 3-14: MD and CFMD simulation boxes. A) FAT/paxillin complex (1520 protein atoms) in a 5x5x8.5nm rectangular box filled with of explicit water (33,126 SPC water molecules) and 50 counter-ions (25 Na<sup>+</sup> and 22 CL<sup>-</sup>) used for equilibrium simulations (Table 3-1, EQ.WOT.P1P2). B) Augmented FAT/paxillin complex (1821 protein atoms) in a 9.5x11x11nm rectangular box filled with of explicit water (97,719 SPC water molecules) and 125 counter-ions (65 Na<sup>+</sup> and 60 CL<sup>-</sup>) used for axial load simulations (Table 3-1, AX.WT.P1P2), shown at t = 0 ns. C) Augmented FAT/paxillin complex at the end of simulation (t = 20 ns)..... 35

Figure 3-15: Illustration of the induced steric clash between H1 and P2 caused by pulling the N-terminus of H1 tail in a direction perpendicular to the plane containing the axes of P1 and P2 (in the direction out of the plane of the paper). .... 39

Figure 3-16: Axial and perpendicular loads applied to the augmented FAT/paxillin complex with H4 tail and P1/P2 constrained. A) In the presence of both LD motifs (P1 and P2), the mechanical load is applied to the N-terminus of H1 tail in a direction parallel to the H1 axis. B) In the absence of P2, the load is applied to the N-terminus of H1 tail in a direction perpendicular to the plane containing the H1 and H4 axes. .... 40

Figure 3-17: Illustration of how the FAT domain self-orientes to follow the load direction (PR.WT.P1). A) FAT domain before applying the load to the H1's N-terminus. B) FAT domain after it self-oriented to follow the load direction. It was presumed that all the directions that are perpendicular to the axis of P1 are nearly equivalent. ....	41
Figure 3-18: Illustration of energy landscape where the colors represent the depth of the well. A) Top view. B) Third dimension which is the depth of the well.....	44
Figure 3-19: H1 position characterization. A) Top and bottom distances between H1 and a virtual helix (in gray). The top distance is between the N-terminal of H1 (center of mass of K923-N927) and the average point of the C-terminal of H2 (center of mass of T963-T967) and N-terminal of H4 (center of mass of L1035-D1039). The bottom distance is between the C-terminal of H1 (center of mass of E937-K941) and the average point of the N-terminal of H2 (center of mass of V951-K955) and C-terminal of H4 (center of mass of T1022-A1026). B) The potential position of H1 if it leaves the bundle. ....	45
Figure 3-20: Residues neighboring the Y925 residue. An expanded view of the region flanking Y925 at the N-terminal of H1. The backbone dihedral angle $\psi_i$ ( $N_i-C\alpha_i-C_i-N_{i+1}$ ) that describes H1 secondary structural conformation. For an $\alpha$ -helix, $\psi \approx -50^\circ$ and for a $\beta$ -strand, $\psi \approx 170^\circ$ .....	47
Figure 3-21: Illustration of a hydrogen donor-acceptor pair formed as O-N-H (donor N+, acceptor O-). A hydrogen bond was assured to be formed if the	

distance between O and N ( $d_{HB}$ ) was to be less than 0.35 nm and the angle $\Theta_{HB}$ formed by O-N-H was less than $30^\circ$ .....	48
Figure 3-22: $3_{10}$ , $\alpha$ and $\pi$ helices formed by various hydrogen donor-accepter pairs starting with residue i.....	49
Figure 3-23: Illustration of the three types of hydrogen donor-accepter pairs ( $\alpha$ , $\alpha/3_{10}$ and $3_{10}$ ) that formed during the simulations, as well as the no hydrogen bond case, denoted by the symbol “Ø.”.....	50
Figure 3-24: Illustrations of different parts of the FAT domain in different final states. Those notations that are described in Table 3-2 used for classification of the final states that FAT domain.....	53
Figure 4-1: Energy landscape of H1 position represented by $d_{top}$ and $d_{bottom}$ in the presence and/or the absence of P1 and P2. H1 position has a small distribution (minima) which means H1 does not appear to have the propensity to leave the bundle under only thermal fluctuation. Each plot represents a cumulative time of 80 ns of simulation time. (Table 3-1, EQ.WOT.P1P2, EQ.WOT. P1, EQ.WOT.P2, and EQ.WOT.Ø).....	57
Figure 4-2: Energy landscape of H1 position represented by $d_{top}$ and $d_{bottom}$ in the absence of P1. $d_{top}$ versus time illustrates the presence of the two local minima (blue spots) on the energy landscape plot for Run#4. $d_{top}$ does not fluctuate between two states, which demonstrates the stability of H1 position relative to the bundle. (Table 3-1, EQ.WOT.P2).....	58
Figure 4-3: Energy landscape of the dihedral angle $\psi$ of the five N-terminal residues of H1 (K923, V924, Y925, E926 and N927) in the presence and/or the absence of P1 and P2. Except N923 that have greater flexibility, since it	

connects with the floppy tail (H1 tail),  $\psi$  angle of other residues has a small distribution (minima). This means H1 does not appear to have the propensity to adopt  $\beta$ -strand conformation under only thermal fluctuation. Each plot represents a cumulative simulation time of 80 ns. (Table 3-1, EQ.WOT.P1P2, EQ.WOT. P1, EQ.WOT.P2, and EQ.WOT.Ø)..... 59

Figure 4-4: Hydrogen bonds types formed in the presence and/or the absence of P1 and P2. H1 primarily forms an  $\alpha$ -helix. Each plot represents a cumulative simulation time of 80 ns. (Table 3-1, EQ.WOT.P1P2, EQ.WOT. P1, EQ.WOT.P2, and EQ.WOT.Ø)..... 61

Figure 4-5: Energy landscape of the H1/H4 salt bridge distances represented by SB1 (R919–D1039) and SB2 (D922–R1042). SB1 and SB2 have a wide distribution which means they are broken. This suggests that they are not primarily responsible for keeping H1 folded within the bundle. Each plot represents a cumulative simulation time of 80 ns. (Table 3-1, EQ.WOT.P1P2, EQ.WOT. P1, EQ.WOT.P2, and EQ.WOT.Ø)..... 63

Figure 4-6: The second salt bridge (SB2: D922-R1042) that is located in the region near the N-terminal of H1 (near Y925). The residue R1042 interacts with another partner which is N916..... 63

Figure 4-7: Cumulative probability of the two salt bridges represented by two distances SB1 (R919–D1039) and SB2 (D922–R1042). If the salt bridge distance has to be less than 0.5 nm, it means they are broken ~80%. This suggests that they are not primarily responsible for keeping H1 folded within the bundle. Each plot represents a cumulative simulation



time of 80 ns. (Table 3-1, EQ.WOT.P1P2, EQ.WOT. P1, EQ.WOT.P2, and EQ.WOT.Ø).	65
Figure 4-8: Energy landscape of H1 position represented by $d_{top}$ and $d_{bottom}$ . H1 position has a small distribution (minima) which means H1 does not appear to have the propensity to leave the bundle under only thermal fluctuation. Each plot represents a cumulative simulation time of 80 ns. (Table 3-1, EQ.WT.P1P2, EQ.WT. P1)	66
Figure 4-9: Energy landscape of H1 position represented by $d_{top}$ and $d_{bottom}$ in the presence of P1 only. Two different preferred states in different simulations illustrate the presence of the two local minima in the previous figure (Figure 4-9: Case +-). Each plot represents a simulation time of 20 ns. (Table 3-1, EQ.WT. P1)	67
Figure 4-10: Energy landscape of the dihedral angle $\psi$ of the five N-terminal residues of H1 (K923, V924, Y925, E926, and N927) in the presence and the absence of P2. Except K923 that have greater flexibility, since it connects with the floppy tail (H1 tail), $\psi$ angle of other residues have a small distribution (minima). This means H1 does not appear to have the propensity to adopt $\beta$ -strand conformation under only thermal fluctuation. Each plot represents a cumulative simulation time of 80 ns. (Table 3-1, EQ.WT.P1P2, EQ.WT.P1)	69
Figure 4-11: Hydrogen bonds types formed in the absence of P2. H1 primarily forms an $\alpha$ -helix. Each plot represents a cumulative simulation time of 80 ns. (Table 3-1, EQ.WT.P1P2, EQ.WT.P1)	70

Figure 4-12: Energy landscape of the H1/H4 salt bridge distances represented by SB1 (R919–D1039) and SB2 (D922–R1042). SB1 and SB2 have a wide distribution which means they are broken. This suggests that they are not primarily responsible for keeping H1 folded within the bundle. Each plot represents a cumulative simulation time of 80 ns. (Table 3-1, EQ.WT.P1P2, EQ.WT.P1). .....	71
Figure 4-13: Cumulative probability of the two salt bridges represented for two distances, SB1 (R919–D1039) and SB2 (D922–R1042). If the salt bridge distance has to be less than 0.5 nm, it means they are broken ~80% of the simulation time. This suggests that they are not primarily responsible for keeping H1 folded within the bundle. Each plot represents a cumulative simulation time of 80 ns. (Table 3-1, EQ.WT.P1P2, EQ.WT.P1). .....	72
Figure 4-14: The structural conformation of H1 under two conditions; H1 within the bundle and H1 isolated. A) H1 while it is attached to the bundle (Figure 3-1). It shows that H1 has the ability to keep its in helical form when it is associated with the bundle. B) H1 when it is isolated (K923-K941). H1 has a propensity to unfold from its C-terminal. ....	73
Figure 4-15: The structural conformation of LD4 under two conditions; LD4 binds to FAT domain and LD4 isolated. A) Snapshots for LD motif while it binds to the FAT domain (Figure 3-1). It shows that LD motif has the ability to keep its in helical form when it is associated with the bundle. B) Snapshots for LD motif when it is isolated (T264-S275). The isolated	

LD does not have the capability to stay folded, which illustrates the effect of the hydrophobic patches that LD binds to..... 74

Figure 4-16: Energy landscape of H1 position represented by  $d_{top}$  and  $d_{bottom}$  in the presence of both P1 and P2. For typical behavior, H1 position has a small distribution (minima) which means H1 does not appear to have the propensity to leave the bundle under constant force applied axially to the N-terminus of H1 tail. Each plot represents a simulation time of 20 ns. (Table 3-1, AX.WT.P1P2)..... 80

Figure 4-17: Energy landscape of the dihedral angle  $\psi$  of the five N-terminal residues of H1 (K923, V924, Y925, E926, and N927) in the presence of both P1 and P2 for H1 typical behavior. Except N923 that has greater flexibility, since it connects with the floppy tail (H1 tail),  $\psi$  angle of other residues have a small distribution (minima). This means H1 does not appear to have the propensity to adopt  $\beta$ -strand conformation under constant force applied axially to the N-terminus of H1 tail. Each plot represents a simulation time of 20 ns. (Table 3-1, AX.WT.P1P2)..... 82

Figure 4-18: Hydrogen bonds types formed in the absence of P2. For H1 typical behavior, H1 primarily forms an  $\alpha$ -helix. Each plot represents a simulation time of 20 ns. (Table 3-1, AX.WT.P1P2)..... 84

Figure 4-19: Energy landscape of the H1/H4 salt bridge distances represented by SB1 (R919–D1039) and SB2 (D922–R1042). SB1 and SB2 have a wide distribution which means they are broken. This suggests that they are not primarily responsible for keeping H1 folded within the bundle. Each plot represents a simulation time of 20 ns. (Table 3-1, AX.WT.P1P2)..... 86

Figure 4-20: The second salt bridge (SB2: D922-R1042) that is located in the region near the N-terminal of H1 (near Y925). The second salt bridge is shown before the simulation started and after. The load applied to the N-terminus of H1 tail pulled N916 away from R1042 making the second salt bridge more stable. ....	87
Figure 4-21: Cumulative probability of the two salt bridges represented for two distances, SB1 (R919–D1039) and SB2 (D922–R1042). If the salt bridge distance has to be less than 0.5 nm, it means they are broken ~60%. This suggests that they are not primarily responsible for keeping H1 folded within the bundle. Each plot represents a simulation time of 20 ns. (Table 3-1, AX.WT.P1P2). ....	88
Figure 4-22: Number electrostatic interactions formed between H1/H4 tail. The interactions between H1/H4 have a wide distribution which means H1/H4 tail prefer to entangled. Each bar represents a simulation time of 20 ns. (Table 3-1, AX.WT.P1P2). ....	89
Figure 4-23: Final state of the structure of the region flanking Y925 for H1 typical behavior under constant force applied axially to the N-terminus of H1 tail. (Table 3-1, AX.WT.P1P2). ....	91
Figure 4-24: Four different matrices are shown for H1 atypical behavior; H1 position, dihedral angle $\psi$ , hydrogen bond state and the salt bridge state. (Table 3-1, AX.WT.P1P2). ....	93
Figure 4-25: Two types of figure are shown for H1 atypical behavior; final state of the structure of the region flanking Y925, and number electrostatic interactions formed between H1/H4 tail. (Table 3-1, AX.WT.P1P2). ....	94

Figure 4-26: Highly hydrophobic residues between H1 and the bundle. The blue colored residues are either Val, Leu, or Ile. These residues create the hydrophobic core that may be responsible for holding H1 to the bundle....	96
Figure 4-27: Energy landscape of H1 position represented by $d_{\text{top}}$ and $d_{\text{bottom}}$ in the absence of P2. For typical behavior, H1 position has a small distribution (minima) which means H1 does not appear to have the propensity to leave the bundle under constant force applied to the N-terminus of H1 tail perpendicular to the P1 axis. Each plot represents a simulation time of 20 ns. (Table 3-1, PR.WT.P1). ....	99
Figure 4-28: Energy landscape of the dihedral angle $\psi$ of the five N-terminal residues of H1 (K923, V924, Y925, E926, and N927) in the presence or the absence of P2 for H1 typical behavior. Except N923 that have greater flexibility, since it connects with the floppy tail (H1 tail), $\psi$ angle of other residues have a small distribution (minima). This means H1 does not appear to have the propensity to adopt $\beta$ -strand conformation under constant force applied to the N-terminus of H1 tail perpendicular to the P1 axis. Each plot represents a simulation time of 20 ns. (Table 3-1, PR.WT.P1).....	101
Figure 4-29: Dihedral angle $\psi$ of the four N-terminal residues of H1 (V924, Y925, E926 and N927) versus time in absence of P2. For Seed#4 Run#1, the $\psi$ angle of V924 and E926 shows that they refold after unfolding (Table 3-1, PR.WT.P1). ....	102

Figure 4-30: Hydrogen bonds types formed in the absence of P2. For H1 typical behavior, H1 primarily forms an $\alpha$ -helix. Each plot represents a simulation time of 20 ns. (Table 3-1, PR.WT.P1). .....	103
Figure 4-31: Energy landscape of the H1/H4 salt bridge distances represented by SB1 (R919–D1039) and SB2 (D922–R1042). SB1 and SB2 have a wide distribution which means they are broken. This suggests that they are not primarily responsible for keeping H1 folded within the bundle. Each plot represents a simulation time of 20 ns. (Table 3-1, PR.WT.P1). .....	105
Figure 4-32: Cumulative probability of the two salt bridges represented for two distances, SB1 (R919–D1039) and SB2 (D922–R1042). If the salt bridge distance has to be less than 0.5 nm, it means they are broken ~70%. This suggests that they are not primarily responsible for keeping H1 folded within the bundle. Each plot represents a simulation time of 20 ns. (Table 3-1, PR.WT.P1). .....	107
Figure 4-33: Number electrostatic interactions formed between H1/H4 tail. The interactions between H1/H4 have a wide distribution which means H1/H4 tail prefer to entangled. Each bar represents a simulation time of 20 ns. (Table 3-1, PR.WT.P1). .....	108
Figure 4-34: Final state of the structure of the region flanking Y925 for H1 typical behavior under constant force applied perpendicularly to the N-terminus of H1 tail. (Table 3-1, PR.WT.P1).....	110
Figure 4-35: Four different matrices are shown for H1 atypical behavior; H1 position, dihedral angle $\psi$ , hydrogen bond state and the salt bridge state. (Table 3-1, PR.WT.P1). .....	112

Figure 4-36: H1 position represented by $d_{\text{top}}$ versus time for H1 atypical behavior.	
The $d_{\text{top}}$ increases rapidly as H1 leaves the bundle.....	113
Figure 4-37: Two types of figure are shown for H1 atypical behavior; final state of the structure of the region flanking Y925, and number electrostatic interactions formed between H1/H4 tail. (Table 3-1, PR.WT.P1). ....	114
Figure 4-38: Energy landscape of H1 position represented by $d_{\text{top}}$ and $d_{\text{bottom}}$ . Looking to the repeatability of H1 atypical behavior found in Seed#1 Run#1, H1 position has a small distribution (minima) which means H1 does not appear to have the propensity to leave the bundle under constant force applied to the N-terminus of H1 tail perpendicular to the P1 axis. The H1 atypical behavior is not repeatable in terms of H1 position. Each plot represents a simulation time of 20 ns. (Table 3-1, PR.WT.P1).....	116
Figure 4-39: Energy landscape of the dihedral angle $\psi$ of the five N-terminal residues of H1 (K923, V924, Y925, E926, and N927) in the presence or the absence of P2 for H1 atypical behavior repeatability. Except Seed#1, Run#8 and Seed#1, Run#10, $\psi$ angle have a small distribution (minima), which means H1 atypical behavior is not repeatable in terms of adopting a $\beta$ -strand. For Seed#1, Run#8 and Seed#1, Run#10, some residues have a tendency to unfold (Seed#1, Run#8: V924, Seed#1, Run#10: V924 and E926). (Table 3-1, PR.WT.P1). ....	118
Figure 4-40: Hydrogen bonds types formed in the absence of P2. For the repeatability of H1 atypical behavior and except Seed#1, Run#10, H1 primarily forms an $\alpha$ -helix. In general, the H1 atypical behavior is not repeatable in	

terms of the hydrogen broken. Each plot represents a simulation time of 20 ns. (Table 3-1, PR.WT.P1). .....	120
Figure 4-41: Energy landscape of the H1/H4 salt bridge distances represented by SB1 (R919–D1039) and SB2 (D922–R1042). SB1 and SB2 have a wide distribution which means they are broken. This suggests that they are not primarily responsible for keeping H1 folded within the bundle. Each plot represents a simulation time of 20 ns. (Table 3-1,PR.WT.P1). .....	121
Figure 4-42: Cumulative probability of the two salt bridges represented for two distances SB1 (R919–D1039) and SB2 (D922–R1042). If the salt bridge distance has to be less than 0.5 nm, it means they are broken ~70%. This suggests that they are not primarily responsible for keeping H1 folded within the bundle. Each plot represents a simulation time of 20 ns. (Table 3-1, PR.WT.P1). .....	122
Figure 4-43: Number electrostatic interactions formed between H1/H4 tail. The interactions between H1/H4 have a wide distribution which means H1/H4 tail prefer to be entangled. Each bar represents a simulation time of 20 ns. (Table 3-1, PR.WT.P1). .....	123
Figure 4-44: Final state of the structure of the region flanking Y925 under constant force applied perpendicularly to the N-terminus of H1 tail. (Table 3-1, PR.WT.P1).....	125



## Chapter 1. Introduction

### 1.1 Focal Adhesion Kinase (FAK)

Focal adhesion kinase (FAK), a non-receptor tyrosine kinase regulated by integrins and expressed in most cell types, plays an important role in signal transduction [1]. Activated FAK is crucial to many biological processes, such as cell proliferation, migration, and survival. These processes are involved in the progression and development of cancer, in which an increased FAK signal might result in one these biological processes being uncontrolled [2].

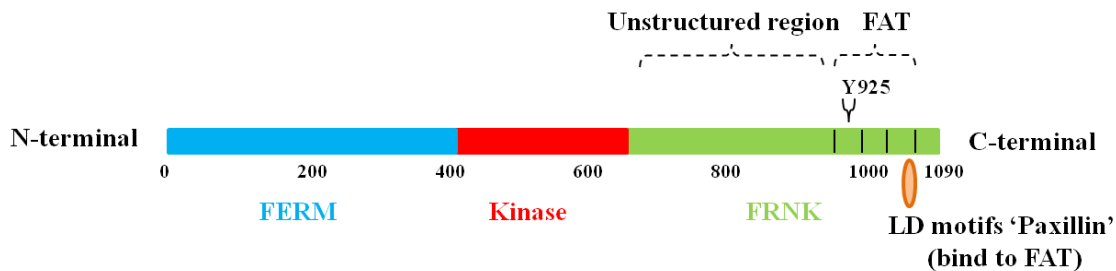


**Figure 1-1: The organization of FAK, which starts with a non-catalytic FERM domain located at the N-terminal; a catalytic kinase domain in the mid section; and a non-catalytic FRNK domain at the C-terminal. The FRNK domain consists of two domains: the unstructured region and FAT domain (modified [1])**

In a number of tumors, including those seen in breast and prostate cancer, the expression of FAK is elevated. Furthermore, experimental overexpression of FAK in cells can increase the growth of cancer cells and invasion. Clinical evidence suggests an important role of FAK in the formation and progression of tumors [3].

The importance of FAK in cell function and the progression and development of cancer suggests the importance of FAK as a potential target for cancer therapy. Inhibition or control of FAK may show promise as a cancer treatment [2].

FAK has multiple domains, which starts with a non-catalytic FERM domain located at the N-terminal; a catalytic kinase domain in the mid section; and a non-catalytic FRNK domain at the C-terminal. The FRNK domain consists of an unstructured region at its N-terminal and FAT (Focal Adhesion Targeting) domain at the C-terminus [1].

## **1.2 Focal Adhesion Targeting Domain (FAT)**

The FAT domain, which consists of four anti-parallel helices bundled together, has a critical phosphorylation site Y925 that has been implicated in cancer growth [4]. Phosphorylation of this site by Src-kinase family promotes the dissociation of FAK from focal adhesions and creates a binding site to the Grb2-SH2 domain.

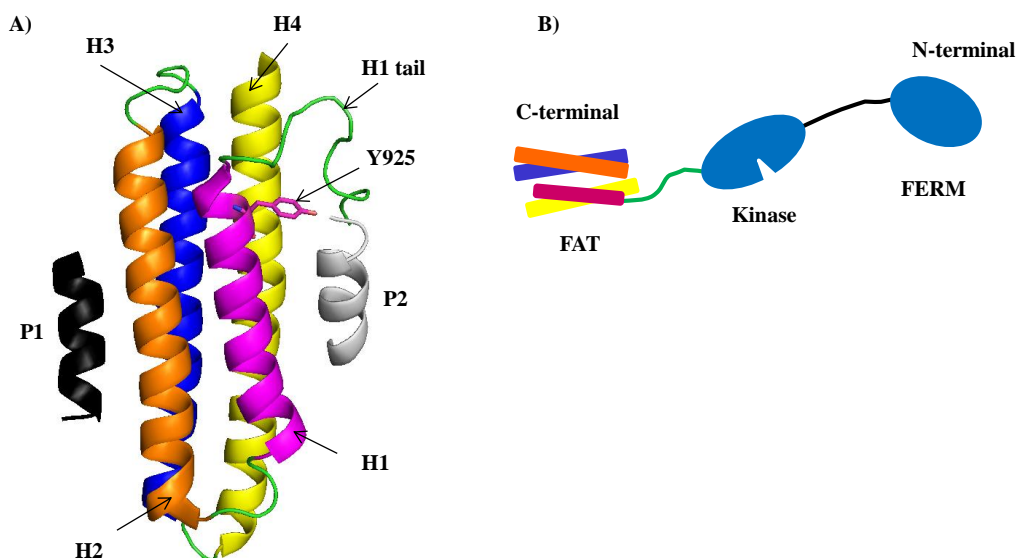


**Figure 1-2: The structure and location of Focal Adhesion Targeting (FAT) domain.** A) Cartoon representation of the FAT/paxillin complex. The construction of this complex is described in detail in chapter 3 (Methodology, Structures, Figure 3-1). The first helix (H1) of this complex is shown in magenta, the second helix (H2) in orange, the third helix (H3) in blue, and the last helix (H4) in yellow. The paxillin LD motifs are represented as follows: LD4, that binds to the first hydrophobic patch HP1, is shown in black (named P1), LD2, that binds to the second hydrophobic patch HP2, is in white (named P2). P1 and P2 will be used in this thesis. B) Illustration of the location of the FAT domain relative to the Kinase and FERM domains.

One phosphorylation site of FAT is Y925, which is located near the N-terminal of the FAT domain. Several hypotheses suggest that conformational changes must take place for this site to be phosphorylated; the actual mechanism is unclear. However, since the phosphorylation of this site is critical, it is important to have a better understanding of what is required to make this site available for phosphorylation. In addition to subjecting this site to thorough investigation, useful insight could be gained and how to create inhibitions preventing its phosphorylation.

### 1.3 Y925 Phosphorylation Requirements

The closed-bundle form of the FAT domain is sufficient to create two binding affinities via the two hydrophobic patches to which paxillin and other scaffolding proteins bind. The FAT domain in its bundled form is a poor substrate for Src-kinase so H1 that carries Y925 has to come out of the bundle [5]. In addition, the region of Y925 has to adopt  $\beta$ -strand conformation to engage the phosphorylation by Src-kinase [6]. Moreover, the Grb2-SH2 domain cannot bind to phosphotyrosine residues unless the area flanking it also adopts  $\beta$ -strand conformation [5] (Figure 1-3). All these requirements for phosphorylation, along with their references, are presented in the literature review.

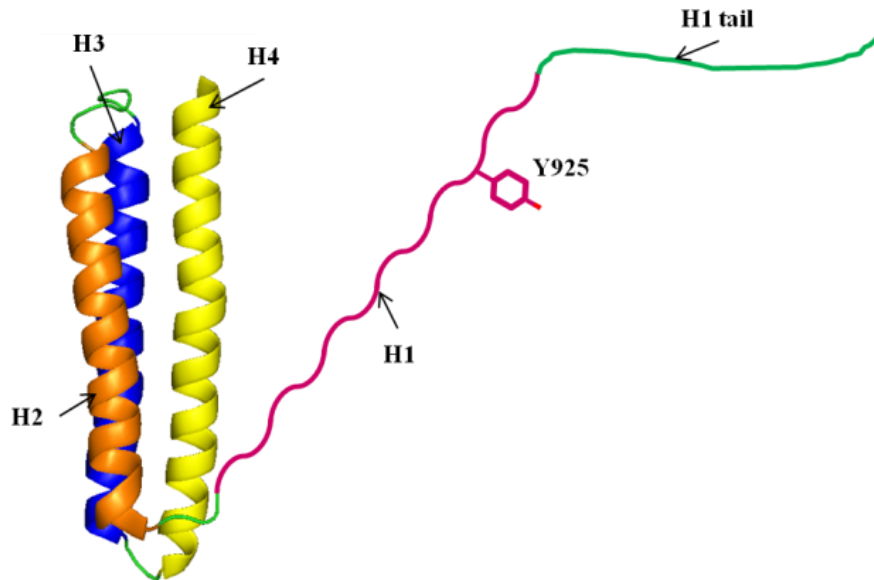


**Figure 1-3: The hypothesized structure of the FAT domain that is required for Y925 phosphorylation. H1 comes out of the bundle as well as the region flanking Y925 adopts a  $\beta$ -strand conformation.**

### 1.4 Understanding Pre-Phosphorylation Process

The previously described requirements for phosphorylation do not demonstrate what makes these structural changes occur; therefore, thorough investigation of this

process is essential to its understanding. Specifically, because it has been suggested that the first helix (H1), which contains Y925, is strongly attached to the bundle, the mechanism by which that energy barrier is overcome to get H1 out of the bundle must be ascertained. To accomplish this goal, which is to understand the mechanism that occurs before phosphorylation, one needs to go look deeply into the FAK environment.

FAK is presumably mechanically activated through extracellular matrix (ECM) proteins and actin cytoskeleton contractility [7-9]. The mechanical activation can be simply performed by molecular stretch, in which the N-terminal of FAK, the FERM/ligand complex, is mechanically pulled to disrupt the complex. This results both in release of auto-inhibition and activation of FAK (Figure 1-4) [10].

Two tethers are required for the existence of this mechanism. The N-terminal of FAK is suggested to be a tether, in which the FERM domain interacts with basic patch ligand [11]. On the other C-terminal side of the FAK, the FAT domain binds to paxillin and creates the opposite tether. Focusing on the FAT/paxillin complex, the load comes from the rest of the FAK through H1, while the LD motifs are considered reactions.

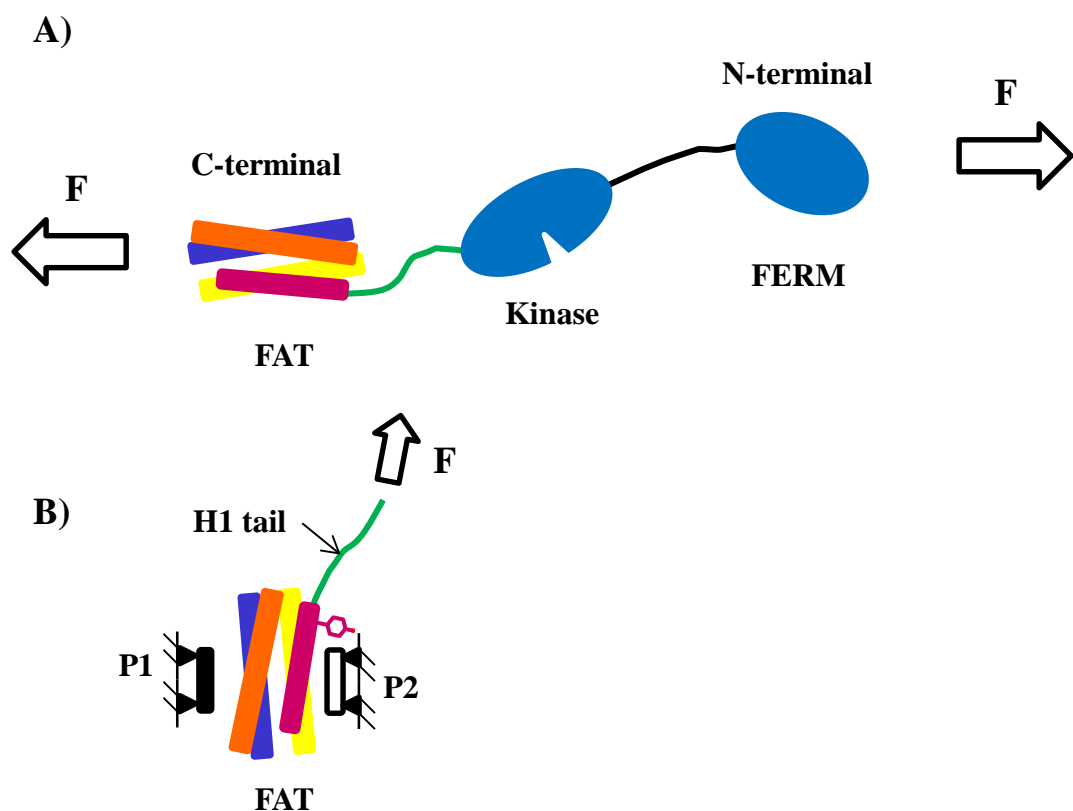


**Figure 1-4: The hypothesized mechanism of the activation of the FAK. A)** The N-terminal of the FAK (FERM domain) acts as a tether while the C-terminal (FAT domain) acts as an opposite tether. When loaded at both terminals, FAK is presumably mechanically activated. **B)** The hypothesized activation mechanism of FAT domain where the load comes from the rest of FAK through H1 tail and LD motifs (P1, P2) act as reactions.

Computational program were used to achieve this goal. Molecular Dynamic Simulation programs, (GROMACS: GRONingen MACHine for Chemical Simulations, CHARMM: Chemistry at HARvard Molecular Mechanics, and others), are able to facilitate an acceptable imitation of the environment in which the protein lives. Specifically, GROMACS, was used, to run Molecular Dynamics (MD) simulations as well as Constant Force Molecular Dynamics (CFMD) simulations. MD is used to look at the protein's behavior at equilibrium, while CFMD is performed to examine the effect of the applied load on the behavior of the protein.

For the FAT domain, it is essential to understand both its mechanical behavior and its propensity to undergo the necessary structural changes required for phosphorylation at equilibrium. Then, CFMD is used to apply the load to the FAT domain in a location and direction thought physiologically reasonable to induce the required conformational changes.

The following chapter includes a detailed review of the literature on the FAT domain, including what is known about the structure, binding affinities, binding partner, and phosphorylation site of the FAT domain, as well as the rationale behind the hypotheses suggesting the requirements needed for phosphorylating the FAT domain.

Methodology follows the literature review and includes a full description of how the FAT/paxillin complex is constructed. In addition, it includes the cases and simulations that must be run for both the equilibrium and loading cases. It also contains an illustration of how a certain hypothesis can be statistically addressed, such as the position of the first helix relative to the bundle, as well as the unfolding of the residues flanking Y925.

The Results section includes a discussion of the matrices chosen. It is divided into two main sections: the equilibrium results and the mechanical loaded results. Connecting the statistical results with the biological implications is the main goal of this chapter.

Finally, Conclusions gives an overall discussion of the results, including what may be required to accomplish the phosphorylation process. It also raises questions that are important to address in future research.

## **Chapter 2. Literature Review**

### **2.1 Focal Adhesion Kinase (FAK)**

FAK, which is 1,090 residues long, consists of a catalytic kinase domain flanked by two non-catalytic domains, the FERM domain (erythrocyte band 4.1 ezrin-radixin-moesin) located in the N-terminus and the C-terminal domain or FRNK (FAK-related-non-kinase) domain (Figure 1-2). The FRNK domain consists of two domains: the unstructured region at the N-terminal and FAT domain (Focal Adhesion Targeting) at the C-terminal [1].

### **2.2 Focal Adhesion Targeting (FAT) Domain**

FAT is approximately 140 amino acids long and is located at the C-terminus of FAK. The importance of the FAT domain comes from the fact that it is sufficient for localizing and targeting FAK to focal-adhesion-associated proteins such as paxillin and talin [12-14]. Even Y925 (within FAT) is not a typical phosphorylation site in vivo [15]; the phosphorylation of this site has been implicated in cancer growth [4], an important topic of further investigation (Y925 in human, mouse sequences and Y926 in avian sequence).

#### **2.2.1 FAT STRUCTURE**

The FAT domain is an antiparallel, “right-handed” four-helix bundle with short loops that is maintained by hydrophobic interactions [13]. It has been shown that the



hydrophobic core of the FAT domain is well defined and highly conserved across species. The first helix, H1, is the shortest one, while the fourth helix, H4, is the longest one (Figure 1-2). The H1 helix of the FAT domain contains Y925 tyrosine which is located at the start of the second turn of H1 and is phosphorylated by Src-kinase family [15].

The analysis of the FAT domain surface has shown that FAT has two hydrophobic-patch binding sites, HP1 at the H2H3 face and HP2 at H1H4 on the opposite side, where the FAT domain binds to paxillin via its two helical LD motifs (Figure 1-2, the white and black helices). A short loop, which contains two proline residues, is between H1 and H2 and is identified as a hinge region because of its flexibility [12, 16].

## **2.3 Paxillin**

Paxillin is an adapter, focal adhesion-associated protein that targets a number of proteins to the focal adhesions and is believed to be responsible for gathering multi-protein complexes to a coordinate signaling [17]. Paxillin is presumed to be a regulator for cell spreading and motility. The N-terminal of paxillin, an unstructured protein, contains a proline-rich region and five copies of approximately 13 peptide residues called LD (leucine-aspartate) repeat motifs, which form amphipathic  $\alpha$ -helices. LD motifs are known to be binding sites for proteins such as FAK, vinculin, and others [18]. The C-terminal of paxillin contains four LIM domains, which are responsible for targeting the paxillin to the focal adhesions [19].

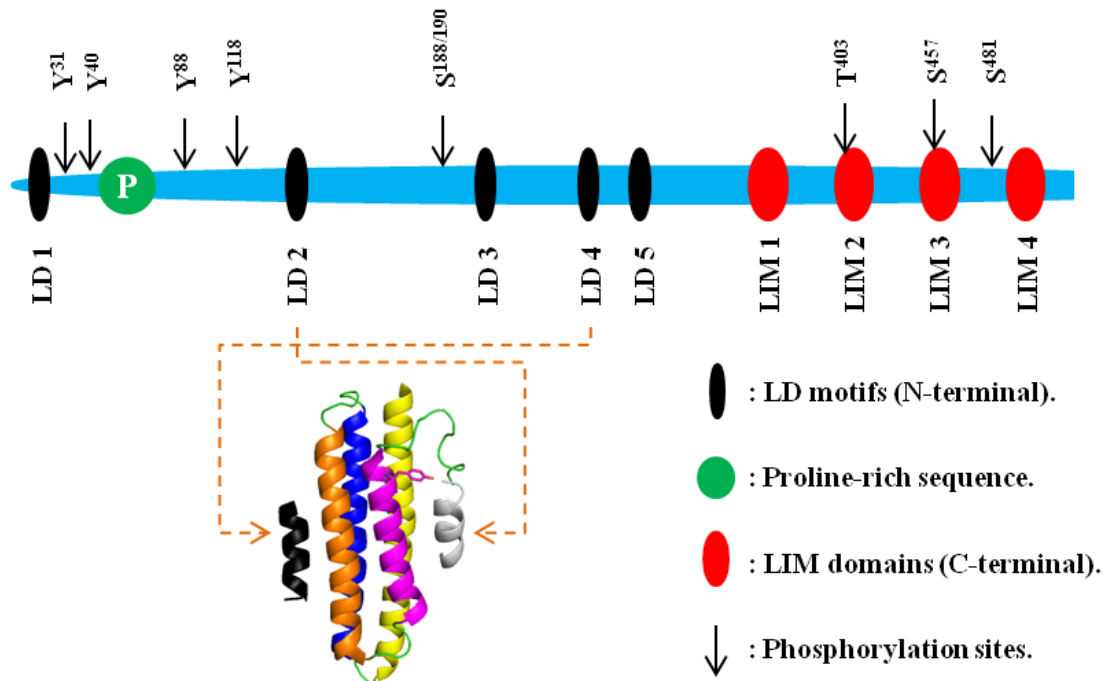


**Figure 2-1: An organization of the different domains of paxillin, including the two LD motifs that bind to the FAT domain (LD4 ‘P1’ at HP1 and LD2 ‘P2’ at HP2) (modified [17]).**

## 2.4 Paxillin Association with FAT

The localization of FAK to the focal adhesions is performed by binding to the paxillin. The two hydrophobic patches HP1 and HP2 of the FAT domain of FAK are the binding sites of the two LD motifs: LD4 (P1) binds to HP1 at H2H3, and LD2 (P2) binds to HP2 at H1H4, near where Y925 is located (For the entire thesis, LD motifs will be called as follows: LD4 ‘P1’ and LD2 ‘P2’). The closed-conformation, bundled form of the FAT domain is presumed to be important for FAT to bind to paxillin [20]. Disrupting these interactions between LD motifs and FAT is likely to break down the localization of FAK. On the C-terminal of paxillin [17], the third LIM domain has a major role in targeting the paxillin to the focal adhesions [19]. In addition, the association of paxillin with FAK or other kinases, such as Src, has an important role in controlling and

promoting the tyrosine phosphorylation of paxillin, which is involved in cell spreading and motility [10].

## **2.5 Phosphorylation of Y925**

Located in the second turn of H1 of the FAT domain, Y925 is known to be the phosphorylation site by Src family tyrosine kinases. Phosphorylation of Y925 creates a binding site of FAT to Grb2-SH2. This provides a mechanism of activation of the ras/MAPK pathway [15]. As a results of Y925 phosphorylation of the FAT domain, FAT is presumed to dissociate from the paxillin, leading to dissociation of FAK from the focal adhesions [20]. The mechanism by which Y925 is phosphorylated and what is required for Y925 to bind FAT to Grb2-SH2 remains unclear.

Experimental results suggest that FAT has to undergo some structural rearrangement, such that Y925 is pointed toward the Src kinase-active site to be phosphorylated [5]. The requirements for creation of access of the Src kinase and Grb2-SH2 to the Y925 phosphorylation site are illustrated below:

### **2.5.1 H1 POSITION**

The unphosphorylated FAT domain is a poor substrate for tyrosine kinases in its bundled, or closed-conformation, form [5]. Therefore, some structural rearrangement of the FAT domain are hypothesized to take place in order to make FAT a tyrosine kinase substrate. Another structure of the FAT domain, called a swapped dimer [5, 21] (Figure 2-2), in which each of the two FAT domains exchanges its first helix, has been observed *in vitro*. Even the infrequent appearance of this type of structure, “which has grown, *in*

*vitro*, in six months comparing it with bundle form that has grown in three weeks,” suggests that H1 has capacity to leave the bundle. Other researchers have suggested that during the formation of the swapped dimer that there will be a transition state in which H1 is less structured. During the transition state, the region around Y925 could adopt the required structure and engage the phosphorylation [20] (Figure 1-3).

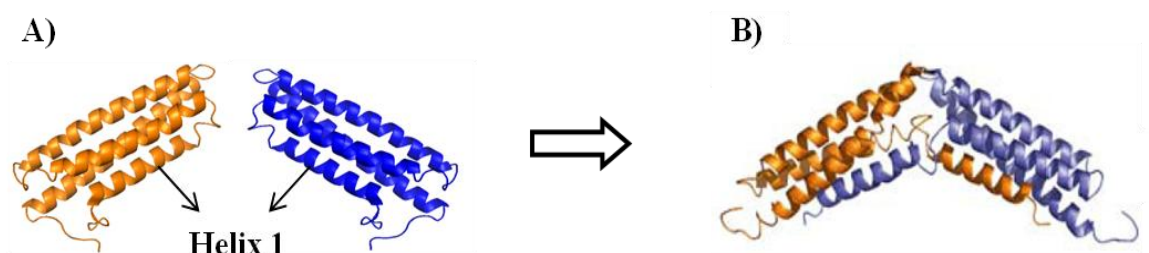


**Figure 2-2: Illustration of an observed swapped dimer created *in vitro* after six months in solution. A) Two different FAT domains in a four-helix bundle form. B) The swapped dimer structure is formed when two FAT domains exchange their first helix (modified [21]).**

In addition, it has been reported that the Vinculin tail, “Vt” [22] and apolipoprotein E ‘apoE’ [23], which have close structural similarities to FAT, undergo a functional folding/unfolding transition [5] (Figure 2-3). The unusual arrangement of the FAT helices and P944XPP peptide “short loop that connects H1 and H2” might enable such transitions [5, 20]

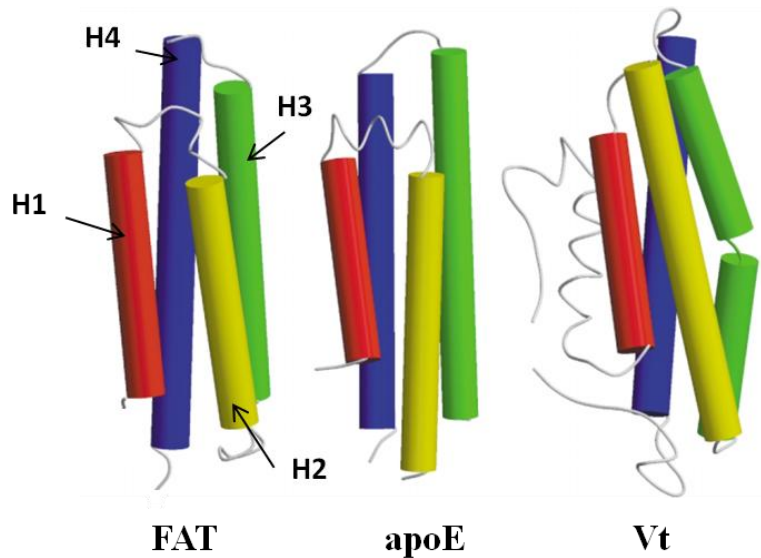


**Figure 2-3: FAT domain, including two structural homologues apolipoprotein E (apoE) and the Vinculin tail (Vt) ( modified [13]).**

As a result, it has been suggested that FAT's H1 must be in an open conformation, specifically with H1 out of the bundle, in order for FAT to engage the phosphorylation [20]. Since H1 is part of the bundle in native form, this means that it has to overcome an energy barrier, by undergoing some unfavorable conformational changes, in order to open out.

### 2.5.2 H1 UNFOLDING

The Src-like tyrosine kinases can bind to a tyrosine located in a region that adopts  $\beta$ -strand structure [6]. In addition, it is known that Grb2-SH2 binds to phospho-tyrosine that is within a  $\beta$ -strand region [24]. The helical conformation of H1 hinders any interaction between Y925 and Grb-SH2 unless it adopts  $\beta$ -strand conformation. This suggests that the phosphorylation of the FAT domain requires that the region flanking Y925 has to be in a  $\beta$ -strand conformation [5] (Figure 1-3).

## 2.6 Salt Bridges between H1 Tail and H4

Based on the published crystal structures, there are two salt bridges, among other factors, contributing to an energy barrier preventing H1 to open out (Figure 2-4). Those salt bridge interactions are between the extensional loop of H1 (for this thesis, called the H1 tail) and H4 which have been observed from the crystal structure [5]. The first salt bridge, ‘SB1’, is between H1 tail R919 and H4 D1039. The second one, ‘SB2’, is between H1 tail D922 and H4 R1042.

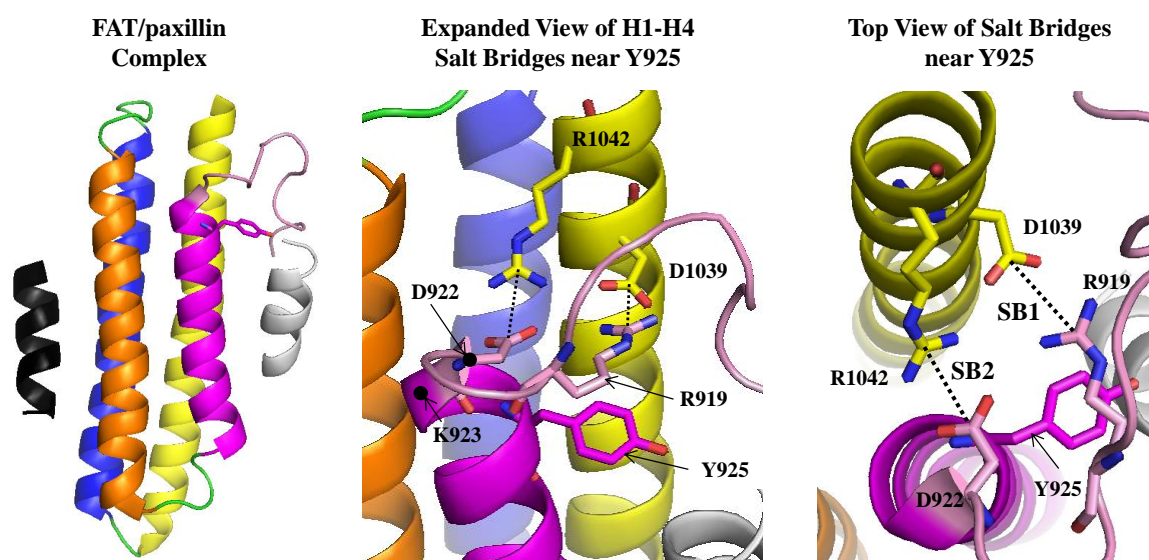
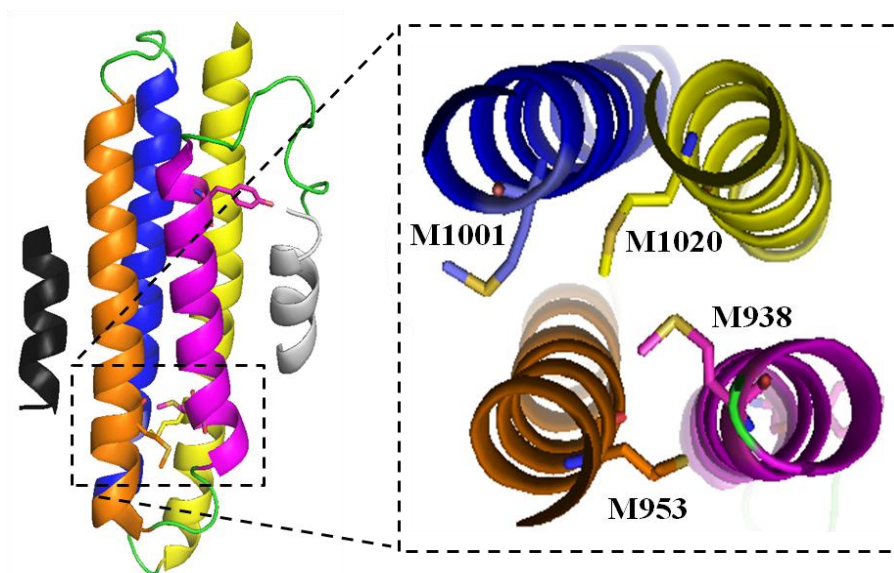


Figure 2-4: Two salt bridges that are located in the region near the N-terminal of H1 (near Y925). Those salt bridges are between H1 tail and H4 (SB1: R919-D1039 and SB2: D922-R1042).

## 2.7 Methionine Zipper between H1, H2, H3 and H4

The “bottom” of the FAT domain (near the C-terminal of H1) involves an obvious cavity form by a hydrophobic cluster consisting of four hydrophobic residues, methionines, which disrupt the packing of the hydrophobic core of the FAT domain

(Figure 2-5) [5, 12]. Since these residues are far away from Y925, it is presumed that they do not have a significant influence of the mechanical behavior region flanking Y925.



**Figure 2-5:** Methionine zipper is formed by four methionine residues, one each from the four helices. The view shown is roughly along the bundle's central axis near region of the C-terminal of H1 where those methionine residues located.

## 2.8 Interactions between Paxillin LD Motifs and FAT Domain

Some interactions between FAT and LD motifs may be important in maintaining the association of FAT domain and paxillin. The aspartic acid from P1, D146, interacts with R962 and/or K955 from H2. Another aspartic acid, D268, from P2 interacts with either H1025 and/or K1032 from H4 [12] (Figure 2-6). Since the main goal of this research is to examine the availability of Y925 for the phosphorylation, the strength of these interactions are not examined.

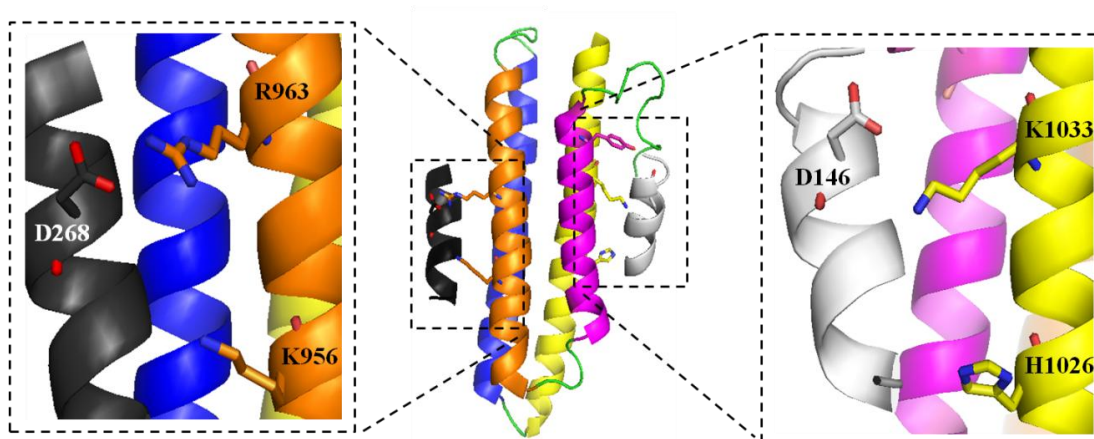


**Figure 2-6: Electrostatic interactions between paxillin and the FAT sub-domain.** The left figure shows the interactions between P1 and H2, while the right figure illustrates the interaction between P2 with H4.

**Table 2-1: A summary of the reported interactions of the FAT/paxillin complex.** Salt bridges are shown in red, methionine zipper is in green and electrostatic interactions are in blue.

	P1	P2	H1	H2	H3	H4
H1			M938 [5, 12]			H1: R919 - H4: D1039 [5] H1: D922 - H4: R1042 [5]
H2	P1: D268 H2: R963 & K956 [12]			M953 [5, 12]		
H3					M1001 [5, 12]	
H4		P2: D146 H4: H1026 & K1033 [12]				M1020 [5, 12]



## Chapter 3. Methodology

To understand the FAT domain's mechanical behavior and examine the availability of Y925 for the phosphorylation, (MD) and Constant Force Molecular Dynamics (CFMD) simulations of FAT/paxillin complex were run using GROMACS [25, 26] and analyzed using scripts written the MATLAB programming language. The methodology chapter has three main sections: Structures, Simulations and Analysis. The structure section illustrates how the structures that are used in the simulation were constructed. The simulation section presents a description of all type of simulations that are run. The analysis section includes all the analysis used for investigating the FAT domain behavior, including the behavior of H1 that contains Y925.

### 3.1 Structures

The FAT/paxillin complex has been constructed and modified in order to be used in the equilibrium MD and loaded CFMD simulations.

#### 3.1.1 FAT/PAXILLIN COMPLEX WITHOUT H4 TAIL AND P1/P2 UNCONSTRAINED

The FAT/paxillin complex that is shown in Figure 1-2 was built through these steps:

1. A crystal structure of FAT/LD4 motif complexes (PDB entry 1ow7) [27] was downloaded from the Protein Bank Database ([www.pdb.org](http://www.pdb.org)). This PDB file includes multiple FAT domains that bind to LD4 motifs from either binding site. As seen in Figure 3-1.A, in the first complex from the left, the LD4 motif (chain D in yellow) binds to the FAT domain (chain A in green) at the second

hydrophobic patch HP2 (between H1/H4). In the second complex, the LD4 motif (chain E in grey) binds to the FAT domain (chain B in magenta) at the first hydrophobic patch HP1 (between H2/H3). The third complex consists of the LD4 motif (chain F in dark pink) binds to the FAT domain (chain C in cyan) at the first hydrophobic patch HP1 (between H2/H3).

2. Using Pymol (Molecular Visualization Program: <http://www.pymol.org/>), the two FAT domains that bind to LD4 motifs (first and third complexes) were selected for alignment.
3. Pymol has options for aligning two molecules. In one option, Pymol minimizes the RMSD (Root Mean Square Deviation; the square root of the mean of the square of the distances between aligned atoms) between aligned molecules. For this study, the backbone atoms of the two selected FAT domains (chain A: N916-T1049 and chain C: I909-G1047) were aligned based on minimizing the RMSD forming the two overlapped FAT domains that bind to LD motifs from two hydrophobic patches shown in Figure 3-1.B.
4. One FAT domain (chain C) and the two LD4 motifs (chain D and chain F) were retained forming the final FAT/paxillin complex as shown in Figure 3-1.C.

The final FAT/paxillin structure with the presence/absence of P1 and P2 was used in all equilibrium simulations (Table 3-1: EQ.WOT.P1P2, EQ.WOT. P2, EQ.WOT.P1 and EQ.WOT.Ø). Detailed descriptions of the cases that are considered for the equilibrium simulations are presented in §0Simulations.

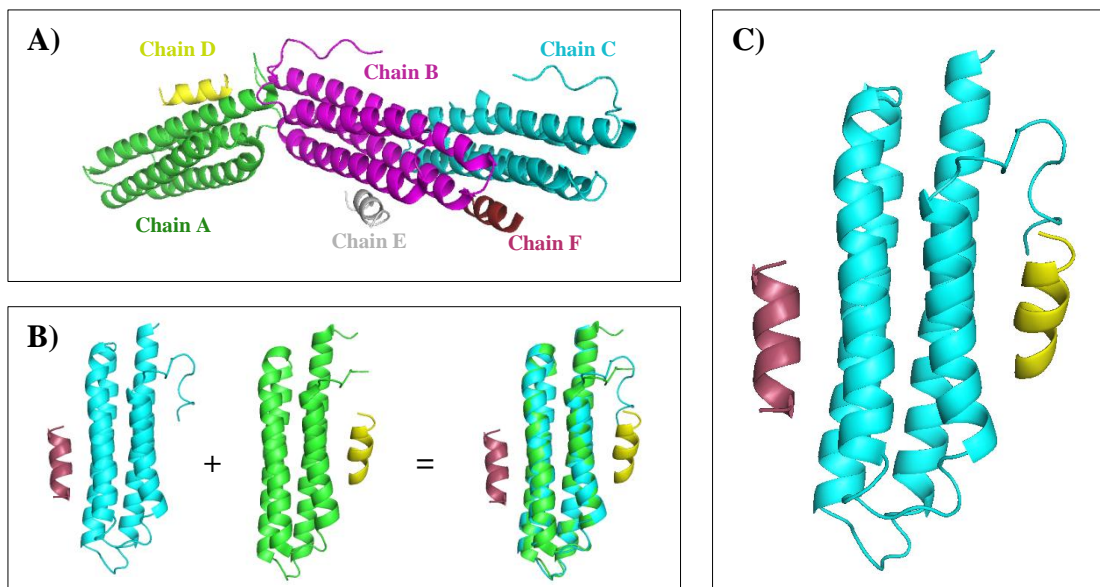


**Figure 3-1: FAT/paxillin complex without H4 tail and P1/P2 unconstrained. A) Three different FAT domains (green, magenta and cyan) that bind to the LD motifs (yellow, grey and dark pink) from either side. B) Selected FAT domains (FAT domain binds to LD motif at HP2 and FAT domain binds to LD motif at HP1) from pdb entry 1ow7 and the overlapped structure. C) FAT/paxillin complex. This structure was used for equilibrium (EQ) without H4 tail (WOT) simulation (Table 3-1).**

### 3.1.2 AUGMENTED FAT/PAXILLIN COMPLEX WITH H4 TAIL AND P1/P2 CONSTRAINED

The FAT/paxillin complex (Figure 3-1.C) was modified for the loaded simulations. As it has been suggested that FAK is mechanically activated, this research investigated mechanically loaded cases using Constant Force Molecular Dynamics (CFMD) simulations. Constant mechanical loads were applied at the N-terminus of H1 (I909) in directions parallel and perpendicular to the H1 axis. The load must be applied to the extensional loop at the FAT domain's N-terminal of that connects the FAT domain with the rest of the FAK domain, the presumptive origin of the mechanical load . In addition, since the paxillin associates the FAT domain to the focal adhesions, the LD motifs to which FAT binds are presumed to act as tethers. However, the key step is to make the load scenarios as realistic as possible before starting any simulations.

### **3.1.2.1 H4 Tail Addition**

Random-coil residues missing from the crystal structure must be added to pdb structure at the C-terminal of the FAT domain, where they belong.

1. Using “builder” command in Pymol, the five residues missing from the pdb (QTRPH) were added to the C-terminal of residue G1047 based on the FAK sequence (Figure 3-2, Figure 3-4).
2. Since the structure of those residues is unknown, their initial structure is assumed to be random coil. The results are not expected to be sensitive to this initial placement as this coil will move in such a way that it finds its natural position after the energy minimization and equilibration processes. This extensional loop is named H4 tail over the entire thesis.

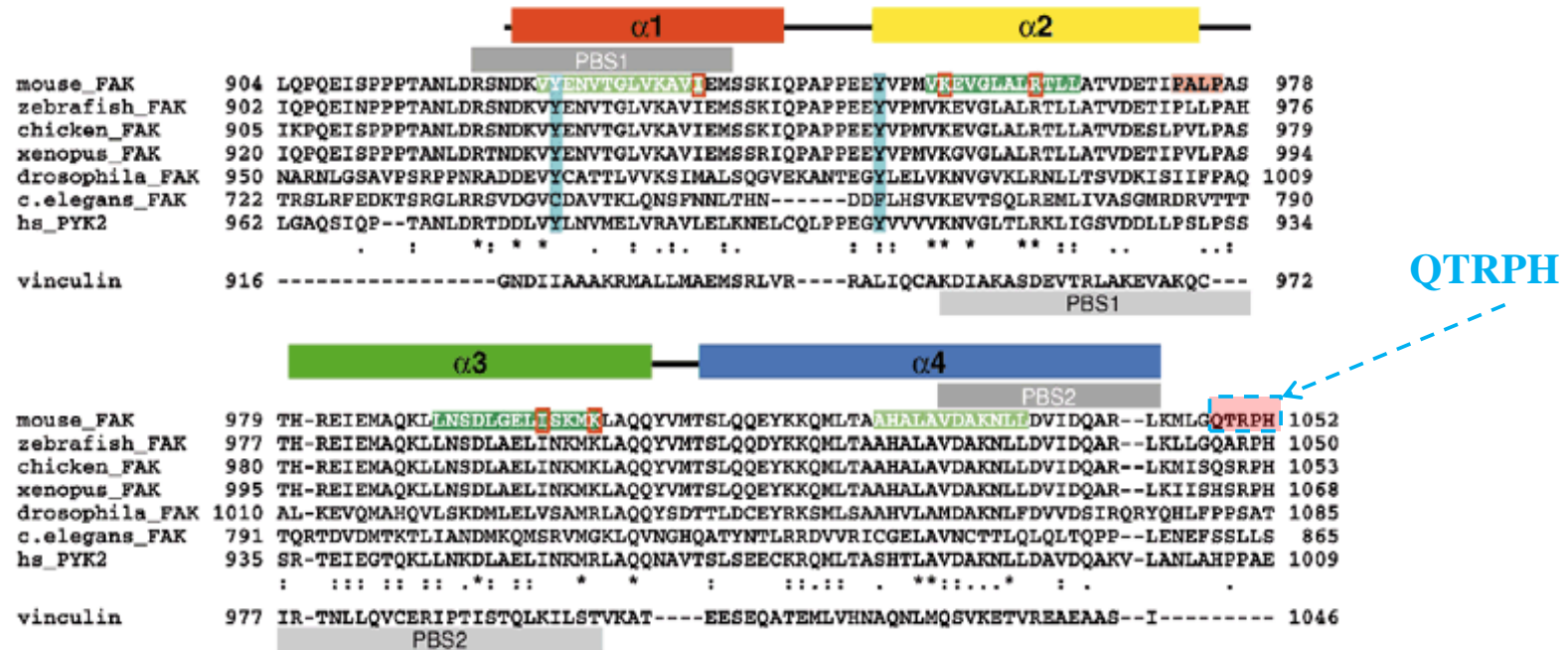
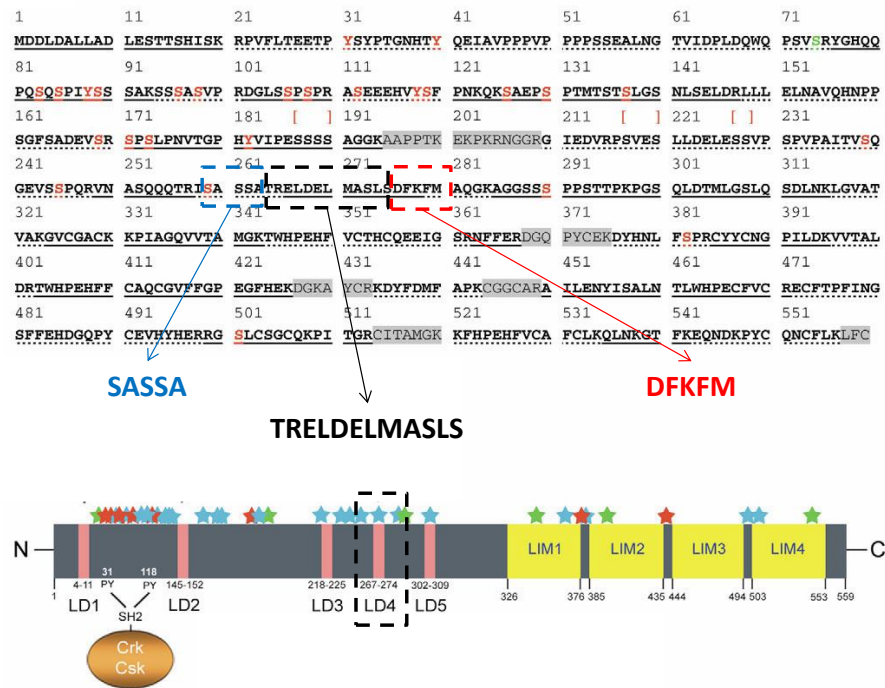


Figure 3-2: FAT sequence for different species. Here, the mouse FAK sequence was used to identify the last five missing residues (QTRPH) of the FAK sequence (modified [13]).

### 3.1.2.2 LD Motifs Extension-Loop Addition

Since the paxillin connects the FAT domain via LD motifs, it connects to the focal adhesions via the LIM domain, it is reasonable to consider the paxillin as a series of tethers. To provide reactions to the applied force, zero displacements were enforced at the ends of the LD motifs during the simulations. Thus LD motifs produce reaction forces to the force applied to N-terminus of the H1 tail. However, to give the FAT domain more conformational freedom, as would be expected in vivo, five residues were added to either end of the LD4 motif. Based on the paxillin sequence (in chicken) and using Paymol's "builder" feature, five residues were added to each end of the LD4 motif: N-terminal, SASSA; C-terminal, DFKFM. (Figure 3-4.C).



**Figure 3-3: Illustration of the paxillin sequence in chicken. The sequence of LD4 is shown in black. The sequence of extensional loop added to the N-terminal of LD4 motif is SASSA (in blue). The sequence of LD4 motif is TRELDLMASLS. The sequence of the extensional loop added to the C-terminal of LD4 motif is DFKFM (modified [28]).**

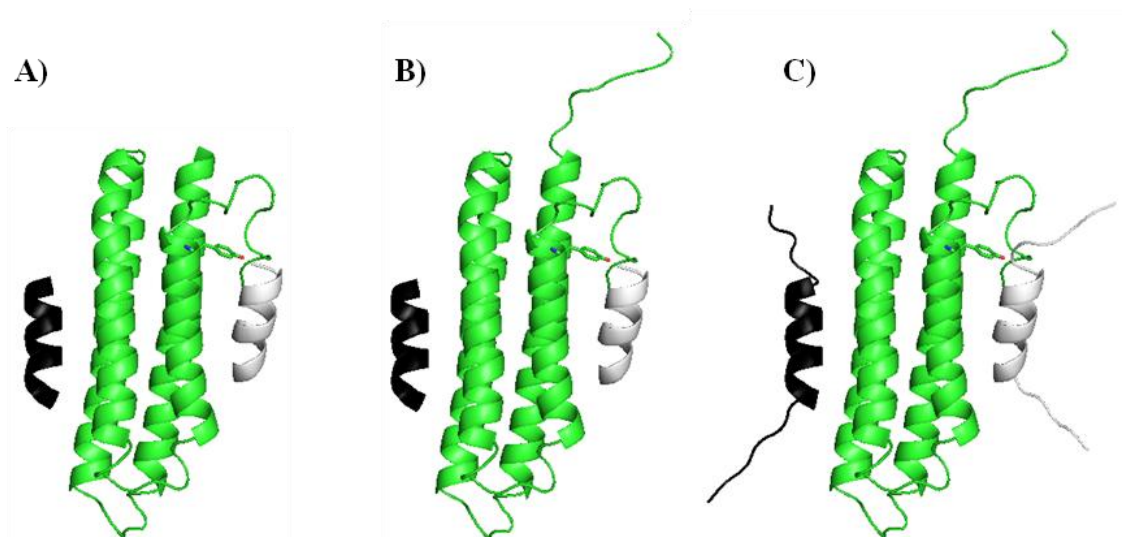


**Figure 3-4: Augmented FAT/paxillin complex with H4 tail and P1/P2 constrained.** A) The FAT/paxillin complex without H4 tail and P1/P2 unconstrained (constructed from 1ow7.pdb, Figure 3-1. C). B) FAT/paxillin complex after adding missing residues (QTRPH) as a random coil using Pymol for H4 helix. This is referred to as the “H4 tail” throughout. C) FAT/paxillin complex after adding five residues to the LD4 motif (N-terminal, SASSA; C-terminal, DFKFM). This structure was used in the mechanically loaded (AX,PR) with H4 tail (WT) simulations (Table 3-1).

This structure, with the presence and the absence of P2 (LD motif that binds to HP2), was used in all equilibrium simulations (Table 3-1: EQ.WT.P1P2, EQ.WT.P1).

### 3.1.1 INITIAL STRUCTURES FOR MECHANICALLY LOADED SIMULATIONS

Two load scenarios were chosen (discussed later in §3.2 Simulations) axial (AX) and perpendicular (PR). To examine the role of the mechanical load on H1 behavior, CFMD simulations were performed on as many different mechanical structures as possible. Using the augmented FAT/paxillin structure (Figure 3-4C), the H1 behavior in all MD simulations was very similar, but the H1/H4 tail behavior was different. Based on these differences in the tail behavior, different seeds were selected. The term ‘seed’, which is used later, refers to distinct initial structures, which were selected from MD simulation trajectories at distinct time steps. From the equilibrium simulations (Table 3-1;



EQ.WT.P1P2, EQ.WT.P1), distinct seeds are selected as initial structures for the mechanical loaded CFMD simulations. The criteria for selection is explained as below:

#### 3.1.1.1 H1/H4 Tail Interactions

After the addition of the H4 tail to the structure, possible electrostatic interactions, which may be found between the two tails were examined. These interactions have the potential to influence the load sharing between the H1/H4 tail. Moreover, they may keep H1 attached to the bundle, as well as regulate or otherwise slow down the unfolding events. Figure 3-5 illustrates a representative interaction in which the H1/H4 tail interact via hydrogen bonds. All 390 possible interactions between H1 tail (I909-N921) and H4 tail (L1043-H1052), were screened over all simulations' trajectories. If any distance between two opposite-charged atoms is less than 0.4 nm, it was recorded as an electrostatic interaction. The equation used to calculate the distance between the opposite charges atoms is given in § 3.3.4 Analysis.

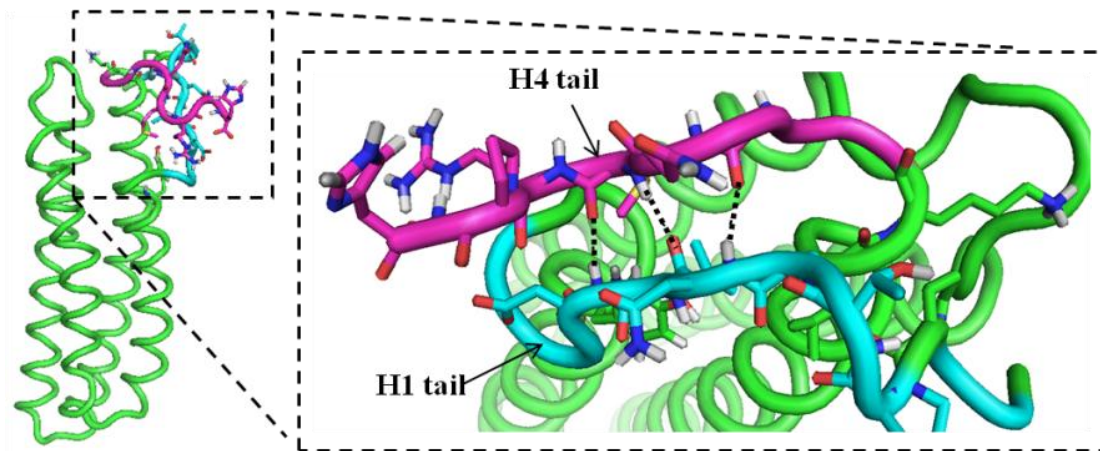
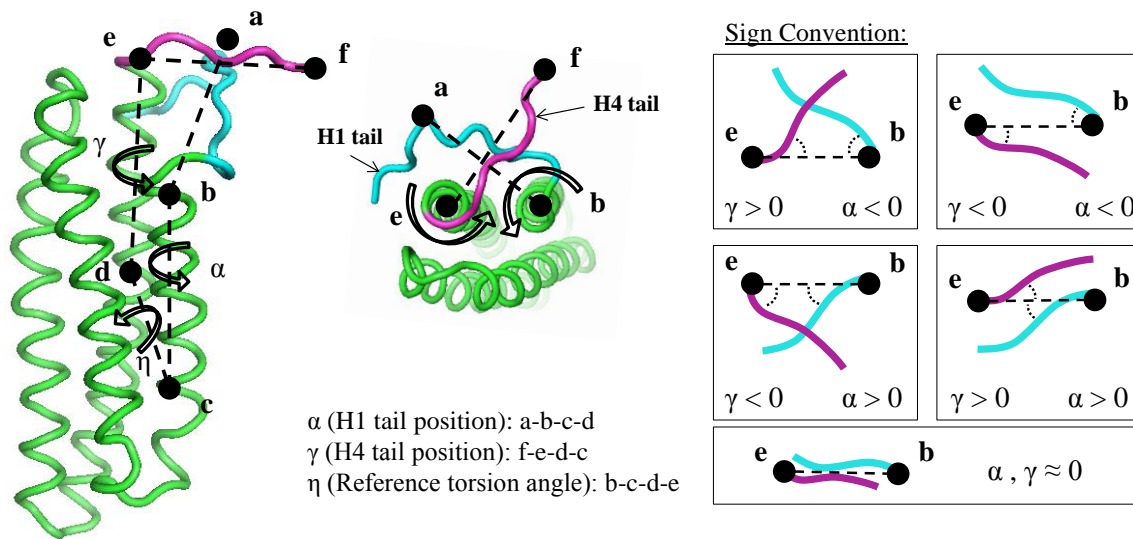


Figure 3-5: Illustration of H1/H4 tail interactions (here are three hydrogen bonds) that were observed during one simulation. The H1 tail is shown in cyan and the H4 tail in magenta.



### 3.1.1.2 H1/H4 Tail Positions

Based on some preliminary mechanically loaded simulations, it was determined that the relative positions of the H1 and H4 tails could be an appropriate criteria on which to choose the initial structures to be used for the mechanically loaded cases. The metric that developed is a combination of torsion angles that describe the rotation of the tails with respect to a fixed reference. It was necessary to select a stable reference or datum as the entire structure moves. Here, six points, describing the center of mass of each respective turn, were used Figure 3-6. Torsion angles “ $\gamma$  and  $\alpha$ ” describe the rotation of each tail with respect to each other. However, to make sure that those angles are truly representative, the torsion angle  $\eta$  which measures the twisting angle between H1 and H4, must be stable. The formula used to calculate these angles is the same formula used for  $\psi$  calculation (see § 3.3.2.2.1 Analysis).



**Figure 3-6: Reference system for defining the position of H1/H4 tail with respect to each other.** The angle  $\alpha$  (a-b-c-d) illustrates the rotation of H1 tail with respect the reference frame formed by (b-c-d-e). The angle  $\gamma$  (f-e-d-c) illustrates the rotation of H4 tail with respect the reference frame formed by (b-c-d-e). The angle  $\eta$  (b-c-d-e) illustrates the twisting of reference frame (H1/H4 axes). The sign of these angles follow the right hand rule where the dash line between the points “e” and “b” is the reference. If  $\alpha$  and  $\gamma$  have the same sign, they are separated. However, if they have different sign, they cross each other. When they are equal to zero, it means they are above each other.

### 3.1.1.3 Selected Seeds for Axial Load Simulation

#### 3.1.1.3.1 H1/H4 Tail Interaction

As seen in Figure 3-7, many interactions developed and/or persisted during the simulations. In some simulations (e.g., Run 4), the tails interacted for nearly 95% of the simulation time, while in others (e.g., Run 2), the tails did not interact at all. In addition to the interaction matrix, the position of the H1/H4 tails with respect to each other is another useful criteria for selecting the appropriate initial structures (i.e., seeds) that were used for the mechanically loaded simulations.

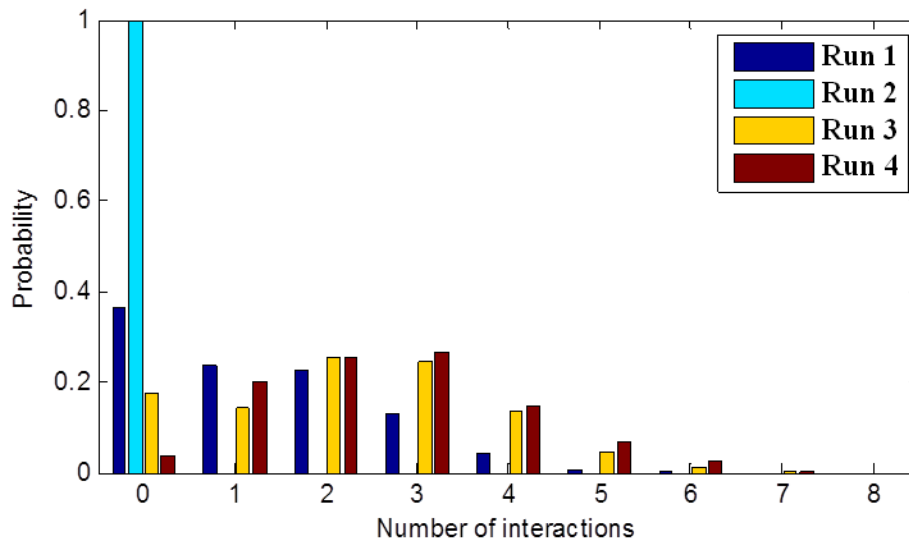


**Figure 3-7: H1/H4 tail electrostatic interactions over time. This figure illustrates the different behaviors of the H1/H4 tail. Run #2 is different for each case while all the other runs show a high probability for H1/H4 tail to interact. Seeds were selected to sample these scenarios. Each bar represents a total time 20 ns. (Table 3-1, EQ.WT.P1P2)**

### ***3.1.1.3.2 H1/H4 Tail Position***

Figure 3-8 shows that (Case ++),  $\eta$  fluctuates  $\pm 5^\circ$  while it stays very close to zero for all different runs. Whether  $\eta$  is a good reference or not depends on how much the tails rotate. The range of the rotation of these tails is about  $\sim 60^\circ$ , so comparing this value with small range of the reference angle suggest that the reference angle that we picked is an acceptable choice. In addition, the figure shows that the position of H1 tail is more stable than the position of H4 that has more mobility. Not only that but also, there is a divergence in the behavior of H4 tail. Run 2 shows that H4 tail does not cross H1 tail, which is supported by the fact that they do not interact most the time (see figure 4-18). All the other runs, however, show a high probability of the H1/H4 tail crossing each other.

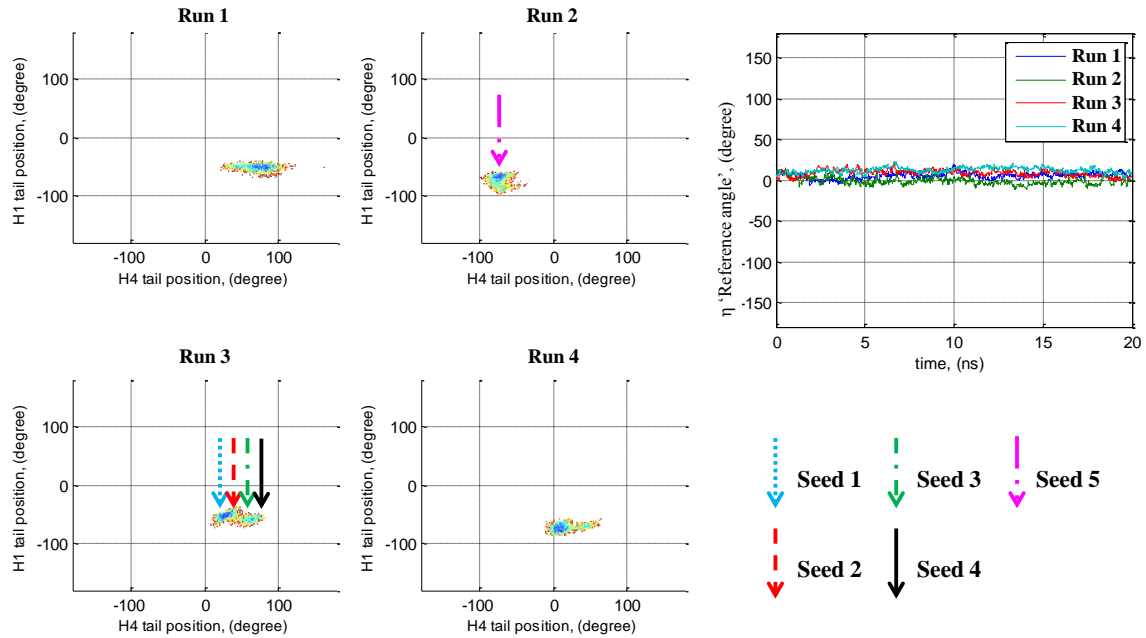


**Figure 3-8: Position of H1/H4 tail with respect to each other. This figure shows the different behavior of the H1/H4 tail. The reference angle  $\eta$  is reasonably stable and taken to be a fixed reference. In Run 2, H1/H4 tail is separated while in other simulation they are cross each other. Seeds 1, 2, 3 and 4 were obtained from Run3 while Seed 5 was selected from Run2. (Table 3-1, EQ.WT.P1P2).**

### 3.1.1.3.3 Initial Structures Used for Axial Load Simulations

Figure 3-9 shows a parallel view (parallel to the H1 axis) of the seeds that were selected from the augmented FAT/paxillin simulated under equilibrium. These seeds are the initial structures used in the axial loaded simulation.

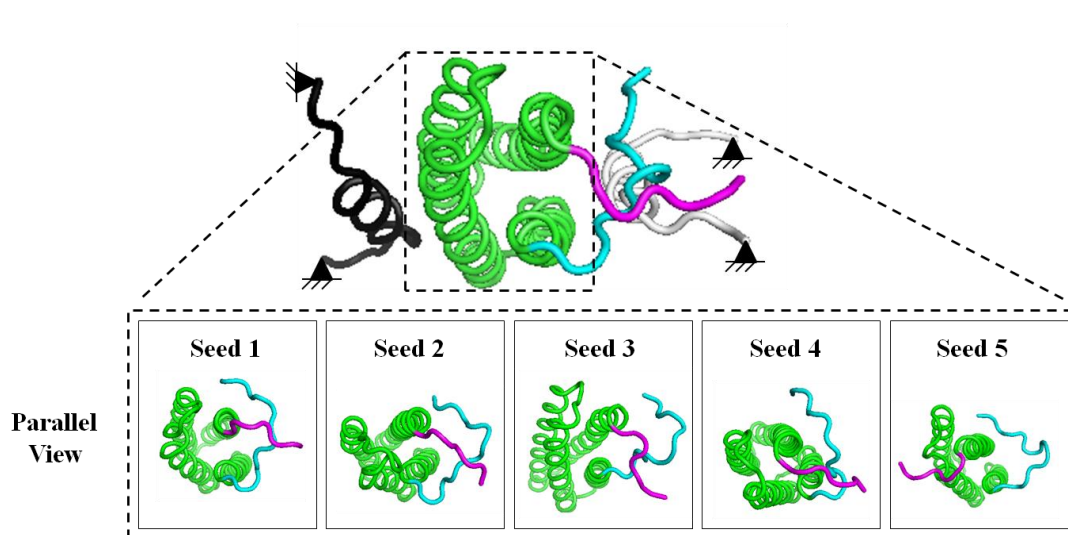


**Figure 3-9:** Five selected seeds for the axial load simulations (Table 3-1, AX.WT.P1P2). A view from H1's N-terminal in a direction normally parallel to the axis of H1 taken from two different simulation runs (Seed 5 from Run 2, Seeds 1-4 from Run 3) of the equilibrium simulations of augmented FAT/paxillin complex (Table 3-1, EQ.WT.P1P2).

### 3.1.1.4 Selected Seeds for Perpendicular Load Simulation

#### 3.1.1.4.1 H1/H4 Tail Interactions

As in Figure 3-10, H1/H4 tail electrostatic interactions persisted throughout the majority of the equilibrium simulation (EQ.WT.P1). In three of the four simulations (Run 1, 2 and 4) the tails interacted for approximately 95% of the total time, while in Run 2 the tails interacted little, if at all. In addition to the interaction metric, the relative position of the H1/H4 tail is a useful metric in identifying the possible initial structures (or seeds) to be used for mechanically loaded simulations.

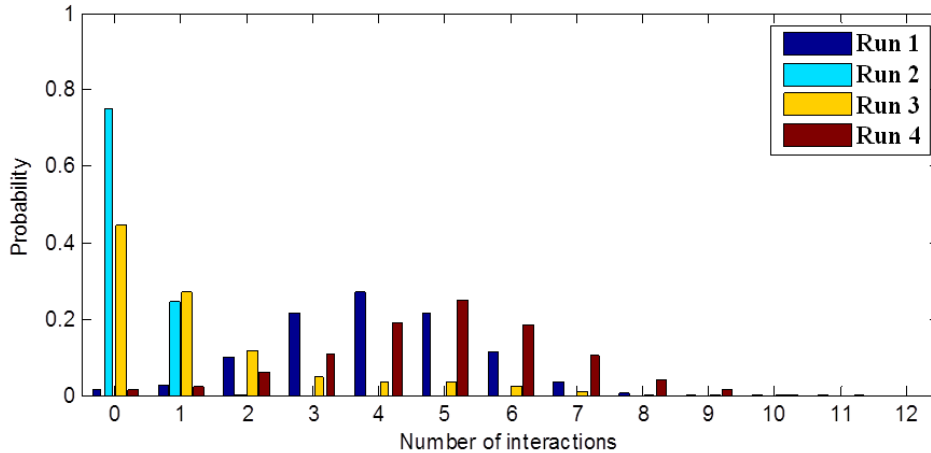


**Figure 3-10: H1/H4 tail electrostatic interactions over time.** This figure illustrates the diverse behavior of the H1/H4 tail. In Run 2 and Run 3, H1/H4 tail have fewer interactions while in all the other runs they show a high probability for H1/H4 tail to interact. Seeds “initial conditions” were selected to elucidate this wide range of behavior. Each bar represents a total time 20 ns. (Table 3-1, EQ.WT.P1)

#### 3.1.1.4.2 H1/H4 Tail Position

At the absence of P2 to interact with FAT’s HP2 (Case +-), Figure 3-11 shows H1/H4 reference angle,  $\eta$  fluctuates  $\pm 5^\circ$  while staying nominally around  $\sim 20^\circ$ . The overall range of the rotation of H1/H4 tail is approximately  $100^\circ$ , so comparing this value with  $\eta$  suggests that the reference used was acceptable. The H1 tail position is more stable than the H4 tail position. Run 2 shows that H4 did not cross H1. Moreover, as seen in Figure 3-10, they do not interact most the time. That said, in three of the four runs the H1/H4 tail show a high proclivity to cross each other.

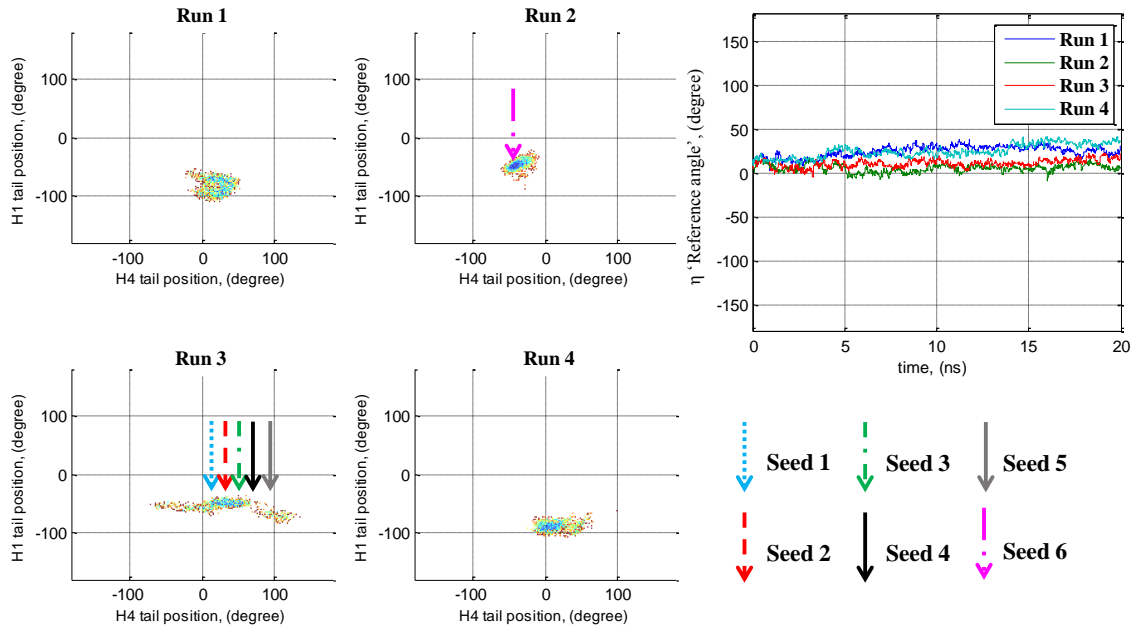


**Figure 3-11: Position of H1/H4 tail with respect to each other. This figure shows the different behavior of the H1/H4 tail. The reference angle  $\eta$  is reasonably stable and taken to be a fixed reference. In Run 2, H1/H4 tail is separated while in other simulation they are cross each other. Seeds 1, 2, 3, 4 and 5 were obtained from Run3 while Seed 6 was selected from Run2. (Table 3-1, EQ.WT.P1).**

### 3.1.1.4.3 Initial Structures Used for Perpendicular Load Simulations

Figure 3-12 illustrates the seeds that were selected from augmented FAT/paxillin under equilibrium in the absence of P2 only for the initial structures used in the perpendicular load simulations.

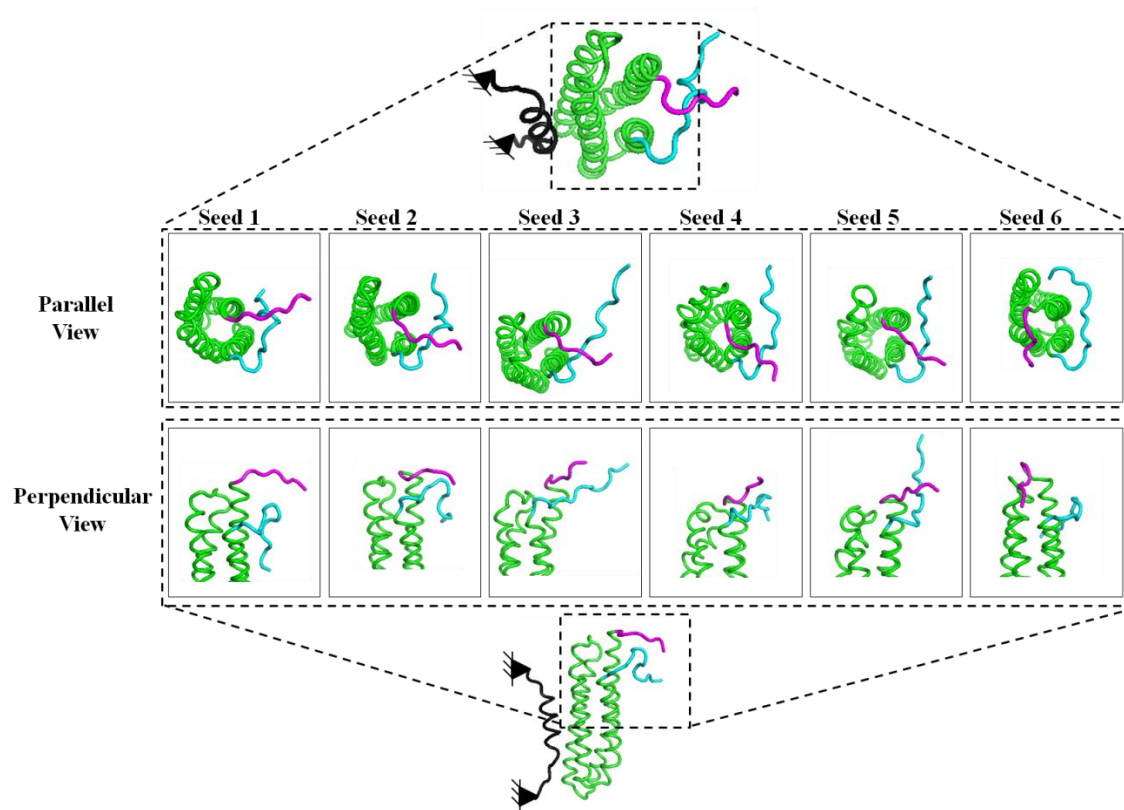


**Figure 3-12: Six selected seeds for the perpendicular load simulations (Table 3-1, PR.WT.P1). Views from H1's N-terminal in a direction normally parallel and perpendicular to the axis of H1 taken from two different simulation runs (Seed 6 from Run 2, Seeds 1-5 from Run 3) of the equilibrium simulations of augmented FAT/paxillin complex (Table 3-1, EQ.WT.P1).**



## 3.2 Simulations

A GROMOS53a6 force field was used to run the Molecular Dynamics simulations performed. A time step of 2fs [29] and periodic boundary conditions were implemented for through all phases of the MD simulations. A parallel-processing version of the LINCS constraint on fast-bond dynamics was used [30]. All the simulations were run on Ranger machine at Texas Advanced Computing Center (TACC, [www.tacc.utexas.edu](http://www.tacc.utexas.edu)).

Different cases of either FAT/paxillin or augmented FAT/paxillin complexes were used in different type of simulations (equilibrium and mechanically loaded simulations). Different cases are defined based on the presence/absence P1 and P2. Each case name is given by [Case +/- +/-]. The first and the second ‘+/-’ indicate the presence/absence of P1 and P2, respectively. For instance, Case + - is interpreted as P1 is present and P2 is absent (Figure 3-13).

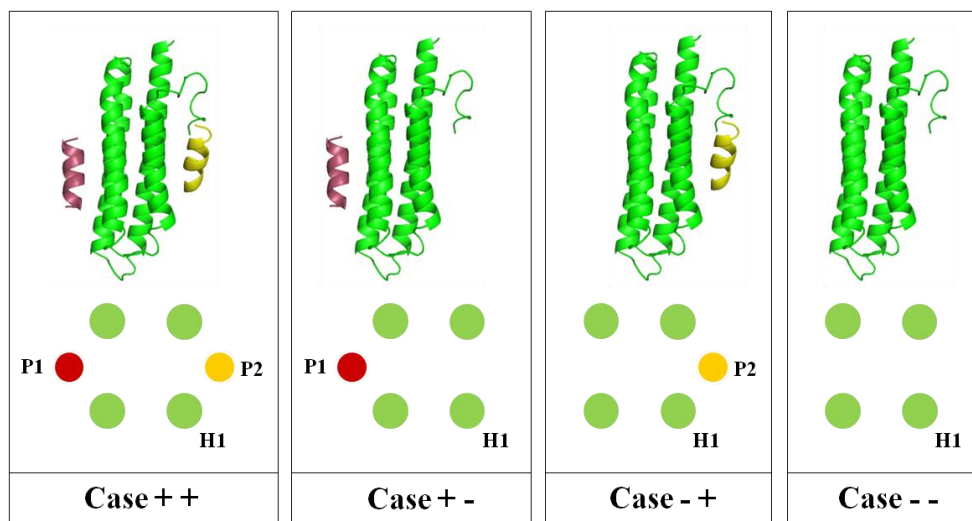


**Figure 3-13: Four types of FAT/paxillin without H4 tail used in the equilibrium simulations. The symbol “+” means that the LD motif is present, and “-” means that LD motif is absent from the FAT/paxillin complex. The first + or - indicates the presence or the absence of P1, while the second indicates the presence or the absence of P2.**

### 3.2.1 PRE-EQUILIBRATION

The FAT/paxillin structures were placed in a box of solvent, explicit water (SPC, Figure 3-14). A minimum distance of 1.2 nm in all directions was used for the equilibrium simulation cases, while a minimum distance of 2 nm was used for the loaded simulations. In order to neutralize the system's total charge, Na<sup>+</sup> and Cl<sup>-</sup> atoms replaced the solvent atoms (water) at a 0.1 M concentration.

### 3.2.2 ENERGY MINIMIZATION AND EQUILIBRATION

Following the energy minimization, each structure was heated to 310°K in three temperature steps (100°K, 200°K, 310°K) with 20 ps spent at each step. The 310°K structure was then pressurized to 1 atm within a total time of 750 ps using a Berendsen thermostat [31], a NoseHoover thermostat with a relaxation constant of 0.1 ps [32, 33] to preserve the 310°K temperature, and a Parrinello-Rahman barostat with a coupling constant of 1 ps [34]. A 1.4 nm cutoff was set for the Coulomb and van der Waals radii. Beyond the cutoff range, the electrostatic interactions were handled using PME electrostatics. By this time, each respective structure had been equilibrated and ready for use in the MD simulations for the equilibrium cases or the CFMD simulations for the loaded cases.

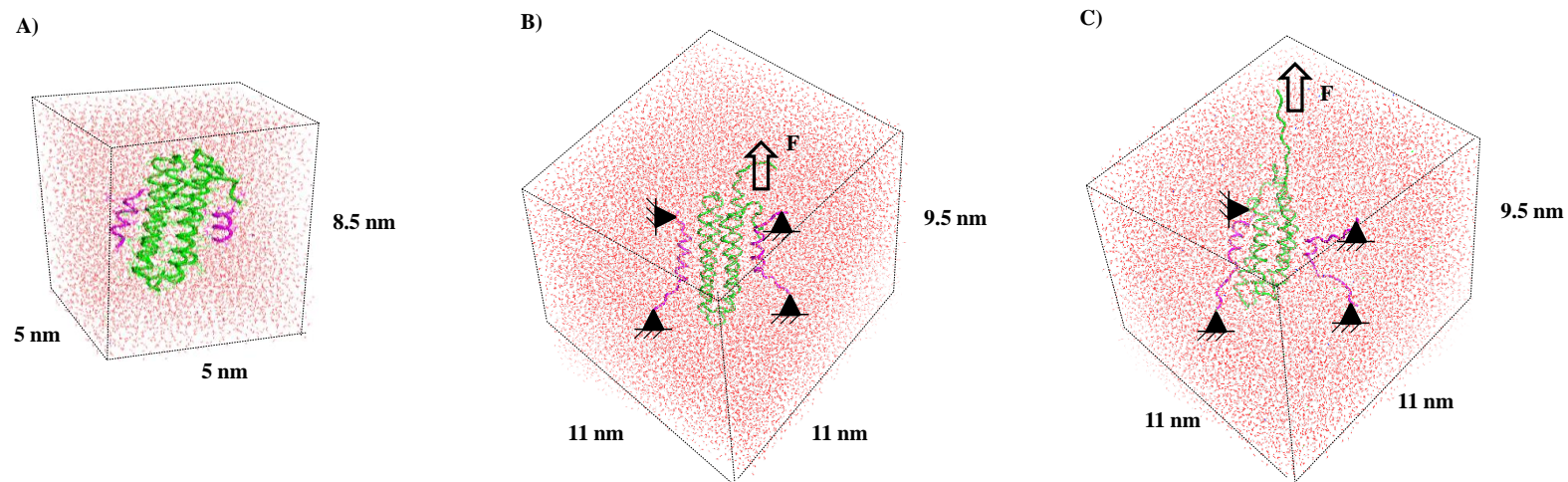


**Figure 3-14: MD and CFMD simulation boxes. A) FAT/paxillin complex (1520 protein atoms) in a 5x5x8.5nm rectangular box filled with of explicit water (33,126 SPC water molecules) and 50 counter-ions (25 Na<sup>+</sup> and 22 CL<sup>-</sup>) used for equilibrium simulations (Table 3-1, EQ.WOT.P1P2). B) Augmented FAT/paxillin complex (1821 protein atoms) in a 9.5x11x11nm rectangular box filled with of explicit water (97,719 SPC water molecules) and 125 counter-ions (65 Na<sup>+</sup> and 60 CL<sup>-</sup>) used for axial load simulations (Table 3-1, AX.WT.P1P2), shown at t = 0 ns. C) Augmented FAT/paxillin complex at the end of simulation (t = 20 ns)**

### 3.2.3 EQUILIBRIUM SIMULATIONS

Two different structures were used in the equilibrium simulations: FAT/paxillin complex without H4 tail and P1/P2 unconstrained (Figure 3-1) and augmented FAT/paxillin complex with H4 tail and P1/P2 constrained (Figure 3-4). FAT/paxillin complex without H4 tail and P1/P2 unconstrained was used to study the propensity, if any, for H1 to leave the bundle and/or adopt a  $\beta$ -strand conformation (Table 3-1, EQ.WOT.P1P2, EQ.WOT.P1, EQ.WOT.P2, EQ.WOT. $\emptyset$ ). The four cases are different in terms of the absence and the presence of LD motifs. The augmented FAT/paxillin complex with H4 tail and P1/P2 constrained was used to study the nature of the reported H1/H4 tail interactions and to identify the mechanically loaded simulations..

#### 3.2.3.1 FAT/Paxillin Complex without H4 Tail and P1/P2 Unconstrained

MD simulations were run for four different cases (Figure 3-13) in the presence/absence of P1 and P2. Each of the four cases was run through its own independent energy minimization and equilibration process. Each case had four runs (repeats), each run lasting 20 ns and starting with different initial conditions (Table 3-1). The relative effects of P1 and P2 on H1 behavior are examined.

#### 3.2.3.2 FAT/Paxillin Complex with H4 Tail and P1/P2 Constrained

MD simulations were run for two different cases (Figure 3-4.C) in presence and absence of P2. Each was run through its own independent energy minimization and equilibration process. Each case had four run (repeats), each lasting 20 ns and starting with different initial conditions (Table 3-1, EQ.WT.P1P2, EQ.WT.P1).

### **3.2.3.3 H1 Isolation**

In order to examine what, if anything, keeps H1 folded, MD simulation of H1 (K923-K941) in isolation was run (Table 3-1, EQ.H1). Hydrogen bonds and the hydrophobicity of the bundle influence the conformational structure of H1. A comparison of H1 behavior as it is in isolation and its behavior as it is within the bundle could illustrate what keeps it folded.

### **3.2.3.4 Paxillin LD Motif Isolation**

Based on their crystal structures, the paxillin LD motifs are presumed to be  $\alpha$ -helices in nature [12]. To examine this assumption, an LD motif (LD4: T264-S275) was isolated and an MD simulation was run for 40 ns to see its preferred conformational structure (Table 3-1, EQ.LD4).

## **3.2.4 MECHANICALLY LOADED SIMULATIONS**

Load is believed to be applied to the FAT domain through H1's N-terminal where it connects to the rest of the FAK. That said, the direction of the applied load is not known. Two orthogonal load directions were considered in the CFMD simulation: parallel to the H1 axis, or axial; and perpendicular to the H1 axis, or perpendicular.

#### 3.2.4.1 Axial Load Simulations

The first load scenario applied to the augmented FAT/paxillin complex was chosen based on the following:

1. The load presumably must be applied to H1 at its N-terminal where it connects the FAT domain to the rest of FAK. The load is distributed on the atoms of the first residue (I909) of the H1 tail. GROMACS's CFMD loading method divides the total load (100 pN) over all atoms of the loaded group (I909) on a mass weighted basis. The force on atom  $i$  is given by  $F_i = \left(\frac{m_i}{M}\right) F_{\text{total}}$ , where  $m_i$  is the mass of the atom and  $M$  is the sum of the masses.
2. It proved too complicated to apply the load in a transverse direction (perpendicular to H1 axis, normal to the plane containing P1/P2 axes), as shown in Figure 3-15. As it had been tried, an induced steric clash between H1 and P2 is caused by pulling the N-terminus of H1 tail in a direction perpendicular to the plane containing the axes of P1 and P2. However, in order to unravel the area flanking Y925, which is the first portion of H1 to which the load is applied, the load had to be applied axially to H1 axis. GROMACS's CFMD loading method maintains the magnitude and direction of the load constant during the entire simulation.

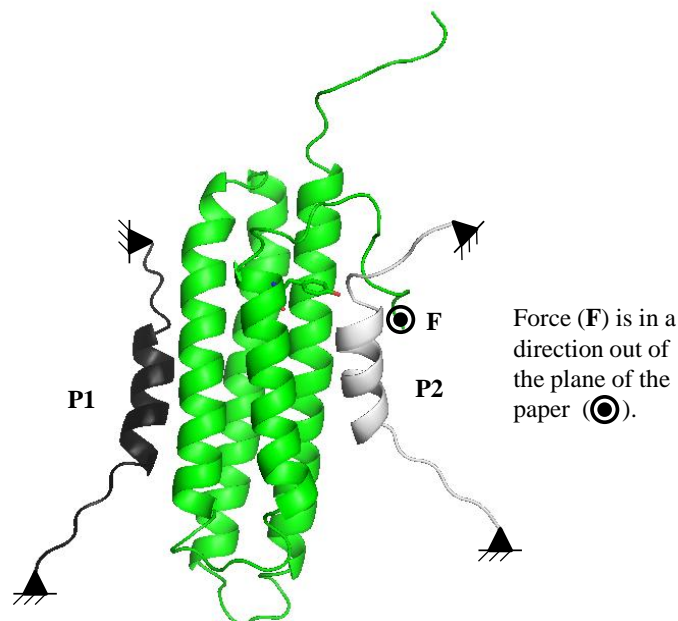


**Figure 3-15: Illustration of the induced steric clash between H1 and P2 caused by pulling the N-terminus of H1 tail in a direction perpendicular to the plane containing the axes of P1 and P2 (in the direction out of the plane of the paper).**

1. If the load is applied to H1's N-terminal, something else has to provide reaction forces. The FAT domain binds to the paxillin through the LD motifs, where they can be considered tethering reactions, so the ends of P1 and P2 had to be constrained. A zero displacement was enforced at the end of the P1 and P2 specifically, at the C $\alpha$  atom of S259 (N-terminus of LD4) and C $\alpha$  atom of M280 (C-terminus of P1). (Figure 3-16.A)

For this load direction, 10 different simulations had different initial structures coming from the MD simulations (Table 3-1, AX.WT.P1P2). The initial structures were selected to be representative of the different equilibrium structure that were observed. The simulations were run using a 100 pN load in a direction parallel to the H1 axis. The reason for such high load was the amount of time a low load simulation may require. So, 100 pN was used to accelerate the process in which H1 comes out of the bundle and/or

adopts  $\beta$ -strand conformation. If this high load achieved the goal in a short time, a simulation would have been performed using a lower load level.

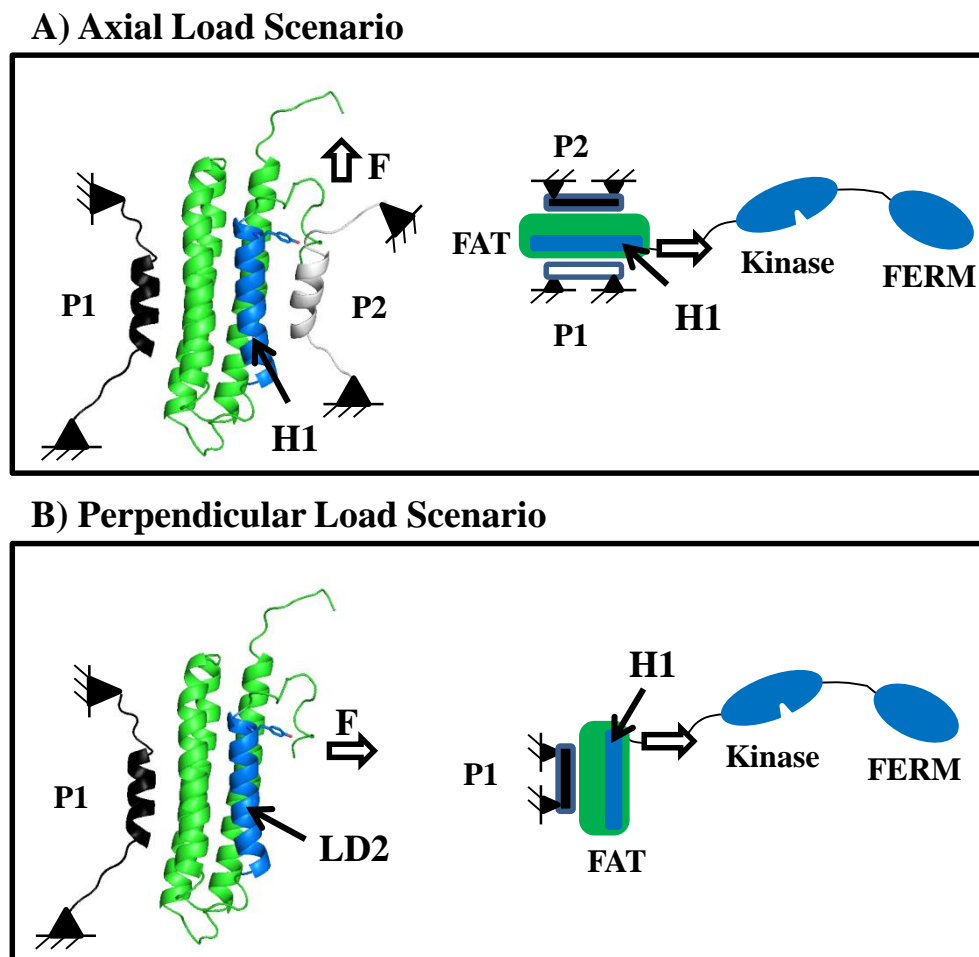


**Figure 3-16: Axial and perpendicular loads applied to the augmented FAT/paxillin complex with H4 tail and P1/P2 constrained. A) In the presence of both LD motifs (P1 and P2), the mechanical load is applied to the N-terminus of H1 tail in a direction parallel to the H1 axis. B) In the absence of P2, the load is applied to the N-terminus of H1 tail in a direction perpendicular to the plane containing the H1 and H4 axes.**

### 3.2.4.2 Perpendicular Load Simulation

Review of the literature suggests that access to Y925 is blocked by extensional loops that come from H1 (i.e., H1 tail) and H4 (i.e., H4 tail) in the presence of P2 (i.e.,



LD2). Others have argued that P2 has to be removed first and the tails pulled away from the Y925 site in order for H1 to come out of the bundle. To examine this, P2 was deleted from the augmented FAT/paxillin complex and the load was applied perpendicular to the FAT domain through the H1 tail, and the ends of the P1 motif were constrained (Figure 3-16). A perpendicular load direction was chosen for this case because, after performing several simulations from various directions, the FAT domain self-oriented following the load direction (Figure 3-17). This suggested that the results were insensitive to the load direction. Six seeds were selected (Figure 3-12), the same as described in the axial load scenario.

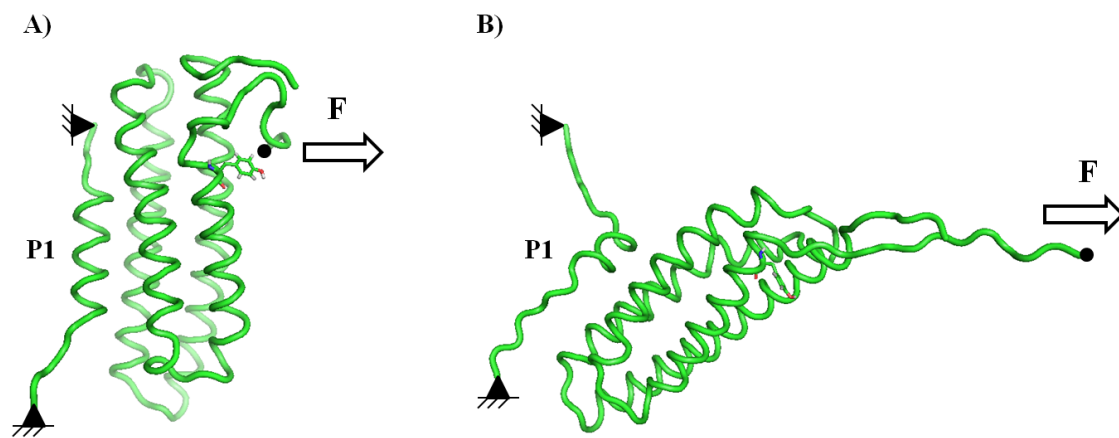


**Figure 3-17: Illustration of how the FAT domain self-orientates to follow the load direction (PR.WT.P1).** A) FAT domain before applying the load to the H1's N-terminus. B) FAT domain after it self-oriented to follow the load direction. It was presumed that all the directions that are perpendicular to the axis of P1 are nearly equivalent.

### 3.2.5 SIMULATION TIMES

Table 3-1 presents an overall description of the structures, cases and simulation time that were used. Symbol representation was used to illustrate the simulation type and initial conditions of the performed simulations.. The name of each simulation case is defined as [Simulation type. H4 tail status. P1 and P2 status]. The equilibrium simulations was labeled as 'EQ' and the mechanical loaded simulations types were denoted according to their loading direction: 'AX' for axial load scenario and 'PR' for perpendicular load scenario. The presence/absence of H4 tail was labeled by 'WOT' (without H4 tail) and 'WT' (with H4 tail). The presence/absence of P1 and P2 denoted by 'P1', when P1 is in presence; 'P2', when P2 is in presence. If both P1 and P2 are absence, it is labeled by Ø. Each structure had many runs (repeats), where each has different initial conditions. Different energy minimization and equilibration process was labeled by 'EE' and different initial velocities were denoted by 'IV'. In the case where different initial structure (Seeds) were used, it is labeled by 'DS'. The duration time of the run was also identified. Each simulation condition and duration was illustrated as: [ Independent initial condition ] x [ Duration time ].

**Table 3-1: Equilibrium and mechanically loaded simulations.**

Simulation type		Structure	Paxillin		Initial conditions x Time [ Independent ] x [ Duration ]	Name
			P1	P2		
Equilibrium (EQ)	w/o H4 tail (WOT)	FAT/paxillin complex (Figure 3-1.C)	+	+	[ 4 (EE) ] x [ 20 ns ]	EQ.WOT.P1P2
			+	-	[ 4 (EE) ] x [ 20 ns ]	EQ.WOT.P1
			-	+	[ 4 (EE) ] x [ 20 ns ]	EQ.WOT.P2
			-	-	[ 4 (EE) ] x [ 20 ns ]	EQ.WOT.Ø
	w/ H4 tail (WT)	Augmented FAT/paxillin complex (Figure 3-4.C)	+	+	[ 2 (EE) x 2 (IV) ] x [ 20 ns ]	EQ.WT.P1P2
			+	-	[ 2 (EE) x 2 (IV) ] x [ 20 ns ]	EQ.WT.P1
	H1 isolated (K923-K941)				[ 1 (EE) ] x [ 20 ns ]	EQ.H1
	LD4 isolated (T264-S275)				[ 1 (EE) ] x [ 40 ns ]	EQ.LD4
	Total time of equilibrium simulations =				540 ns	
Mechanically Loaded	Axial (AX)	Augmented FAT/paxillin complex (Figure 3-4.C)	+	+	[ 5 (DS,EE) x 2 (IV) ] x [ 20 ns ]	AX.WT.P1P2
	Perpendicular (PR)		+	-	[ 5 (DS,EE) x 2 (IV) ] x [ 20 ns ] [ 1 (DS,EE) x 11 (IV) ] x [ 20 ns ]	PR.WT.P1
	Total time of mechanically loaded simulations =				620 ns	
Total =					1160 ns	

Notations:

EE: Different Energy Minimization and Equilibration.

DS: Different Seeds.    +: LD motif is in present.

IV: Different Initial Velocities.

- : LD motif is removed from the structure.

### 3.3 Analysis

The output data was analyzed using different metrics that addressed different aspects of the availability of Y925 as well as the mechanical behavior of FAT under various load conditions.

#### 3.3.1 ENERGY LANDSCAPE ANALYSIS

In cases where one must look at the stability of the structure and its favorable states, energy landscapes plots would be used. Energy landscapes are evaluated using Boltzmann inversion of the probability of variables  $x$  and  $y$  occurring at time  $t$  as follows:

$$E(x, y) = -\ln [P(x, y)]$$

where  $p(x, y)$  is the probability of the variables  $x$  and  $y$  over time.

The blue color (minima) represents a point/region of the highest likelihood. According to this scaling, an point lying in the blue region is about 500 times more likely than an equivalent point lying in the red region (Figure 3-18).

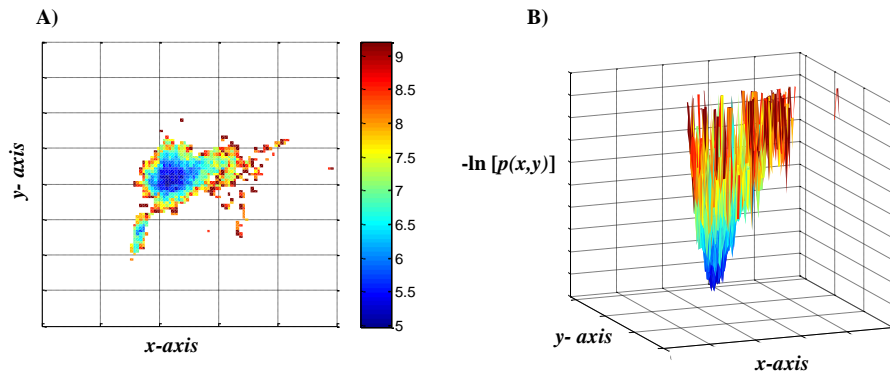


**Figure 3-18: Illustration of energy landscape where the colors represent the depth of the well. A) Top view. B) Third dimension which is the depth of the well.**

### 3.3.2 H1 BEHAVIOR

The main interest is to examine the behavior of H1 in terms of its position and its helical character. Distance metric was chosen to track the position of H1 relative to the bundle. Backbone dihedral angle  $\psi$  is calculated for the first five residues (K923, V924, Y925, E926, and N927) of the N-terminal of H1.

#### 3.3.2.1 H1 Position

To examine the hypothesis that H1 must be out of the bundle in order to allow Y925 phosphorylation, H1's position was evaluated. The position of H1 relative to the bundle is taken to be the distance between H1 and the helices adjacent to it, H2 and H4. To have single plot that is able to indicate the position of the entire H1 (top and bottom portions), the distance between H1 and an virtual helix, which is the equivalent between H2 and H4, was calculated. The energy landscape of top distance  $d_{\text{top}}$  vs. the bottom distance  $d_{\text{bottom}}$  was plotted to determine the most likely position of H1 (Figure 3-19.A).

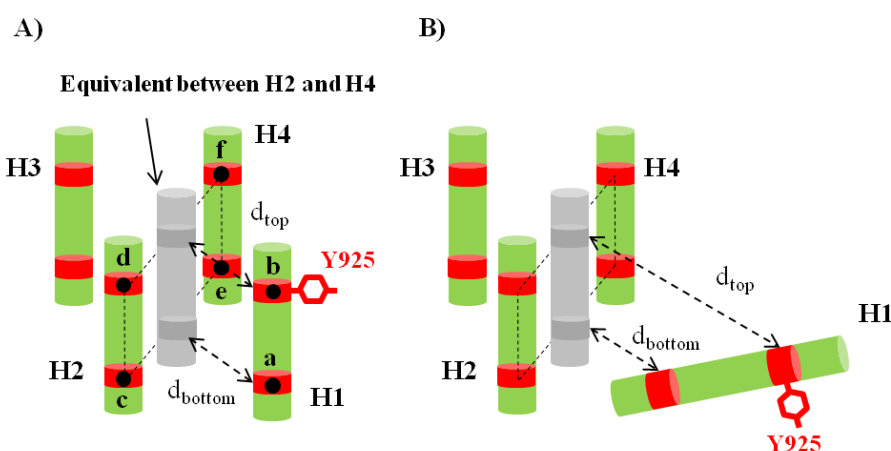


**Figure 3-19: H1 position characterization.** A) Top and bottom distances between H1 and a virtual helix (in gray). The top distance is between the N-terminal of H1 (center of mass of K923-N927) and the average point of the C-terminal of H2 (center of mass of T963-T967) and N-terminal of H4 (center of mass of L1035-D1039). The bottom distance is between the C-terminal of H1 (center of mass of E937-K941) and the average point of the N-terminal of H2 (center of mass of V951-K955)

and C-terminal of H4 (center of mass of T1022-A1026). B) The potential position of H1 if it leaves the bundle.

The top distance and bottom distance, which were used in the analysis, are calculated as follows:

$$d_{top} = \sqrt{\left[b_x - \frac{d_x+f_x}{2}\right]^2 + \left[b_y - \frac{d_y+f_y}{2}\right]^2 + \left[b_z - \frac{d_z+f_z}{2}\right]^2}$$

$$d_{bottom} = \sqrt{\left[a_x - \frac{c_x+e_x}{2}\right]^2 + \left[a_y - \frac{c_y+e_y}{2}\right]^2 + \left[a_z - \frac{c_z+e_z}{2}\right]^2}$$

Where points ‘a and b’ are the centers of mass of two complete turns at the C- and N-terminals of H1 respectively (a: E937-K941, b: K923-N927). Points ‘c and d’ are the centers of mass of complete turns at the N- and C-terminals of H2 respectively (c: V951-K955, d: T963-T967). Points ‘e and f’ are the centers of mass of complete turns at the N- and C-terminals of H4 respectively (e: T1022-A1026, f: L1035-D1039) (Figure 3-19). Since the C-terminal of H1 connects with H2 and the N-terminal of H1 is pulled out, one expects it to be more likely that the top distance of H1 will increase as H1 opens out (Figure 3-19.B).

### 3.3.2.2 H1 Unfolding

According to the known Ramachandran ( $\phi, \psi$ ) plot, for H1 to adopt  $\beta$ -strand conformation, its backbone dihedral angle has to be  $\sim 170^\circ$ . For more detailed to understand the unfolding propagation, if any, the instantaneous status of hydrogen donor-acceptor pairs metric is examined.

#### 3.3.2.2.1 Backbone Dihedral Angle $\psi$

A current hypothesis suggests that the region flanking Y925, “N-terminal of H1,” has to adopt  $\beta$ -strand conformation [5]. This can be tested using the backbone dihedral  $\psi$  ( $N_i-C\alpha_i-C_i-N_i$ ) which demonstrates the conformation of the backbone main chain. For an

$\alpha$ -helix,  $\psi \approx -50^\circ$ , while for a  $\beta$ -strand:  $\psi \approx 170^\circ$  (Figure 3-20). Using for points  $(N_i, C\alpha_i, C_i, N_{i+1})$ ,  $\psi$  that were evaluated in the analysis is calculated as follow:

$$\psi = \text{atan2}(|\mathbf{b}_2| \mathbf{b}_1 \cdot [\mathbf{b}_2 \times \mathbf{b}_3], [\mathbf{b}_1 \times \mathbf{b}_2] \cdot [\mathbf{b}_2 \times \mathbf{b}_3])$$

where  $\mathbf{b}_1$ ,  $\mathbf{b}_2$ , and  $\mathbf{b}_3$  are vectors defined as:  $\mathbf{b}_1 = \overline{C\alpha_i - N_i}$ ,  $\mathbf{b}_2 = \overline{C_i - C\alpha_i}$ , and  $\mathbf{b}_3 = \overline{N_{i+1} - C_i}$ .

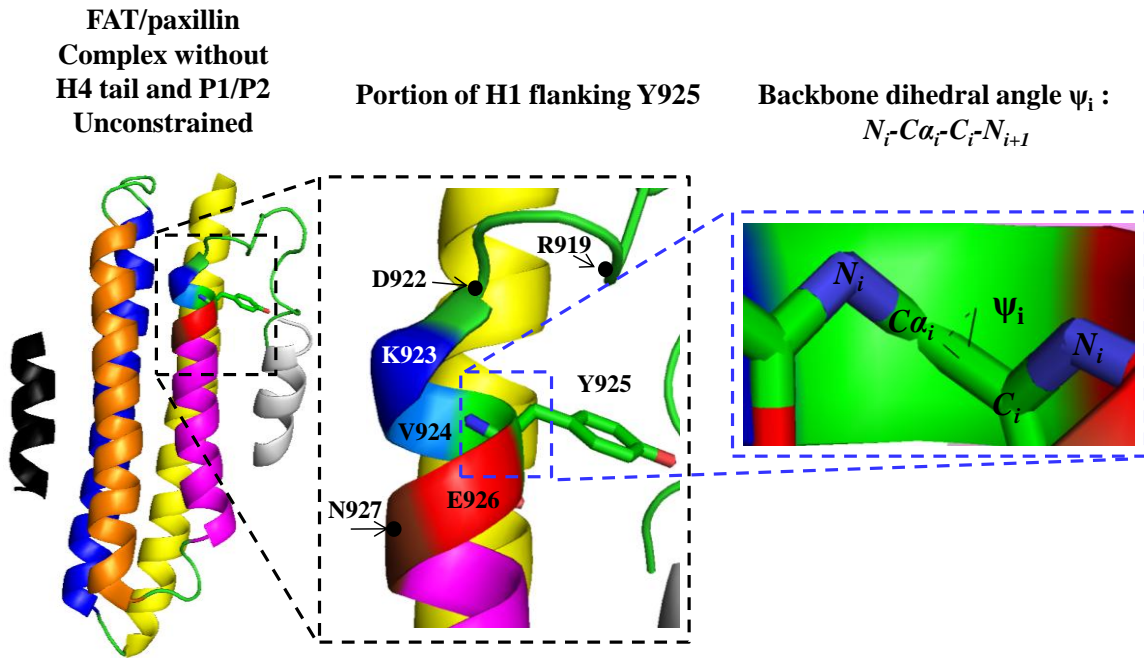
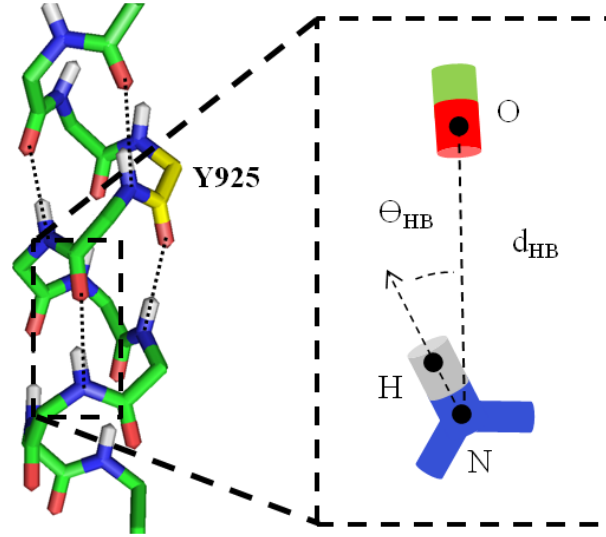


Figure 3-20: Residues neighboring the Y925 residue. An expanded view of the region flanking Y925 at the N-terminal of H1. The backbone dihedral angle  $\psi_i$  ( $N_i - C\alpha_i - C_i - N_{i+1}$ ) that describes H1 secondary structural conformation. For an  $\alpha$ -helix,  $\psi \approx -50^\circ$  and for a  $\beta$ -strand,  $\psi \approx 170^\circ$ .

### 3.3.2.2.2 Hydrogen Bonds via Donor-Acceptor Pairs

Details regarding unfolding are revealed via the states of the hydrogen donor-acceptor pairs (Figure 3-21). To maintain the helical character in a secondary structure level of the protein, hydrogen bonds are formed between a backbone oxygen from one residue and an amine hydrogen from another residue. To form a hydrogen bond, two

conditions need to be satisfied: i) The distance between the oxygen (acceptor) and nitrogen (donor) ‘ $d_{HB}$ ’ must be less than 0.35 nm and the angle ‘ $\Theta_{HB}$ ’ must be less than  $30^\circ$ .



**Figure 3-21: Illustration of a hydrogen donor-acceptor pair formed as O-N-H (donor N+, acceptor O-). A hydrogen bond was assured to be formed if the distance between O and N ( $d_{HB}$ ) was to be less than 0.35 nm and the angle  $\Theta_{HB}$  formed by O-N-H was less than  $30^\circ$ .**

The hydrogen donor-acceptor pair was calculated as follows:

$$\vec{d}_{HB} = [O_x - N_x]\mathbf{i} + [O_y - N_y]\mathbf{j} + [O_z - N_z]\mathbf{k}$$

$$\vec{HN} = [H_x - N_x]\mathbf{i} + [H_y - N_y]\mathbf{j} + [H_z - N_z]\mathbf{k}$$

where  $O$ ,  $N$ , and  $H$  are the centers of mass of the atoms forming the hydrogen bonds: oxygen, nitrogen, and hydrogen, respectively, and  $\mathbf{i}$ ,  $\mathbf{j}$ , and  $\mathbf{k}$  are the unit vectors.

The hydrogen bond distance ‘ $d_{HB}$ ’ is:

$$d_{HB} = |\vec{d}_{HB}|$$

The hydrogen bond angle ‘ $\Theta_{HB}$ ’ is:

$$\theta_{HB} = \text{ACOS} \left[ \frac{\vec{d}_{HB} \cdot \vec{HN}}{|\vec{d}_{HB}| \cdot |\vec{HN}|} \right]$$



Hydrogen acceptor-donor pair analysis provides information about the type of helix:  $3_{10}$ -helix, 'i:i+3';  $\alpha$ -helix, 'i:i+4';  $\pi$ -helix, 'i:i+5' where 'i' represents the residue number (Figure 3-22).

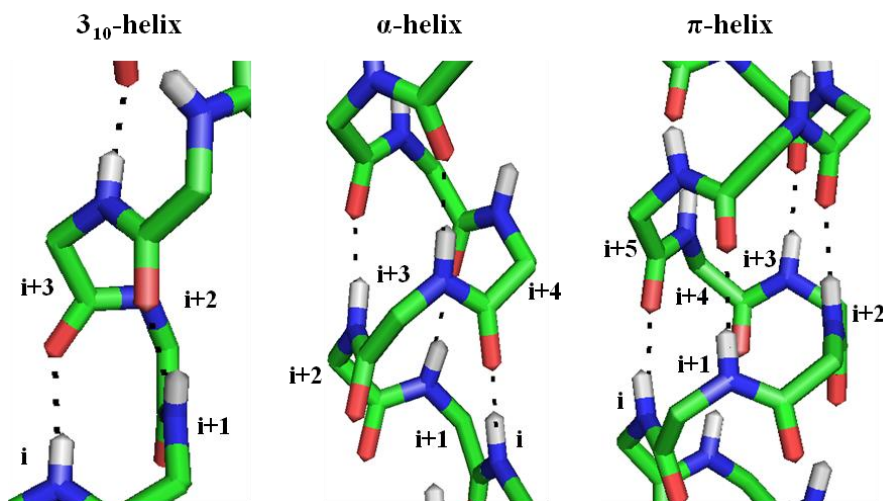
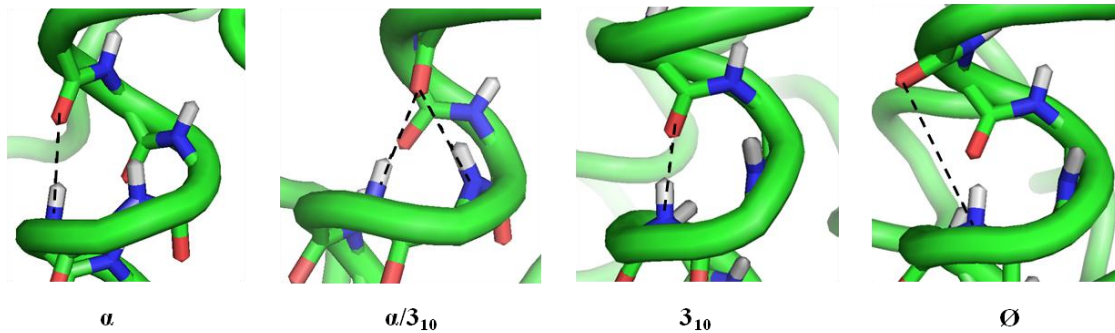


Figure 3-22:  $3_{10}$ ,  $\alpha$  and  $\pi$  helices formed by various hydrogen donor-acceptor pairs starting with residue i.

During all MD and CFMD simulations, only four types of hydrogen donor-acceptor pair appeared. Primarily, the helix formed a hydrogen bond between i:i+4 residues, which is called an  $\alpha$  helix-type bond. There is a very low propensity to form the  $3_{10}$  hydrogen bond between i:i+3 residues. In yet another type of hydrogen bond, a combination of  $\alpha$  and  $3_{10}$ , the residue "i" forms a double hydrogen bond,  $\alpha/3_{10}$ , between residues i:i+3/i+4. In addition to these types, no or a broken hydrogen bond that occurs sometimes was labeled "Ø." Figure 3-23 illustrates the types of hydrogen donor-acceptor pairs observed during the simulations.



**Figure 3-23: Illustration of the three types of hydrogen donor-acceptor pairs ( $\alpha$ ,  $\alpha/3_{10}$  and  $3_{10}$ ) that formed during the simulations, as well as the no hydrogen bond case, denoted by the symbol “ $\emptyset$ .”**

### 3.3.3 SALT BRIDGES BETWEEN H1 TAIL AND H4

Based on the published crystal structures, the two important salt bridges between H1 and H4 were observed. Salt bridge 1 (SB1) is formed by the interactions between the side chains of R919-D1039 while Salt bridge 2 (SB2) is formed by the interactions between the side chains of D922-R1042 [5]. The distance between the centers of mass of the terminal, side-chain carbon atoms, CZ and CG, from arginine (R) and aspartic acid (D), respectively, was evaluated (Figure 2-4) as follows:

$$SB_i = \sqrt{[CZ_x - CG_x]^2 + [CZ_y - CG_y]^2 + [CZ_z - CG_z]^2}$$

where  $i=1,2$  represents the first or the second salt bridge.

### 3.3.4 H1/H4 TAIL INTERACTION

Based on primarily simulation, it appeared that the H1/H4 tail may share the applied load resulting H1 holding to the bundle as well as slowing down any unfolding events. As a result, all possible interactions that can be formed between H1/H4 tail have been surveyed as discussed previously. Examining the correlations between forming such an electrostatic interaction and the unfolding events gives better idea about the influence,

if any, of H1/H4 tail interactions on H1 behavior. The electrostatic interaction distance ( $d_{EI}$ ) between any opposite charged atoms was calculated as follows:

$$d_{EI} = \sqrt{[(-ve)_x - (+ve)_x]^2 + [(-ve)_y - (+ve)_y]^2 + [(-ve)_z - (+ve)_z]^2}$$

where ‘-ve’ represents the negative charge atom and ‘+ve’ represents the positive charge atom. The negative charges atoms are either the backbone oxygen atoms or the terminal side-chain oxygen atoms. The same for the positive charged atoms, they are either backbone nitrogen atoms or terminal side-chain nitrogen atoms.

### 3.3.5 FINAL STATE OF FAT’S STRUCTURE UNDER APPLIED LOAD

For different CFMD simulations, FAT domain undergoes different structural states. Table 3-2 and Figure 3-24 illustrate a classification of different final states of the FAT structure. The classification is based on H1 position, H1unfolding H1/H4 tail interaction, and the area between the H2-H3 helices. Symbol representation was used to describe these final states. For H1 position, H1 is either in or out of the bundle labeled by ‘In and Out’ respectively. For H1 Unfolding, there is a degree of unfolding of the first five residues (K923, V924, Y925, E926, and N927), ‘H’ means they are folded in a helical form and ‘SUF’ illustrates the unfolding of the first two residues (K923, V924) while ‘UF’ means that all the five residues unfolded. For H1/H4 tail interactions, when the C-terminal of H4 tail forms a  $\beta$ -sheet with N-terminal of H1 tail via hydrogen bonds, it is labeled by ‘ $\beta$ , EX’ where the label ‘ $\beta$ , NEX’ means that the  $\beta$ -sheet is formed between the C-terminal of H4 tail and mid section of H1 tail. In the case where the C-terminal of H4 tail entangled with the C-terminal of H1 tail, it is denoted by ‘ $\tau$ ’. If H1/H4 are separate, it is labeled by ‘S’. In addition, it was observed that the C-terminal of H2

and the N-terminal of H3 was sometime unfolded, which is denoted by ‘U23’, but if they are folded it is denoted by ‘F23’.

**Table 3-2: Classification of different FAT structures in the final states that were observed during the simulations. Each symbol describes a different structure a portion of the FAT domain would adopt. Those states are illustrated in Figure 3-24 .**

Classification	Symbol	Qualitative Description
H1 Position	In	H1 stays in the bundle.
	Out	H1 is out of the bundle.
H1 Unfolding	H	H1 is in a helical form.
	SUF	The first two residues of N-terminal of H1 (K923 and V924) start to unfold.
	UF	The region flanks Y925 is unfolded (K923, V924, Y925, E926, and N927)
H1/H4 Tail Interactions	$\beta$ , EX	H1/H4 tail form $\beta$ -sheet via hydrogen bonds. The C-terminal of H4 tail interacts with N-terminal of H1 tail.
	$\beta$ , NEX	H1/H4 tail form $\beta$ -sheet via hydrogen bonds. The C-terminal of H4 tail interacts with mid section of H1 tail.
	$\tau$	H1/H4 tail have interactions where the C-terminal of H4 tail interacts with the C-terminal of the H1 tail (i.e., near the N-terminal of H1 helix).
	S	H1/H4 tail do not have interactions (i.e., they are separate).
H2-H3 Structure	U23	The C-terminal of H2 and the N-terminal of H3 are unfolded.
	F23	The C-terminal of H2 and the N-terminal of H3 are folded.

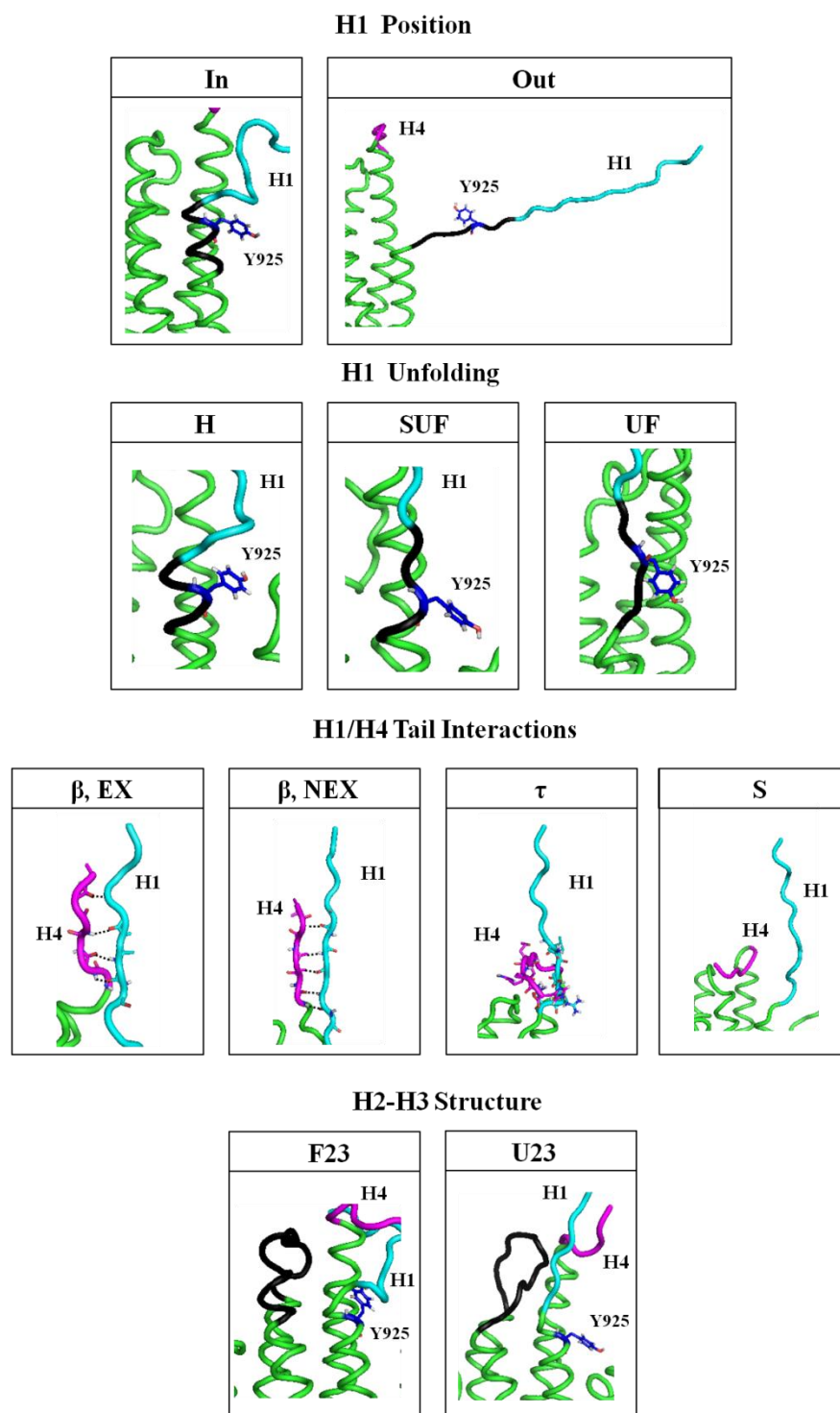


**Figure 3-24: Illustrations of different parts of the FAT domain in different final states. Those notations that are described in Table 3-2 used for classification of the final states that FAT domain.**

In the next chapter, the results of the metrics chosen are presented and discussed statistically. In addition, the biological implications behind those statistics will be discussed.

## **Chapter 4. Results**

The primary goal is to determine the conditions required for the FAT domain (specifically; its H1 helix) to undergo the hypothesized structural changes, in which H1 comes out of the bundle and/or adopts  $\beta$ -strand conformation. These conformational changes presumably allow Y925 to be phosphorylated. In addition, it is important to examine the influence of the paxillin LD motifs, which bind to FAT, on the behavior of the H1. Under equilibrium and mechanical load, four metrics were evaluated for examining H1 behavior:

1. H1 position
2. H1 unfolding
3. H1/H4 salt bridges
4. H1/H4 tail interactions.

### **4.1 Equilibrium Results**

#### **4.1.1 FAT/PAXILLIN COMPLEX WITHOUT H4 TAIL AND P1/P2 UNCONSTRAINED**

Under equilibrium, the FAT/paxillin complex had been investigated in which the presence or absence of P1 and P2 was varied. (Figure 3-4 and Table 3-1, EQ.WOT.P1P2, EQ.WOT.P1, EQ.WOT.P2, and EQ.WOT. $\emptyset$ ).

#### **4.1.1.1 H1 Position**

Under equilibrium conditions, the position of H1 does not vary significantly. As seen in Figure 4-1, the blue colored regions (minima) of the H1 position have small distribution. The relative position of H1 to the bundle is very stable, which means H1 does not appear to have a propensity to leave the bundle for any case that was simulated.

Based on the literature, electrostatic and hydrophobic interactions between H1 (residues 917-922) and H4 present an energy barrier keeping H1 attached to the bundle. This observation and H1 position results are consistent. However, in order for Y925 to engage the phosphorylation, H1 has to leave the bundle. Therefore, under only thermal fluctuation, it does not seem that H1 has the capacity to leave the bundle. Furthermore, even in the absence of both P1 and P2 (Case - -), the relative position of H1 to the bundle is stable, which means H1 is strongly attached to the bundle regardless of the presence or absence of the paxillin LD motifs. It appears that P1/P2 do not have a significant influence on the stability of H1.



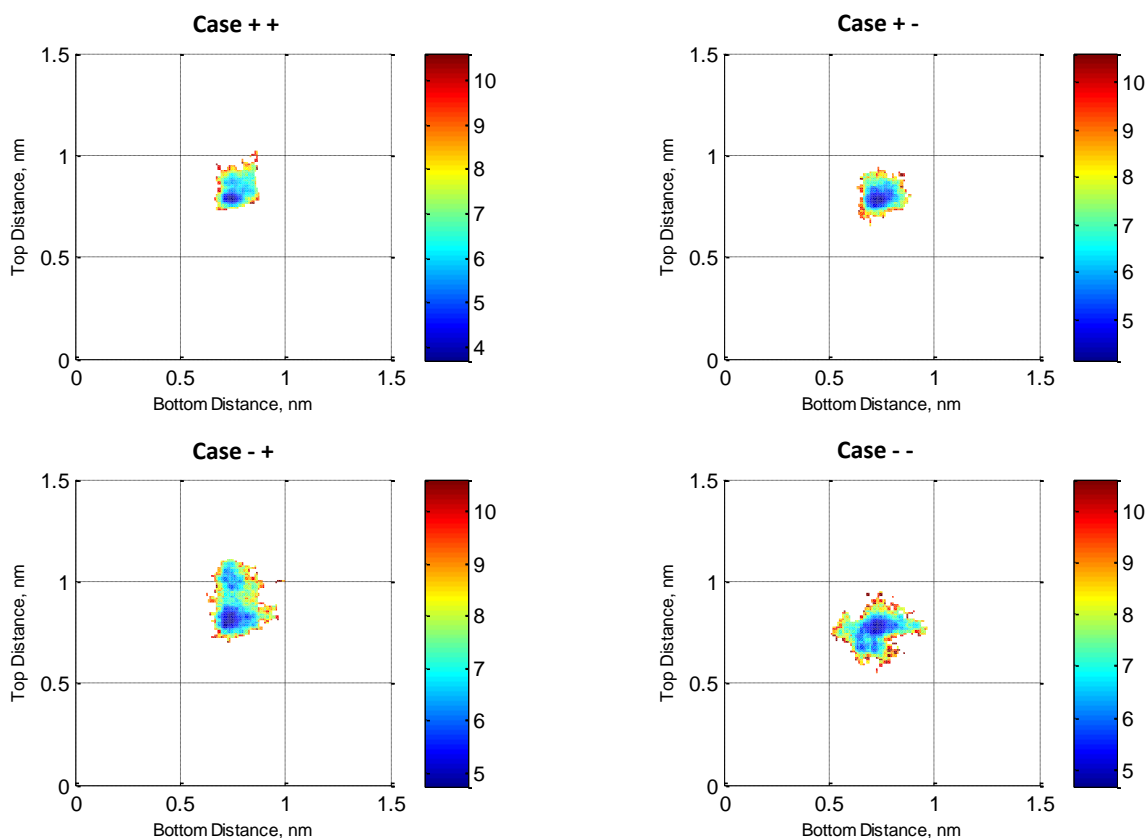


**Figure 4-1: Energy landscape of H1 position represented by  $d_{top}$  and  $d_{bottom}$  in the presence and/or the absence of P1 and P2. H1 position has a small distribution (minima) which means H1 does not appear to have the propensity to leave the bundle under only thermal fluctuation. Each plot represents a cumulative time of 80 ns of simulation time. (Table 3-1, EQ.WOT.P1P2, EQ.WOT. P1, EQ.WOT.P2, and EQ.WOT.Ø).**

The Case -+ (P1 is absent), is slightly different than other cases. In all four runs, the H1 position is very similar to those in the other cases seen in Figure 4-1 except the fourth run, which has two local minimis (two states, Figure 4-2). However, the top distance of H1 increased by 0.2 nm and stayed stable, which is an indication of the stability of the relative position of H1 with respect to the bundle.

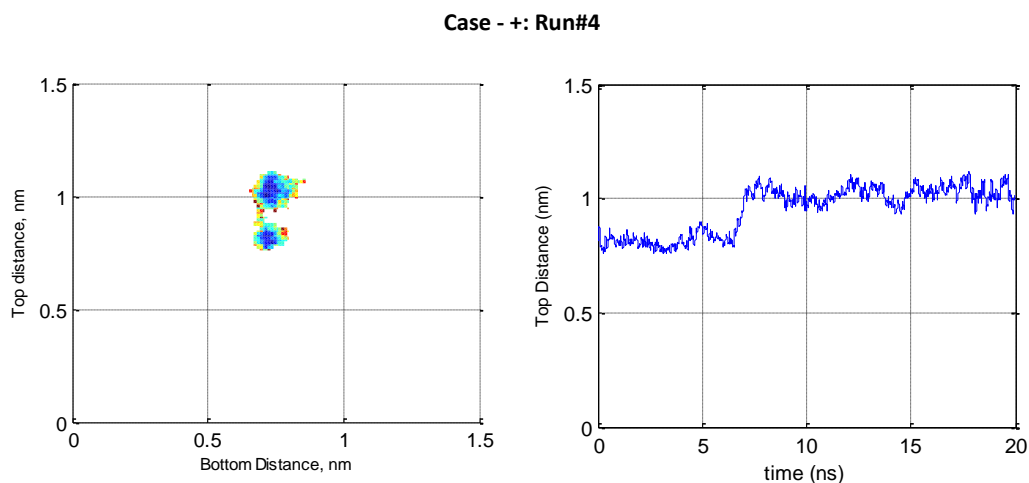


**Figure 4-2: Energy landscape of H1 position represented by  $d_{top}$  and  $d_{bottom}$  in the absence of P1.  $d_{top}$  versus time illustrates the presence of the two local minima (blue spots) on the energy landscape plot for Run#4.  $d_{top}$  does not fluctuate between two states, which demonstrates the stability of H1 position relative to the bundle. (Table 3-1, EQ.WOT.P2).**

#### 4.1.1.2 H1 Unfolding

To examine the unfolding of H1, if any, two important metrics were evaluated: backbone dihedral angle  $\psi$  and hydrogen donor-accepter pairs (illustrated previously in § 3.3.2.2 analysis).

##### 4.1.1.2.1 Backbone Dihedral Angle $\psi$

As in Figure 4-3, except residue K923, the  $\psi$  angles of the other top four residues of the N-terminal of H1 (V924, Y925, E926, and N927) have a small distribution (the mean value is  $\sim -50^\circ$  degree). This means they are folded in a helical form for any case simulated. However, the first residue at the N-terminus of H1 (K923) is expected to have high flexibility, since it connects with H1 tail (i.e., H1 tail is free to move). That said, the flexibility of K923 does not affect the stability of the other residues flanking Y925.

For Y925 to engage the phosphorylation, the region flanking Y925 has to adopt  $\beta$ -strand conformation as it was discussed in §2.5 Literature Review. Under only thermal fluctuation, the  $\psi$  metric suggests that residues flanking Y925 do not appear to have propensity to adopt  $\beta$ -strand conformation. In addition, even in the absence of both P1 and P2 (Case - -), H1 has the ability to stay folded in a helical form. This suggests that maintaining the helical form of H1 is nearly independent of the FAT association with paxillin.

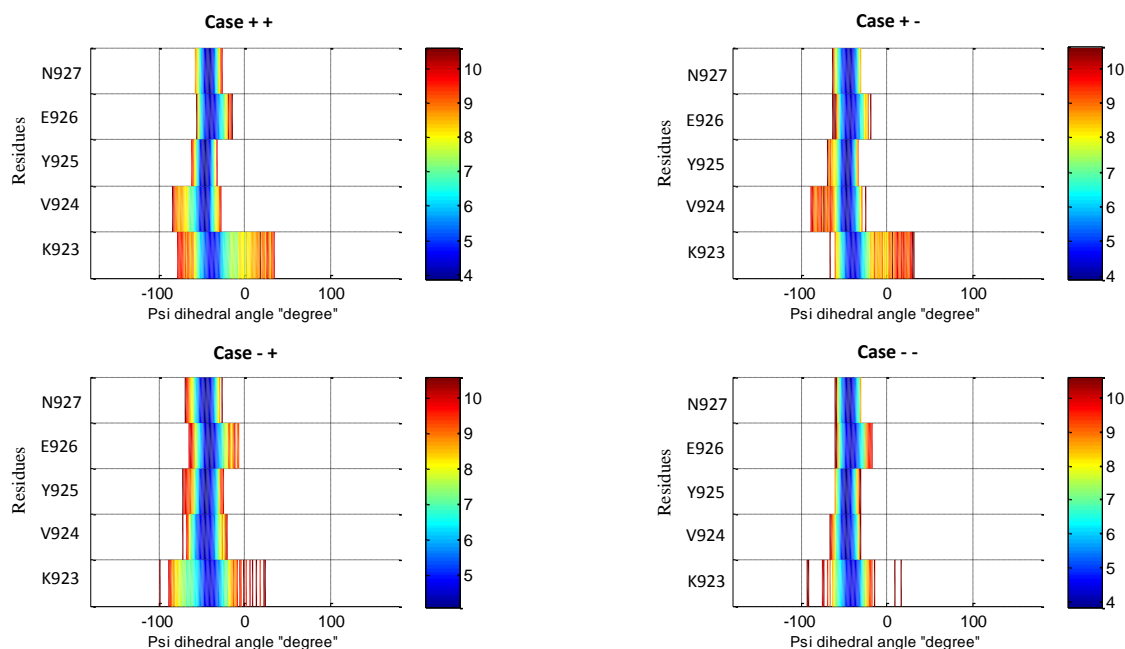


**Figure 4-3: Energy landscape of the dihedral angle  $\psi$  of the five N-terminal residues of H1 (K923, V924, Y925, E926 and N927) in the presence and/or the absence of P1 and P2. Except N923 that have greater flexibility, since it connects with the floppy tail (H1 tail),  $\psi$  angle of other residues has a small distribution (minima). This means H1 does not appear to have the propensity to adopt  $\beta$ -strand conformation under only thermal fluctuation. Each plot represents a cumulative simulation time of 80 ns. (Table 3-1, EQ.WOT.P1P2, EQ.WOT. P1, EQ.WOT.P2, and EQ.WOT.Ø)**

#### 4.1.1.2.1 Hydrogen Donor-Acceptor Pairs

Figure 4-4 shows the probability of forming different types of hydrogen bond for the first five residues at the N-terminal of H1 (K923, V924, Y925, E926, and N927). Most the time, they form an  $\alpha$ -helix hydrogen bond type. On the other hand,  $\pi$  and  $3_{10}$ -helix hydrogen bond type formed very rarely. The hydrogen bond of K923 is broken about  $\sim 25\%$  of the time. However, the hydrogen bonds of other four residues are broken about 3% to 7% of the time. The residue K923 is expected to have more broken hydrogen bond since it connects to the H1 tail. Hydrogen donor-acceptor pairs metric is useful in examining the propagation of the unfolding, if any. Based on what Figure 4-4 shows, the unfolding of K923 does not propagate into the other four residues where they are stable. Moreover, the absence of both P1 and P2 does not affect H1 behavior in terms of maintaining their  $\alpha$ -helical form. This is consistent with the previous suggestion that the stability of the H1 is independent of FAT association with the paxillin.

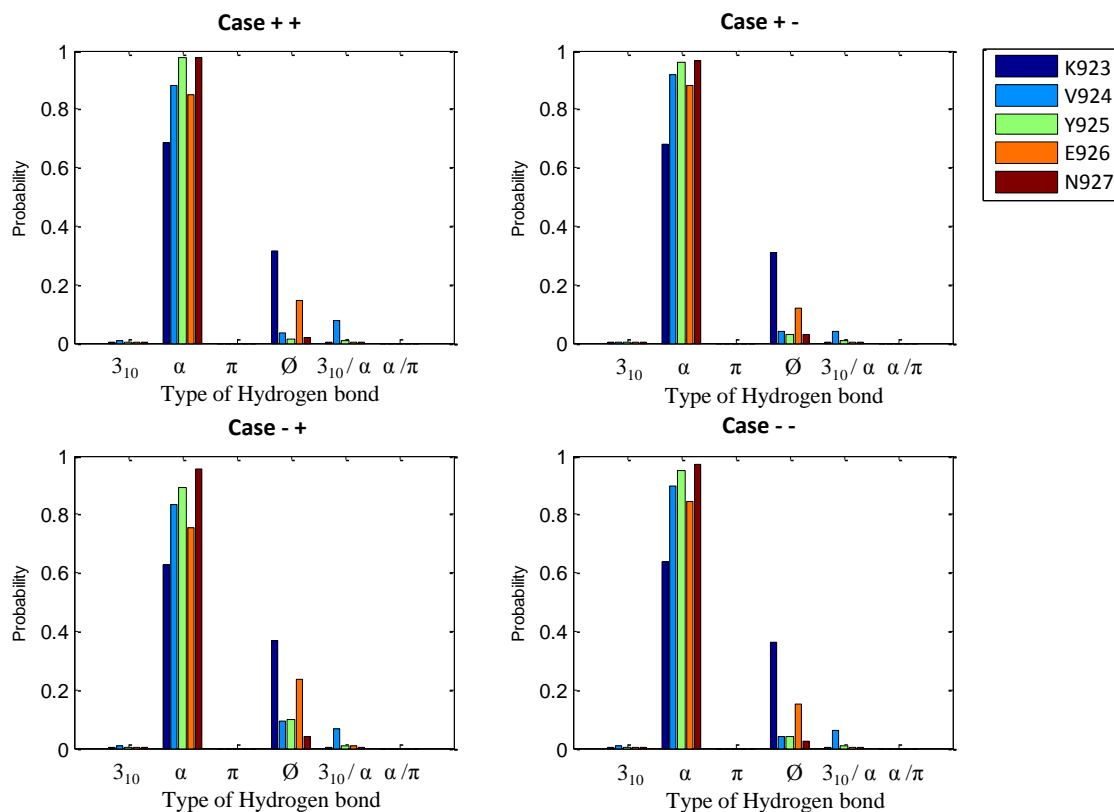


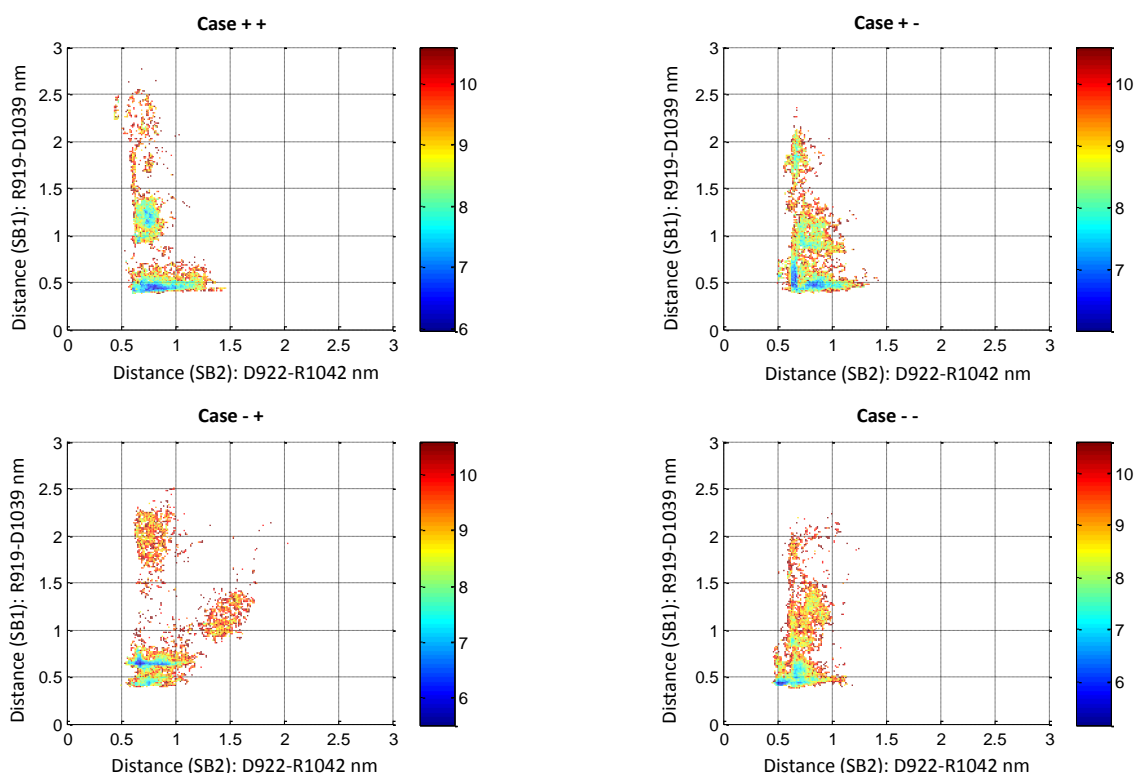
**Figure 4-4: Hydrogen bonds types formed in the presence and/or the absence of P1 and P2. H1 primarily forms an  $\alpha$ -helix. Each plot represents a cumulative simulation time of 80 ns. (Table 3-1, EQ.WOT.P1P2, EQ.WOT. P1, EQ.WOT.P2, and EQ.WOT. $\emptyset$ )**

Recalling the necessity of H1 to adopt  $\beta$ -strand conformation for making Y925 accessible for phosphorylation, H1 does not have the capacity to accomplish this requirement under only thermal fluctuation.

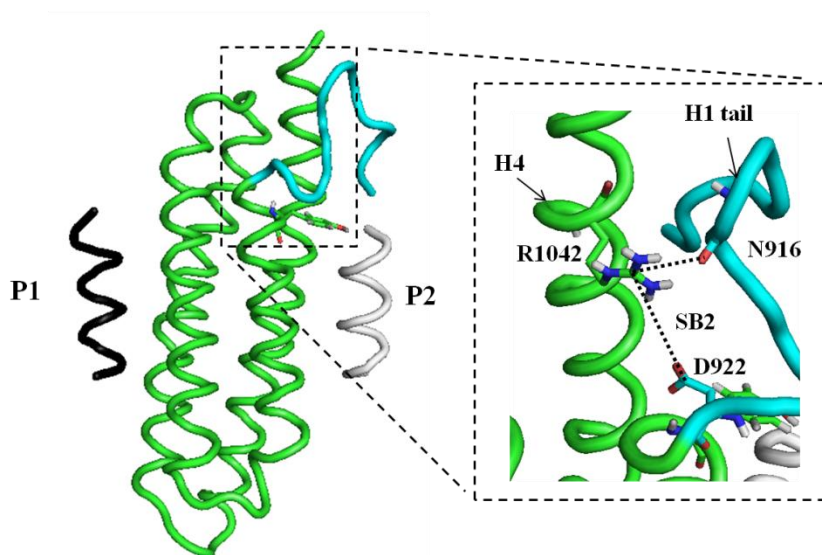
#### 4.1.1.3 Salt Bridges between H1 Tail and H4

Figure 4-5 shows the wide distribution of the salt bridge distances (SB1: R919-D1039 and SB2: D922-R1042) formed between H1 tail and H4. This wide distribution means that they are not stable and broken most the time. The first salt bridge (SB1) has a wider distribution than the second one (SB2). Even the second salt bridge, with a shorter

range of fluctuation, appears to be broken more often than the first. The reason, why the second salt bridge is broken more often, is because R1042 finds another partner, namely N916, backbone oxygen (Figure 4-6). The first salt bridge has a wide distribution because it is formed between the residue R919, farther inside H1 tail that has more mobility, and residue D1039 in H4.



**Figure 4-5: Energy landscape of the H1/H4 salt bridge distances represented by SB1 (R919–D1039) and SB2 (D922–R1042). SB1 and SB2 have a wide distribution which means they are broken. This suggests that they are not primarily responsible for keeping H1 folded within the bundle. Each plot represents a cumulative simulation time of 80 ns. (Table 3-1, EQ.WOT.P1P2, EQ.WOT.P1, EQ.WOT.P2, and EQ.WOT.Ø).**



**Figure 4-6: The second salt bridge (SB2: D922-R1042) that is located in the region near the N-terminal of H1 (near Y925). The residue R1042 interacts with another partner which is N916.**

As seen in Figure 4-7, if the salt bridge distance must be less than 0.5 nm, then the second salt bridge, SB2 (D922–R1042), is broken most the time for any case, whereas the first salt bridge, SB1 (919–D1039), persists 30% of the time. The relative position of H1 tail to the bundle is stable, which makes SB1 persist longer and point the residue, N916, to R1042 closer than D922.

However, it has been suggested that these salt bridges, among other factors, are responsible of maintaining relative position of H1 with the bundle. This result suggests that it does not appear that these salt bridges have a significant role in keeping H1 attached to the bundle.



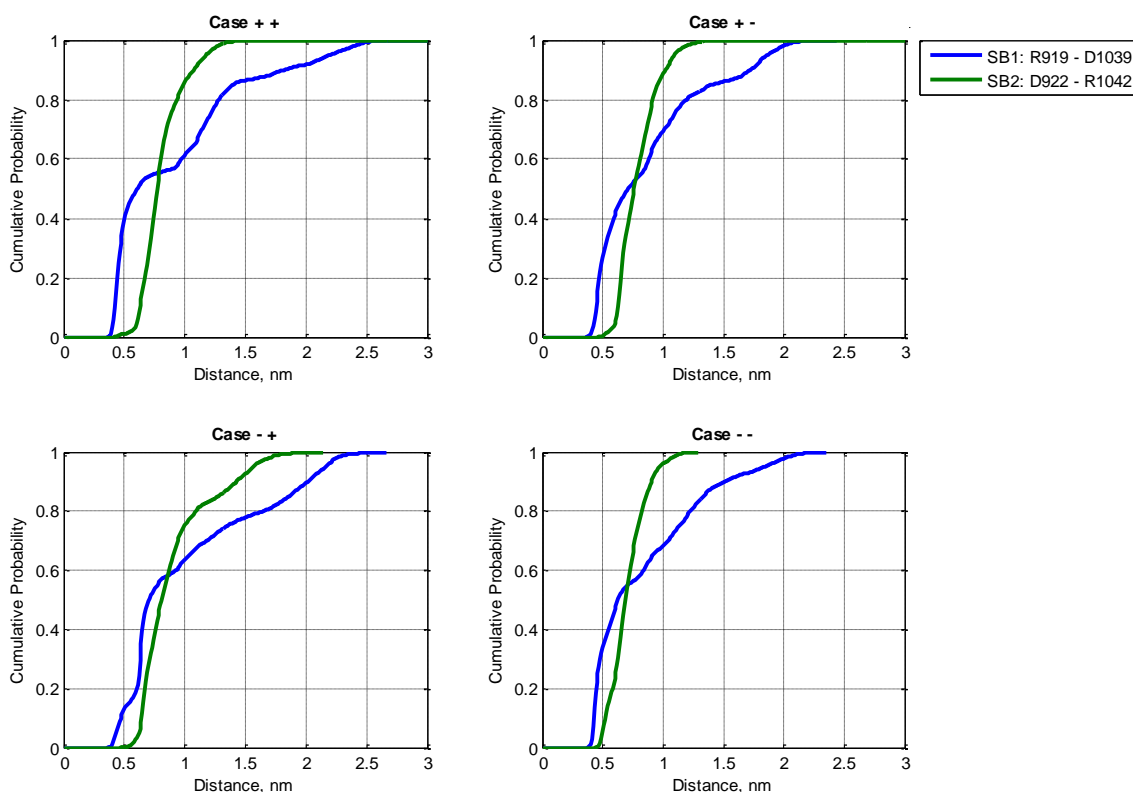


**Figure 4-7: Cumulative probability of the two salt bridges represented by two distances SB1 (R919–D1039) and SB2 (D922–R1042). If the salt bridge distance has to be less than 0.5 nm, it means they are broken ~80%. This suggests that they are not primarily responsible for keeping H1 folded within the bundle. Each plot represents a cumulative simulation time of 80 ns. (Table 3-1, EQ.WOT.P1P2, EQ.WOT.P1, EQ.WOT.P2, and EQ.WOT.Ø).**

#### 4.1.2 AUGMENTED FAT/PAXILLIN COMPLEX WITH H4 TAIL AND P1/P2 CONSTRAINED

For equilibrium simulations, the augmented FAT/paxillin structure was used and the presence/absence of P2 was varied (Figure 3-4.C and Table 3-1, EQ.WT.P1P2, EQ.WT.P1). This structure was introduced to the mechanically loaded simulation, so understanding its behavior under equilibrium is important. It is very important to examine the effect of the three modifications applied to FAT/paxillin complex of H1 behavior: the

addition H4 tail, the addition of the random coils to P1 and P2, and enforcing a zero displacement condition to the ends of P1 and P2.

#### 4.1.2.1 H1 Position

Figure 4-8 shows the blue colored regions (minima) of H1 position that have small distribution. The relative position of H1 to neighboring helices is very stable which means H1 does not appear to have a propensity to leave the bundle for two simulated cases. In the absence of P2 (binds to HP2), H1 is still attached to the bundle. Moreover, the modifications made to the FAT/paxillin complex do not influence the stability of the position of H1 relative to the bundle. As a result, H1 is strongly attached to the bundle regardless any augmented changes made or the absence of P2.

It seems that under thermal fluctuations only, H1 does not have the ability to overcome the energy barrier, that keeps H1 attached to the bundle. If this is the case, Y925 might not be accessible for the phosphorylation in which H1 has to be out of the bundle

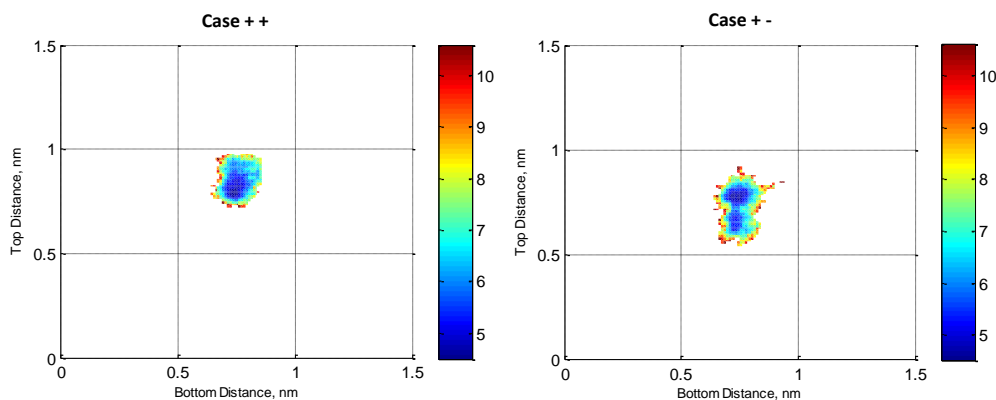


**Figure 4-8: Energy landscape of H1 position represented by  $d_{top}$  and  $d_{bottom}$ . H1 position has a small distribution (minima) which means H1 does not appear to have the propensity to leave the bundle under only thermal fluctuation. Each plot represents a cumulative simulation time of 80 ns. (Table 3-1, EQ.WT.P1P2, EQ.WT. P1).**

Figure 4-9 illustrates why the two blue colored regions (minima) for the Case +- exist. They are different stable states in different runs, not different stable states in one simulation. The top distance between H1 and the bundle for Run#1 and Run#4 is slightly smaller than it is in Run#2 and Run#3. After compiling their data in one plot, these two blue spots in Figure 4-8 appeared.

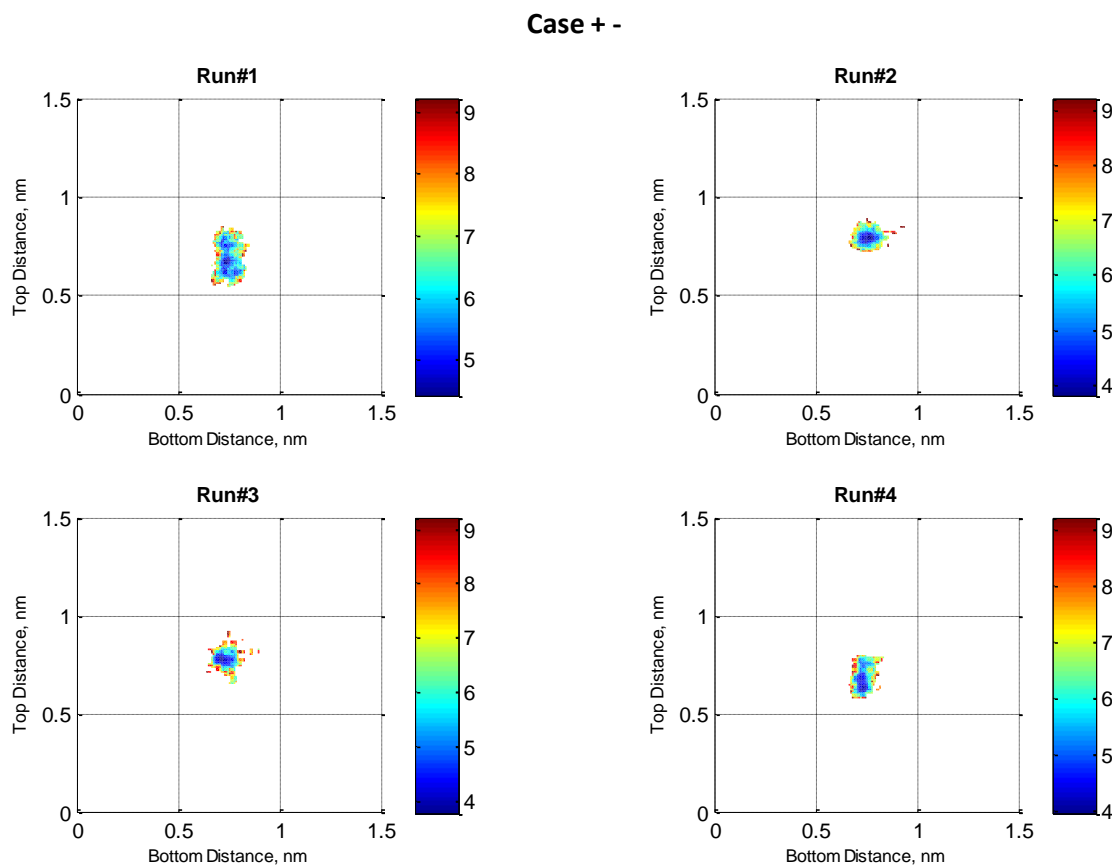


**Figure 4-9: Energy landscape of H1 position represented by  $d_{\text{top}}$  and  $d_{\text{bottom}}$  in the presence of P1 only. Two different preferred states in different simulations illustrate the presence of the two local minima in the previous figure (Figure 4-9: Case +-). Each plot represents a simulation time of 20 ns. (Table 3-1, EQ.WT. P1).**

### 4.1.2.2 H1 Unfolding

#### 4.1.2.2.1 Backbone Dihedral Angle $\psi$

As seen in Figure 4-10, except residue K923, the  $\psi$  angles of the other top four residues of the H1's N-terminal (V924, Y925, E926, and N927) have a small distribution (the mean value is  $\sim -50^\circ$  degree). This means they are folded in a helical form in the presence/absence of P2. However, the first residue at the N-terminus of H1 (K923) is expected, as discussed before, to have greater flexibility, since it connects with the H1 tail (i.e., H1 tail is free to move). Even though, the flexibility of K923 does not affect the stability of the other residues flanking Y925. Furthermore, the augmented changes made to the FAT/paxillin structure do not appear to significantly affect the ability of H1 to stay folded. The region flanking Y925 does not appear to have the propensity to adopt  $\beta$ -strand conformation. Even if residue K923 has a propensity to unfold, all other residues are stable and not affected by its flexibility. As a result, H1 does not have the propensity to adopt  $\beta$ -strand conformation under only thermal fluctuation. This means H1 might not have the ability to undergo the structural rearrangements needed for making Y925 accessible for phosphorylation.

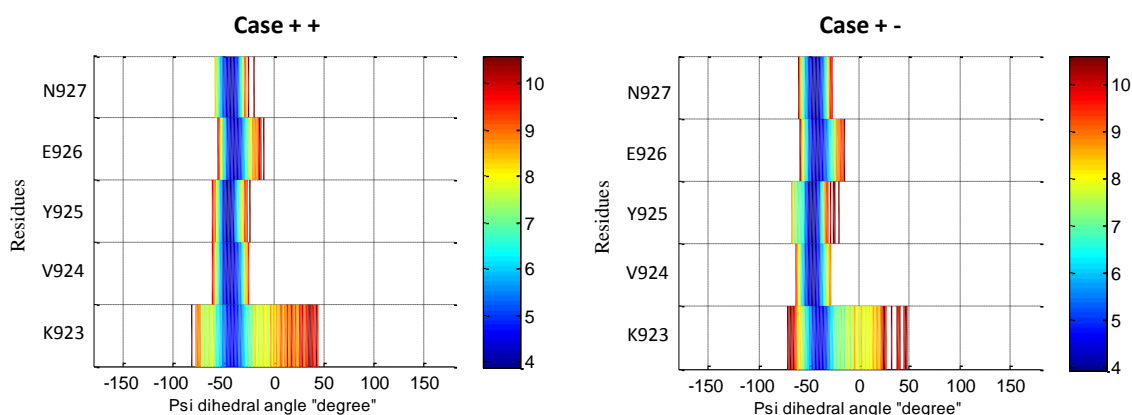


**Figure 4-10: Energy landscape of the dihedral angle  $\psi$  of the five N-terminal residues of H1 (K923, V924, Y925, E926, and N927) in the presence and the absence of P2. Except K923 that have greater flexibility, since it connects with the floppy tail (H1 tail),  $\psi$  angle of other residues have a small distribution (minima). This means H1 does not appear to have the propensity to adopt  $\beta$ -strand conformation under only thermal fluctuation. Each plot represents a cumulative simulation time of 80 ns. (Table 3-1, EQ.WT.P1P2, EQ.WT.P1).**

#### 4.1.2.2.1 Hydrogen Donor-Acceptor Pairs

Figure 4-11 shows the probability of different types of hydrogen bond formed by the first five residues at the N-terminal of H1 (K923, V924, Y925, E926, and N927). Most the time, they form an  $\alpha$ -helix hydrogen bond type. The other hydrogen bond types were formed very rarely. The hydrogen bond of K923 is broken about  $\sim 30\%$  of the time. However, the hydrogen bonds of other four residues are broken about 3% to 10% of the simulation time. The residue K923 is expected to have more broken hydrogen bond; as discussed before, since it connects to the H1 tail. Examining the propagation of the unfolding, if any, hydrogen donor-acceptor pairs metric is useful. Based on what is shown in Figure 4-11, the unfolding of K923 does not propagate into the other four residues which they are stable. Moreover, the augmented changes made to the FAT/paxillin complex and the absence of P2 do not disrupt H1  $\alpha$ -helical form.

In the presence of P1 and P2 (Case ++), the hydrogen bond of the first residue is more likely to be broken than in the absence of P2 (Case +-). This is possibly because the motion constraint that the presence of the constrained P2 provides, but in general, the difference is not significant.

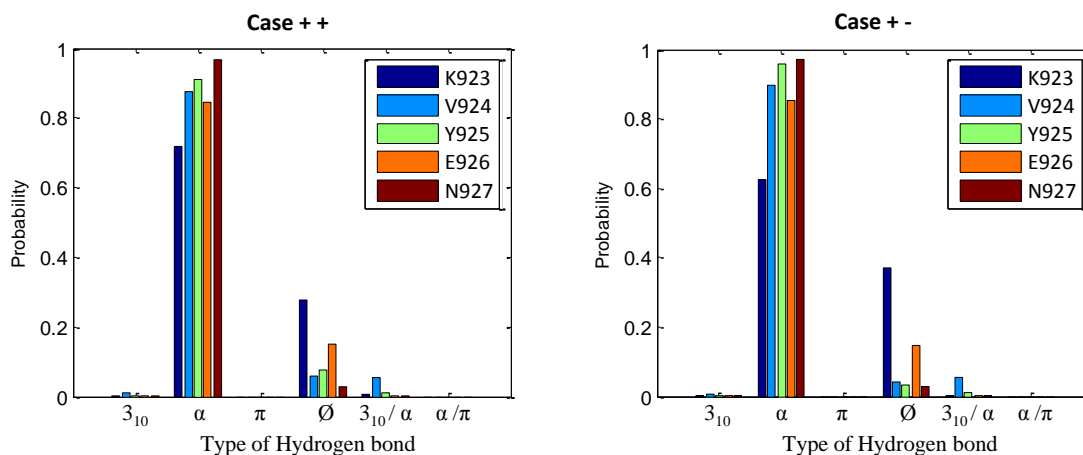


**Figure 4-11: Hydrogen bonds types formed in the absence of P2. H1 primarily forms an  $\alpha$ -helix. Each plot represents a cumulative simulation time of 80 ns. (Table 3-1, EQ.WT.P1P2, EQ.WT.P1).**

#### 4.1.2.3 Salt Bridges between H1 Tail and H4

Figure 4-12 shows the wide distribution of distances between residues formed by the two salt bridges (SB1: R919-D1039, SB2: D922–R1042). This wide distribution means they are broken most the time. For Case +- (in the absence of P2), the first salt bridge (SB1: R919-D1039) has a wider distribution than the second one (SB2: D922–R1042). As discussed before, because R1042 finds another partner N916, backbone oxygen, Figure 4-6, the second salt bridge is broken more. For Case ++ (P1 and P2 are in presence), the first salt bridge has smaller distribution because the relative motion of H1 tail to the bundle is constrained by the presence of P2 (P2 is constrained). In addition, the

augmented changes made to FAT/paxillin structure do not provide supports to these two salt bridges. Their persistence is similar to that found in previous simulations (FAT/paxillin complex without H4 tail and P1/P2 unconstrained, Figure 3-1).

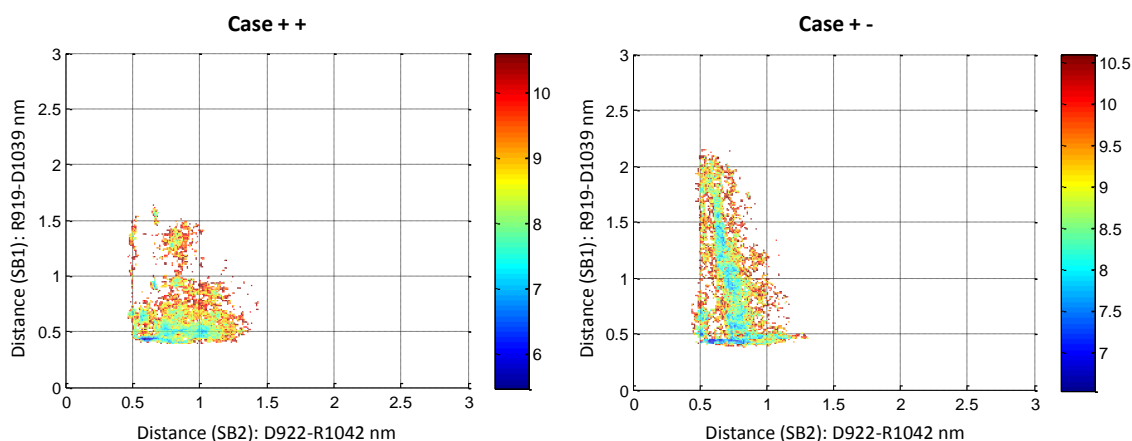


**Figure 4-12: Energy landscape of the H1/H4 salt bridge distances represented by SB1 (R919–D1039) and SB2 (D922–R1042). SB1 and SB2 have a wide distribution which means they are broken. This suggests that they are not primarily responsible for keeping H1 folded within the bundle. Each plot represents a cumulative simulation time of 80 ns. (Table 3-1, EQ.WT.P1P2, EQ.WT.P1).**

As in Figure 4-13, if the salt bridge distance must be less than 0.5 nm, then the second salt bridge, SB2: D922–R1042, is broken most the time for any simulated case, whereas the first one persists 20~40% of the time. Besides other factors, the two salt bridges between H1 and H4 are often cited as being responsible for keeping H1 attached to the bundle. However, these results show the opposite: they are not stable, which means they might not have a significant contribution in holding H1 to the bundle.

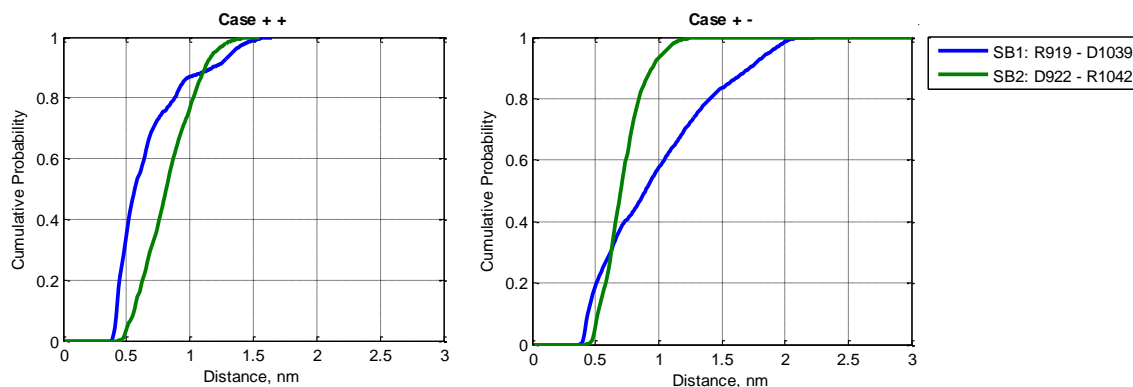


**Figure 4-13: Cumulative probability of the two salt bridges represented for two distances, SB1 (R919–D1039) and SB2 (D922–R1042). If the salt bridge distance has to be less than 0.5 nm, it means they are broken ~80% of the simulation time. This suggests that they are not primarily responsible for keeping H1 folded within the bundle. Each plot represents a cumulative simulation time of 80 ns. (Table 3-1, EQ.WT.P1P2, EQ.WT.P1).**

#### 4.1.3 H1 ISOLATION

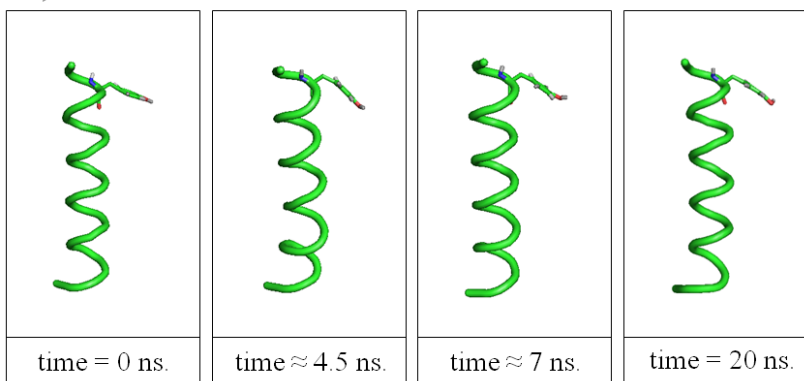
Previous results suggest that H1 prefers to stay folded in an  $\alpha$ -helical form within the bundle. In addition, the two salt bridges are broken most often and they do not appear to be the key of holding H1 to the bundle. There must, therefore, along with the hydrogen bonds, be another factor contributing to maintaining the helical form of H1, as well as holding it to the bundle. Therefore, it is important to consider the possible effect of the hydrophobicity of the FAT domain core on H1 and examine the H1 behavior as it is isolated.

Figure 4-14 shows H1 behavior under two types of simulations: A) MD for the entire FAT system, and B) MD for H1 isolated from FAT. H1 stays in a helical form as it attached to the bundle and it unfolds when it is isolated. Even though, H1 started to unfold from its C-terminal (where the H1/H2 hinge connects to) while the region flanking Y925 at the N-terminal struggled for long time in keeping its helical form. This illustrates the influence of the hydrophobicity of the FAT core on H1, as well as the propensity of H1 to unfold from its C-terminal. It has been suggested that this hinge between H1 and



H2 has the ability to promote such an unfolding transition to the H1 helix. This results are consistent with both the important role of the hydrophobicity on H1 behavior, as well as the propensity of H1 to unfold from its C-terminal (where Y925 is located at N-terminal portion).

**A) H1 while it is attached to the bundle.**



**B) H1 when it is isolated.**

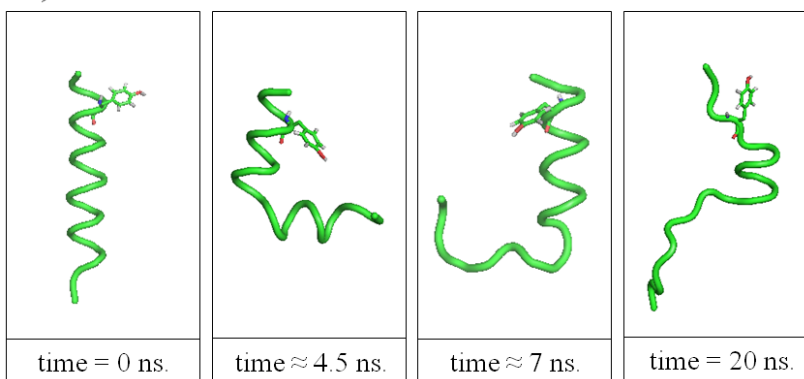


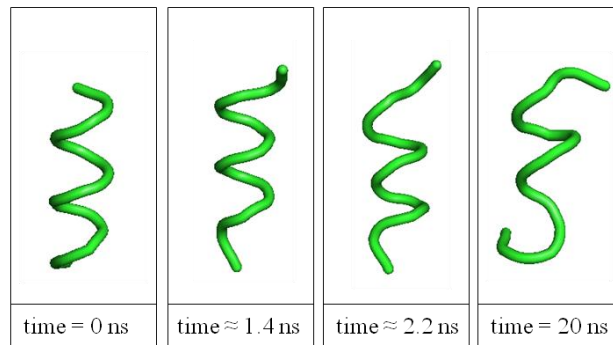
**Figure 4-14: The structural conformation of H1 under two conditions; H1 within the bundle and H1 isolated. A) H1 while it is attached to the bundle (Figure 3-1). It shows that H1 has the ability to keep its in helical form when it is associated with the bundle. B) H1 when it is isolated (K923-K941). H1 has a propensity to unfold from its C-terminal.**

#### 4.1.4 PAXILLIN LD MOTIF ISOLATION

To examine the assumption that suggests LD motif is  $\alpha$ -helix in its native form, MD simulation was run for an isolated LD4 motif. Figure 4-15 shows LD4 behavior under two type of simulation: LD motif when it is isolated, LD motif bound to the FAT

domain. When isolated, the LD motif unfolded in 2 ns which means that LD motif does not appear to have the ability maintain its helical form by itself. However, when LD motif binds to the FAT domain, it stays in a helical form. This contradicts what is stated in the literature and illustrates the role of hydrophobicity of the hydrophobic patches HP1 and HP2 on the conformational structure of the LD motifs as they associate with the FAT domain. It does not seem that LD motifs stabilize the bundle form of the FAT domain, but the FAT domain has the capacity to stabilize the helical form of LD motifs when they are in association.

**A) LD4 while it binds to the bundle.**



**B) when it is isolated.**

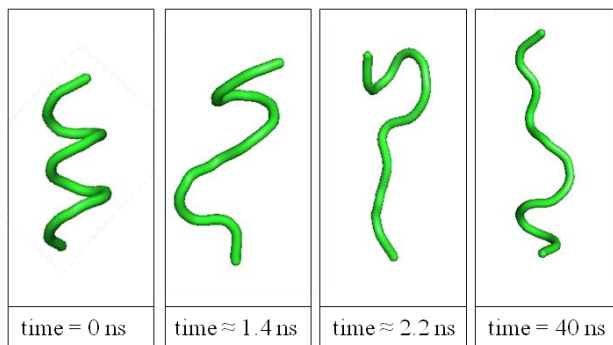


**Figure 4-15: The structural conformation of LD4 under two conditions; LD4 binds to FAT domain and LD4 isolated. A) Snapshots for LD motif while it binds to the FAT domain (Figure 3-1). It shows that LD motif has the ability to keep its in helical form when it is associated with the bundle. B) Snapshots for LD motif when it is isolated (T264-S275). The isolated LD does not have the capability to stay folded, which illustrates the effect of the hydrophobic patches that LD binds to.**

#### 4.1.5 EQUILIBRIUM RESULT SUMMARY

The total time of equilibrium simulations, 560 ns, was run for different cases (in the presence/absence of P1 and P2) and different structure (FAT/paxillin complex without H4 tail and P1/P2 unconstrained, and augmented FAT/paxillin complex with H4 tail and P1/P2 constrained). For all these equilibrium simulations, H1 position metric strongly suggests that independent of binding to the paxillin, H1 does not have the propensity to leave the bundle under only thermal fluctuation. In addition, H1 unfolding metrics suggest that H1 stays folded in  $\alpha$ -helical form. In the case where H1 is isolated, H1 has the propensity to unfold from its C-terminal (not from the N-terminal where the Y925 is located). This result is consistent with what has been suggested in the literature about the energy barrier that prevents H1 to leave the bundle. However, the two reported salt bridges (SB1: R919-D1039, SB2: D922–R1042) were weak and not able to persist, which contradicts what stated in the literature that these salt brides have a role in holding H1 to the bundle.

As discussed before, it has been suggested for Y925, which isolated at the N-terminal of H1, to be accessible for phosphorylation, H1 has to come out of the bundle and adopt a  $\beta$ -strand conformation. Whereas under only thermal fluctuation, it does not appear that the FAT domain is able to undergo the required structural rearrangements needed for phosphorylation. This suggests that under only thermal fluctuation, Y925 is not frequently accessible for phosphorylation. Moreover, the salt bridges metric raises a question of the ability of the interactions, observed from the crystal structure of a protein, to persist in the dynamic in vivo environment.

For Y925 to be accessible for phosphorylation, mechanical loads or/and chemical interaction(s) have to take place to promote the required structural changes. From

mechanical standpoint, the FAK has been hypothesized to be mechanically activated. The next section presents results of H1 behavior under applied load.

## **4.2 Loaded Scenario Results**

As discussed in the equilibrium results, the thermal fluctuation does not appear to have the capacity to promote the required structural rearrangement of the FAT domain needed for making Y925 accessible for the phosphorylation. H1 neither leaves the bundle nor adopts a  $\beta$ -strand conformation under only thermal fluctuation. As a result, axial and perpendicular mechanical loaded simulations were run (illustrated in §3.2.4 Simulations). The H1 behavior, in terms of its relative position and unfolding, under the influence of the load was examined using Constant Force Molecular Dynamics (CFMD) simulations on as many different initial structures as possible (discussed in §3.1.1 Simulations).

### **4.2.1 AXIAL LOAD SCENARIO RESULTS**

Five different initial structures (seeds, Figure 3-9) were chosen based on the behavior of H1/H4 tail, their relative position to each other as well as how many interactions they have (Figure 3-8). Each seed was run twice, with different initial velocities (Table 3-1, AX.WT.P1P2). A 100 pN constant force is applied to the N-terminus of H1 tail in a direction parallel to the H1 axis with P1/P2 were constrained. The results of the axial load simulation show two types of H1 behavior: typical and atypical (Table 4-1).

**Table 4-1: H1 typical and atypical behaviors under axial load, applied to the N-terminus of H1 tail and P1/P2 constrained. Eight out of ten simulations have typical behavior, while two have atypical behavior. (Table 3-1, AX.WT, P1P2).**

Initial Structures		H1 Behavior Type		H1 Behavior Description	
		Typical	Atypical	H1 Position	H1 Unfolding
Seed#1	Run#1	Yes	-	In the bundle	In a helical form
	Run#2	Yes	-	In the bundle	In a helical form
Seed#2	Run#1	Yes	-	In the bundle	In a helical form
	Run#2	-	Yes	In the bundle	The first two residues, K923 and V924, of H1 unfold.
Seed#3	Run#1	Yes	-	In the bundle	In a helical form
	Run#2	Yes	-	In the bundle	In a helical form
Seed#4	Run#1	Yes	-	In the bundle	In a helical form
	Run#2	Yes	-	In the bundle	In a helical form
Seed#5	Run#1	-	Yes	In the bundle	The first two residues, K923 and V924, of H1 unfold.
	Run#2	Yes	-	In the bundle	In a helical form

#### **4.2.1.1 H1 Typical Behavior**

Eight simulations out of ten have the same H1 behavior (Table 4-1). These eight simulations started with different initial conditions (seeds and initial velocities). Regardless the differences in their initial conditions, the behavior of H1 is very similar. The typical behavior of H1 is similar to its behavior under equilibrium.

##### ***4.2.1.1.1 H1 Position***

As seen in Figure 4-16, the blue-colored regions (minima) of the H1 position have small distribution. For all the different initial conditions applied, the relative position of H1 to the bundle is very stable, which means H1 does not appear to have a propensity to leave the bundle. As suggested in literature, electrostatic and hydrophobic interactions between H1 (residues A917-D922) and H4 present an energy barrier keeping H1 attached to the bundle. A 100 pN constant load applied does not appear to have the ability to overcome this energy barrier. Under equilibrium and axial load, FAT domain moves as a rigid body and the 100 pN axial load does not have the capacity to open the FAT domain. However, in order for Y925 to engage the phosphorylation, H1 has to leave the bundle. It seems that Y925 is not easily accessible for phosphorylation.

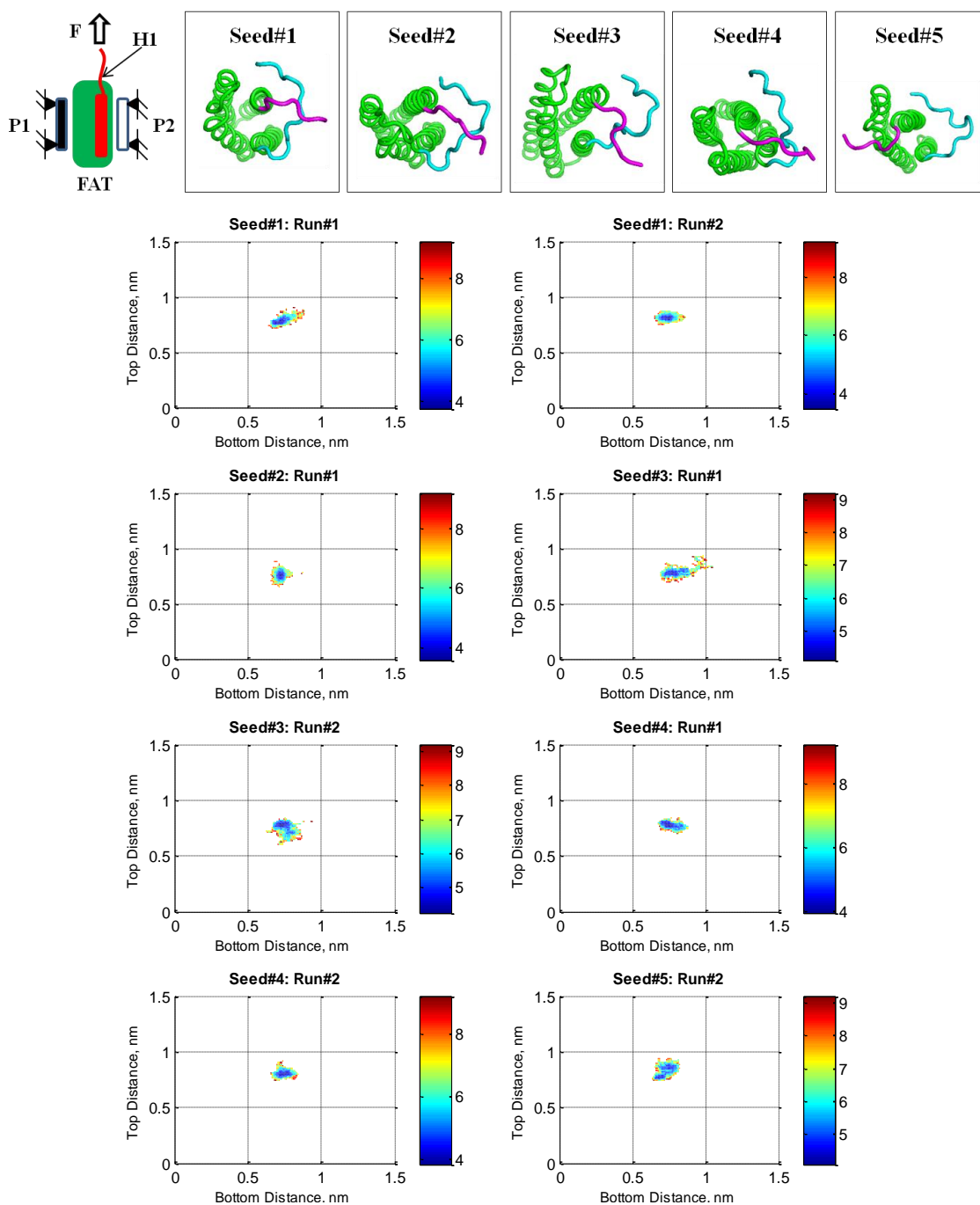


**Figure 4-16: Energy landscape of H1 position represented by  $d_{\text{top}}$  and  $d_{\text{bottom}}$  in the presence of both P1 and P2. For typical behavior, H1 position has a small distribution (minima) which means H1 does not appear to have the propensity to leave the bundle under constant force applied axially to the N-terminus of H1 tail. Each plot represents a simulation time of 20 ns. (Table 3-1, AX.WT.P1P2).**



#### ***4.2.1.1.2 H1 Unfolding***

##### **4.2.1.1.2.1 Backbone Dihedral Angle $\psi$**

From Figure 4-17, except residue K923, the  $\psi$  angles of the other top four residues of the H1's N-terminal (V924, Y925, E926, and N927) have a small distribution (the mean value is  $\sim -50^0$  degree). This means they are folded in a helical form. However, the first residue at the N-terminus of H1 (K923) is expected, as discussed before, to have a greater flexibility, since it connects with H1 tail (i.e., H1 tail is free to move). The flexibility of K923 does not affect the stability of the other residues flanking Y925.

Under equilibrium and an applied 100 pN axial load, the region flanking Y925 does not appear to have the propensity to adopt  $\beta$ -strand conformation. Even when residue K923 has a propensity to unfold, all other residues are stable and not affected by its flexibility. This means H1 has a high resistance to any structural rearrangements needed for making Y925 accessible for phosphorylation.

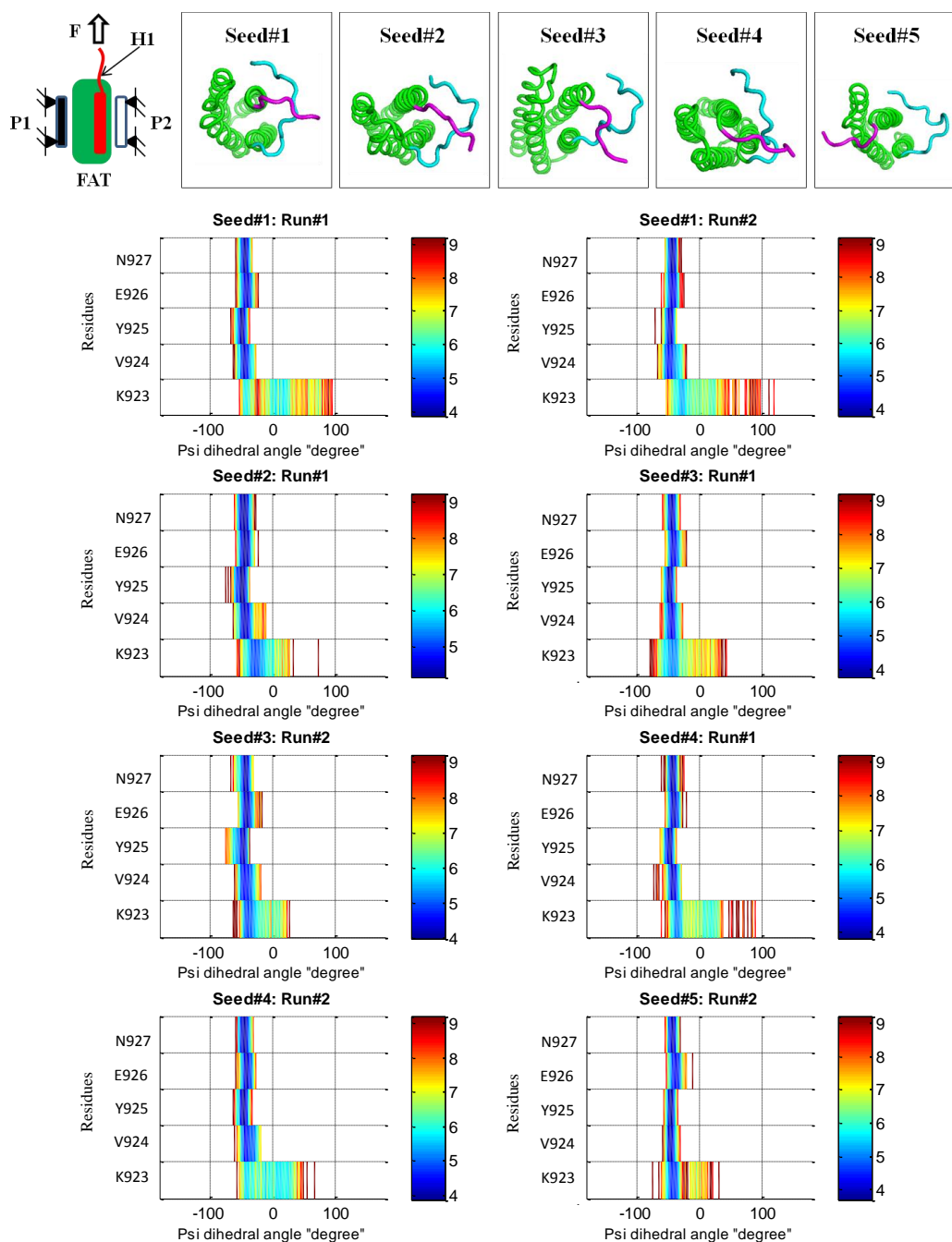


**Figure 4-17: Energy landscape of the dihedral angle  $\psi$  of the five N-terminal residues of H1 (K923, V924, Y925, E926, and N927) in the presence of both P1 and P2 for H1 typical behavior. Except N927 that has greater flexibility, since it connects with the floppy tail (H1 tail),  $\psi$  angle of other residues have a small distribution (minima). This means H1 does not appear to have the propensity to adopt  $\beta$ -strand conformation under constant force applied axially to the N-terminus of H1 tail. Each plot represents a simulation time of 20 ns. (Table 3-1, AX.WT.P1P2).**

#### 4.2.1.1.2.2 Hydrogen Donor-Acceptor Pairs

Figure 4-18 shows the probability of different hydrogen bond types formed by the first five residues at the N-terminal of H1 (K923, V924, Y925, E926, and N927). Most the time, they form an  $\alpha$ -helix hydrogen bond type for any different initial conditions applied. The  $\pi$  and  $3_{10}$ -helix hydrogen bond type formed very rarely. The hydrogen bond of K923 is broken about  $\sim 50\%$  of the time. However, the hydrogen bonds of other four residues are broken about 3% to 7% of the time. The residue K923 is expected to have more broken hydrogen bond since it connects to the H1 tail.

Hydrogen donor-acceptor pairs metric is useful in examining the propagation of the unfolding, if any. Based on what Figure 4-18 shows, the unfolding of K923 does not propagate into the other four residues where they are stable. Neither thermal fluctuation nor 100 pN axial load appear to excite the region flanking Y925 and promote the needed conformational rearrangements for the phosphorylation.

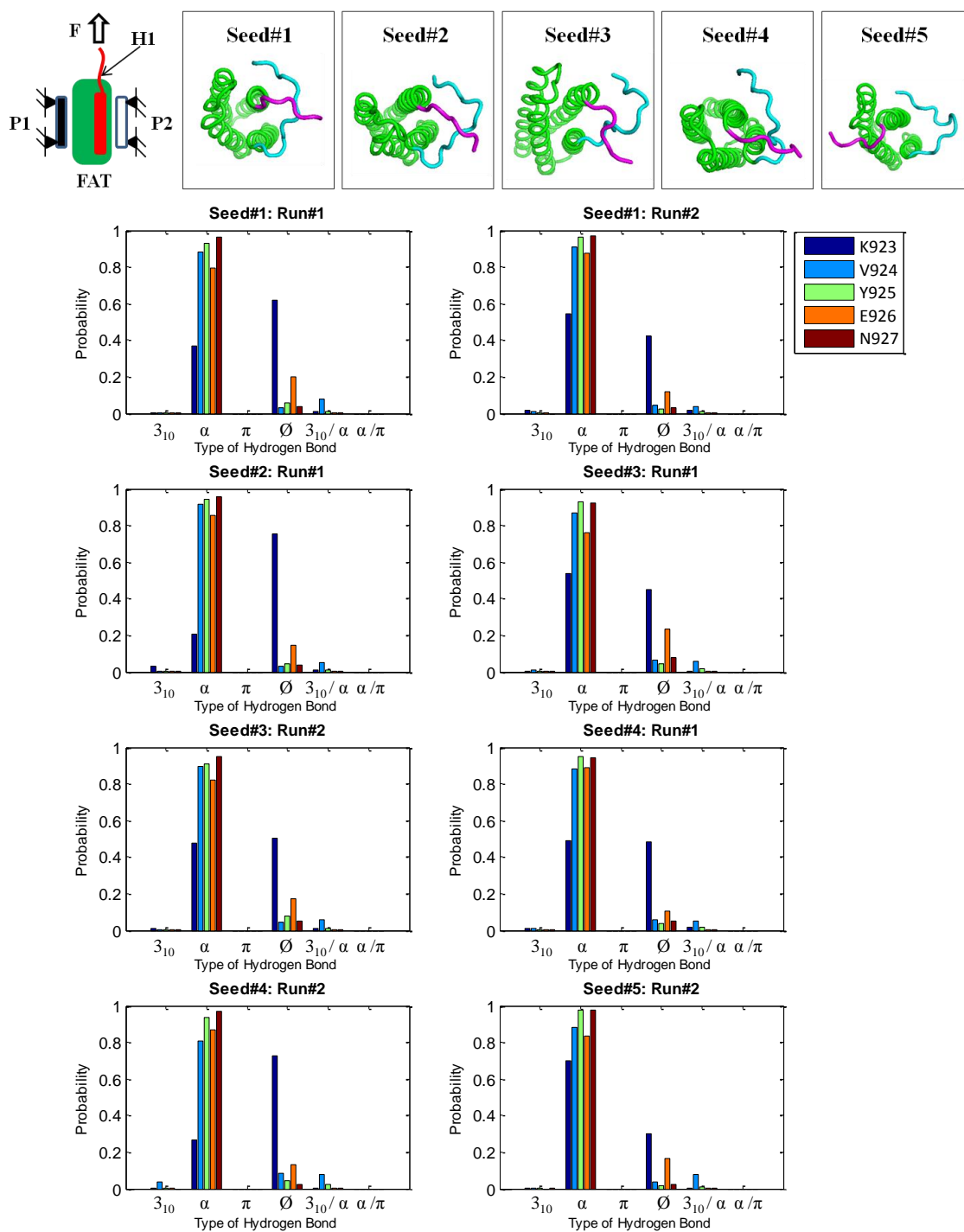


**Figure 4-18: Hydrogen bonds types formed in the absence of P2. For H1 typical behavior, H1 primarily forms an  $\alpha$ -helix. Each plot represents a simulation time of 20 ns. (Table 3-1, AX.WT.P1P2).**

#### ***4.2.1.1.3 Salt Bridges between H1 Tail and H4***

Figure 4-19 shows the wide distribution of distances between residues that formed the two salt bridges (SB1: R919-D1039, SB2: D922–R1042). This wide distribution of the distance means they are broken most the time. The first salt bridge (SB1) has a wider distribution than the second one (SB2), which is because of the load applied to H1 tail. The H1 tail is pulled in the load direction breaking the first salt bridge more often and pulling the residue, N916, that sometime interacts with R1042, which leads to making the second salt bridge more stable. (Figure 4-20). The applied load makes the first salt bridge weaker and the second salt bridge stronger.

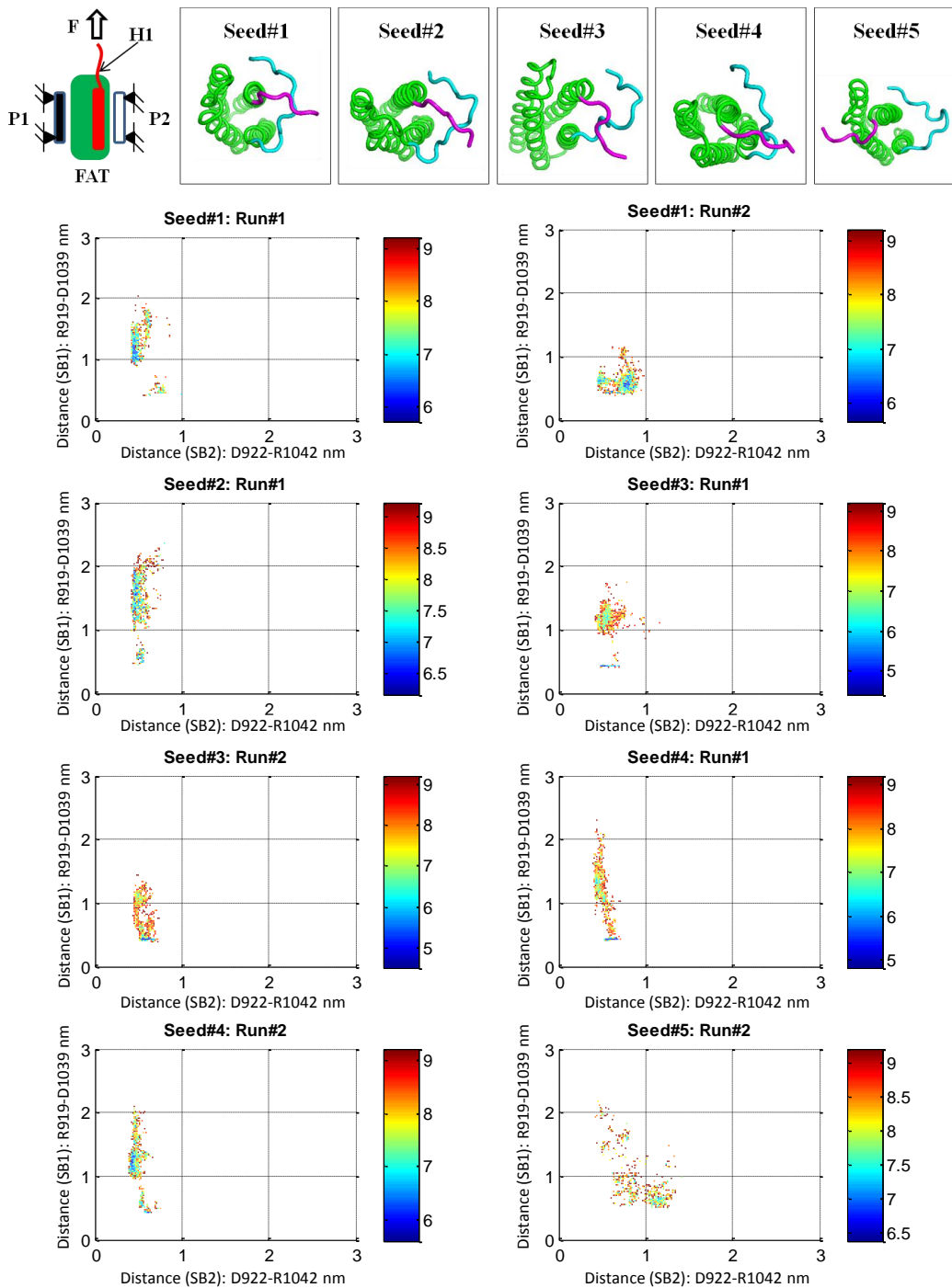


**Figure 4-19: Energy landscape of the H1/H4 salt bridge distances represented by SB1 (R919–D1039) and SB2 (D922–R1042). SB1 and SB2 have a wide distribution which means they are broken. This suggests that they are not primarily responsible for keeping H1 folded within the bundle. Each plot represents a simulation time of 20 ns. (Table 3-1, AX.WT.P1P2).**

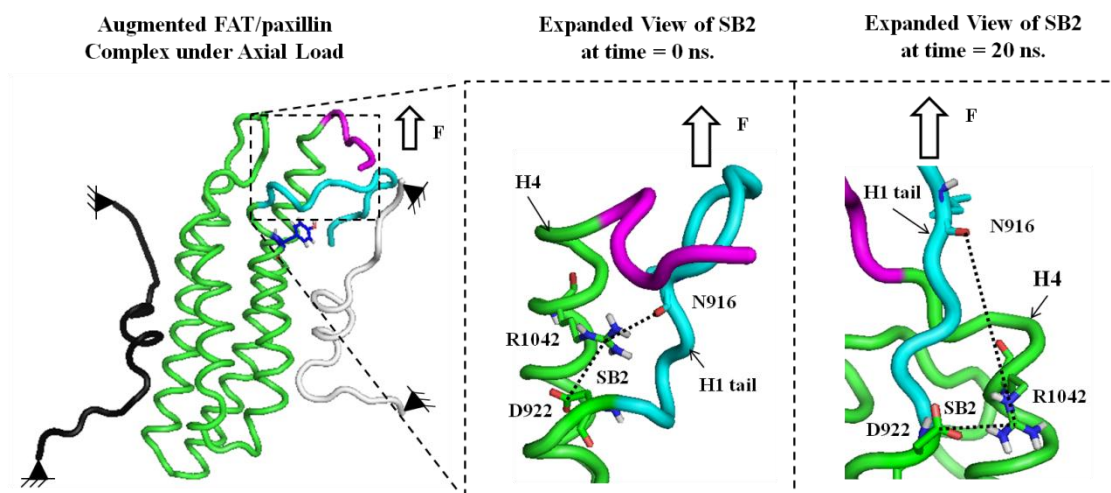


**Figure 4-20: The second salt bridge (SB2: D922-R1042) that is located in the region near the N-terminal of H1 (near Y925). The second salt bridge is shown before the simulation started and after. The load applied to the N-terminus of H1 tail pulled N916 away from R1042 making the second salt bridge more stable.**

As in Figure 4-21, if the salt bridge distance must be less than 0.5 nm, then the first salt bridge, SB1: D922–R1042, is broken most the time, whereas the second one, SB2: R919–D1039, persists 30% of the time. Under the influence of the axial load, the relative position of H1 tail to the bundle increases, which makes the first salt bridge broken more and pointing the residue, D922, to R1042 closer than N916 (Figure 4-20).

However, it has been suggested that these salt bridges, among other factors, are responsible of maintaining relative position of H1 with the bundle. This result suggests that it does not appear that these salt bridges have a significant role in keeping H1 attached to the bundle. In addition, salt bridge metric suggests that the strength of the interactions between the residues are affected by the applied load.

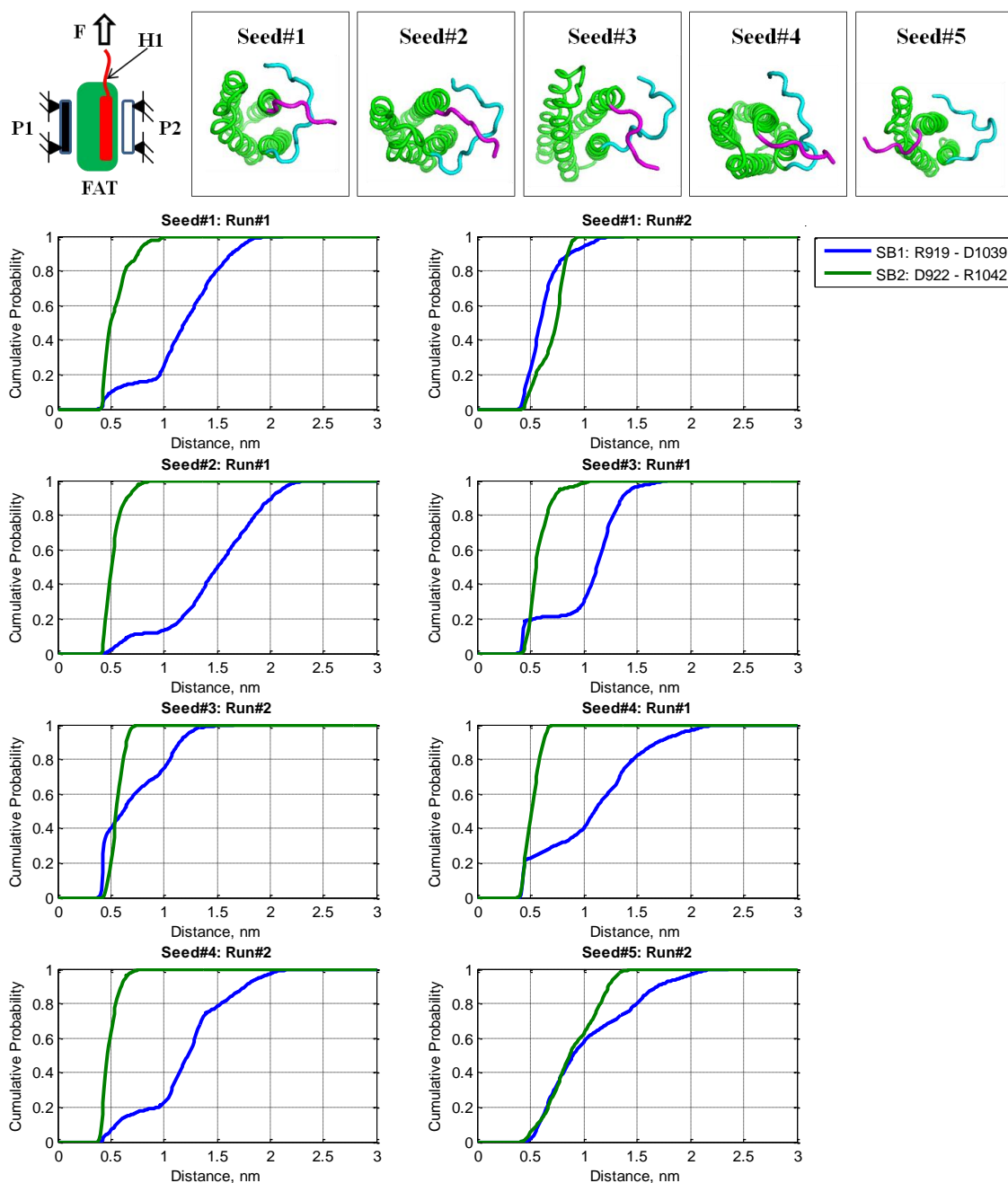


**Figure 4-21: Cumulative probability of the two salt bridges represented for two distances, SB1 (R919–D1039) and SB2 (D922–R1042). If the salt bridge distance has to be less than 0.5 nm, it means they are broken ~60%. This suggests that they are not primarily responsible for keeping H1 folded within the bundle. Each plot represents a simulation time of 20 ns. (Table 3-1, AX.WT.P1P2).**



#### 4.2.1.1.4 H1/H4 Tail Interaction

Figure 4-22 shows the quality of interactions formed between the H1/H4 tail. The number of H1/H4 tail interactions is widely distributed, the Seed#2 Run#1 and Seed#5 Run#2 are different than the other. In Seed#5 Run#2, H1/H4 tail have mostly no interactions, where the initial structure has no interaction between H1/H4 tail and they are separated. In Seed#2 Run#1, they have 1~3 electrostatic interactions while in other simulations, H1/H4 tail prefers to be entangled through 4 ~7 electrostatic interaction. In Seed#5 Run#2, the two salt bridges are broken and H1/H4 tail are separate, yet H1 is strongly attached to the bundle in a helical form. This suggests that they are another factors that holding H1 to the bundle. (discussed in § 4.2.1.3 Axial Load Result

Summary)

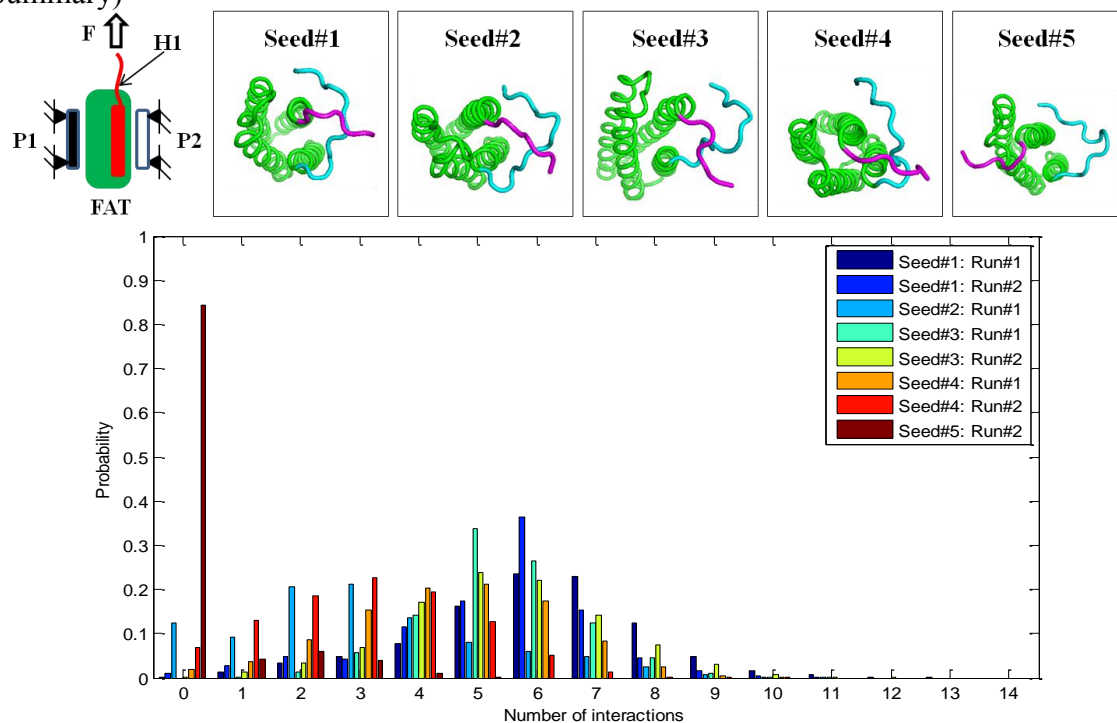


**Figure 4-22: Number electrostatic interactions formed between H1/H4 tail. The interactions between H1/H4 have a wide distribution which means H1/H4 tail prefer to entangled. Each bar represents a simulation time of 20 ns. (Table 3-1, AX.WT.P1P2).**

#### 4.2.1.1.5 FAT Structure in its Final States

Table 4-2 and Figure 4-23 show the FAT structure's final states in terms of H position, H1 unfolding, H1/H4 tail interactions and H2-H3 structure. In 100% of the eight simulations, H1 stays folded in the bundle. In 50% of the simulations, H1/H4 tail form  $\beta$ -sheet via a number of hydrogen bonds. About 37%, they are entangled via number of electrostatic interactions. This suggests that H1/H4 tail prefer to interact with each other more often. In only one simulation (Seed#5 Run#2), H1/H4 tail are mostly separate. (H1/H4 tail interactions are listed in (Appendix D). In this simulation, H1 stays folded in the bundle, which suggests that H1/H4 tail does not appear to be the key regulator of resisting H1 unfolding or keeping H1 attached to the bundle.

**Table 4-2: Final state of the structure of the region flanking Y925 for H1 typical behavior under constant force applied axially to the N-terminus of H1 tail. (Table 3-1, AX.WT.P1P2).**

	H1 Position		H1 Unfolding			H1/H4 Tail Interactions				H2-H3 Structure	
	In	Out	F	SUF	UN	$\beta$ , EX	$\beta$ , NEX	$\tau$	S	F23	U23
Probability %	8/8	0/8	8/8	0/8	0/8	1/8	3/8	3/8	1/8	6/8	2/8

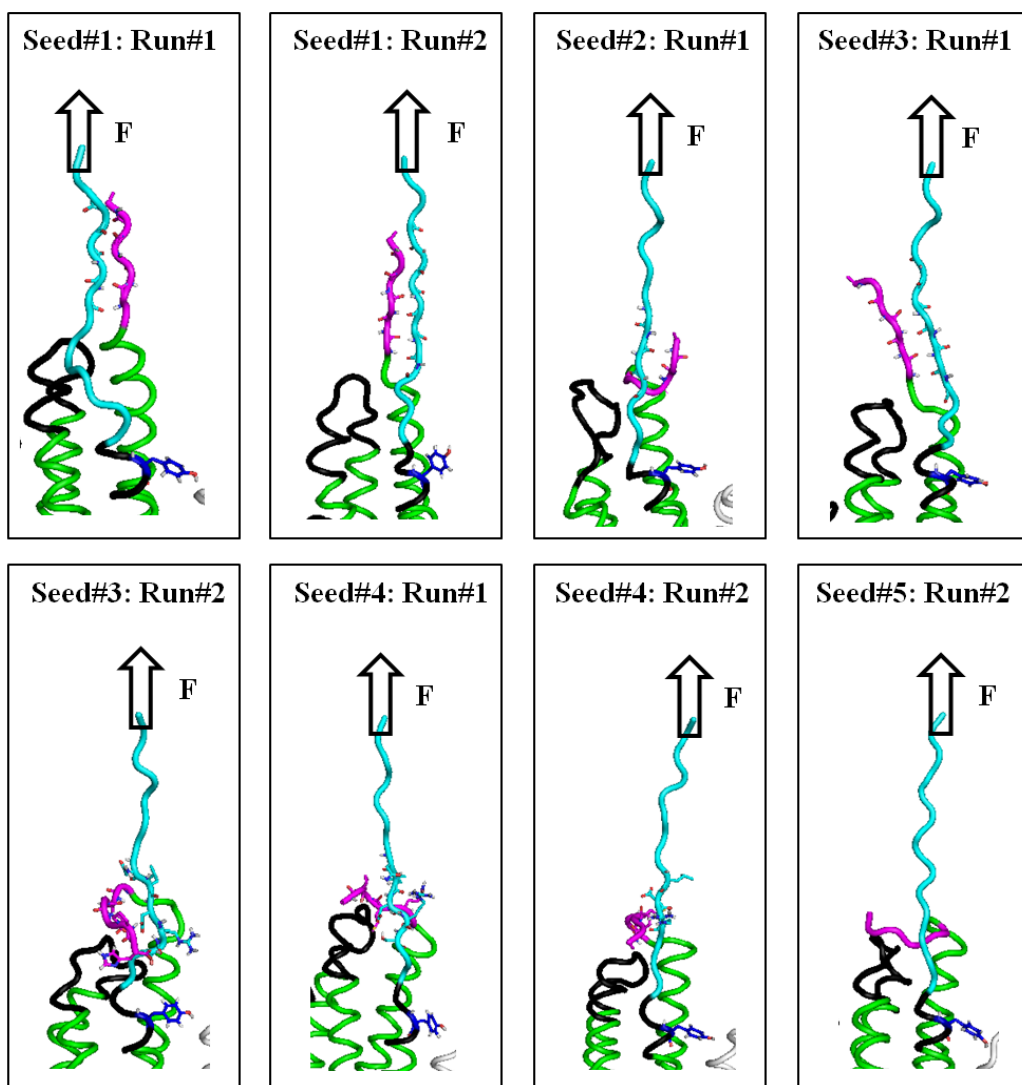


Figure 4-23: Final state of the structure of the region flanking Y925 for H1 typical behavior under constant force applied axially to the N-terminus of H1 tail. (Table 3-1, AX.WT.P1P2).

#### 4.2.1.2 H1 Atypical Behavior

The two other runs out of ten show different behavior of H1 (Table 4-1). They start with different initial structures (Seed#2 and Seed#5). In Seed#2, the H1/H4 tail interact with each other, while in Seed#5, they are separate.

In Figure 4-24, there are four different metrics: H1 position, dihedral angle  $\psi$ , hydrogen state and salt bridge state. For both simulations, the relative position of H1 has a small distribution (blue colored region) which means H1 is attached to the bundle. Also, the  $\psi$  angle of the second residue of H1's N-terminal (V924) shows that it unfolds. The residue (V924) has more broken hydrogen bond. The hydrogen bond metric shows that the unfolding of the first residue of H1 (K923) propagates into only the second residue (V924) where the other residues are stable. In addition, in Seed#5, Run#1, the second salt bridge (D922-R1042) is broken more often than the one in the Seed#2, Run#2. However, the first salt bridge (R919-D1039) is broken most the time.

In general, even the first two residues of N-terminal of H1 unfold, their unfolding do not propagate into the H1 helix to create  $\beta$ -strand conformation. Moreover, even these two residues show a propensity to unfold, H1 does not appear to have the capacity to leave the bundle. This atypical behavior of H1 does not achieve the required structural changes needed for Y925 phosphorylation, where H1 must leave the bundle and adopt  $\beta$ -strand conformation.

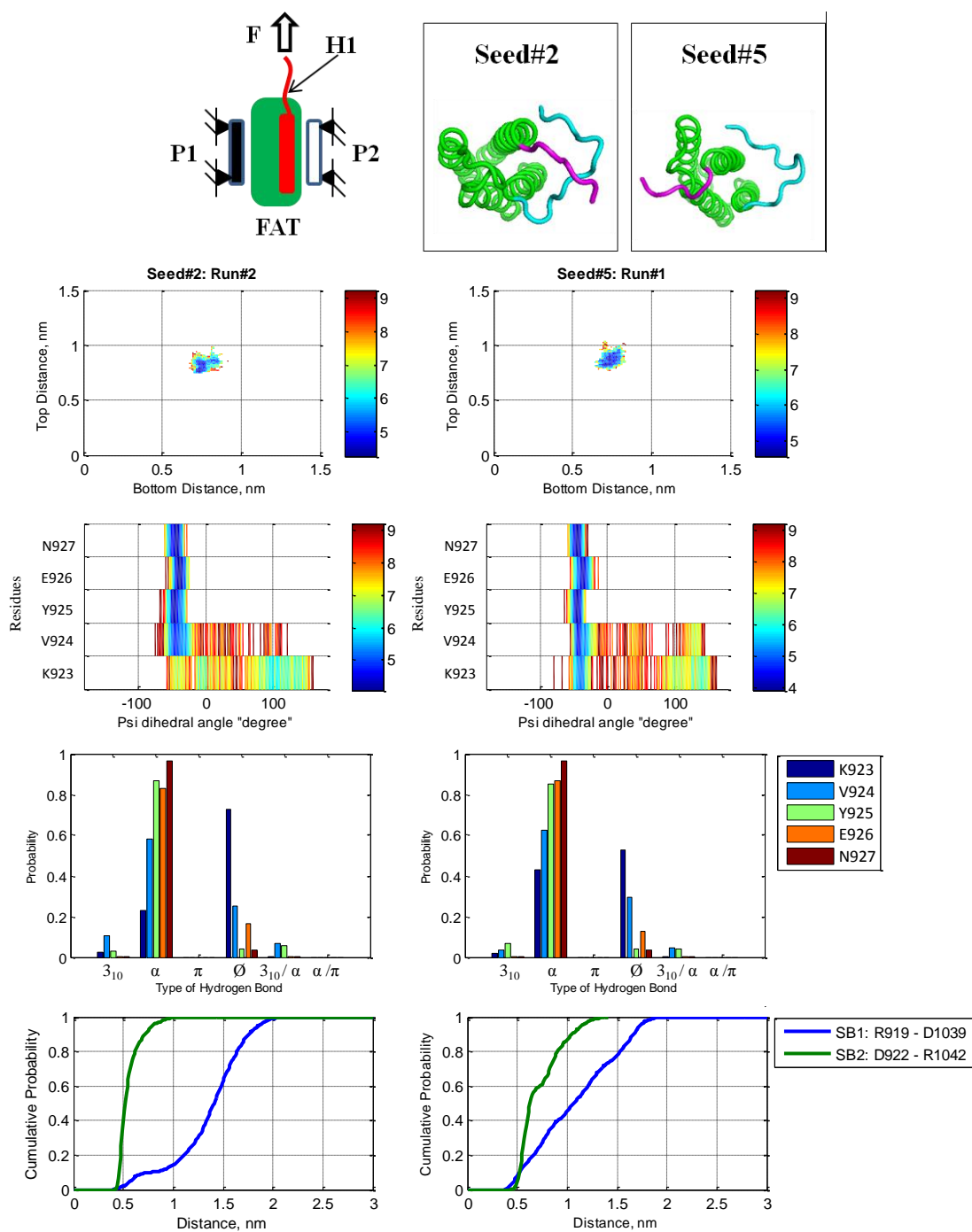


**Figure 4-24: Four different matrices are shown for H1 atypical behavior; H1 position, dihedral angle  $\psi$ , hydrogen bond state and the salt bridge state. (Table 3-1, AX.WT.P1P2).**

Figure 4-25 shows that the structure of the region flanking Y925 in its final state, as well as the probability of the number of interactions formed between the H1/H4 tail. The atypical behaviors of H1/H4 tail are different: one forms  $\beta$ -sheet via number of hydrogen bonds, while in the second, H1/H4 tail are separate. Even when H1/H4 tail share the applied load via forming  $\beta$ -sheet, it does not persist the unfolding of H1. This suggests that the interactions formed between H1/H4 tail might not have a significant effect on holding H1 to the bundle.

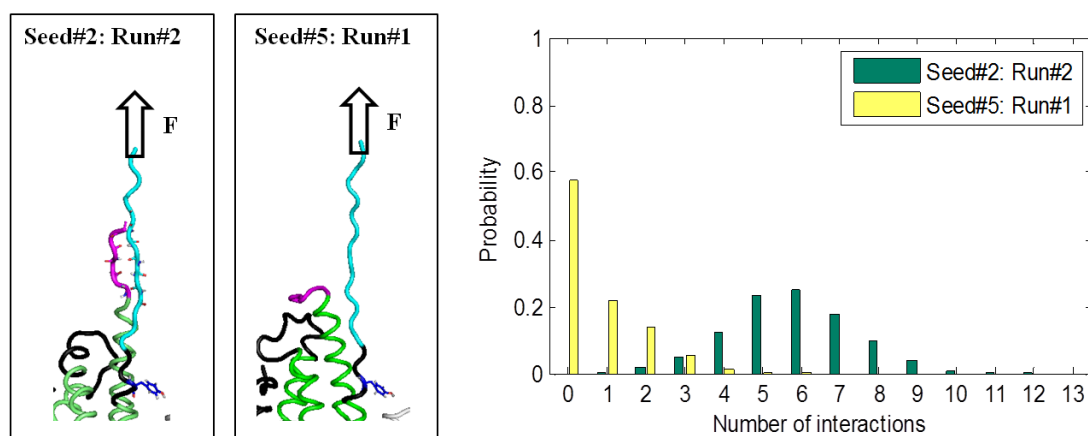


**Figure 4-25: Two types of figure are shown for H1 atypical behavior; final state of the structure of the region flanking Y925, and number electrostatic interactions formed between H1/H4 tail. (Table 3-1, AX.WT.P1P2).**

#### **4.2.1.3 Axial Load Scenario Result Summary**

For axial load scenario, a total of 200 ns simulation time was run. All simulations starts with different initial conditions (seeds, equilibration process and initial velocities). In general, none of these simulations shows that H1 comes out of the bundle. Also, there is a low propensity of the second residue (V924, besides K923) to unfold while all other residues are stable in a helical form. The two salt bridges are broken more often. H1/H4 tail prefer to interact with each other. In more than 80% of the simulations ran, the H1/H4 tail stay entangled via hydrogen and/or electrostatic interactions.

In some simulations, the salt bridges are broken and H1/H4 tail are separate, however, H1 is attached to the bundle. It has been suggested that in addition to the salt bridges, hydrophobic interactions (between highly hydrophobic residues, e.g., Val, Leu, and Ile) between H1 and the bundle create an energy barrier preventing H1 from leaving the bundle (Figure 4-26). They could be important in holding H1 to the bundle.

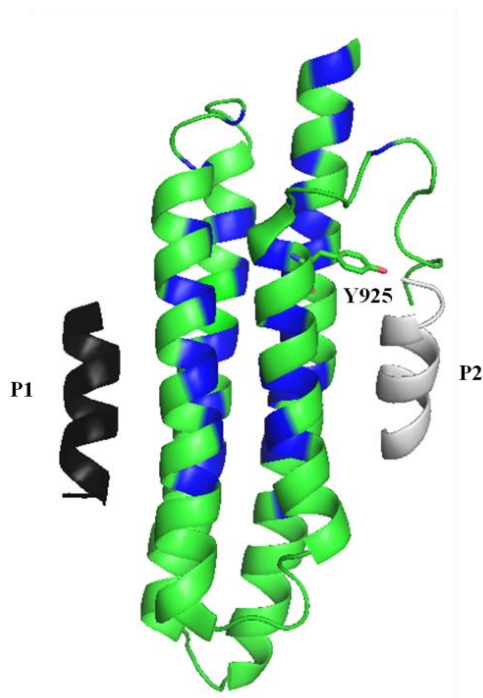


**Figure 4-26: Highly hydrophobic residues between H1 and the bundle. The blue colored residues are either Val, Leu, or Ile. These residues create the hydrophobic core that may be responsible for holding H1 to the bundle.**

Under 100 pN axial load applied to N-terminus to H1 tail, H1 does not appear to have a propensity to leave the bundle. The region flanking Y925 prefers to stay in a helical form. As discussed before, for Y925 phosphorylation, H1 has to leave the bundle and adopt  $\beta$ -strand conformation. So, it seems that the axial load scenario does not appear to have the capacity to promote the required structural changes for making Y925 accessible for phosphorylation.

**Table 4-3: Final state of the structure of the region flanking Y925 for H1 typical and atypical behaviors under constant force applied axially to the N-terminus of H1 tail. (Table 3-1, AX.WT.P1P2).**

	H1 Position		H1 Unfolding			H1/H4 Tail Interactions				H2-H3 Structure	
	In	Out	F	SUF	UN	$\beta$ , EX	$\beta$ , NEX	$\tau$	S	F23	U23
Probability %	10/10	0/10	8/10	2/10	0/10	1/10	4/10	2/8	3/10	8/10	2/10



#### 4.2.2 PERPENDICULAR LOAD SCENARIO RESULTS

Six different initial structures (Seeds, Figure 3-12) were chosen based on the behavior of H1/H4 tail, their relative position to each other, as well as how many interactions they have (Figure 3-11). Each seed was run twice, with different initial velocities (Table 3-1, PR.WT.P1). A 100 pN constant force is applied to the N-terminus of H1 tail in a direction perpendicular to the H1 axis and P1 was constrained. The results of the perpendicular load simulation show two types of H1 behavior: typical and atypical (Table 4-4).

**Table 4-4: H1 typical and atypical behaviors under perpendicular load, applied to the N-terminus of H1 tail and P1 constrained. Nine out of twelve simulations have typical behavior, while three have atypical behavior. (Table 3-1, PR.WT. P1P2).**

Initial Structures		H1 Behavior Type		H1 Behavior Description	
		Typical	Atypical	H1 Position	H1 Unfolding
Seed#1	Run#1	-	Yes	Out of the bundle	In a $\beta$ -strand conformation
	Run#2	Yes	-	In the bundle	In a helical form
Seed#2	Run#1	-	Yes	In the bundle	In a $\beta$ -strand conformation
	Run#2	Yes	-	In the bundle	In a helical form
Seed#3	Run#1	Yes	-	In the bundle	In a helical form
	Run#2	Yes	-	In the bundle	In a helical form
Seed#4	Run#1	Yes	-	In the bundle	In a helical form
	Run#2	Yes	-	In the bundle	In a helical form
Seed#5	Run#1	Yes	-	In the bundle	In a helical form
	Run#2	Yes	-	In the bundle	In a helical form
Seed#6	Run#1	-	Yes	In the bundle	The first two residues, K923 and V924, of H1 unfold.
	Run#2	Yes	-	In the bundle	In a helical form

##### 4.2.2.1 H1 Typical Behavior

Nine simulations out of twelve have nominally the same H1 behavior (Table 4-4). These nine simulations started with different initial conditions (seeds and initial

velocities). Regardless of the differences in their initial conditions, the behavior of H1 is very similar. The typical behavior of H1 is similar to its behavior under equilibrium.

#### ***4.2.2.1.1 H1 Position***

Figure 4-27 shows the blue-colored regions (minima) of the H1 position have small distribution. For all different initial conditions applied, the relative position of H1 to the bundle is very stable, which means H1 does not appear to have a propensity to leave the bundle. As discussed before, electrostatic and hydrophobic interactions between H1 (residues 917-922) and H4 present an energy barrier keeping H1 attached to the bundle. For these simulations, 100 pN constant load applied does not appear to have the ability to overcome this energy barrier. FAT domain tends to move as a rigid body and the 100 pN perpendicular load does not have the capacity to open the FAT domain out.

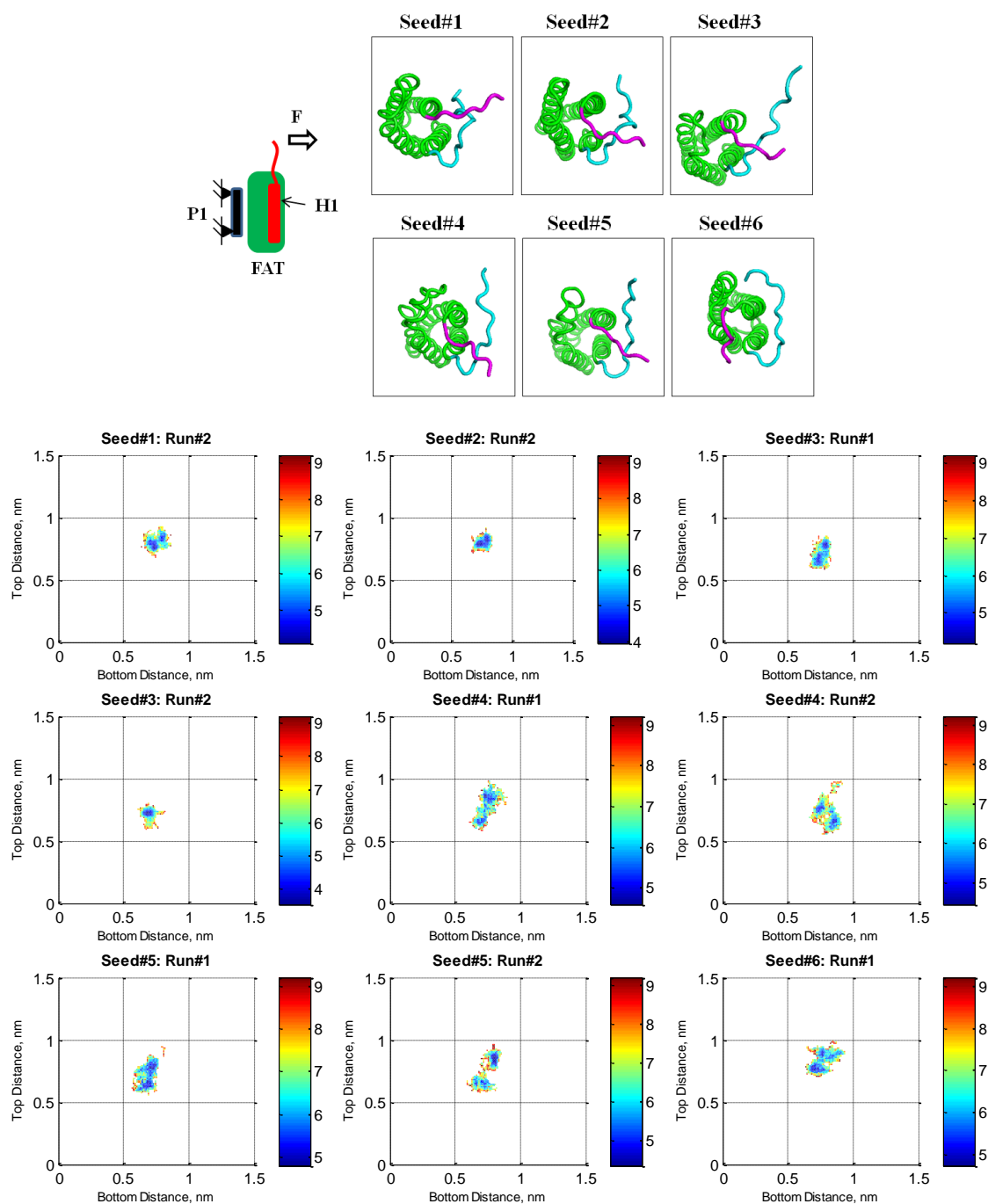


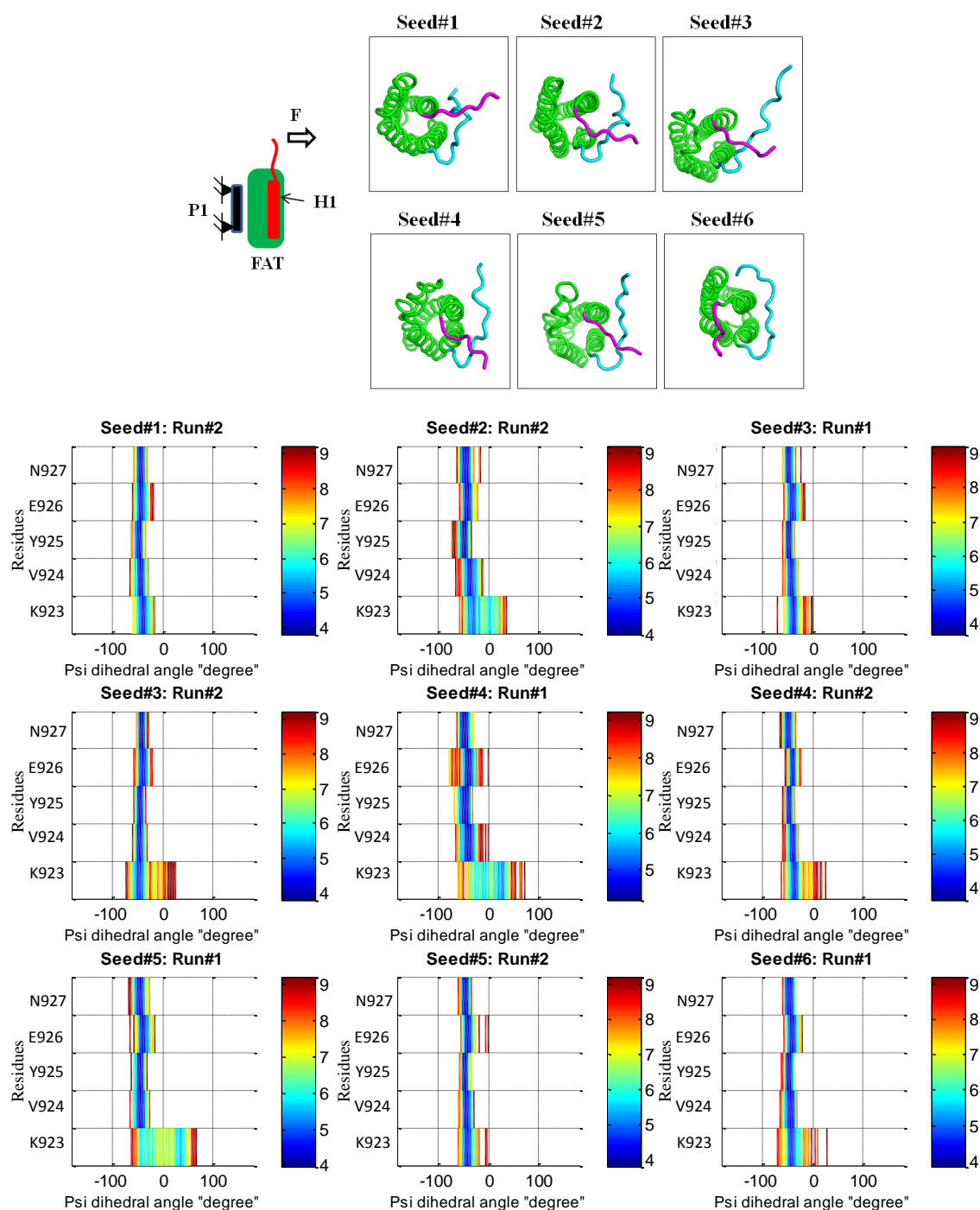
**Figure 4-27: Energy landscape of H1 position represented by  $d_{top}$  and  $d_{bottom}$  in the absence of P2. For typical behavior, H1 position has a small distribution (minima) which means H1 does not appear to have the propensity to leave the bundle under constant force applied to the N-terminus of H1 tail perpendicular to the P1 axis. Each plot represents a simulation time of 20 ns. (Table 3-1, PR.WT.P1).**

#### **4.2.2.1.2 H1 Unfolding**

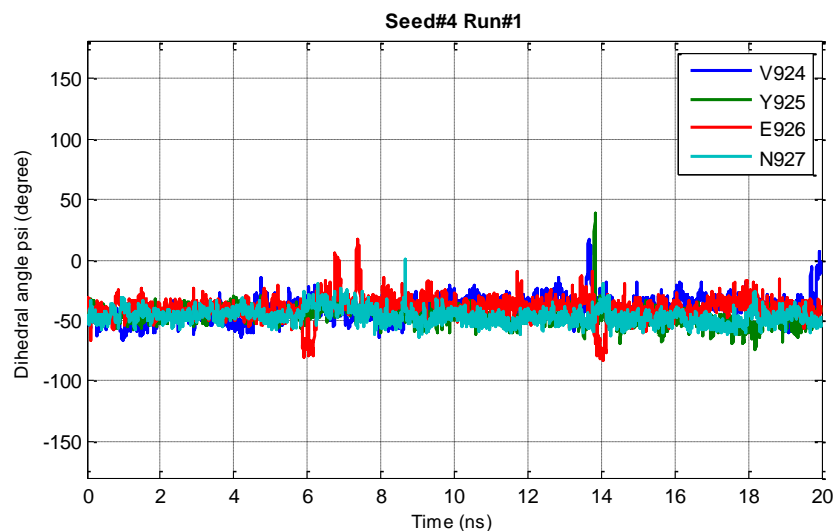
##### **4.2.2.1.2.1 Backbone Dihedral Angle $\psi$**

Figure 4-28 shows that except residue K923, the  $\psi$  angles of the other top four residues of the H1's N-terminal (V924, Y925, E926, and N927) have a small distribution (the mean value is  $\sim -50^0$  degree). This means they are folded in a helical form. However, the first residue at the N-terminus of H1 (K923) is expected, as discussed before, to have a greater flexibility, since it connects with H1 tail (i.e., H1 tail is free to move). The flexibility of K923 does not affect the stability of the other residues flanking Y925. This figure also shows that in Seed#4 Run#1, the residue V926 is the most damaged one. However, Figure 4-29 shows that the residues V926 refolded back after the unfolding and they do not stay unfolded.

For all simulations had been discussed, the region flanking Y925 does not appear to have the propensity to adopt  $\beta$ -strand conformation. Even residue K923 has a propensity to unfold, all other residues are stable and not affected by its flexibility. This means H1 has a high resistance to any structural rearrangements needed for making Y925 accessible for phosphorylation.



**Figure 4-28: Energy landscape of the dihedral angle  $\psi$  of the five N-terminal residues of H1 (K923, V924, Y925, E926, and N927) in the presence or the absence of P2 for H1 typical behavior. Except N923 that have greater flexibility, since it connects with the floppy tail (H1 tail),  $\psi$  angle of other residues have a small distribution (minima). This means H1 does not appear to have the propensity to adopt  $\beta$ -strand conformation under constant force applied to the N-terminus of H1 tail perpendicular to the P1 axis. Each plot represents a simulation time of 20 ns. (Table 3-1, PR.WT.P1).**



**Figure 4-29: Dihedral angle  $\psi$  of the four N-terminal residues of H1 (V924, Y925, E926 and N927) versus time in absence of P2. For Seed#4 Run#1, the  $\psi$  angle of V924 and E926 shows that they refold after unfolding (Table 3-1, PR.WT.P1).**

#### 4.2.2.1.2.2 Hydrogen Donor-Acceptor Pairs

Figure 4-30 shows the probability of different hydrogen bond types formed by the first five residues at the N-terminal of H1 (K923, V924, Y925, E926, and N927). Most the time, they form an  $\alpha$ -helix hydrogen bond type for any different initial conditions applied. The  $\pi$  and  $3_{10}$ -helix hydrogen bond type formed very rarely. The hydrogen bond of K923 is broken about  $\sim 50\%$  of the time. However, the hydrogen bonds of other four residues are broken about 3  $\sim$  15% of the time. The residue K923 is expected to have more broken hydrogen bond since it connects to the H1 tail.

Hydrogen donor-acceptor pairs metric is useful in examining the propagation of the unfolding, if any. Based on what Figure 4-30 shows, the unfolding of K923, in most of the simulations, does not propagate into the other four residues where they are stable.

Neither thermal fluctuation nor 100 pN load appear to excite the region flanking Y925 and promote the needed conformational rearrangements for the phosphorylation.

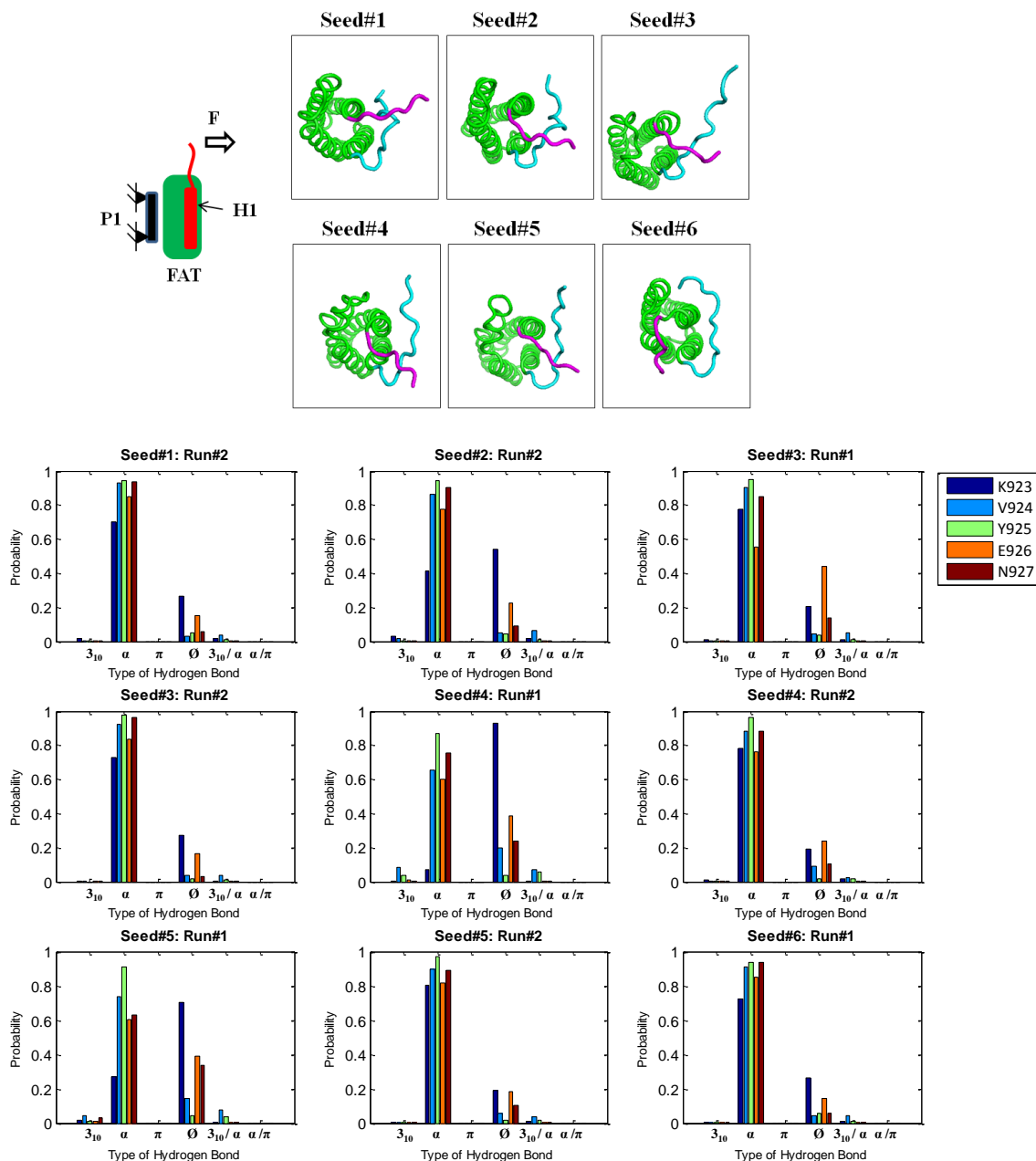


**Figure 4-30: Hydrogen bonds types formed in the absence of P2. For H1 typical behavior, H1 primarily forms an  $\alpha$ -helix. Each plot represents a simulation time of 20 ns. (Table 3-1, PR.WT.P1).**

#### ***4.2.2.1.3 Salt Bridges between H1 Tail and H4***

Figure 4-31 shows the wide distribution of distances between residues that formed the two salt bridges (SB1: R919-D1039, SB2: D922–R1042). This wide distribution of the distance means they are broken most the time. The first salt bridge (SB1) has a wider distribution than the second one (SB2), which is because of the load applied to H1 tail. The H1 tail is pulled in a direction that breaks the first salt bridge more often and pulls the residue, N916, that sometime interacts with R1042, making the second salt bridge more stable. (Figure 4-31). The applied load makes the first salt bridge weaker and the second salt bridge stronger.



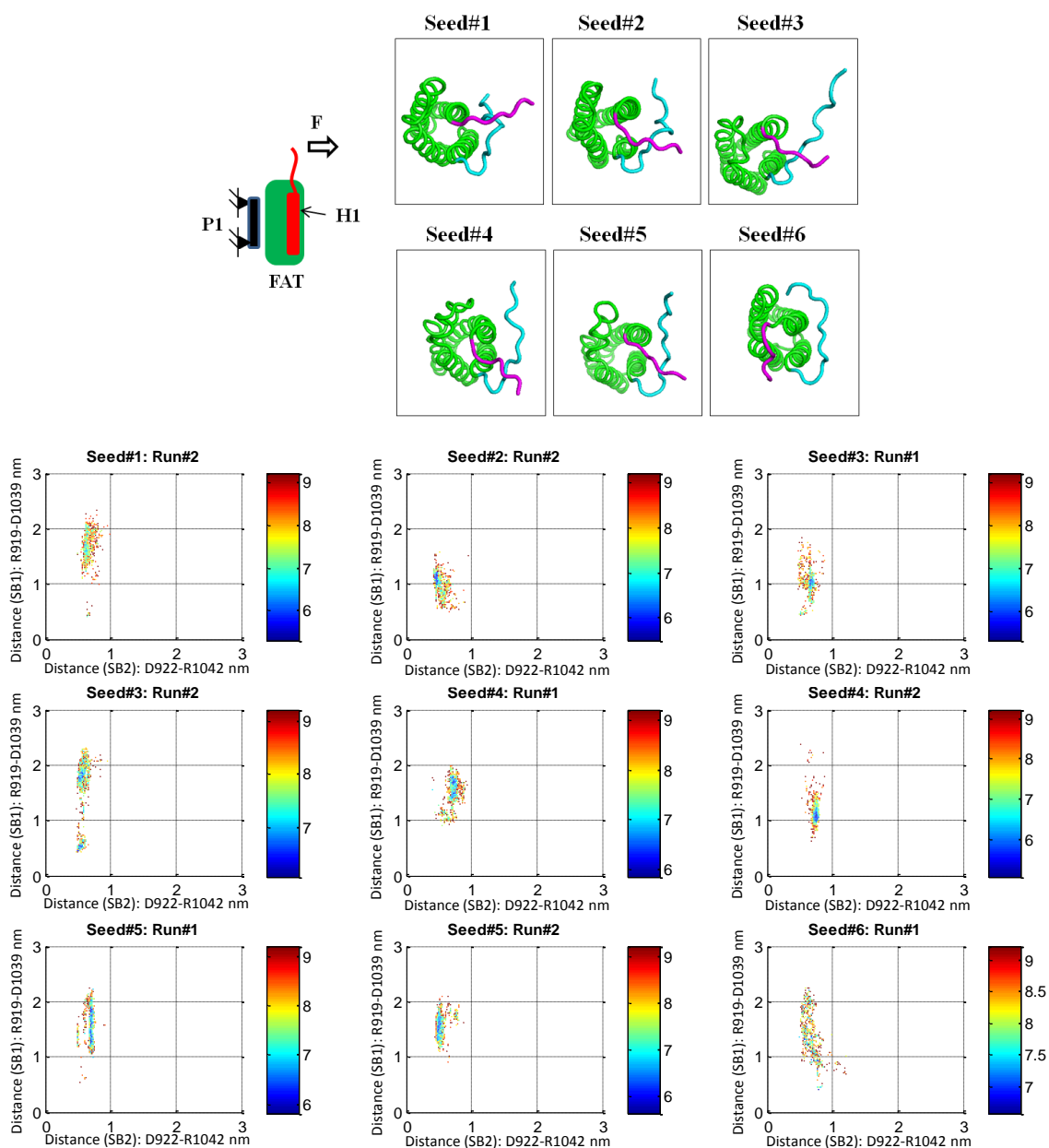


**Figure 4-31: Energy landscape of the H1/H4 salt bridge distances represented by SB1 (R919–D1039) and SB2 (D922–R1042). SB1 and SB2 have a wide distribution which means they are broken. This suggests that they are not primarily responsible for keeping H1 folded within the bundle. Each plot represents a simulation time of 20 ns. (Table 3-1, PR.WT.P1).**

As seen in Figure 4-32, if the salt bridge distance must be less than 0.5 nm, then the first salt bridge, SB1: R919–D1039, is broken most the time, whereas the second one, SB2: D922–R1042, persists 30% of the time. Under the influence of the perpendicular load, the relative position of H1 tail to the bundle increases, which makes the first salt bridge break more of time and point the residue, D922, to R1042 closer than N916 (Figure 4-20).

However, as discussed before, these salt bridges have been suggested, among other factors, to be responsible of maintaining relative position of H1 with the bundle. This result suggests that it does not appear that these salt bridges have a significant role in keeping H1 attached to the bundle. In addition, salt bridge metric suggests that the strength of the interactions between the residues are affected by the applied load which is consistent with the axial load results.

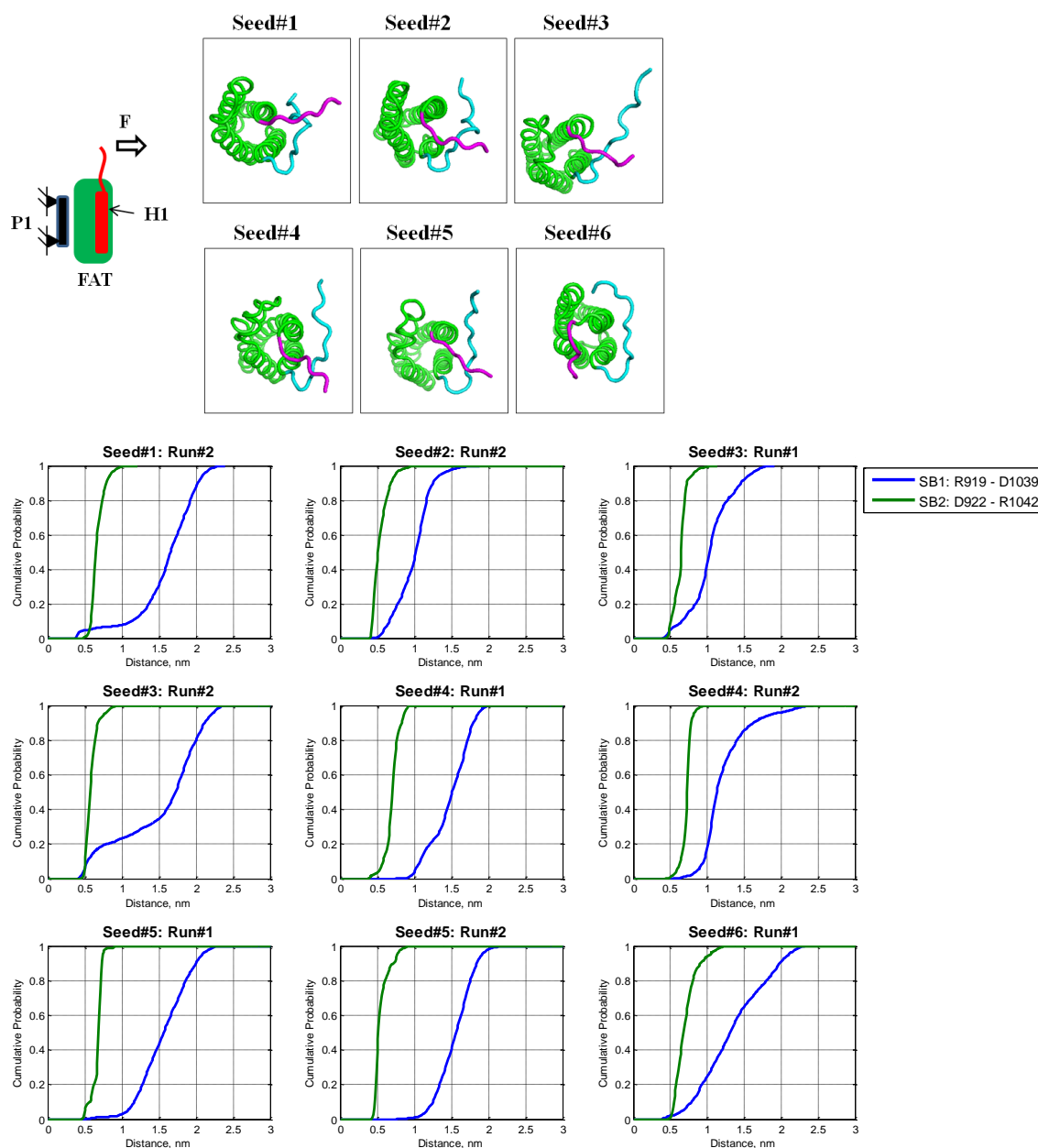


**Figure 4-32: Cumulative probability of the two salt bridges represented for two distances, SB1 (R919-D1039) and SB2 (D922-R1042). If the salt bridge distance has to be less than 0.5 nm, it means they are broken ~70%. This suggests that they are not primarily responsible for keeping H1 folded within the bundle. Each plot represents a simulation time of 20 ns. (Table 3-1, PR.WT.P1).**

#### 4.2.2.1.4 H1/H4 Tail Interaction

Figure 4-33 shows how many interactions formed between the H1/H4 tail. The number of H1/H4 tail interactions is widely distributed, in which Seed#3 Run#2 and Seed#6 Run#1 are different than the others. In these two simulations, H1/H4 tail have almost no interactions, where their initial structures are different in terms of H1/H4 tail behavior. In Seed#3, they interact with each other, while in Seed#6, they are separate. In second runs of Seed#1 and Seed#5, H1/H4 tail have 1~3 electrostatic interactions in between while in other five simulations, H1/H4 tail are entangled through 4 ~7 electrostatic interactions. In Seed#3, Run#2 and Seed#6, Run#1, even the two salt bridges are broken and the H1/H4 tail are separate, H1 is strongly attached to the bundle in a helical form. This suggests that there are another factors that holding H1 to the bundle which is hydrophobic interactions that has been discussed § 4.2.1.3 Axial Load Result Summary.

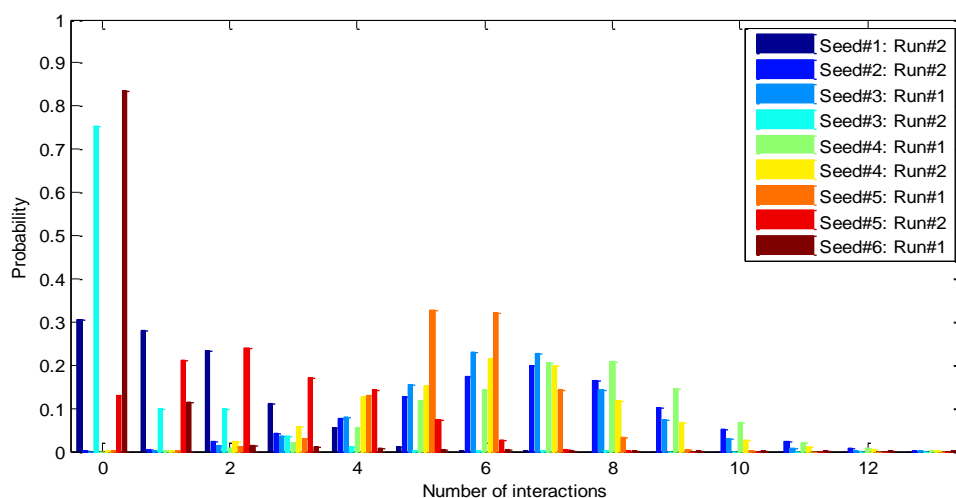


**Figure 4-33: Number electrostatic interactions formed between H1/H4 tail. The interactions between H1/H4 have a wide distribution which means H1/H4 tail prefer to entangled. Each bar represents a simulation time of 20 ns. (Table 3-1, PR.WT.P1).**

#### 4.2.2.1.5 *FAT Structure in its Final States*

Table 4-5 shows show the FAT structure's final states in terms of H position, H1 unfolding, H1/H4 tail interactions and H2-H3 structure. For 100% of the nine simulations, H1 stays folded in the bundle. In more than 50% of the simulations, H1/H4 tail form  $\beta$ -sheet via a number of hydrogen bonds. In about 25%, they are entangled via number of electrostatic interactions. This suggests that H1/H4 tail prefer to interact with each other more often. In two simulations (Seed#3, Run#2 and Seed#6, Run#1), H1/H4 tail are mostly separate. (H1/H4 tail interactions are listed in (Appendix D). In these two simulations, H1 stays folded in the bundle, which suggests that H1/H4 tail does not appear to be the key regulator of resisting H1 unfolding or keeping H1 attached to the bundle.

**Table 4-5: Final state of the structure of the region flanking Y925 for H1 typical behavior under constant force applied perpendicularly to the N-terminus of H1 tail. (Table 3-1, PR.WT.P1).**

	H1 Position		H1 Unfolding			H1/H4 Tail Interactions				H2-H3 Structure	
	In	Out	F	SUF	UN	$\beta$ , EX	$\beta$ , NEX	$\tau$	S	F23	U23
Probability %	9/9	0/9	9/9	0/9	0/9	0/9	5/9	2/8	2/9	7/9	2/9

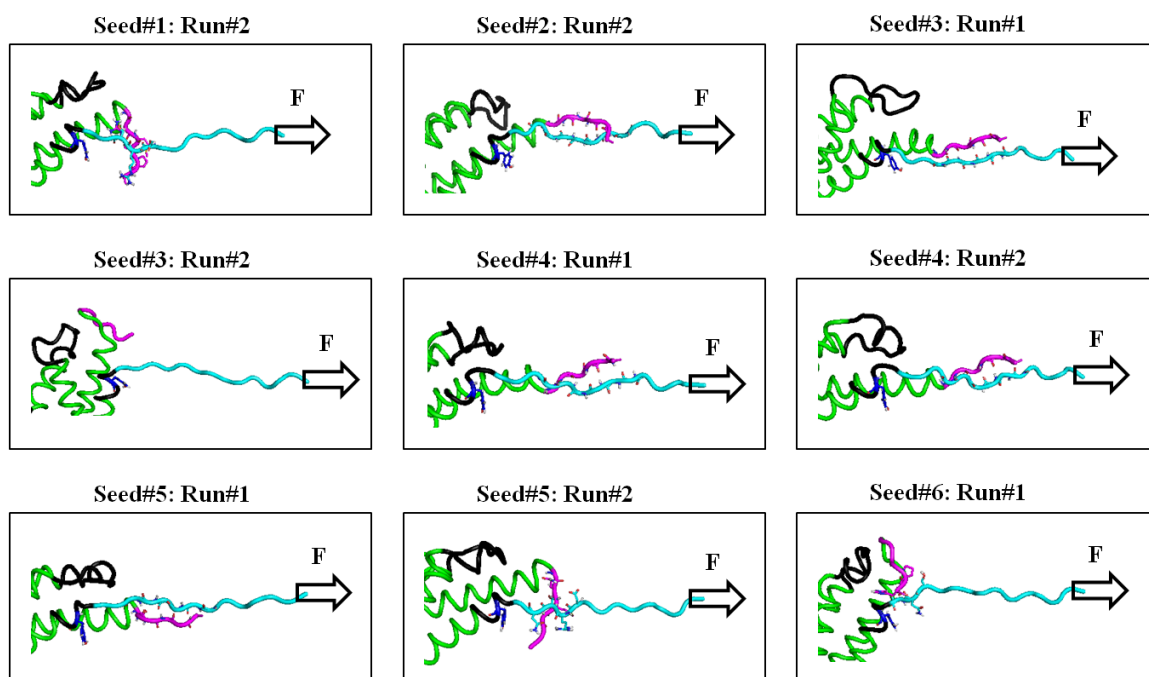


**Figure 4-34: Final state of the structure of the region flanking Y925 for H1 typical behavior under constant force applied perpendicularly to the N-terminus of H1 tail. (Table 3-1, PR.WT.P1).**

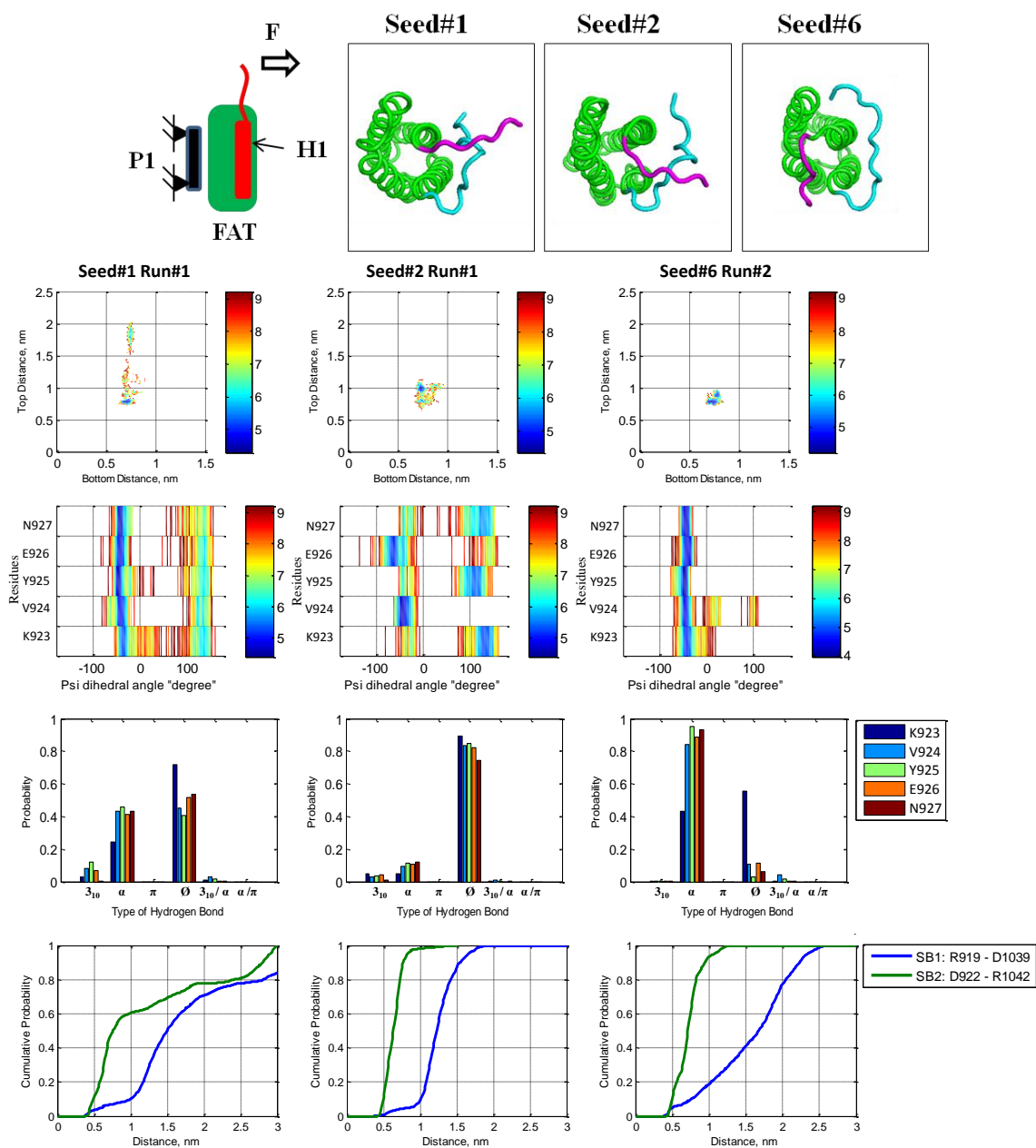
#### 4.2.2.2 H1 Atypical Behavior

Figure 4-35 shows four different metrics: H1 position, dihedral angle  $\psi$ , hydrogen state and salt bridge state. For two simulations (Seed#2, Run#1 and Seed#2, Run#1), the relative position of H1 has a small distribution (blue-colored region) which means H1 is attached to the bundle. However, in Seed#1, Run#1, the top distance between H1 and neighbor helices has a wide distribution. For this simulation, Figure 4-36 shows that the top distance between H1 and neighbor helices increases rapidly which means H1 come out of the bundle.

Also, in Seed#1, Run#1 and Seed#2, Run#1, the  $\psi$  angle of the top five residues unfolded and reach  $170^\circ$ , which means they adopt  $\beta$ -strand conformation. In Seed#6 Run#1, only the top two residues of H1 (K923 and V924) have a propensity to unfold while the others remain folded.

In Seed#1, Run#1 and Seed#2, Run#1, the hydrogen bonds of the top five residues of H1 are mostly broken. Whereas, in Seed#6, Run#1, the unfolding of the first two residues of H1 (K923, V924) does not propagate into the other residues. In addition, for all the three simulations, the salt bridges are broken more often.

In only one simulation, atypical behavior of H1 achieved the required structural changes needed for Y925 phosphorylation, where H1 leaves the bundle and adopt  $\beta$ -strand conformation.



**Figure 4-35: Four different matrices are shown for H1 atypical behavior; H1 position, dihedral angle  $\psi$ , hydrogen bond state and the salt bridge state. (Table 3-1, PR.WT.P1).**



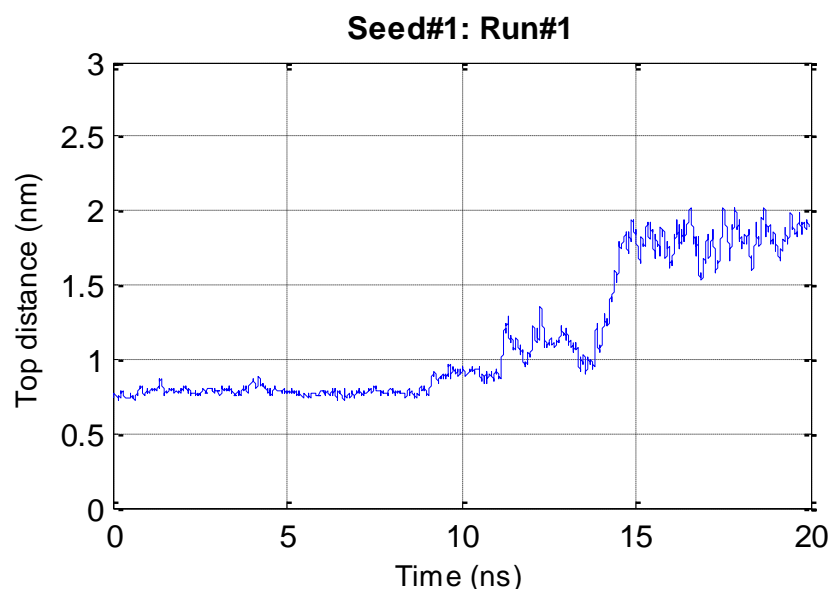


**Figure 4-36: H1 position represented by  $d_{top}$  versus time for H1 atypical behavior. The  $d_{top}$  increases rapidly as H1 leaves the bundle.**

Figure 4-37 shows that the structure of the region flanking Y925 in its final state, as well as the probability of the number of interactions formed between the H1/H4 tail. The atypical behaviors of H1/H4 tail are different: in one simulation, they form  $\beta$ -sheet via number of hydrogen bonds (Seed#2, Run#1), while in two other simulations (Seed#1, Run#1 and Seed#6, Run#2), the H1/H4 tail are separate.

Even when H1/H4 tail share the applied load via forming  $\beta$ -sheet, H1 does not come out of the bundle. Moreover, H1 stays in the bundle while H1/H4 tail are separate. This suggests that the interactions formed between H1/H4 tail might not have a significant effect on holding H1 to the bundle.

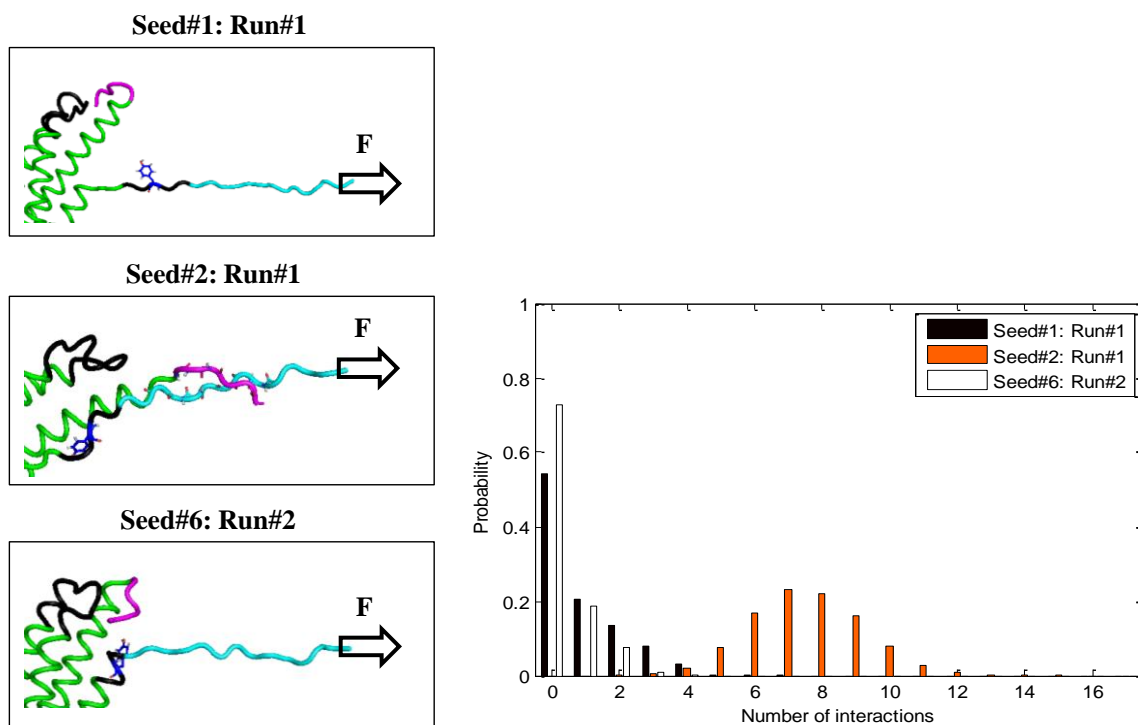


**Figure 4-37: Two types of figure are shown for H1 atypical behavior; final state of the structure of the region flanking Y925, and number electrostatic interactions formed between H1/H4 tail. (Table 3-1, PR.WT.P1).**

Since Seed#1 shows one simulation that FAT undergoes the required structural rearrangement needed for Y925 phosphorylation, it is important to run more simulations for this seed with different initial velocities. The goal is to examine the repeatability of the atypical type of behavior in which H1 is out of the bundle and it adopts a  $\beta$ -strand conformation.

#### 4.2.2.3 Repeatability of H1 Atypical Behavior

Under mechanical load applied perpendicular to the N-terminus of H1 tail, nine more simulations of Seed#1 were run to examine the repeatability of the atypical

behavior of H1, where the region flanking Y925 adopts  $\beta$ -strand and comes out of the bundle.

#### ***4.2.2.3.1 H1 Position***

As seen in Figure 4-38, the blue-colored regions (minima) of the H1 position have small distribution. For all different initial velocities applied, the relative position of H1 to the bundle is very stable. This means H1 prefers to be within the bundle and atypical behavior, where H1 comes out of the bundle, is not repeatable. This emphasizes how strong the energy barrier that keeps H1 within the bundle.

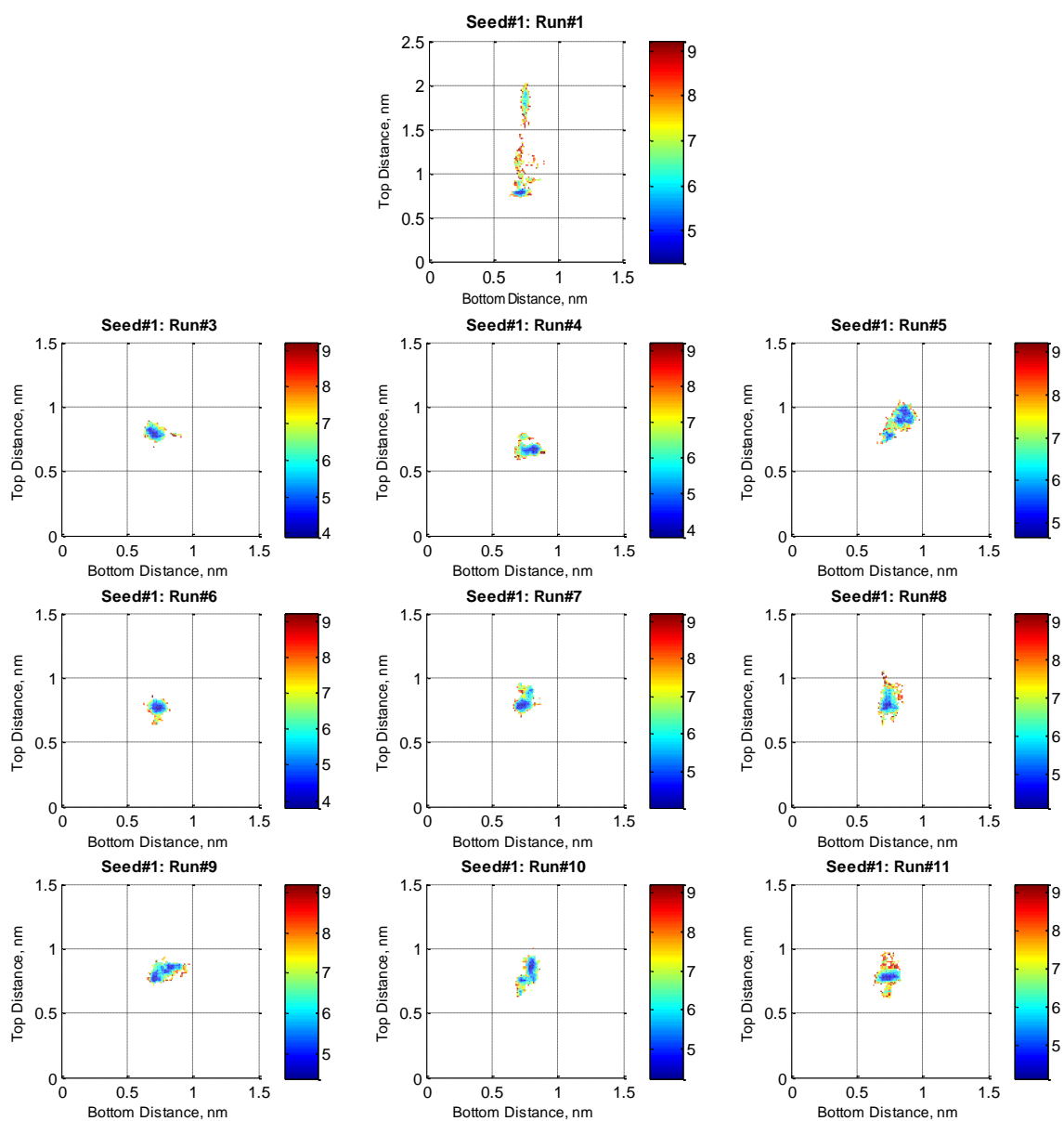


**Figure 4-38: Energy landscape of H1 position represented by  $d_{top}$  and  $d_{bottom}$ . Looking to the repeatability of H1 atypical behavior found in Seed#1 Run#1, H1 position has a small distribution (minima) which means H1 does not appear to have the propensity to leave the bundle under constant force applied to the N-terminus of H1 tail perpendicular to the P1 axis. The H1 atypical behavior is not repeatable in terms of H1 position. Each plot represents a simulation time of 20 ns. (Table 3-1, PR.WT.P1).**

#### **4.2.2.3.2 H1 Unfolding**

##### **4.2.2.3.2.1 Backbone Dihedral Angle $\psi$**

As in Figure 4-39, the  $\psi$  angle of the top five residues (except K923) for six different simulations, has small distribution which means they have the capacity to keep their helical conformations. In Seed#1, Run8, only the first two residues have the propensity to unfold, while other residues are very stable. In Seed#1, Run#10, only three residues out of five have the propensity to unfold. In general, it appears that the atypical behavior of H1, where the region flanking 925 adopts  $\beta$ -strand conformation, is not repeatable.

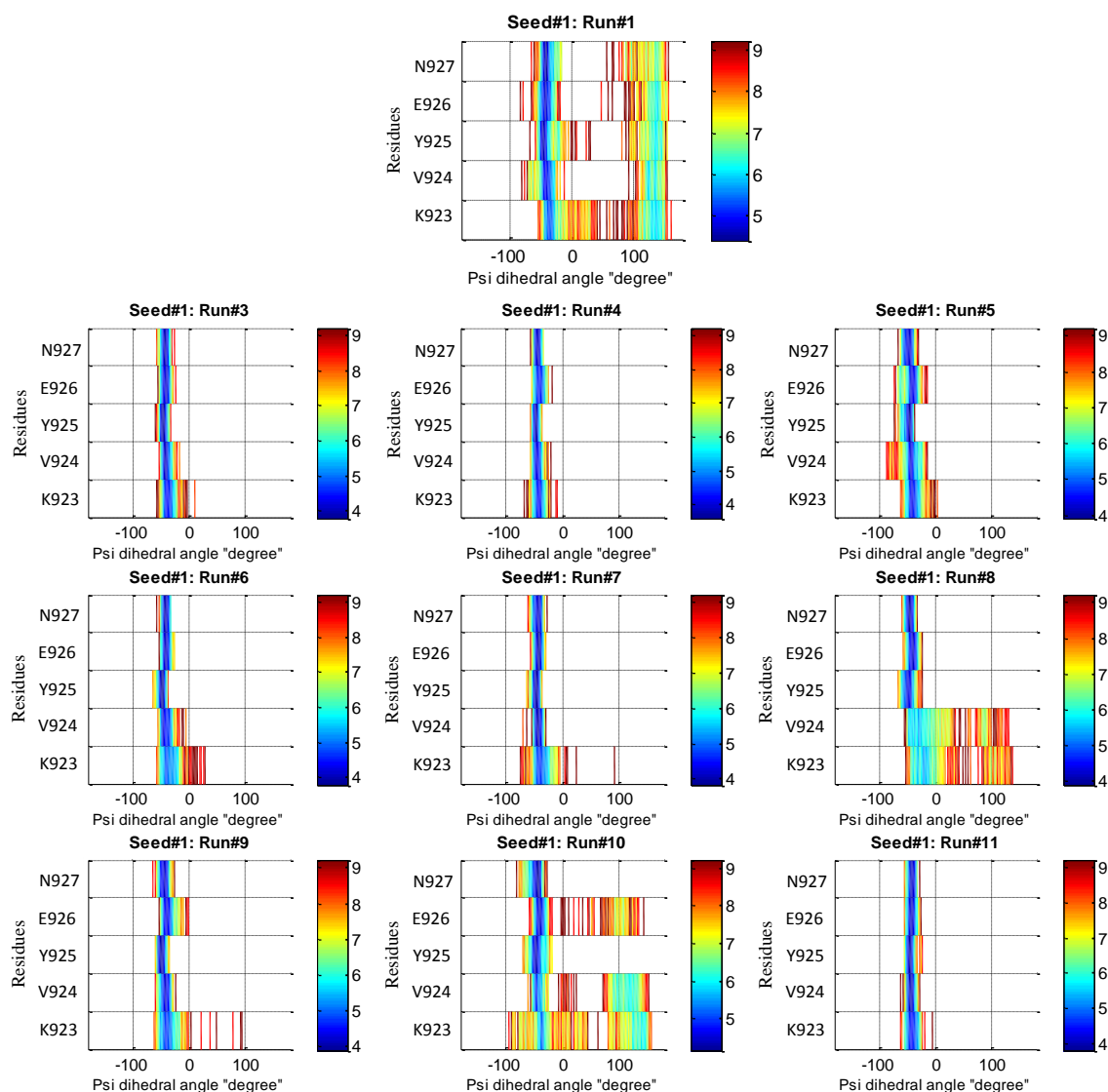


**Figure 4-39: Energy landscape of the dihedral angle  $\psi$  of the five N-terminal residues of H1 (K923, V924, Y925, E926, and N927) in the presence or the absence of P2 for H1 atypical behavior repeatability. Except Seed#1, Run#8 and Seed#1, Run#10,  $\psi$  angle have a small distribution (minima), which means H1 atypical behavior is not repeatable in terms of adopting a  $\beta$ -strand. For Seed#1, Run#8 and Seed#1, Run#10, some residues have a tendency to unfold (Seed#1, Run#8: V924, Seed#1, Run#10: V924 and E926). (Table 3-1, PR.WT.P1).**

#### 4.2.2.3.2.2 Hydrogen Donor-Acceptor Pairs

Figure 4-43 shows that the only simulation that has similarity with atypical behavior is Seed#1, Run#10, in which the hydrogen bonds of the first five residues are broken are mostly broken. Otherwise, in the other simulations the first five residues of H1 form  $\alpha$ -helix hydrogen bond type. This supports the previous results that suggest the atypical behavior is not repeatable.

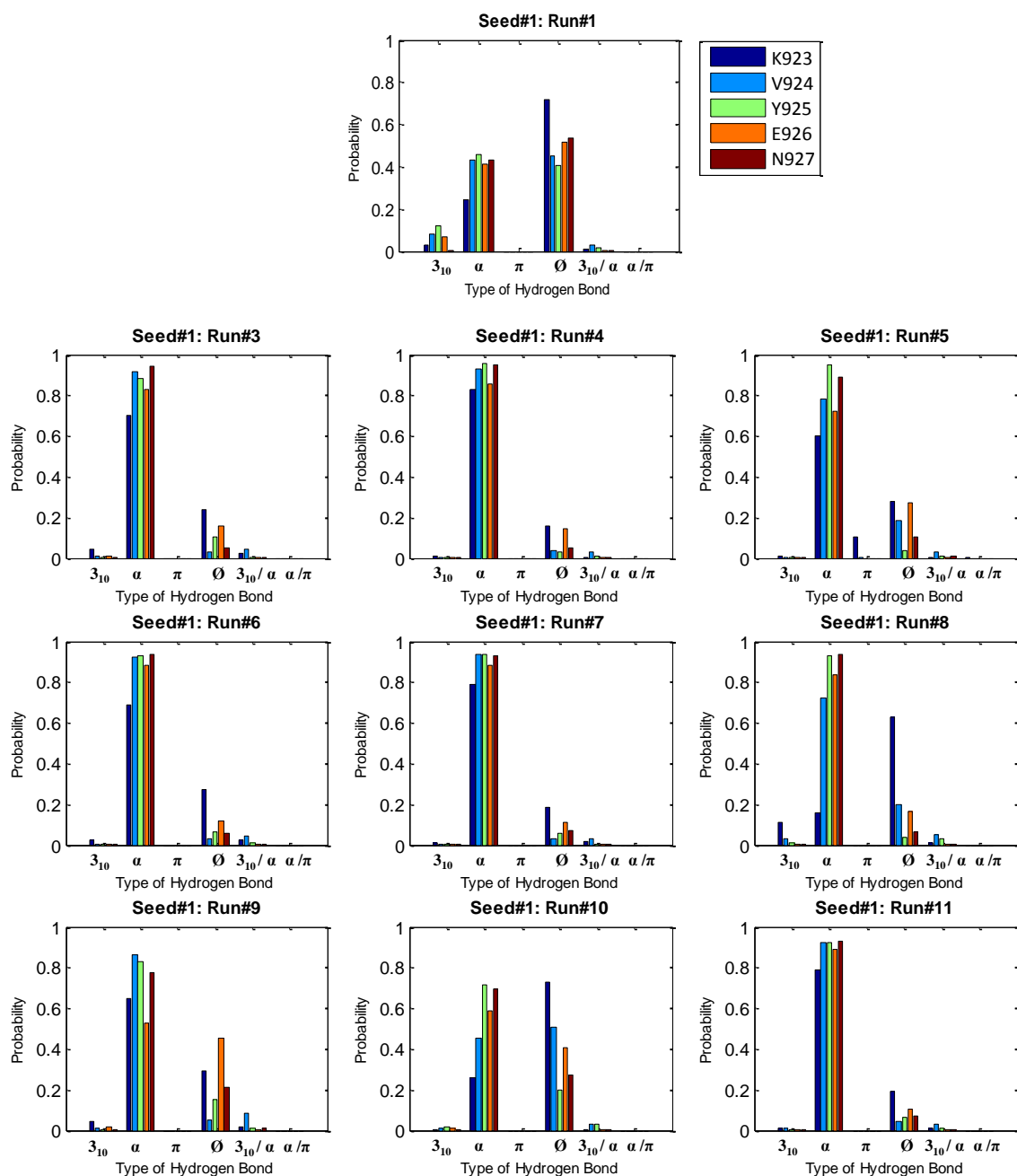


**Figure 4-40: Hydrogen bonds types formed in the absence of P2. For the repeatability of H1 atypical behavior and except Seed#1, Run#10, H1 primarily forms an  $\alpha$ -helix. In general, the H1 atypical behavior is not repeatable in terms of the hydrogen broken. Each plot represents a simulation time of 20 ns. (Table 3-1, PR.WT.P1).**



### 4.2.2.3.3 Salt Bridges between H1 Tail and H4

As seen in Figure 4-41 and Figure 4-42, the wide distribution of the two salt bridge distances suggests that they are broken most the time. This is consistent with the previous results that these salt bridges are not the key regulator of holding H1 to the bundle.

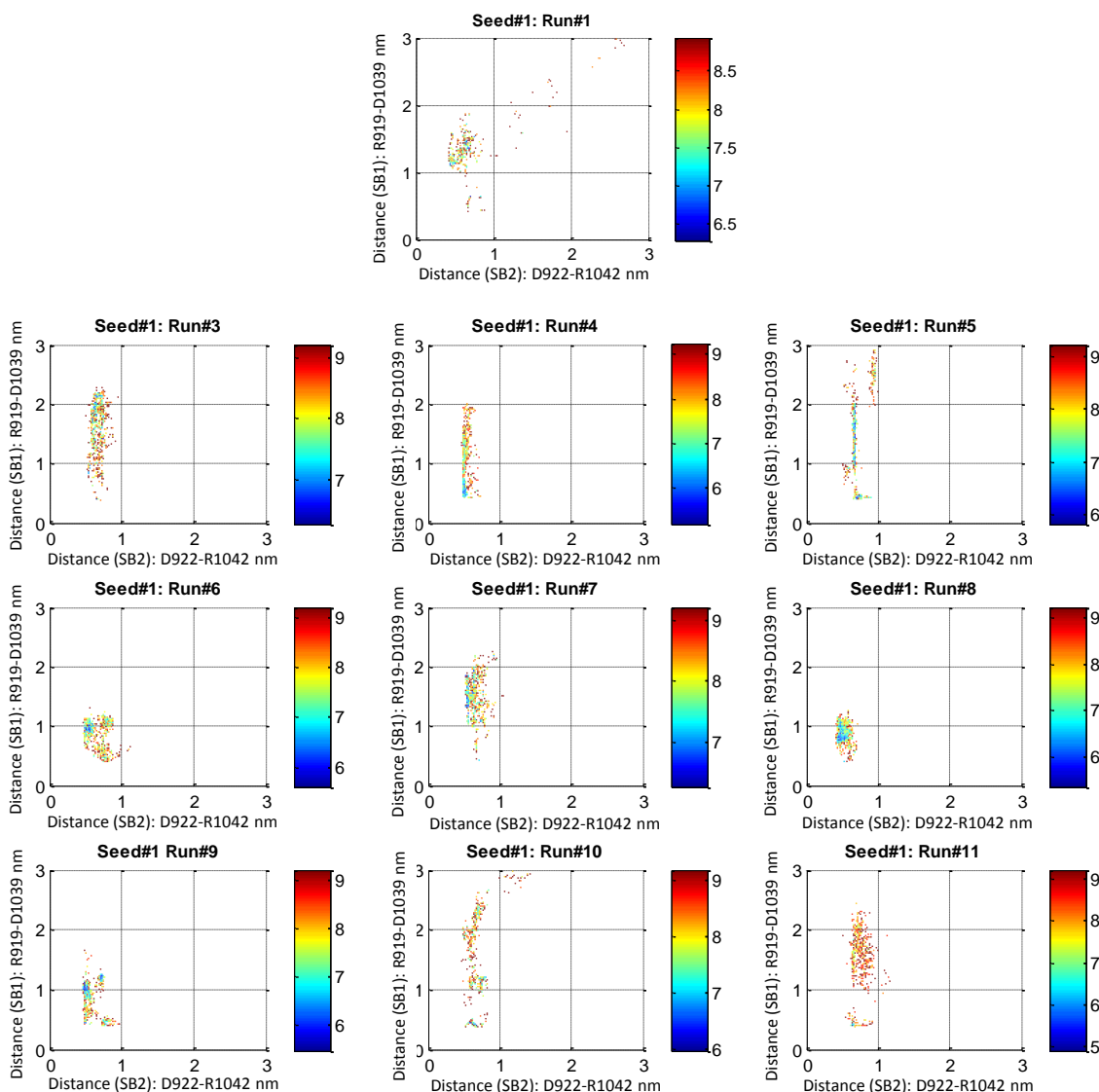


**Figure 4-41: Energy landscape of the H1/H4 salt bridge distances represented by SB1 (R919–D1039) and SB2 (D922–R1042). SB1 and SB2 have a wide distribution which means they are broken. This suggests that they are not primarily responsible for keeping H1 folded within the bundle. Each plot represents a simulation time of 20 ns. (Table 3-1, PR.WT.P1).**

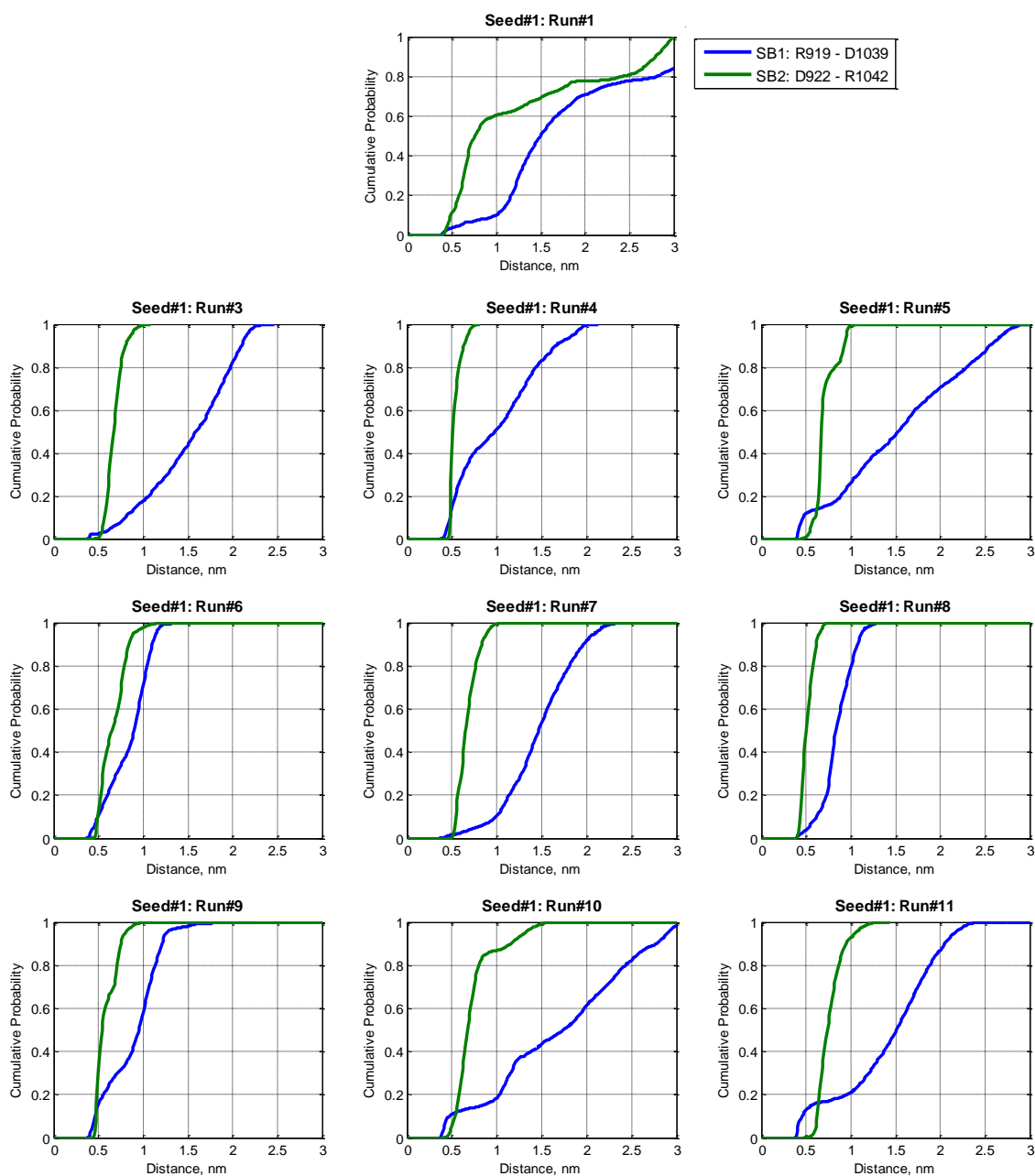


**Figure 4-42: Cumulative probability of the two salt bridges represented for two distances SB1 (R919–D1039) and SB2 (D922–R1042). If the salt bridge distance has to be less than 0.5 nm, it means they are broken ~70%. This suggests that they are not primarily responsible for keeping H1 folded within the bundle. Each plot represents a simulation time of 20 ns. (Table 3-1, PR.WT.P1).**

#### 4.2.2.3.4 H1/H4 Tail Interaction

Figure 4-43 shows how many interactions formed between the H1/H4 tail. The number of H1/H4 tail interactions is widely distributed, which means H1/H4 tail prefers to be entangled through either hydrogen bonds or electrostatic interactions. In Seed#1, Run#11, even the two salt bridges are broken, the H1/H4 tail are separate, H1 is strongly attached to the bundle in a helical form. This suggests that they are another factors that holding H1 to the bundle. (discussed § 4.2.1.3 Axial Load Result Summary)

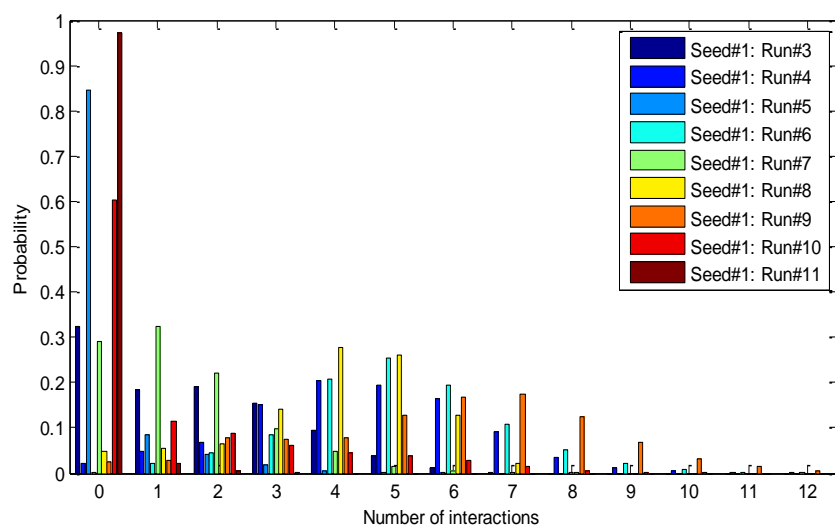


**Figure 4-43: Number electrostatic interactions formed between H1/H4 tail. The interactions between H1/H4 have a wide distribution which means H1/H4 tail prefer to be entangled. Each bar represents a simulation time of 20 ns. (Table 3-1, PR.WT.P1).**

#### 4.2.2.3.5 FAT Structure in its Final States

Figure 4-44 show the FAT structure's final states in terms of H1 position, H1 unfolding, H1/H4 tail interactions and H2-H3 structure. For all nine simulations, H1 stays folded in the bundle. In 30% of the simulations, the H1/H4 tail form  $\beta$ -sheet via a number of hydrogen bonds. In about 20%, they are entangled via number of electrostatic

interactions. This suggests that H1/H4 tail prefer to interact with each other more often. In two simulations (Seed#1, Run#3 and Run#11), the H1/H4 tail are almost separate. (H1/H4 tail interactions are listed in (Appendix D). In these two simulations, H1 stays folded in the bundle, which suggests that H1/H4 tail does not appear to be the key regulator of resisting H1 unfolding or keeping H1 attached to the bundle. In Seed#1, Run#5, the FAT domain disassociates from the paxillin. This type of behavior raises the question of the loading capability of the FAT/paxillin complex. How much the maximum load can be hold by the paxillin needs more investigations.

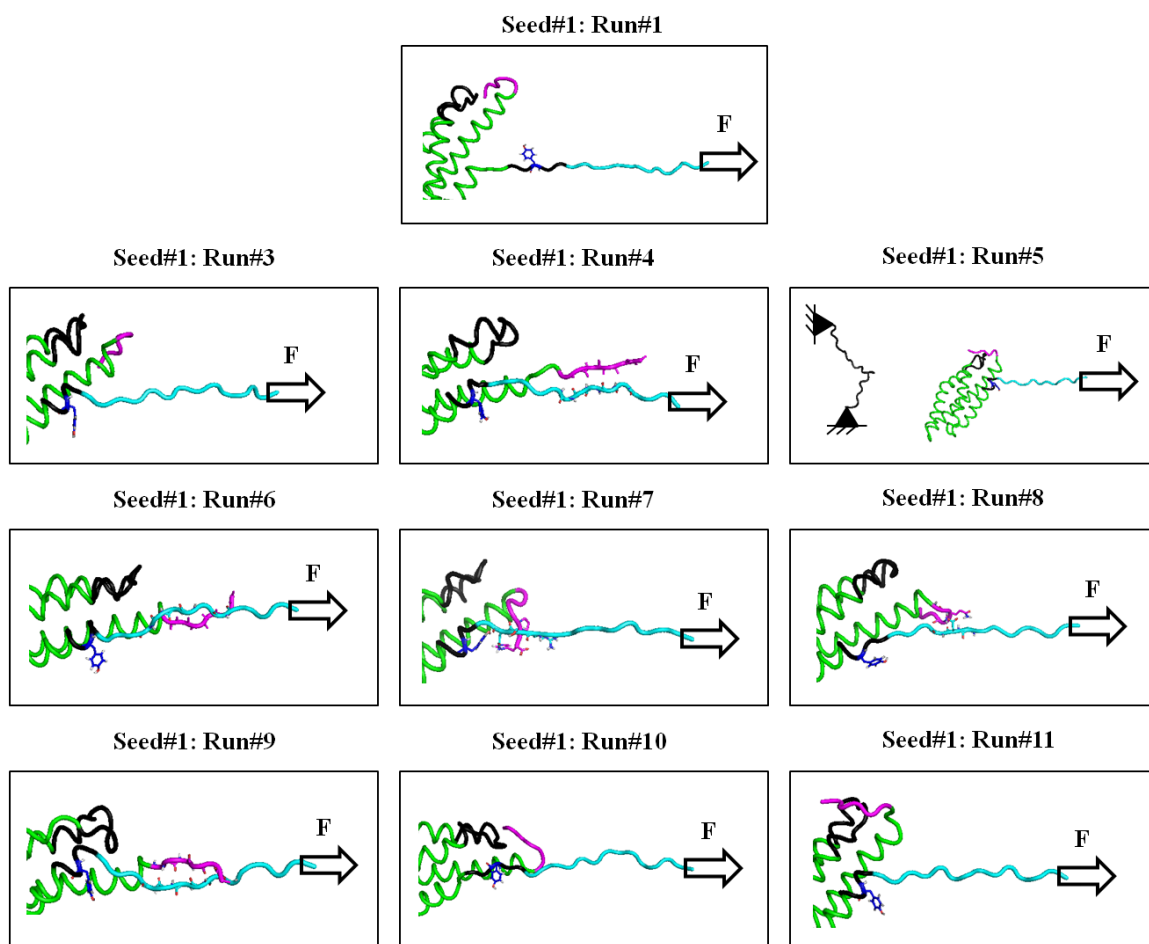


**Figure 4-44: Final state of the structure of the region flanking Y925 under constant force applied perpendicularly to the N-terminus of H1 tail. (Table 3-1, PR.WT.P1).**

#### 4.2.2.4 Perpendicular Load Scenario Result Summary

For perpendicular load scenario, a total of 320 ns simulation time was run. All simulations starts with different initial conditions (seeds, equilibration process and initial velocities). In general, they show H1 has high propensity to be attached to the bundle. Also, H1 prefers to stay in a helical form. In most of the simulations, H1/H4 tail prefer to interact with each other. (See Table 4-6)

In only one simulation, H1 comes out of the bundle and the region flanking Y295 adopts a complete  $\beta$ -strand conformation. The same seed that shows this type of behavior, was run nine additional times with different initial velocities to examine the repeatability of this interesting type of behavior. However, none of the nine simulations shows the same behavior. This illustrates the low appearance of this type of behavior where H1 come out the bundle and the region flanking Y925 adopts  $\beta$ -strand conformation.

In one simulation, the FAT domain disassociates from the paxillin, which raises the question of the loading capability of the FAT/paxillin complex. It is important to examine how much load could paxillin holds.

**Table 4-6: Final state of the structure of the region flanking Y925 for H1 typical and atypical behaviors under constant force applied perpendicularly to the N-terminus of H1 tail. (Table 3-1, PR.WT.P1).**

	H1 Position		H1 Unfolding			H1/H4 Tail Interactions				H2-H3 Structure	
	In	Out	F	SUF	UN	$\beta$ , EX	$\beta$ , NEX	$\tau$	S	F23	U23
Probability	20/21	1/21	16/21	2/21	3/21	1/21	8/21	4/21	8/21	17/21	4/21

## Chapter 5. Conclusions

It has been reported that Y925 in the FAT domain is a critical phosphorylation site, key in cancer initiation and progression. In order for Y925 to be phosphorylated, it has been suggested that H1 has to come out of the bundle and the region flanking this tyrosine residue has to adopt  $\beta$ -strand conformation. What it takes the FAT domain to adopt the hypothesized structure, to engage the phosphorylation, remains unclear. So, it is very important to examine these hypotheses to have better understanding of FAT domain behavior which may contribute in anti-cancer therapy development. To accomplish this, Molecular Dynamics (MD) simulations and Constant Force Molecular Dynamics (CFMD) simulations were run. Two structures were used in the simulation: (i) the FAT/paxillin complex without H4 tail and P1/P2 unconstrained and (ii) the augmented FAT/paxillin complex with H4 tail and P1/P2 constrained. These two structures were used in different cases where the presence/absence of P1 and P2 was varied. All the simulations were run on a variety of initial conditions (different energy minimization and equilibration process, different initial velocities, different initial structures or “seeds”). The behavior of H1 that contains Y925 was examined using four different metrics: H1 position, H1 unfolding, salt bridge state, and H1/H4 tail interactions.

### 5.1 Under Equilibrium, Y925 Phosphorylation Conditions Not Met

**Under thermal fluctuations only, H1 does not appear to have a proclivity to leave the bundle and/or adopt  $\beta$ -strand conformation.** Both two FAT/paxillin structures were used in equilibrium simulation where the presence/absence of P1/P2 was varied. In addition, an isolated H1 helix and an isolated LD4 motif were simulated under

equilibrium conditions. The total equilibrium simulation time is 540 ns. Based on the equilibrium results, H1 is highly attached to the bundle and it does not appear to have a capacity to leave the bundle under only thermal fluctuation. Moreover, H1 does not appear to have propensity to adopt  $\beta$ -strand conformation or at least to unfold under its own thermal vibration. The salt bridges (SB1: R919-D1042, SB2: D922-R1042) between H1 tail and H4 have been suggested, among other factors, to hold H1 to the bundle. However, these two salt bridges are frequently broken which means they are not the key in holding H1 to the bundle. Moreover, in the absence of both LD motifs, H1 is strongly attached to the bundle and remains folded, so the LD motifs do not appear to affect the stability of the FAT domain. The isolated H1 simulation shows that H1 has the propensity to unfold from its C-terminal, keeping in mind that Y925 is located at the N-terminal. The C-terminal of H1 connects to a hinge region (contains two proline residues) that has been suggested to have the ability to promote such H1 unfolding from its C-terminal. In the isolated LD4 simulation, LD motif does have the capacity to keep its helical character. However, in literature, it has been assumed to be in helical form in nature. In summary, under only thermal fluctuation, H1 does not demonstrate the capacity to undergo the required structural rearrangement needed for Y925 phosphorylation. This result, besides the fact that FAK is hypothesized to be mechanically activated, are motivations to examine the influence of the applied load on H1 behavior.

Two applied mechanical load scenarios were chosen: axial and perpendicular. For the constrained axial load scenario, a 100 pN constant load was applied to the N-terminus of H1 tail in a direction parallel to the H1 axis and in the presence of both constrained P1 and P2 which are constrained. This load scenario was chosen based on the assumption



that axial load direction should most efficiently unravel H1. For the perpendicular load scenario, the same load was applied to the N-terminus of H1 in a direction perpendicular to the P1 axis but in the presence of P1 only. This load scenario was chosen based on the idea that P2, which blocks the access to Y925, has to first leave in order for the perpendicular load to open the FAT domain. The total loaded simulation time for the two load scenarios (axial and perpendicular) is 620 ns.

## **5.2 Under Axial Load, Y925 Phosphorylation Conditions Not Met**

**Under axial load, CFMD simulations show high propensity of H1 to stay folded and highly attached.** Moreover, the salt bridges do not appear to have an influence on H1 position or H1 unfolding since they are broken most of the time. Also, the second salt bridge (SB2: D922-R1042) persists longer under the load influence, than in equilibrium, in which it is weaker. This suggests that the interactions found in the crystal structure may not persist in the dynamic in vivo environment. Load may play role in either breaking or supporting the salt bridges. Even by applying 100 pN for a total of 200 ns long, there is no simulation that H1 undergo the hypothesized structure of the FAT domain in which H1 is out of the bundle and the area flanking Y925 adopts a  $\beta$ -strand conformation.

## **5.3 Under Perpendicular Load, Y925 Phosphorylation Conditions Not Met**

**Perpendicular load simulations also show high propensity of H1 to be attached to the bundle as well as retain its helical form.** In addition, the salt bridges do not appear to have an influence on H1 unfolding or the H1 position, as has been found in

axial load scenario. Under either perpendicular or axial load, the behavior of the salt bridges is similar. After applying a 100 pN (in either the axial or perpendicular direction), for a cumulative total of 240 ns long, only one simulation out of 12 simulations adopts the hypothesized structure in which H1 is out of the bundle and the area flanking Y925 adopts a complete  $\beta$ -strand conformation. As a result, nine more simulations were run in which they have the same initial structure (as the one that undergoes the needed structural conformation changes for Y925 phosphorylation) but each with different initial velocities. These simulations were run to examine the repeatability of this type of behavior. However, this type of behavior, where H1 is highly attached to the bundle and it does not have a propensity to unfold, was not found to be repeatable. Moreover, one of these nine simulations, the FAT is pulled away from the paxillin, raising the question of how much load the FAT/paxillin interactions can carry. In the future work, it will be important to examine the strength of the interaction between FAT and paxillin.

#### **5.4 Mechanical Load is Insufficient Over the Examined Timescales**

**All the results suggest that either the mechanical load alone is insufficient to make Y925 accessible for phosphorylation or it is a very slow process.** Furthermore, it might be something more than load has to take place for making Y925 accessible for phosphorylation such as chemical interactions. This could be a good motivation for looking for other factors that could contribute in getting Y925 available for phosphorylation.

## Chapter 6. Future Work

From equilibrium and loading simulations, it appears that H1 has very high propensity to stay folded within the bundle. It has been reported that Y925, located in the N-terminal of the first helix (H1) of FAT, is phosphorylated. However, this suggests that either this kind of process takes a long time or/and different conditions have to occur.

Longer CFMD simulations (more than 20 ns each) should be run to assess the time required for H1 to undergo that the structural changes needed for Y925 phosphorylation. Along the line with the necessity of extending the CFMD simulations, the unfolding propagation, if any, will be investigated via “satates” and net fluxes between states. The hydrogen donor-acceptor pairs and the  $\psi$  dihedral angle of the first five residues of the N-terminal of H1 (including Y925) will be key states. These calculations generate the possible states that the region flanking Y925 occupies, which gives a specific assessment of the unfolding initiation and propagation that could occur.

Since only two load scenarios (axial and perpendicular) with one load level (100 pN) were considered, different load directions with different load levels should be considered in any additional CFMD simulations. It may be that the most realistic load scenario is more complicated than the simple ones examined in this study. So, it is important to make the load scenarios as realistic as possible. As a result, constraining the ends of LD motifs, for example, should re-examined. In addition, for physiological reasons, lower load levels should be examined.

The strength of all possible interactions (electrostatic and hydrophobic) between H1 and the neighbor helices, including LD motifs, should be evaluated as a function of the applied load. Correlations between the strength of these interactions and the

availability of Y925 should be calculated. This will give a better understanding of the key regulators as they may gate of the Y925 phosphorylation.

H1/H2 hinge has been suggested to have a role in promoting the structural changes needed for Y925 phosphorylation. Moreover, MD simulation of the isolated H1 shows that H1 has a propensity to unfold from its C-terminal, which is one arm of the H1/H2 hinge. It is possible that H1 may unfold from its C-terminal and not from the N-terminal (where Y925 located). So, it is important to investigate the behavior of H1's C-terminal residues. To accomplish, the  $\psi$  dihedral angle and hydrogen donor-acceptor pairs states will be examined.

## Appendix A. PDB Files

### 1. The FAT/paxillin complex constructed using raw file 1ow7.pdb (§3.1.1 Structures):

```
HEADER      TRANSFERASE                      28-MAR-03   1OW7
TITLE       PAXILLIN LD4 MOTIF BOUND TO THE FOCAL ADHESION TARGETING
TITLE       2 (FAT) DOMAIN OF THE FOCAL ADHESION KINASE
COMPND      MOL_ID: 1;
COMPND      2 MOLECULE: FOCAL ADHESION KINASE 1;
COMPND      3 CHAIN: A, B, C;
COMPND      4 FRAGMENT: FOCAL ADHESION TARGETING DOMAIN;
COMPND      5 SYNONYM: FADK 1, PP125FAK, PROTEIN- TYROSINE KINASE 2;
COMPND      6 EC: 2.7.1.112;
COMPND      7 ENGINEERED: YES;
COMPND      8 MOL_ID: 2;
COMPND      9 MOLECULE: PAXILLIN;
COMPND     10 CHAIN: D, E, F;
COMPND     11 FRAGMENT: PAXILLIN LD4 MOTIF;
COMPND     12 ENGINEERED: YES
SOURCE      MOL_ID: 1;
SOURCE      2 ORGANISM_SCIENTIFIC: HOMO SAPIENS;
SOURCE      3 ORGANISM_COMMON: HUMAN;
SOURCE      4 ORGANISM_TAXID: 9606;
SOURCE      5 GENE: PTK2 OR FAK1 OR FAK;
SOURCE      6 EXPRESSION_SYSTEM: ESCHERICHIA COLI BL21(DE3);
SOURCE      7 EXPRESSION_SYSTEM_TAXID: 469008;
SOURCE      8 EXPRESSION_SYSTEM_STRAIN: BL21(DE3);
SOURCE      9 EXPRESSION_SYSTEM_VECTOR_TYPE: PLASMID;
SOURCE     10 EXPRESSION_SYSTEM_PLASMID: PGEX-6P2;
SOURCE     11 MOL_ID: 2;
SOURCE     12 SYNTHETIC: YES;
SOURCE     13 OTHER_DETAILS: SEQUENCE DERIVED FROM HUMAN PAXILLIN
KEYWDS      4 HELICAL BUNDLE, AMPHIPHATIC HELIX, TRANSFERASE
EXPDTA      X-RAY DIFFRACTION
```

AUTHOR M.K.HOELLERER,M.E.M.NOBLE,G.LABESSE,J.M.WERNER,S.T.AROLD  
 REVDAT 2 24-FEB-09 10W7 1 VERSN  
 REVDAT 1 21-OCT-03 10W7 0  
 JRNL AUTH M.K.HOELLERER,M.E.M.NOBLE,G.LABESSE,J.M.WERNER,  
 JRNL AUTH 2 S.T.AROLD  
 JRNL TITL MOLECULAR RECOGNITION OF PAXILLIN LD MOTIFS BY THE  
 JRNL TITL 2 FOCAL ADHESION TARGETING DOMAIN  
 JRNL REF STRUCTURE V. 11 1207 2003  
 JRNL REFN ISSN 0969-2126  
 JRNL PMID 14527389  
 JRNL DOI 10.1016/J.STR.2003.08.010  
 REMARK 1  
 REMARK 2  
 REMARK 2 RESOLUTION. 2.60 ANGSTROMS.  
 REMARK 3  
 REMARK 3 REFINEMENT.  
 REMARK 3 PROGRAM : REFMAC 5.1.24  
 REMARK 3 AUTHORS : MURSHUDOV,VAGIN,DODSON  
 REMARK 3  
 REMARK 3 REFINEMENT TARGET : MAXIMUM LIKELIHOOD  
 REMARK 3  
 REMARK 3 DATA USED IN REFINEMENT.  
 REMARK 3 RESOLUTION RANGE HIGH (ANGSTROMS) : 2.60  
 REMARK 3 RESOLUTION RANGE LOW (ANGSTROMS) : 111.80  
 REMARK 3 DATA CUTOFF (SIGMA(F)) : 0.000  
 REMARK 3 COMPLETENESS FOR RANGE (%) : 78.2  
 REMARK 3 NUMBER OF REFLECTIONS : 23071  
 REMARK 3  
 REMARK 3 FIT TO DATA USED IN REFINEMENT.  
 REMARK 3 CROSS-VALIDATION METHOD : THROUGHOUT  
 REMARK 3 FREE R VALUE TEST SET SELECTION : RANDOM  
 REMARK 3 R VALUE (WORKING + TEST SET) : 0.239  
 REMARK 3 R VALUE (WORKING SET) : 0.237  
 REMARK 3 FREE R VALUE : 0.269  
 REMARK 3 FREE R VALUE TEST SET SIZE (%) : 5.200  
 REMARK 3 FREE R VALUE TEST SET COUNT : 1189  
 REMARK 3  
 REMARK 3 FIT IN THE HIGHEST RESOLUTION BIN.  
 REMARK 3 TOTAL NUMBER OF BINS USED : 20

REMARK 3 BIN RESOLUTION RANGE HIGH (A) : 2.60  
 REMARK 3 BIN RESOLUTION RANGE LOW (A) : 2.67  
 REMARK 3 REFLECTION IN BIN (WORKING SET) : 785  
 REMARK 3 BIN COMPLETENESS (WORKING+TEST) (%) : NULL  
 REMARK 3 BIN R VALUE (WORKING SET) : 0.4350  
 REMARK 3 BIN FREE R VALUE SET COUNT : 48  
 REMARK 3 BIN FREE R VALUE : 0.4630  
 REMARK 3  
 REMARK 3 NUMBER OF NON-HYDROGEN ATOMS USED IN REFINEMENT.  
 REMARK 3 PROTEIN ATOMS : 3470  
 REMARK 3 NUCLEIC ACID ATOMS : 0  
 REMARK 3 HETEROGEN ATOMS : 0  
 REMARK 3 SOLVENT ATOMS : 50  
 REMARK 3  
 REMARK 3 B VALUES.  
 REMARK 3 FROM WILSON PLOT (A\*\*2) : 76.00  
 REMARK 3 MEAN B VALUE (OVERALL, A\*\*2) : 74.70  
 REMARK 3 OVERALL ANISOTROPIC B VALUE.  
 REMARK 3 B11 (A\*\*2) : 7.65000  
 REMARK 3 B22 (A\*\*2) : -3.19000  
 REMARK 3 B33 (A\*\*2) : -4.46000  
 REMARK 3 B12 (A\*\*2) : 0.00000  
 REMARK 3 B13 (A\*\*2) : 0.00000  
 REMARK 3 B23 (A\*\*2) : 0.00000  
 REMARK 3  
 REMARK 3 ESTIMATED OVERALL COORDINATE ERROR.  
 REMARK 3 ESU BASED ON R VALUE (A) : 0.460  
 REMARK 3 ESU BASED ON FREE R VALUE (A) : 0.311  
 REMARK 3 ESU BASED ON MAXIMUM LIKELIHOOD (A) : NULL  
 REMARK 3 ESU FOR B VALUES BASED ON MAXIMUM LIKELIHOOD (A\*\*2) : NULL  
 REMARK 3  
 REMARK 3 CORRELATION COEFFICIENTS.  
 REMARK 3 CORRELATION COEFFICIENT FO-FC : 0.935  
 REMARK 3 CORRELATION COEFFICIENT FO-FC FREE : 0.909  
 REMARK 3  
 REMARK 3 RMS DEVIATIONS FROM IDEAL VALUES COUNT RMS WEIGHT  
 REMARK 3 BOND LENGTHS REFINED ATOMS (A) : 3509 ; 0.012 ; 0.022  
 REMARK 3 BOND LENGTHS OTHERS (A) : 3367 ; 0.000 ; 0.020  
 REMARK 3 BOND ANGLES REFINED ATOMS (DEGREES) : 4744 ; 1.713 ; 2.010

REMARK	3	BOND ANGLES OTHERS	(DEGREES):	7895 ; 3.480 ; 3.000
REMARK	3	TORSION ANGLES, PERIOD 1	(DEGREES):	442 ; 1.430 ; 5.000
REMARK	3	TORSION ANGLES, PERIOD 2	(DEGREES):	NULL ; NULL ; NULL
REMARK	3	TORSION ANGLES, PERIOD 3	(DEGREES):	NULL ; NULL ; NULL
REMARK	3	TORSION ANGLES, PERIOD 4	(DEGREES):	NULL ; NULL ; NULL
REMARK	3	CHIRAL-CENTER RESTRAINTS	(A**3):	585 ; 0.112 ; 0.200
REMARK	3	GENERAL PLANES REFINED ATOMS	(A):	3761 ; 0.008 ; 0.020
REMARK	3	GENERAL PLANES OTHERS	(A):	538 ; 0.005 ; 0.020
REMARK	3	NON-BONDED CONTACTS REFINED ATOMS	(A):	1038 ; 0.251 ; 0.200
REMARK	3	NON-BONDED CONTACTS OTHERS	(A):	3922 ; 0.294 ; 0.200
REMARK	3	NON-BONDED TORSION REFINED ATOMS	(A):	NULL ; NULL ; NULL
REMARK	3	NON-BONDED TORSION OTHERS	(A):	1835 ; 0.107 ; 0.200
REMARK	3	H-BOND (X...Y) REFINED ATOMS	(A):	57 ; 0.174 ; 0.200
REMARK	3	H-BOND (X...Y) OTHERS	(A):	NULL ; NULL ; NULL
REMARK	3	POTENTIAL METAL-ION REFINED ATOMS	(A):	NULL ; NULL ; NULL
REMARK	3	POTENTIAL METAL-ION OTHERS	(A):	NULL ; NULL ; NULL
REMARK	3	SYMMETRY VDW REFINED ATOMS	(A):	15 ; 0.278 ; 0.200
REMARK	3	SYMMETRY VDW OTHERS	(A):	73 ; 0.309 ; 0.200
REMARK	3	SYMMETRY H-BOND REFINED ATOMS	(A):	5 ; 0.142 ; 0.200
REMARK	3	SYMMETRY H-BOND OTHERS	(A):	NULL ; NULL ; NULL
REMARK	3	SYMMETRY METAL-ION REFINED ATOMS	(A):	NULL ; NULL ; NULL
REMARK	3	SYMMETRY METAL-ION OTHERS	(A):	NULL ; NULL ; NULL
REMARK	3			
REMARK	3	ISOTROPIC THERMAL FACTOR RESTRAINTS.	COUNT	RMS WEIGHT
REMARK	3	MAIN-CHAIN BOND REFINED ATOMS	(A**2):	2252 ; 2.828 ; 1.500
REMARK	3	MAIN-CHAIN BOND OTHER ATOMS	(A**2):	NULL ; NULL ; NULL
REMARK	3	MAIN-CHAIN ANGLE REFINED ATOMS	(A**2):	3644 ; 5.037 ; 2.000
REMARK	3	SIDE-CHAIN BOND REFINED ATOMS	(A**2):	1257 ; 4.743 ; 3.000
REMARK	3	SIDE-CHAIN ANGLE REFINED ATOMS	(A**2):	1100 ; 7.598 ; 4.500
REMARK	3			
REMARK	3	ANISOTROPIC THERMAL FACTOR RESTRAINTS.	COUNT	RMS WEIGHT
REMARK	3	RIGID-BOND RESTRAINTS	(A**2):	NULL ; NULL ; NULL
REMARK	3	SPHERICITY; FREE ATOMS	(A**2):	NULL ; NULL ; NULL
REMARK	3	SPHERICITY; BONDED ATOMS	(A**2):	NULL ; NULL ; NULL
REMARK	3			
REMARK	3	NCS RESTRAINTS STATISTICS		
REMARK	3	NUMBER OF DIFFERENT NCS GROUPS :	NULL	
REMARK	3			
REMARK	3	TLS DETAILS		



REMARK 3 NUMBER OF TLS GROUPS : NULL  
 REMARK 3  
 REMARK 3 BULK SOLVENT MODELLING.  
 REMARK 3 METHOD USED : BABINET MODEL WITH MASK  
 REMARK 3 PARAMETERS FOR MASK CALCULATION  
 REMARK 3 VDW PROBE RADIUS : 1.40  
 REMARK 3 ION PROBE RADIUS : 0.80  
 REMARK 3 SHRINKAGE RADIUS : 0.80  
 REMARK 3  
 REMARK 3 OTHER REFINEMENT REMARKS: 1) THE SECOND LD4 MOTIF (CHAIN F,  
 REMARK 3 BOUND TO MOLECULE C) WAS FITTED INTO THE UNBIASED 3FO-2FC MAPS  
 REMARK 3 (CNS). ITS POSITION AND ORIENTATION WERE INFERRED FROM  
 REMARK 3 HOMOLOGY WITH THE WELL-DEFINED OTHER LD4 - FAT INTERACTION  
 REMARK 3 (CHAINS A AND C), AND ARE SUPPORTED BY NMR DATA (SEE  
 REMARK 3 PUBLICATION). 2) THE CRYSTAL DIFFRACTED ANISOTROPICALLY TO 2.8  
 REMARK 3 AND 2.6 Å RESOLUTION. THE WEAK, BUT CONSISTENT, DATA TO 2.6 Å  
 REMARK 3 WERE INCLUDED, AS THEY SIGNIFICANTLY IMPROVED THE ELECTRON  
 REMARK 3 DENSITY.  
 REMARK 4  
 REMARK 4 1OW7 COMPLIES WITH FORMAT V. 3.15, 01-DEC-08  
 REMARK 100  
 REMARK 100 THIS ENTRY HAS BEEN PROCESSED BY RCSB ON 31-MAR-03.  
 REMARK 100 THE RCSB ID CODE IS RCSB018728.  
 REMARK 200  
 REMARK 200 EXPERIMENTAL DETAILS  
 REMARK 200 EXPERIMENT TYPE : X-RAY DIFFRACTION  
 REMARK 200 DATE OF DATA COLLECTION : 30-JUN-02  
 REMARK 200 TEMPERATURE (KELVIN) : 100  
 REMARK 200 PH : 6.3  
 REMARK 200 NUMBER OF CRYSTALS USED : 1  
 REMARK 200  
 REMARK 200 SYNCHROTRON (Y/N) : Y  
 REMARK 200 RADIATION SOURCE : ESRF  
 REMARK 200 BEAMLINE : BM30A  
 REMARK 200 X-RAY GENERATOR MODEL : NULL  
 REMARK 200 MONOCHROMATIC OR LAUE (M/L) : M  
 REMARK 200 WAVELENGTH OR RANGE (Å) : 0.98  
 REMARK 200 MONOCHROMATOR : SILICON  
 REMARK 200 OPTICS : TWO CRYSTALS MONOCHROMATOR

REMARK 200 BETWEEN TWO CYLINDRICAL  
 REMARK 200 PARABOLIC MIRRORS  
 REMARK 200  
 REMARK 200 DETECTOR TYPE : CCD  
 REMARK 200 DETECTOR MANUFACTURER : MARRESEARCH  
 REMARK 200 INTENSITY-INTEGRATION SOFTWARE : MOSFLM  
 REMARK 200 DATA SCALING SOFTWARE : CCP4 (SCALA)  
 REMARK 200  
 REMARK 200 NUMBER OF UNIQUE REFLECTIONS : 23071  
 REMARK 200 RESOLUTION RANGE HIGH (A) : 2.600  
 REMARK 200 RESOLUTION RANGE LOW (A) : 29.600  
 REMARK 200 REJECTION CRITERIA (SIGMA(I)) : NULL  
 REMARK 200  
 REMARK 200 OVERALL.  
 REMARK 200 COMPLETENESS FOR RANGE (%) : 88.7  
 REMARK 200 DATA REDUNDANCY : 2.700  
 REMARK 200 R MERGE (I) : 0.07900  
 REMARK 200 R SYM (I) : 0.06400  
 REMARK 200 <I/SIGMA(I)> FOR THE DATA SET : 8.9000  
 REMARK 200  
 REMARK 200 IN THE HIGHEST RESOLUTION SHELL.  
 REMARK 200 HIGHEST RESOLUTION SHELL, RANGE HIGH (A) : 2.60  
 REMARK 200 HIGHEST RESOLUTION SHELL, RANGE LOW (A) : 2.69  
 REMARK 200 COMPLETENESS FOR SHELL (%) : 79.3  
 REMARK 200 DATA REDUNDANCY IN SHELL : 1.70  
 REMARK 200 R MERGE FOR SHELL (I) : 0.86000  
 REMARK 200 R SYM FOR SHELL (I) : 0.62000  
 REMARK 200 <I/SIGMA(I)> FOR SHELL : 0.300  
 REMARK 200  
 REMARK 200 DIFFRACTION PROTOCOL: SINGLE WAVELENGTH  
 REMARK 200 METHOD USED TO DETERMINE THE STRUCTURE: MOLECULAR REPLACEMENT  
 REMARK 200 SOFTWARE USED: AMORE  
 REMARK 200 STARTING MODEL: PDBENTRY 1K05  
 REMARK 200  
 REMARK 200 REMARK: NULL  
 REMARK 280  
 REMARK 280 CRYSTAL  
 REMARK 280 SOLVENT CONTENT, VS (%) : 74.01  
 REMARK 280 MATTHEWS COEFFICIENT, VM (ANGSTROMS\*\*3/DA) : 4.77

REMARK 280

REMARK 280 CRYSTALLIZATION CONDITIONS: SODIUM CHLORIDE, GLYCEROL, HEPES,  
 REMARK 280 PH 6.3, VAPOR DIFFUSION, HANGING DROP, TEMPERATURE 292K

REMARK 290

REMARK 290 CRYSTALLOGRAPHIC SYMMETRY

REMARK 290 SYMMETRY OPERATORS FOR SPACE GROUP: C 2 2 21

REMARK 290

REMARK 290	SYMOP	SYMMETRY
REMARK 290	NNNMMM	OPERATOR
REMARK 290	1555	X, Y, Z
REMARK 290	2555	-X, -Y, Z+1/2
REMARK 290	3555	-X, Y, -Z+1/2
REMARK 290	4555	X, -Y, -Z
REMARK 290	5555	X+1/2, Y+1/2, Z
REMARK 290	6555	-X+1/2, -Y+1/2, Z+1/2
REMARK 290	7555	-X+1/2, Y+1/2, -Z+1/2
REMARK 290	8555	X+1/2, -Y+1/2, -Z

REMARK 290

REMARK 290 WHERE NNN -> OPERATOR NUMBER

REMARK 290 MMM -> TRANSLATION VECTOR

REMARK 290

REMARK 290 CRYSTALLOGRAPHIC SYMMETRY TRANSFORMATIONS

REMARK 290 THE FOLLOWING TRANSFORMATIONS OPERATE ON THE ATOM/HETATM

REMARK 290 RECORDS IN THIS ENTRY TO PRODUCE CRYSTALLOGRAPHICALLY

REMARK 290 RELATED MOLECULES.

REMARK 290	SMTRY1	1	1.000000	0.000000	0.000000	0.000000
REMARK 290	SMTRY2	1	0.000000	1.000000	0.000000	0.000000
REMARK 290	SMTRY3	1	0.000000	0.000000	1.000000	0.000000
REMARK 290	SMTRY1	2	-1.000000	0.000000	0.000000	0.000000
REMARK 290	SMTRY2	2	0.000000	-1.000000	0.000000	0.000000
REMARK 290	SMTRY3	2	0.000000	0.000000	1.000000	48.09950
REMARK 290	SMTRY1	3	-1.000000	0.000000	0.000000	0.000000
REMARK 290	SMTRY2	3	0.000000	1.000000	0.000000	0.000000
REMARK 290	SMTRY3	3	0.000000	0.000000	-1.000000	48.09950
REMARK 290	SMTRY1	4	1.000000	0.000000	0.000000	0.000000
REMARK 290	SMTRY2	4	0.000000	-1.000000	0.000000	0.000000
REMARK 290	SMTRY3	4	0.000000	0.000000	-1.000000	0.000000
REMARK 290	SMTRY1	5	1.000000	0.000000	0.000000	44.49700
REMARK 290	SMTRY2	5	0.000000	1.000000	0.000000	109.83250

REMARK 290	SMTRY3	5	0.000000	0.000000	1.000000	0.000000
REMARK 290	SMTRY1	6	-1.000000	0.000000	0.000000	44.49700
REMARK 290	SMTRY2	6	0.000000	-1.000000	0.000000	109.83250
REMARK 290	SMTRY3	6	0.000000	0.000000	1.000000	48.09950
REMARK 290	SMTRY1	7	-1.000000	0.000000	0.000000	44.49700
REMARK 290	SMTRY2	7	0.000000	1.000000	0.000000	109.83250
REMARK 290	SMTRY3	7	0.000000	0.000000	-1.000000	48.09950
REMARK 290	SMTRY1	8	1.000000	0.000000	0.000000	44.49700
REMARK 290	SMTRY2	8	0.000000	-1.000000	0.000000	109.83250
REMARK 290	SMTRY3	8	0.000000	0.000000	-1.000000	0.000000
REMARK 290						
REMARK 290 REMARK: NULL						
REMARK 300						
REMARK 300 BIOMOLECULE: 1						
REMARK 300 SEE REMARK 350 FOR THE AUTHOR PROVIDED AND/OR PROGRAM						
REMARK 300 GENERATED ASSEMBLY INFORMATION FOR THE STRUCTURE IN						
REMARK 300 THIS ENTRY. THE REMARK MAY ALSO PROVIDE INFORMATION ON						
REMARK 300 BURIED SURFACE AREA.						
REMARK 350						
REMARK 350 COORDINATES FOR A COMPLETE MULTIMER REPRESENTING THE KNOWN						
REMARK 350 BIOLOGICALLY SIGNIFICANT OLIGOMERIZATION STATE OF THE						
REMARK 350 MOLECULE CAN BE GENERATED BY APPLYING BIOMT TRANSFORMATIONS						
REMARK 350 GIVEN BELOW. BOTH NON-CRYSTALLOGRAPHIC AND						
REMARK 350 CRYSTALLOGRAPHIC OPERATIONS ARE GIVEN.						
REMARK 350						
REMARK 350 BIOMOLECULE: 1						
REMARK 350 AUTHOR DETERMINED BIOLOGICAL UNIT: HEXAMERIC						
REMARK 350 APPLY THE FOLLOWING TO CHAINS: A, B, C, D, E, F						
REMARK 350	BIOMT1	1	1.000000	0.000000	0.000000	0.000000
REMARK 350	BIOMT2	1	0.000000	1.000000	0.000000	0.000000
REMARK 350	BIOMT3	1	0.000000	0.000000	1.000000	0.000000
REMARK 375						
REMARK 375 SPECIAL POSITION						
REMARK 375 THE FOLLOWING ATOMS ARE FOUND TO BE WITHIN 0.15 ANGSTROMS						
REMARK 375 OF A SYMMETRY RELATED ATOM AND ARE ASSUMED TO BE ON SPECIAL						
REMARK 375 POSITIONS.						
REMARK 375						
REMARK 375 ATOM RES CSSEQI						
REMARK 375	HOH B	60	LIES ON A SPECIAL POSITION.			

REMARK 375        HOH C    4   LIES ON A SPECIAL POSITION.

REMARK 465

REMARK 465 MISSING RESIDUES

REMARK 465 THE FOLLOWING RESIDUES WERE NOT LOCATED IN THE

REMARK 465 EXPERIMENT. (M=MODEL NUMBER; RES=RESIDUE NAME; C=CHAIN

REMARK 465 IDENTIFIER; SSSEQ=SEQUENCE NUMBER; I=INSERTION CODE.)

REMARK 465

REMARK 465	M	RES	C	SSSEQI
REMARK 465		SER	A	892
REMARK 465		SER	A	893
REMARK 465		PRO	A	894
REMARK 465		ALA	A	895
REMARK 465		ASP	A	896
REMARK 465		SER	A	897
REMARK 465		TYR	A	898
REMARK 465		ASN	A	899
REMARK 465		GLU	A	900
REMARK 465		GLY	A	901
REMARK 465		VAL	A	902
REMARK 465		LYS	A	903
REMARK 465		LEU	A	904
REMARK 465		GLN	A	905
REMARK 465		PRO	A	906
REMARK 465		GLN	A	907
REMARK 465		GLU	A	908
REMARK 465		ILE	A	909
REMARK 465		SER	A	910
REMARK 465		PRO	A	911
REMARK 465		PRO	A	912
REMARK 465		PRO	A	913
REMARK 465		THR	A	914
REMARK 465		ALA	A	915
REMARK 465		ARG	A	1050
REMARK 465		PRO	A	1051
REMARK 465		HIS	A	1052
REMARK 465		SER	B	892
REMARK 465		SER	B	893
REMARK 465		PRO	B	894
REMARK 465		ALA	B	895

REMARK 465	ASP B	896
REMARK 465	SER B	897
REMARK 465	TYR B	898
REMARK 465	ASN B	899
REMARK 465	GLU B	900
REMARK 465	GLY B	901
REMARK 465	VAL B	902
REMARK 465	LYS B	903
REMARK 465	LEU B	904
REMARK 465	GLN B	905
REMARK 465	PRO B	906
REMARK 465	GLN B	907
REMARK 465	GLU B	908
REMARK 465	GLN B	1048
REMARK 465	THR B	1049
REMARK 465	ARG B	1050
REMARK 465	PRO B	1051
REMARK 465	HIS B	1052
REMARK 465	SER C	892
REMARK 465	SER C	893
REMARK 465	PRO C	894
REMARK 465	ALA C	895
REMARK 465	ASP C	896
REMARK 465	SER C	897
REMARK 465	TYR C	898
REMARK 465	ASN C	899
REMARK 465	GLU C	900
REMARK 465	GLY C	901
REMARK 465	VAL C	902
REMARK 465	LYS C	903
REMARK 465	LEU C	904
REMARK 465	GLN C	905
REMARK 465	PRO C	906
REMARK 465	GLN C	907
REMARK 465	GLU C	908
REMARK 465	GLN C	1048
REMARK 465	THR C	1049
REMARK 465	ARG C	1050
REMARK 465	PRO C	1051

REMARK 465 HIS C 1052

REMARK 465 ALA D 1

REMARK 465 ALA E 1

REMARK 465 ALA F 1

REMARK 500

REMARK 500 GEOMETRY AND STEREOCHEMISTRY

REMARK 500 SUBTOPIC: TORSION ANGLES

REMARK 500

REMARK 500 TORSION ANGLES OUTSIDE THE EXPECTED RAMACHANDRAN REGIONS:

REMARK 500 (M=MODEL NUMBER; RES=RESIDUE NAME; C=CHAIN IDENTIFIER;

REMARK 500 SSEQ=SEQUENCE NUMBER; I=INSERTION CODE).

REMARK 500

REMARK 500 STANDARD TABLE:

REMARK 500 FORMAT: (10X,I3,1X,A3,1X,A1,I4,A1,4X,F7.2,3X,F7.2)

REMARK 500

REMARK 500 EXPECTED VALUES: GJ KLEYWEGT AND TA JONES (1996). PHI/PSI-

REMARK 500 CHOLOGY: RAMACHANDRAN REVISITED. STRUCTURE 4, 1395 - 1400

REMARK 500

REMARK 500	M	RES	CSSEQI	PSI	PHI
REMARK 500	SER	A	920	-39.71	-39.13
REMARK 500	TYR	A1007		32.90	-91.74
REMARK 500	MET	A1009		13.73	81.75
REMARK 500	MET	B1009		-3.32	72.96
REMARK 500	ASN	C 916		21.89	-71.05
REMARK 500	LYS	C 941		-94.67	-97.28
REMARK 500	ILE	C 942		-47.69	4.76
REMARK 500	PRO	C 944		-78.50	-55.50
REMARK 500	ALA	C 945		142.87	-29.64
REMARK 500	TYR	C1016		-1.48	-56.86

REMARK 500

REMARK 500 REMARK: NULL

REMARK 900

REMARK 900 RELATED ENTRIES

REMARK 900 RELATED ID: 1K05 RELATED DB: PDB

REMARK 900 CRYSTAL STRUCTURE OF THE FOCAL ADHESION TARGETING DOMAIN OF

REMARK 900 FOCAL ADHESION KINASE

DBREF	10W7	A	892	1052	UNP	Q05397	FAK1_HUMAN	892	1052
DBREF	10W7	B	892	1052	UNP	Q05397	FAK1_HUMAN	892	1052
DBREF	10W7	C	892	1052	UNP	Q05397	FAK1_HUMAN	892	1052

DBREF	1OW7	D	1	13	PDB	1OW7	1OW7			1	13					
DBREF	1OW7	E	1	13	PDB	1OW7	1OW7			1	13					
DBREF	1OW7	F	1	13	PDB	1OW7	1OW7			1	13					
SEQRES	1	A	161	SER	SER	PRO	ALA	ASP	SER	TYR	ASN	GLU	GLY	VAL	LYS	LEU
SEQRES	2	A	161	GLN	PRO	GLN	GLU	ILE	SER	PRO	PRO	PRO	THR	ALA	ASN	LEU
SEQRES	3	A	161	ASP	ARG	SER	ASN	ASP	LYS	VAL	TYR	GLU	ASN	VAL	THR	GLY
SEQRES	4	A	161	LEU	VAL	LYS	ALA	VAL	ILE	GLU	MET	SER	SER	LYS	ILE	GLN
SEQRES	5	A	161	PRO	ALA	PRO	PRO	GLU	GLU	TYR	VAL	PRO	MET	VAL	LYS	GLU
SEQRES	6	A	161	VAL	GLY	LEU	ALA	LEU	ARG	THR	LEU	LEU	ALA	THR	VAL	ASP
SEQRES	7	A	161	GLU	THR	ILE	PRO	LEU	LEU	PRO	ALA	SER	THR	HIS	ARG	GLU
SEQRES	8	A	161	ILE	GLU	MET	ALA	GLN	LYS	LEU	LEU	ASN	SER	ASP	LEU	GLY
SEQRES	9	A	161	GLU	LEU	ILE	ASN	LYS	MET	LYS	LEU	ALA	GLN	GLN	TYR	VAL
SEQRES	10	A	161	MET	THR	SER	LEU	GLN	GLN	GLU	TYR	LYS	LYS	GLN	MET	LEU
SEQRES	11	A	161	THR	ALA	ALA	HIS	ALA	LEU	ALA	VAL	ASP	ALA	LYS	ASN	LEU
SEQRES	12	A	161	LEU	ASP	VAL	ILE	ASP	GLN	ALA	ARG	LEU	LYS	MET	LEU	GLY
SEQRES	13	A	161	GLN	THR	ARG	PRO	HIS								
SEQRES	1	B	161	SER	SER	PRO	ALA	ASP	SER	TYR	ASN	GLU	GLY	VAL	LYS	LEU
SEQRES	2	B	161	GLN	PRO	GLN	GLU	ILE	SER	PRO	PRO	PRO	THR	ALA	ASN	LEU
SEQRES	3	B	161	ASP	ARG	SER	ASN	ASP	LYS	VAL	TYR	GLU	ASN	VAL	THR	GLY
SEQRES	4	B	161	LEU	VAL	LYS	ALA	VAL	ILE	GLU	MET	SER	SER	LYS	ILE	GLN
SEQRES	5	B	161	PRO	ALA	PRO	PRO	GLU	GLU	TYR	VAL	PRO	MET	VAL	LYS	GLU
SEQRES	6	B	161	VAL	GLY	LEU	ALA	LEU	ARG	THR	LEU	LEU	ALA	THR	VAL	ASP
SEQRES	7	B	161	GLU	THR	ILE	PRO	LEU	LEU	PRO	ALA	SER	THR	HIS	ARG	GLU
SEQRES	8	B	161	ILE	GLU	MET	ALA	GLN	LYS	LEU	LEU	ASN	SER	ASP	LEU	GLY
SEQRES	9	B	161	GLU	LEU	ILE	ASN	LYS	MET	LYS	LEU	ALA	GLN	GLN	TYR	VAL
SEQRES	10	B	161	MET	THR	SER	LEU	GLN	GLN	GLU	TYR	LYS	LYS	GLN	MET	LEU
SEQRES	11	B	161	THR	ALA	ALA	HIS	ALA	LEU	ALA	VAL	ASP	ALA	LYS	ASN	LEU
SEQRES	12	B	161	LEU	ASP	VAL	ILE	ASP	GLN	ALA	ARG	LEU	LYS	MET	LEU	GLY
SEQRES	13	B	161	GLN	THR	ARG	PRO	HIS								
SEQRES	1	C	161	SER	SER	PRO	ALA	ASP	SER	TYR	ASN	GLU	GLY	VAL	LYS	LEU
SEQRES	2	C	161	GLN	PRO	GLN	GLU	ILE	SER	PRO	PRO	PRO	THR	ALA	ASN	LEU
SEQRES	3	C	161	ASP	ARG	SER	ASN	ASP	LYS	VAL	TYR	GLU	ASN	VAL	THR	GLY
SEQRES	4	C	161	LEU	VAL	LYS	ALA	VAL	ILE	GLU	MET	SER	SER	LYS	ILE	GLN
SEQRES	5	C	161	PRO	ALA	PRO	PRO	GLU	GLU	TYR	VAL	PRO	MET	VAL	LYS	GLU
SEQRES	6	C	161	VAL	GLY	LEU	ALA	LEU	ARG	THR	LEU	LEU	ALA	THR	VAL	ASP
SEQRES	7	C	161	GLU	THR	ILE	PRO	LEU	LEU	PRO	ALA	SER	THR	HIS	ARG	GLU
SEQRES	8	C	161	ILE	GLU	MET	ALA	GLN	LYS	LEU	LEU	ASN	SER	ASP	LEU	GLY
SEQRES	9	C	161	GLU	LEU	ILE	ASN	LYS	MET	LYS	LEU	ALA	GLN	GLN	TYR	VAL
SEQRES	10	C	161	MET	THR	SER	LEU	GLN	GLN	GLU	TYR	LYS	LYS	GLN	MET	LEU



SEQRES	11	C	161	THR	ALA	ALA	HIS	ALA	LEU	ALA	VAL	ASP	ALA	LYS	ASN	LEU	
SEQRES	12	C	161	LEU	ASP	VAL	ILE	ASP	GLN	ALA	ARG	LEU	LYS	MET	LEU	GLY	
SEQRES	13	C	161	GLN	THR	ARG	PRO	HIS									
SEQRES	1	D	13	ALA	THR	ARG	GLU	LEU	ASP	GLU	LEU	MET	ALA	SER	LEU	SER	
SEQRES	1	E	13	ALA	THR	ARG	GLU	LEU	ASP	GLU	LEU	MET	ALA	SER	LEU	SER	
SEQRES	1	F	13	ALA	THR	ARG	GLU	LEU	ASP	GLU	LEU	MET	ALA	SER	LEU	SER	
FORMUL	7	HOH		*50 (H2 O)													
HELIX	1		1	ASP	A	922	ILE	A	942	1							21
HELIX	2		2	PRO	A	946	ILE	A	972	1							27
HELIX	3		3	PRO	A	973	LEU	A	975	5							3
HELIX	4		4	THR	A	979	TYR	A	1007	1							29
HELIX	5		5	LEU	A	1012	GLY	A	1047	1							36
HELIX	6		6	ASP	B	922	ILE	B	942	1							21
HELIX	7		7	PRO	B	946	GLU	B	970	1							25
HELIX	8		8	THR	B	971	LEU	B	975	5							5
HELIX	9		9	PRO	B	976	SER	B	978	5							3
HELIX	10		10	THR	B	979	TYR	B	1007	1							29
HELIX	11		11	SER	B	1011	LEU	B	1046	1							36
HELIX	12		12	ASP	C	922	LYS	C	941	1							20
HELIX	13		13	PRO	C	946	ILE	C	972	1							27
HELIX	14		14	THR	C	979	TYR	C	1007	1							29
HELIX	15		15	THR	C	1010	GLY	C	1047	1							38
HELIX	16		16	GLU	D	4	LEU	D	12	1							9
HELIX	17		17	GLU	E	4	ALA	E	10	1							7
HELIX	18		18	THR	F	2	LEU	F	12	1							11
CRYST1	88.994	219.665	96.199	90.00	90.00	90.00	C	2	2	21							24
ORIGX1		1.000000	0.000000	0.000000		0.000000											
ORIGX2		0.000000	1.000000	0.000000		0.000000											
ORIGX3		0.000000	0.000000	1.000000		0.000000											
SCALE1		0.011237	0.000000	0.000000		0.000000											
SCALE2		0.000000	0.004552	0.000000		0.000000											
SCALE3		0.000000	0.000000	0.010395		0.000000											
ATOM	12	N	ILE	C	909		-7.120	90.264	27.594	1.00	84.95						N
ATOM	13	CA	ILE	C	909		-6.328	91.240	26.773	1.00	86.58						C
ATOM	14	C	ILE	C	909		-6.742	92.707	26.925	1.00	85.87						C
ATOM	15	O	ILE	C	909		-7.924	93.047	26.881	1.00	86.73						O
ATOM	16	CB	ILE	C	909		-6.375	90.883	25.252	1.00	85.93						C
ATOM	17	CG1	ILE	C	909		-5.547	91.908	24.460	1.00	84.17						C
ATOM	18	CG2	ILE	C	909		-7.829	90.811	24.763	1.00	79.59						C

ATOM	19	CD1	ILE	C	909	-5.233	91.508	23.026	1.00	82.55	C
ATOM	20	N	SER	C	910	-5.760	93.584	27.092	1.00	85.82	N
ATOM	21	CA	SER	C	910	-6.064	95.004	27.245	1.00	88.03	C
ATOM	22	C	SER	C	910	-6.002	95.773	25.931	1.00	87.92	C
ATOM	23	O	SER	C	910	-5.363	95.336	24.962	1.00	90.37	O
ATOM	24	CB	SER	C	910	-5.117	95.644	28.260	1.00	87.19	C
ATOM	25	OG	SER	C	910	-3.892	94.924	28.339	1.00	88.96	O
ATOM	26	N	PRO	C	911	-6.707	96.919	25.869	1.00	85.92	N
ATOM	27	CA	PRO	C	911	-6.692	97.727	24.649	1.00	82.06	C
ATOM	28	C	PRO	C	911	-5.458	98.621	24.779	1.00	76.36	C
ATOM	29	O	PRO	C	911	-4.891	98.763	25.878	1.00	72.62	O
ATOM	30	CB	PRO	C	911	-8.003	98.513	24.750	1.00	81.26	C
ATOM	31	CG	PRO	C	911	-8.052	98.813	26.204	1.00	83.81	C
ATOM	32	CD	PRO	C	911	-7.705	97.441	26.818	1.00	84.68	C
ATOM	33	N	PRO	C	912	-5.029	99.238	23.668	1.00	69.40	N
ATOM	34	CA	PRO	C	912	-3.851	100.103	23.695	1.00	63.70	C
ATOM	35	C	PRO	C	912	-3.917	101.091	24.857	1.00	60.56	C
ATOM	36	O	PRO	C	912	-4.996	101.538	25.235	1.00	61.26	O
ATOM	37	CB	PRO	C	912	-3.923	100.804	22.338	1.00	65.28	C
ATOM	38	CG	PRO	C	912	-4.655	99.848	21.490	1.00	64.22	C
ATOM	39	CD	PRO	C	912	-5.745	99.375	22.395	1.00	65.66	C
ATOM	40	N	PRO	C	913	-2.763	101.438	25.446	1.00	58.77	N
ATOM	41	CA	PRO	C	913	-2.797	102.386	26.571	1.00	61.24	C
ATOM	42	C	PRO	C	913	-3.755	103.530	26.256	1.00	63.36	C
ATOM	43	O	PRO	C	913	-3.840	103.956	25.109	1.00	67.19	O
ATOM	44	CB	PRO	C	913	-1.349	102.849	26.685	1.00	59.78	C
ATOM	45	CG	PRO	C	913	-0.577	101.661	26.222	1.00	59.63	C
ATOM	46	CD	PRO	C	913	-1.386	101.084	25.074	1.00	59.35	C
ATOM	47	N	THR	C	914	-4.458	104.042	27.266	1.00	65.08	N
ATOM	48	CA	THR	C	914	-5.436	105.093	27.011	1.00	69.04	C
ATOM	49	C	THR	C	914	-4.815	106.370	26.491	1.00	73.88	C
ATOM	50	O	THR	C	914	-3.717	106.786	26.919	1.00	72.02	O
ATOM	51	CB	THR	C	914	-6.315	105.419	28.250	1.00	69.24	C
ATOM	52	CG2	THR	C	914	-5.485	106.060	29.340	1.00	69.56	C
ATOM	53	OG1	THR	C	914	-7.361	106.329	27.874	1.00	67.64	O
ATOM	54	N	ALA	C	915	-5.531	106.964	25.535	1.00	76.34	N
ATOM	55	CA	ALA	C	915	-5.106	108.193	24.885	1.00	78.39	C
ATOM	56	C	ALA	C	915	-5.407	109.387	25.786	1.00	81.78	C
ATOM	57	O	ALA	C	915	-4.725	110.418	25.718	1.00	84.63	O

ATOM	58	CB	ALA	C	915	-5.821	108.341	23.538	1.00	73.31	C
ATOM	59	N	ASN	C	916	-6.399	109.226	26.660	1.00	82.80	N
ATOM	60	CA	ASN	C	916	-6.816	110.305	27.546	1.00	82.11	C
ATOM	61	C	ASN	C	916	-5.834	110.665	28.679	1.00	79.48	C
ATOM	62	O	ASN	C	916	-6.252	111.247	29.670	1.00	75.73	O
ATOM	63	CB	ASN	C	916	-8.204	109.979	28.131	1.00	88.81	C
ATOM	64	CG	ASN	C	916	-9.073	109.113	27.184	1.00	94.91	C
ATOM	65	ND2	ASN	C	916	-9.575	107.988	27.704	1.00	96.94	N
ATOM	66	OD1	ASN	C	916	-9.289	109.455	26.012	1.00	99.35	O
ATOM	67	N	LEU	C	917	-4.549	110.328	28.531	1.00	76.82	N
ATOM	68	CA	LEU	C	917	-3.513	110.651	29.529	1.00	76.15	C
ATOM	69	C	LEU	C	917	-2.212	111.089	28.847	1.00	76.67	C
ATOM	70	O	LEU	C	917	-1.728	110.419	27.941	1.00	78.80	O
ATOM	71	CB	LEU	C	917	-3.179	109.444	30.403	1.00	78.46	C
ATOM	72	CG	LEU	C	917	-4.159	108.769	31.351	1.00	80.00	C
ATOM	73	CD1	LEU	C	917	-3.506	107.526	31.939	1.00	78.87	C
ATOM	74	CD2	LEU	C	917	-4.546	109.731	32.447	1.00	85.50	C
ATOM	75	N	ASP	C	918	-1.611	112.173	29.311	1.00	78.12	N
ATOM	76	CA	ASP	C	918	-0.394	112.668	28.673	1.00	82.31	C
ATOM	77	C	ASP	C	918	0.858	111.919	29.108	1.00	81.67	C
ATOM	78	O	ASP	C	918	1.210	111.929	30.285	1.00	84.04	O
ATOM	79	CB	ASP	C	918	-0.238	114.174	28.947	1.00	88.22	C
ATOM	80	CG	ASP	C	918	1.043	114.760	28.347	1.00	94.03	C
ATOM	81	OD1	ASP	C	918	2.096	114.097	28.473	1.00	98.43	O
ATOM	82	OD2	ASP	C	918	1.002	115.882	27.776	1.00	97.26	O
ATOM	83	N	ARG	C	919	1.552	111.315	28.140	1.00	77.81	N
ATOM	84	CA	ARG	C	919	2.757	110.518	28.399	1.00	71.26	C
ATOM	85	C	ARG	C	919	4.063	111.292	28.346	1.00	73.28	C
ATOM	86	O	ARG	C	919	5.138	110.691	28.354	1.00	77.64	O
ATOM	87	CB	ARG	C	919	2.842	109.384	27.386	1.00	60.42	C
ATOM	88	CG	ARG	C	919	1.550	108.657	27.167	1.00	57.11	C
ATOM	89	CD	ARG	C	919	1.107	107.962	28.421	1.00	54.34	C
ATOM	90	NE	ARG	C	919	-0.182	107.321	28.226	1.00	57.02	N
ATOM	91	CZ	ARG	C	919	-0.705	106.445	29.072	1.00	55.74	C
ATOM	92	NH1	ARG	C	919	-0.039	106.116	30.173	1.00	54.16	N
ATOM	93	NH2	ARG	C	919	-1.874	105.878	28.794	1.00	54.13	N
ATOM	94	N	SER	C	920	3.984	112.613	28.284	1.00	74.38	N
ATOM	95	CA	SER	C	920	5.195	113.421	28.187	1.00	76.74	C
ATOM	96	C	SER	C	920	6.091	113.252	29.365	1.00	75.30	C

ATOM	97	O	SER C 920	7.317	113.241	29.232	1.00	72.65	O
ATOM	98	CB	SER C 920	4.871	114.909	28.089	1.00	79.67	C
ATOM	99	OG	SER C 920	4.047	115.190	26.977	1.00	89.57	O
ATOM	100	N	ASN C 921	5.466	113.149	30.529	1.00	77.59	N
ATOM	101	CA	ASN C 921	6.220	113.042	31.761	1.00	80.00	C
ATOM	102	C	ASN C 921	5.910	111.775	32.547	1.00	79.61	C
ATOM	103	O	ASN C 921	6.108	111.720	33.763	1.00	83.99	O
ATOM	104	CB	ASN C 921	5.972	114.304	32.602	1.00	78.49	C
ATOM	105	CG	ASN C 921	6.493	115.567	31.912	1.00	79.04	C
ATOM	106	ND2	ASN C 921	5.604	116.532	31.661	1.00	74.33	N
ATOM	107	OD1	ASN C 921	7.684	115.660	31.596	1.00	79.77	O
ATOM	108	N	ASP C 922	5.440	110.756	31.831	1.00	73.79	N
ATOM	109	CA	ASP C 922	5.106	109.470	32.427	1.00	70.09	C
ATOM	110	C	ASP C 922	6.337	108.555	32.462	1.00	69.92	C
ATOM	111	O	ASP C 922	6.608	107.825	31.504	1.00	71.98	O
ATOM	112	CB	ASP C 922	3.996	108.781	31.630	1.00	65.82	C
ATOM	113	CG	ASP C 922	3.281	107.715	32.440	1.00	66.60	C
ATOM	114	OD1	ASP C 922	3.871	107.216	33.425	1.00	64.17	O
ATOM	115	OD2	ASP C 922	2.130	107.378	32.093	1.00	68.31	O
ATOM	116	N	LYS C 923	7.085	108.609	33.559	1.00	67.80	N
ATOM	117	CA	LYS C 923	8.267	107.779	33.713	1.00	66.08	C
ATOM	118	C	LYS C 923	7.884	106.297	33.809	1.00	62.54	C
ATOM	119	O	LYS C 923	8.695	105.440	33.505	1.00	65.36	O
ATOM	120	CB	LYS C 923	9.080	108.228	34.942	1.00	67.57	C
ATOM	121	CG	LYS C 923	10.228	109.196	34.620	1.00	73.58	C
ATOM	122	CD	LYS C 923	11.553	108.468	34.336	1.00	78.66	C
ATOM	123	CE	LYS C 923	12.152	107.810	35.606	1.00	85.47	C
ATOM	124	NZ	LYS C 923	13.465	107.085	35.397	1.00	79.94	N
ATOM	125	N	VAL C 924	6.661	105.978	34.222	1.00	57.97	N
ATOM	126	CA	VAL C 924	6.266	104.569	34.284	1.00	59.25	C
ATOM	127	C	VAL C 924	6.178	103.993	32.855	1.00	60.92	C
ATOM	128	O	VAL C 924	6.643	102.879	32.595	1.00	60.50	O
ATOM	129	CB	VAL C 924	4.903	104.386	35.012	1.00	59.50	C
ATOM	130	CG1	VAL C 924	4.414	102.937	34.899	1.00	51.04	C
ATOM	131	CG2	VAL C 924	5.065	104.748	36.465	1.00	55.92	C
ATOM	132	N	TYR C 925	5.578	104.768	31.947	1.00	59.17	N
ATOM	133	CA	TYR C 925	5.413	104.412	30.538	1.00	58.27	C
ATOM	134	C	TYR C 925	6.798	104.265	29.891	1.00	62.45	C
ATOM	135	O	TYR C 925	7.025	103.397	29.044	1.00	61.60	O

ATOM	136	CB	TYR	C	925	4.613	105.514	29.839	1.00	54.96	C
ATOM	137	CG	TYR	C	925	3.947	105.102	28.554	1.00	54.96	C
ATOM	138	CD1	TYR	C	925	4.609	105.202	27.336	1.00	58.50	C
ATOM	139	CD2	TYR	C	925	2.659	104.582	28.559	1.00	58.34	C
ATOM	140	CE1	TYR	C	925	4.003	104.793	26.144	1.00	59.20	C
ATOM	141	CE2	TYR	C	925	2.039	104.161	27.376	1.00	58.79	C
ATOM	142	CZ	TYR	C	925	2.721	104.270	26.171	1.00	60.73	C
ATOM	143	OH	TYR	C	925	2.130	103.849	25.001	1.00	57.74	O
ATOM	144	N	GLU	C	926	7.725	105.123	30.299	1.00	65.25	N
ATOM	145	CA	GLU	C	926	9.083	105.089	29.780	1.00	68.80	C
ATOM	146	C	GLU	C	926	9.809	103.861	30.320	1.00	69.97	C
ATOM	147	O	GLU	C	926	10.430	103.099	29.570	1.00	69.90	O
ATOM	148	CB	GLU	C	926	9.820	106.358	30.202	1.00	75.59	C
ATOM	149	CG	GLU	C	926	11.293	106.408	29.819	1.00	90.96	C
ATOM	150	CD	GLU	C	926	11.965	107.723	30.223	1.00	101.09	C
ATOM	151	OE1	GLU	C	926	11.383	108.464	31.050	1.00	109.17	O
ATOM	152	OE2	GLU	C	926	13.079	108.010	29.724	1.00	106.84	O
ATOM	153	N	ASN	C	927	9.717	103.666	31.629	1.00	68.66	N
ATOM	154	CA	ASN	C	927	10.376	102.541	32.254	1.00	67.67	C
ATOM	155	C	ASN	C	927	9.822	101.200	31.828	1.00	68.74	C
ATOM	156	O	ASN	C	927	10.574	100.227	31.768	1.00	72.39	O
ATOM	157	CB	ASN	C	927	10.352	102.684	33.773	1.00	68.05	C
ATOM	158	CG	ASN	C	927	11.327	103.738	34.259	1.00	70.92	C
ATOM	159	ND2	ASN	C	927	11.334	103.976	35.562	1.00	70.63	N
ATOM	160	OD1	ASN	C	927	12.072	104.335	33.465	1.00	69.96	O
ATOM	161	N	VAL	C	928	8.523	101.126	31.546	1.00	64.92	N
ATOM	162	CA	VAL	C	928	7.941	99.868	31.076	1.00	61.66	C
ATOM	163	C	VAL	C	928	8.547	99.631	29.700	1.00	60.07	C
ATOM	164	O	VAL	C	928	9.082	98.562	29.420	1.00	60.30	O
ATOM	165	CB	VAL	C	928	6.392	99.942	30.981	1.00	60.82	C
ATOM	166	CG1	VAL	C	928	5.872	98.889	30.022	1.00	60.29	C
ATOM	167	CG2	VAL	C	928	5.771	99.725	32.365	1.00	58.20	C
ATOM	168	N	THR	C	929	8.485	100.652	28.851	1.00	63.07	N
ATOM	169	CA	THR	C	929	9.054	100.578	27.512	1.00	61.40	C
ATOM	170	C	THR	C	929	10.504	100.131	27.584	1.00	62.87	C
ATOM	171	O	THR	C	929	10.971	99.358	26.749	1.00	63.14	O
ATOM	172	CB	THR	C	929	9.003	101.927	26.841	1.00	58.88	C
ATOM	173	CG2	THR	C	929	9.757	101.909	25.557	1.00	63.85	C
ATOM	174	OG1	THR	C	929	7.646	102.254	26.554	1.00	62.34	O

ATOM	175	N	GLY	C	930	11.216	100.623	28.589	1.00	64.51	N
ATOM	176	CA	GLY	C	930	12.602	100.244	28.739	1.00	64.78	C
ATOM	177	C	GLY	C	930	12.737	98.768	29.037	1.00	68.72	C
ATOM	178	O	GLY	C	930	13.534	98.079	28.411	1.00	73.17	O
ATOM	179	N	LEU	C	931	11.958	98.289	30.002	1.00	71.25	N
ATOM	180	CA	LEU	C	931	11.973	96.891	30.393	1.00	69.93	C
ATOM	181	C	LEU	C	931	11.542	96.037	29.233	1.00	66.95	C
ATOM	182	O	LEU	C	931	12.208	95.065	28.914	1.00	67.13	O
ATOM	183	CB	LEU	C	931	11.026	96.633	31.565	1.00	73.68	C
ATOM	184	CG	LEU	C	931	10.990	95.208	32.125	1.00	77.88	C
ATOM	185	CD1	LEU	C	931	12.404	94.755	32.513	1.00	77.15	C
ATOM	186	CD2	LEU	C	931	10.054	95.182	33.332	1.00	79.64	C
ATOM	187	N	VAL	C	932	10.424	96.365	28.603	1.00	65.09	N
ATOM	188	CA	VAL	C	932	10.009	95.537	27.488	1.00	69.46	C
ATOM	189	C	VAL	C	932	11.164	95.398	26.517	1.00	73.87	C
ATOM	190	O	VAL	C	932	11.497	94.297	26.098	1.00	72.32	O
ATOM	191	CB	VAL	C	932	8.820	96.110	26.756	1.00	63.05	C
ATOM	192	CG1	VAL	C	932	8.589	95.329	25.483	1.00	62.98	C
ATOM	193	CG2	VAL	C	932	7.609	96.025	27.642	1.00	59.58	C
ATOM	194	N	LYS	C	933	11.776	96.530	26.185	1.00	79.21	N
ATOM	195	CA	LYS	C	933	12.912	96.599	25.274	1.00	80.58	C
ATOM	196	C	LYS	C	933	14.141	95.773	25.707	1.00	83.29	C
ATOM	197	O	LYS	C	933	14.731	95.054	24.891	1.00	83.49	O
ATOM	198	CB	LYS	C	933	13.294	98.064	25.107	1.00	81.60	C
ATOM	199	CG	LYS	C	933	13.286	98.550	23.670	1.00	84.45	C
ATOM	200	CD	LYS	C	933	12.877	100.009	23.543	1.00	84.61	C
ATOM	201	CE	LYS	C	933	11.568	100.112	22.774	1.00	83.57	C
ATOM	202	NZ	LYS	C	933	11.236	101.508	22.371	1.00	88.80	N
ATOM	203	N	ALA	C	934	14.542	95.872	26.973	1.00	83.91	N
ATOM	204	CA	ALA	C	934	15.700	95.101	27.431	1.00	86.68	C
ATOM	205	C	ALA	C	934	15.429	93.604	27.294	1.00	88.36	C
ATOM	206	O	ALA	C	934	16.351	92.809	27.107	1.00	92.75	O
ATOM	207	CB	ALA	C	934	16.048	95.439	28.880	1.00	87.14	C
ATOM	208	N	VAL	C	935	14.159	93.227	27.407	1.00	85.45	N
ATOM	209	CA	VAL	C	935	13.733	91.839	27.268	1.00	81.49	C
ATOM	210	C	VAL	C	935	13.888	91.417	25.814	1.00	81.92	C
ATOM	211	O	VAL	C	935	14.375	90.328	25.520	1.00	83.58	O
ATOM	212	CB	VAL	C	935	12.247	91.673	27.699	1.00	79.53	C
ATOM	213	CG1	VAL	C	935	11.545	90.605	26.852	1.00	72.69	C

ATOM	214	CG2	VAL	C	935	12.184	91.310	29.164	1.00	75.15	C
ATOM	215	N	ILE	C	936	13.469	92.291	24.910	1.00	82.93	N
ATOM	216	CA	ILE	C	936	13.551	92.020	23.489	1.00	85.97	C
ATOM	217	C	ILE	C	936	15.010	91.975	23.021	1.00	92.14	C
ATOM	218	O	ILE	C	936	15.336	91.325	22.022	1.00	90.57	O
ATOM	219	CB	ILE	C	936	12.766	93.078	22.709	1.00	80.76	C
ATOM	220	CG1	ILE	C	936	11.295	93.014	23.104	1.00	78.23	C
ATOM	221	CG2	ILE	C	936	12.879	92.827	21.232	1.00	82.49	C
ATOM	222	CD1	ILE	C	936	10.444	94.028	22.396	1.00	76.28	C
ATOM	223	N	GLU	C	937	15.891	92.658	23.746	1.00	98.38	N
ATOM	224	CA	GLU	C	937	17.309	92.662	23.401	1.00	105.29	C
ATOM	225	C	GLU	C	937	17.875	91.261	23.702	1.00	106.70	C
ATOM	226	O	GLU	C	937	18.752	90.751	22.996	1.00	109.35	O
ATOM	227	CB	GLU	C	937	18.034	93.754	24.208	1.00	109.34	C
ATOM	228	CG	GLU	C	937	19.500	93.990	23.811	1.00	114.00	C
ATOM	229	CD	GLU	C	937	19.745	93.851	22.306	1.00	117.38	C
ATOM	230	OE1	GLU	C	937	18.904	94.339	21.512	1.00	115.32	O
ATOM	231	OE2	GLU	C	937	20.785	93.257	21.925	1.00	117.56	O
ATOM	232	N	MET	C	938	17.361	90.644	24.761	1.00	108.24	N
ATOM	233	CA	MET	C	938	17.762	89.296	25.136	1.00	107.56	C
ATOM	234	C	MET	C	938	16.978	88.301	24.275	1.00	108.86	C
ATOM	235	O	MET	C	938	17.521	87.303	23.809	1.00	107.20	O
ATOM	236	CB	MET	C	938	17.444	89.039	26.605	1.00	103.15	C
ATOM	237	CG	MET	C	938	17.085	87.600	26.890	1.00	100.99	C
ATOM	238	SD	MET	C	938	16.864	87.280	28.638	1.00	102.23	S
ATOM	239	CE	MET	C	938	18.424	87.925	29.302	1.00	96.91	C
ATOM	240	N	SER	C	939	15.696	88.584	24.061	1.00	112.38	N
ATOM	241	CA	SER	C	939	14.840	87.692	23.279	1.00	117.67	C
ATOM	242	C	SER	C	939	15.323	87.446	21.848	1.00	119.77	C
ATOM	243	O	SER	C	939	15.197	86.328	21.338	1.00	118.72	O
ATOM	244	CB	SER	C	939	13.392	88.216	23.235	1.00	118.43	C
ATOM	245	OG	SER	C	939	13.138	88.966	22.054	1.00	120.19	O
ATOM	246	N	SER	C	940	15.871	88.474	21.200	1.00	122.53	N
ATOM	247	CA	SER	C	940	16.335	88.328	19.820	1.00	124.52	C
ATOM	248	C	SER	C	940	17.828	88.067	19.662	1.00	125.63	C
ATOM	249	O	SER	C	940	18.302	87.764	18.559	1.00	123.74	O
ATOM	250	CB	SER	C	940	15.955	89.558	19.002	1.00	124.34	C
ATOM	251	OG	SER	C	940	16.234	89.323	17.633	1.00	124.58	O
ATOM	252	N	LYS	C	941	18.561	88.199	20.763	1.00	127.31	N

ATOM	253	CA	LYS C 941	19.995	87.954	20.756	1.00130.31	C
ATOM	254	C	LYS C 941	20.260	86.516	21.259	1.00133.31	C
ATOM	255	O	LYS C 941	20.191	85.556	20.483	1.00134.26	O
ATOM	256	CB	LYS C 941	20.706	88.985	21.646	1.00129.68	C
ATOM	257	CG	LYS C 941	22.179	89.203	21.304	1.00133.13	C
ATOM	258	CD	LYS C 941	23.024	87.947	21.534	1.00136.10	C
ATOM	259	CE	LYS C 941	24.242	87.899	20.601	1.00136.33	C
ATOM	260	NZ	LYS C 941	25.034	89.168	20.595	1.00133.87	N
ATOM	261	N	ILE C 942	20.531	86.399	22.563	1.00135.72	N
ATOM	262	CA	ILE C 942	20.832	85.149	23.304	1.00135.88	C
ATOM	263	C	ILE C 942	20.989	83.747	22.671	1.00135.69	C
ATOM	264	O	ILE C 942	21.954	83.048	23.011	1.00136.41	O
ATOM	265	CB	ILE C 942	19.861	84.953	24.508	1.00135.80	C
ATOM	266	CG1	ILE C 942	20.569	84.151	25.618	1.00134.32	C
ATOM	267	CG2	ILE C 942	18.583	84.210	24.062	1.00133.16	C
ATOM	268	CD1	ILE C 942	19.708	83.865	26.818	1.00133.90	C
ATOM	269	N	GLN C 943	20.075	83.315	21.798	1.00134.34	N
ATOM	270	CA	GLN C 943	20.188	81.993	21.193	1.00132.88	C
ATOM	271	C	GLN C 943	21.674	81.652	21.016	1.00132.35	C
ATOM	272	O	GLN C 943	22.173	80.690	21.625	1.00132.00	O
ATOM	273	CB	GLN C 943	19.414	81.962	19.851	1.00132.04	C
ATOM	274	CG	GLN C 943	17.982	81.446	20.006	1.00131.86	C
ATOM	275	CD	GLN C 943	17.936	79.947	20.263	1.00131.58	C
ATOM	276	NE2	GLN C 943	17.400	79.551	21.420	1.00128.52	N
ATOM	277	OE1	GLN C 943	18.384	79.155	19.431	1.00131.63	O
ATOM	278	N	PRO C 944	22.408	82.449	20.194	1.00131.19	N
ATOM	279	CA	PRO C 944	23.835	82.210	19.966	1.00127.40	C
ATOM	280	C	PRO C 944	24.699	82.162	21.238	1.00124.05	C
ATOM	281	O	PRO C 944	25.070	81.116	21.760	1.00122.03	O
ATOM	282	CB	PRO C 944	24.201	83.391	19.093	1.00128.29	C
ATOM	283	CG	PRO C 944	23.087	83.384	18.151	1.00129.04	C
ATOM	284	CD	PRO C 944	21.968	83.466	19.213	1.00130.52	C
ATOM	285	N	ALA C 945	24.992	83.349	21.743	1.00122.53	N
ATOM	286	CA	ALA C 945	25.806	83.568	22.946	1.00122.04	C
ATOM	287	C	ALA C 945	25.841	82.540	24.075	1.00120.54	C
ATOM	288	O	ALA C 945	24.840	81.906	24.400	1.00119.65	O
ATOM	289	CB	ALA C 945	25.494	84.961	23.538	1.00121.84	C
ATOM	290	N	PRO C 946	27.033	82.368	24.685	1.00120.48	N
ATOM	291	CA	PRO C 946	27.308	81.442	25.797	1.00120.10	C



ATOM	292	C	PRO C 946	27.088	82.176	27.137	1.00118.51	C
ATOM	293	O	PRO C 946	26.599	83.308	27.138	1.00117.33	O
ATOM	294	CB	PRO C 946	28.772	81.055	25.571	1.00121.49	C
ATOM	295	CG	PRO C 946	29.366	82.309	24.986	1.00120.89	C
ATOM	296	CD	PRO C 946	28.288	82.759	24.011	1.00120.40	C
ATOM	297	N	PRO C 947	27.429	81.554	28.284	1.00118.59	N
ATOM	298	CA	PRO C 947	27.252	82.190	29.601	1.00120.40	C
ATOM	299	C	PRO C 947	28.096	83.451	29.875	1.00122.86	C
ATOM	300	O	PRO C 947	27.870	84.150	30.863	1.00121.93	O
ATOM	301	CB	PRO C 947	27.594	81.069	30.570	1.00119.50	C
ATOM	302	CG	PRO C 947	27.130	79.871	29.861	1.00118.56	C
ATOM	303	CD	PRO C 947	27.576	80.097	28.434	1.00118.85	C
ATOM	304	N	GLU C 948	29.105	83.725	29.052	1.00126.09	N
ATOM	305	CA	GLU C 948	29.921	84.935	29.256	1.00128.05	C
ATOM	306	C	GLU C 948	29.179	86.102	28.618	1.00129.22	C
ATOM	307	O	GLU C 948	29.651	87.246	28.633	1.00129.11	O
ATOM	308	CB	GLU C 948	31.281	84.804	28.563	1.00128.79	C
ATOM	309	CG	GLU C 948	32.407	84.236	29.412	1.00129.22	C
ATOM	310	CD	GLU C 948	33.351	83.374	28.595	1.00129.49	C
ATOM	311	OE1	GLU C 948	34.515	83.783	28.369	1.00127.95	O
ATOM	312	OE2	GLU C 948	32.907	82.282	28.171	1.00130.34	O
ATOM	313	N	GLU C 949	27.998	85.811	28.081	1.00130.67	N
ATOM	314	CA	GLU C 949	27.249	86.828	27.372	1.00132.06	C
ATOM	315	C	GLU C 949	25.753	87.036	27.699	1.00131.00	C
ATOM	316	O	GLU C 949	25.239	88.139	27.493	1.00130.08	O
ATOM	317	CB	GLU C 949	27.510	86.591	25.880	1.00134.83	C
ATOM	318	CG	GLU C 949	29.022	86.702	25.559	1.00139.33	C
ATOM	319	CD	GLU C 949	29.411	86.198	24.172	1.00142.36	C
ATOM	320	OE1	GLU C 949	28.784	86.638	23.181	1.00144.45	O
ATOM	321	OE2	GLU C 949	30.356	85.376	24.080	1.00140.95	O
ATOM	322	N	TYR C 950	25.041	86.011	28.181	1.00129.73	N
ATOM	323	CA	TYR C 950	23.648	86.241	28.575	1.00125.37	C
ATOM	324	C	TYR C 950	23.553	86.517	30.088	1.00123.89	C
ATOM	325	O	TYR C 950	22.607	87.168	30.529	1.00124.67	O
ATOM	326	CB	TYR C 950	22.678	85.099	28.172	1.00124.27	C
ATOM	327	CG	TYR C 950	23.065	83.664	28.475	1.00124.30	C
ATOM	328	CD1	TYR C 950	23.439	83.256	29.757	1.00123.25	C
ATOM	329	CD2	TYR C 950	22.993	82.694	27.471	1.00123.52	C
ATOM	330	CE1	TYR C 950	23.729	81.904	30.027	1.00122.44	C

ATOM	331	CE2	TYR	C	950	23.276	81.354	27.728	1.00122.74	C
ATOM	332	CZ	TYR	C	950	23.645	80.961	29.000	1.00123.33	C
ATOM	333	OH	TYR	C	950	23.933	79.628	29.219	1.00122.73	O
ATOM	334	N	VAL	C	951	24.527	86.057	30.879	1.00121.89	N
ATOM	335	CA	VAL	C	951	24.483	86.321	32.314	1.00122.76	C
ATOM	336	C	VAL	C	951	24.330	87.824	32.567	1.00126.35	C
ATOM	337	O	VAL	C	951	23.721	88.226	33.566	1.00128.44	O
ATOM	338	CB	VAL	C	951	25.731	85.811	33.041	1.00121.55	C
ATOM	339	CG1	VAL	C	951	25.719	86.295	34.493	1.00119.27	C
ATOM	340	CG2	VAL	C	951	25.732	84.296	33.010	1.00122.16	C
ATOM	341	N	PRO	C	952	24.913	88.677	31.687	1.00127.99	N
ATOM	342	CA	PRO	C	952	24.782	90.131	31.868	1.00126.63	C
ATOM	343	C	PRO	C	952	23.495	90.571	31.136	1.00125.51	C
ATOM	344	O	PRO	C	952	22.759	91.421	31.623	1.00124.87	O
ATOM	345	CB	PRO	C	952	26.048	90.694	31.202	1.00126.03	C
ATOM	346	CG	PRO	C	952	27.016	89.550	31.238	1.00127.51	C
ATOM	347	CD	PRO	C	952	26.122	88.382	30.895	1.00128.76	C
ATOM	348	N	MET	C	953	23.236	89.989	29.960	1.00124.90	N
ATOM	349	CA	MET	C	953	22.025	90.287	29.161	1.00124.90	C
ATOM	350	C	MET	C	953	20.768	90.152	30.033	1.00123.24	C
ATOM	351	O	MET	C	953	19.695	90.642	29.674	1.00123.57	O
ATOM	352	CB	MET	C	953	21.900	89.307	27.982	1.00128.34	C
ATOM	353	CG	MET	C	953	21.893	89.921	26.586	1.00132.89	C
ATOM	354	SD	MET	C	953	21.585	88.654	25.299	1.00139.20	S
ATOM	355	CE	MET	C	953	23.116	87.639	25.355	1.00133.99	C
ATOM	356	N	VAL	C	954	20.914	89.433	31.149	1.00120.10	N
ATOM	357	CA	VAL	C	954	19.851	89.218	32.134	1.00115.86	C
ATOM	358	C	VAL	C	954	20.044	90.326	33.162	1.00114.76	C
ATOM	359	O	VAL	C	954	19.100	91.026	33.523	1.00115.64	O
ATOM	360	CB	VAL	C	954	19.980	87.827	32.841	1.00115.37	C
ATOM	361	CG1	VAL	C	954	19.528	87.912	34.295	1.00114.62	C
ATOM	362	CG2	VAL	C	954	19.132	86.800	32.120	1.00111.15	C
ATOM	363	N	LYS	C	955	21.281	90.484	33.625	1.00112.03	N
ATOM	364	CA	LYS	C	955	21.611	91.524	34.594	1.00110.08	C
ATOM	365	C	LYS	C	955	20.988	92.853	34.129	1.00108.57	C
ATOM	366	O	LYS	C	955	20.634	93.707	34.946	1.00107.99	O
ATOM	367	CB	LYS	C	955	23.136	91.641	34.715	1.00109.26	C
ATOM	368	CG	LYS	C	955	23.618	92.778	35.592	1.00112.85	C
ATOM	369	CD	LYS	C	955	23.180	92.635	37.038	1.00113.69	C

ATOM	370	CE	LYS	C	955	23.684	93.818	37.851	1.00117.31	C
ATOM	371	NZ	LYS	C	955	23.412	93.674	39.305	1.00120.85	N
ATOM	372	N	GLU	C	956	20.849	93.000	32.810	1.00106.12	N
ATOM	373	CA	GLU	C	956	20.259	94.183	32.181	1.00104.23	C
ATOM	374	C	GLU	C	956	18.766	94.254	32.481	1.00101.34	C
ATOM	375	O	GLU	C	956	18.304	95.191	33.132	1.00101.80	O
ATOM	376	CB	GLU	C	956	20.462	94.139	30.661	1.00107.40	C
ATOM	377	CG	GLU	C	956	21.683	94.881	30.150	1.00115.30	C
ATOM	378	CD	GLU	C	956	21.296	96.029	29.238	1.00120.67	C
ATOM	379	OE1	GLU	C	956	20.256	95.899	28.554	1.00123.99	O
ATOM	380	OE2	GLU	C	956	22.023	97.048	29.192	1.00123.79	O
ATOM	381	N	VAL	C	957	18.018	93.275	31.974	1.00 97.84	N
ATOM	382	CA	VAL	C	957	16.575	93.179	32.202	1.00 91.30	C
ATOM	383	C	VAL	C	957	16.287	93.287	33.705	1.00 89.63	C
ATOM	384	O	VAL	C	957	15.201	93.722	34.111	1.00 89.13	O
ATOM	385	CB	VAL	C	957	16.024	91.823	31.670	1.00 86.99	C
ATOM	386	CG1	VAL	C	957	14.696	91.487	32.325	1.00 81.87	C
ATOM	387	CG2	VAL	C	957	15.859	91.885	30.162	1.00 83.49	C
ATOM	388	N	GLY	C	958	17.258	92.877	34.521	1.00 86.73	N
ATOM	389	CA	GLY	C	958	17.100	92.942	35.963	1.00 86.30	C
ATOM	390	C	GLY	C	958	17.253	94.357	36.489	1.00 87.09	C
ATOM	391	O	GLY	C	958	16.602	94.736	37.470	1.00 87.61	O
ATOM	392	N	LEU	C	959	18.122	95.134	35.836	1.00 88.08	N
ATOM	393	CA	LEU	C	959	18.390	96.533	36.203	1.00 87.22	C
ATOM	394	C	LEU	C	959	17.248	97.427	35.696	1.00 84.42	C
ATOM	395	O	LEU	C	959	16.860	98.399	36.361	1.00 81.73	O
ATOM	396	CB	LEU	C	959	19.752	96.998	35.617	1.00 90.23	C
ATOM	397	CG	LEU	C	959	21.069	96.402	36.183	1.00 94.61	C
ATOM	398	CD1	LEU	C	959	22.235	96.526	35.174	1.00 91.08	C
ATOM	399	CD2	LEU	C	959	21.416	97.110	37.493	1.00 96.47	C
ATOM	400	N	ALA	C	960	16.710	97.079	34.525	1.00 80.88	N
ATOM	401	CA	ALA	C	960	15.614	97.822	33.912	1.00 78.40	C
ATOM	402	C	ALA	C	960	14.308	97.632	34.678	1.00 77.74	C
ATOM	403	O	ALA	C	960	13.397	98.449	34.574	1.00 77.60	O
ATOM	404	CB	ALA	C	960	15.435	97.385	32.474	1.00 77.27	C
ATOM	405	N	LEU	C	961	14.216	96.536	35.424	1.00 77.06	N
ATOM	406	CA	LEU	C	961	13.037	96.242	36.225	1.00 75.44	C
ATOM	407	C	LEU	C	961	13.202	96.911	37.577	1.00 77.45	C
ATOM	408	O	LEU	C	961	12.229	97.333	38.204	1.00 76.85	O

ATOM	409	CB	LEU	C	961	12.883	94.737	36.432	1.00	73.48	C
ATOM	410	CG	LEU	C	961	11.791	94.360	37.440	1.00	72.22	C
ATOM	411	CD1	LEU	C	961	10.410	94.596	36.828	1.00	67.24	C
ATOM	412	CD2	LEU	C	961	11.961	92.903	37.858	1.00	73.06	C
ATOM	413	N	ARG	C	962	14.440	96.984	38.042	1.00	81.45	N
ATOM	414	CA	ARG	C	962	14.714	97.632	39.314	1.00	86.24	C
ATOM	415	C	ARG	C	962	14.209	99.069	39.193	1.00	83.35	C
ATOM	416	O	ARG	C	962	13.524	99.572	40.085	1.00	83.50	O
ATOM	417	CB	ARG	C	962	16.218	97.617	39.594	1.00	96.72	C
ATOM	418	CG	ARG	C	962	16.627	98.192	40.952	1.00	107.84	C
ATOM	419	CD	ARG	C	962	18.157	98.202	41.147	1.00	114.40	C
ATOM	420	NE	ARG	C	962	18.488	98.556	42.529	1.00	123.62	N
ATOM	421	CZ	ARG	C	962	19.715	98.810	42.983	1.00	127.32	C
ATOM	422	NH1	ARG	C	962	20.761	98.751	42.164	1.00	129.36	N
ATOM	423	NH2	ARG	C	962	19.890	99.139	44.262	1.00	127.50	N
ATOM	424	N	THR	C	963	14.550	99.700	38.066	1.00	81.04	N
ATOM	425	CA	THR	C	963	14.159	101.075	37.737	1.00	77.34	C
ATOM	426	C	THR	C	963	12.641	101.222	37.673	1.00	76.41	C
ATOM	427	O	THR	C	963	12.077	102.135	38.271	1.00	78.85	O
ATOM	428	CB	THR	C	963	14.703	101.532	36.342	1.00	77.75	C
ATOM	429	CG2	THR	C	963	14.212	102.939	36.011	1.00	73.04	C
ATOM	430	OG1	THR	C	963	16.136	101.527	36.336	1.00	76.39	O
ATOM	431	N	LEU	C	964	11.984	100.333	36.931	1.00	72.53	N
ATOM	432	CA	LEU	C	964	10.537	100.405	36.784	1.00	71.29	C
ATOM	433	C	LEU	C	964	9.855	100.296	38.114	1.00	71.98	C
ATOM	434	O	LEU	C	964	8.906	101.030	38.397	1.00	72.44	O
ATOM	435	CB	LEU	C	964	10.006	99.298	35.868	1.00	68.42	C
ATOM	436	CG	LEU	C	964	8.478	99.135	35.810	1.00	64.26	C
ATOM	437	CD1	LEU	C	964	7.791	100.441	35.463	1.00	57.94	C
ATOM	438	CD2	LEU	C	964	8.152	98.068	34.782	1.00	62.07	C
ATOM	439	N	LEU	C	965	10.341	99.370	38.931	1.00	74.48	N
ATOM	440	CA	LEU	C	965	9.764	99.152	40.246	1.00	75.89	C
ATOM	441	C	LEU	C	965	9.991	100.384	41.094	1.00	74.88	C
ATOM	442	O	LEU	C	965	9.085	100.824	41.815	1.00	73.74	O
ATOM	443	CB	LEU	C	965	10.368	97.896	40.879	1.00	76.31	C
ATOM	444	CG	LEU	C	965	9.876	96.665	40.106	1.00	76.66	C
ATOM	445	CD1	LEU	C	965	10.606	95.443	40.588	1.00	76.56	C
ATOM	446	CD2	LEU	C	965	8.357	96.507	40.275	1.00	75.94	C
ATOM	447	N	ALA	C	966	11.190	100.954	40.972	1.00	72.90	N

ATOM	448	CA	ALA C 966	11.550	102.167	41.701	1.00	71.93	C
ATOM	449	C	ALA C 966	10.582	103.315	41.362	1.00	70.46	C
ATOM	450	O	ALA C 966	10.082	103.991	42.268	1.00	72.48	O
ATOM	451	CB	ALA C 966	12.976	102.562	41.371	1.00	69.12	C
ATOM	452	N	THR C 967	10.313	103.520	40.070	1.00	67.44	N
ATOM	453	CA	THR C 967	9.398	104.565	39.627	1.00	63.01	C
ATOM	454	C	THR C 967	7.976	104.304	40.072	1.00	64.40	C
ATOM	455	O	THR C 967	7.271	105.235	40.454	1.00	65.31	O
ATOM	456	CB	THR C 967	9.358	104.693	38.112	1.00	64.08	C
ATOM	457	CG2	THR C 967	8.359	105.741	37.688	1.00	64.42	C
ATOM	458	OG1	THR C 967	10.644	105.078	37.638	1.00	67.54	O
ATOM	459	N	VAL C 968	7.524	103.056	40.012	1.00	63.53	N
ATOM	460	CA	VAL C 968	6.156	102.809	40.440	1.00	65.67	C
ATOM	461	C	VAL C 968	6.079	103.144	41.926	1.00	69.31	C
ATOM	462	O	VAL C 968	5.044	103.603	42.400	1.00	68.50	O
ATOM	463	CB	VAL C 968	5.682	101.338	40.194	1.00	64.11	C
ATOM	464	CG1	VAL C 968	4.207	101.203	40.574	1.00	57.49	C
ATOM	465	CG2	VAL C 968	5.860	100.949	38.731	1.00	60.33	C
ATOM	466	N	ASP C 969	7.181	102.944	42.650	1.00	75.56	N
ATOM	467	CA	ASP C 969	7.206	103.246	44.080	1.00	83.87	C
ATOM	468	C	ASP C 969	7.015	104.739	44.334	1.00	87.31	C
ATOM	469	O	ASP C 969	6.393	105.127	45.328	1.00	90.96	O
ATOM	470	CB	ASP C 969	8.512	102.774	44.730	1.00	90.65	C
ATOM	471	CG	ASP C 969	8.646	101.247	44.743	1.00	99.31	C
ATOM	472	OD1	ASP C 969	7.585	100.569	44.687	1.00	99.15	O
ATOM	473	OD2	ASP C 969	9.804	100.741	44.822	1.00	102.67	O
ATOM	474	N	GLU C 970	7.551	105.579	43.451	1.00	87.78	N
ATOM	475	CA	GLU C 970	7.383	107.025	43.592	1.00	87.87	C
ATOM	476	C	GLU C 970	6.020	107.494	43.066	1.00	86.64	C
ATOM	477	O	GLU C 970	5.565	108.587	43.390	1.00	89.18	O
ATOM	478	CB	GLU C 970	8.467	107.757	42.828	1.00	87.52	C
ATOM	479	CG	GLU C 970	9.852	107.398	43.245	1.00	98.17	C
ATOM	480	CD	GLU C 970	10.886	108.142	42.426	1.00	107.97	C
ATOM	481	OE1	GLU C 970	10.958	107.886	41.196	1.00	110.90	O
ATOM	482	OE2	GLU C 970	11.615	108.980	43.015	1.00	110.97	O
ATOM	483	N	THR C 971	5.355	106.657	42.284	1.00	82.40	N
ATOM	484	CA	THR C 971	4.087	107.046	41.711	1.00	79.25	C
ATOM	485	C	THR C 971	2.865	106.634	42.512	1.00	80.67	C
ATOM	486	O	THR C 971	1.841	107.311	42.466	1.00	81.99	O

ATOM	487	CB	THR	C	971	3.993	106.485	40.276	1.00	79.59	C
ATOM	488	CG2	THR	C	971	2.685	106.873	39.595	1.00	75.08	C
ATOM	489	OG1	THR	C	971	5.091	106.996	39.512	1.00	72.72	O
ATOM	490	N	ILE	C	972	2.962	105.531	43.244	1.00	81.67	N
ATOM	491	CA	ILE	C	972	1.817	105.045	44.024	1.00	83.42	C
ATOM	492	C	ILE	C	972	1.269	106.051	45.048	1.00	80.81	C
ATOM	493	O	ILE	C	972	0.046	106.236	45.160	1.00	74.87	O
ATOM	494	CB	ILE	C	972	2.166	103.743	44.776	1.00	83.46	C
ATOM	495	CG1	ILE	C	972	2.802	102.745	43.820	1.00	84.93	C
ATOM	496	CG2	ILE	C	972	0.902	103.090	45.323	1.00	83.58	C
ATOM	497	CD1	ILE	C	972	3.825	101.854	44.487	1.00	89.93	C
ATOM	498	N	PRO	C	973	2.169	106.709	45.805	1.00	79.99	N
ATOM	499	CA	PRO	C	973	1.744	107.687	46.814	1.00	79.69	C
ATOM	500	C	PRO	C	973	0.568	108.529	46.339	1.00	80.30	C
ATOM	501	O	PRO	C	973	-0.466	108.639	47.004	1.00	81.02	O
ATOM	502	CB	PRO	C	973	2.995	108.535	47.016	1.00	76.57	C
ATOM	503	CG	PRO	C	973	4.097	107.565	46.802	1.00	75.19	C
ATOM	504	CD	PRO	C	973	3.637	106.739	45.625	1.00	76.30	C
ATOM	505	N	LEU	C	974	0.765	109.106	45.162	1.00	77.51	N
ATOM	506	CA	LEU	C	974	-0.186	109.972	44.493	1.00	75.93	C
ATOM	507	C	LEU	C	974	-1.568	109.412	44.101	1.00	74.44	C
ATOM	508	O	LEU	C	974	-2.544	110.144	44.073	1.00	75.32	O
ATOM	509	CB	LEU	C	974	0.491	110.533	43.243	1.00	76.44	C
ATOM	510	CG	LEU	C	974	-0.441	111.137	42.189	1.00	80.68	C
ATOM	511	CD1	LEU	C	974	-0.996	112.470	42.673	1.00	80.27	C
ATOM	512	CD2	LEU	C	974	0.336	111.310	40.882	1.00	84.93	C
ATOM	513	N	LEU	C	975	-1.675	108.129	43.801	1.00	73.62	N
ATOM	514	CA	LEU	C	975	-2.967	107.620	43.354	1.00	75.01	C
ATOM	515	C	LEU	C	975	-3.926	107.317	44.492	1.00	74.03	C
ATOM	516	O	LEU	C	975	-3.518	107.273	45.653	1.00	75.19	O
ATOM	517	CB	LEU	C	975	-2.734	106.391	42.475	1.00	75.34	C
ATOM	518	CG	LEU	C	975	-1.607	106.735	41.489	1.00	78.17	C
ATOM	519	CD1	LEU	C	975	-0.730	105.515	41.226	1.00	79.70	C
ATOM	520	CD2	LEU	C	975	-2.208	107.321	40.208	1.00	79.20	C
ATOM	521	N	PRO	C	976	-5.222	107.135	44.178	1.00	72.08	N
ATOM	522	CA	PRO	C	976	-6.211	106.835	45.216	1.00	74.16	C
ATOM	523	C	PRO	C	976	-5.691	105.762	46.154	1.00	75.80	C
ATOM	524	O	PRO	C	976	-4.933	104.894	45.741	1.00	79.03	O
ATOM	525	CB	PRO	C	976	-7.413	106.388	44.405	1.00	72.85	C

ATOM	526	CG	PRO C 976	-7.355	107.346	43.252	1.00	69.07	C
ATOM	527	CD	PRO C 976	-5.882	107.359	42.880	1.00	68.30	C
ATOM	528	N	ALA C 977	-6.082	105.823	47.421	1.00	80.66	N
ATOM	529	CA	ALA C 977	-5.611	104.827	48.381	1.00	80.60	C
ATOM	530	C	ALA C 977	-6.081	103.447	47.977	1.00	79.40	C
ATOM	531	O	ALA C 977	-5.274	102.504	47.939	1.00	78.47	O
ATOM	532	CB	ALA C 977	-6.120	105.152	49.803	1.00	79.02	C
ATOM	533	N	SER C 978	-7.378	103.357	47.658	1.00	77.53	N
ATOM	534	CA	SER C 978	-8.031	102.094	47.311	1.00	79.82	C
ATOM	535	C	SER C 978	-7.295	101.299	46.265	1.00	83.07	C
ATOM	536	O	SER C 978	-7.200	100.076	46.359	1.00	88.50	O
ATOM	537	CB	SER C 978	-9.484	102.323	46.851	1.00	77.34	C
ATOM	538	OG	SER C 978	-9.563	102.906	45.566	1.00	79.95	O
ATOM	539	N	THR C 979	-6.742	101.997	45.285	1.00	82.72	N
ATOM	540	CA	THR C 979	-6.036	101.333	44.206	1.00	77.91	C
ATOM	541	C	THR C 979	-4.576	100.906	44.454	1.00	78.02	C
ATOM	542	O	THR C 979	-3.975	100.280	43.582	1.00	79.71	O
ATOM	543	CB	THR C 979	-6.049	102.220	42.970	1.00	74.94	C
ATOM	544	CG2	THR C 979	-7.463	102.693	42.648	1.00	62.47	C
ATOM	545	OG1	THR C 979	-5.230	103.361	43.230	1.00	75.64	O
ATOM	546	N	HIS C 980	-3.995	101.207	45.610	1.00	77.48	N
ATOM	547	CA	HIS C 980	-2.596	100.836	45.805	1.00	79.32	C
ATOM	548	C	HIS C 980	-2.347	99.360	45.884	1.00	78.62	C
ATOM	549	O	HIS C 980	-1.223	98.914	45.667	1.00	76.26	O
ATOM	550	CB	HIS C 980	-2.002	101.472	47.063	1.00	82.98	C
ATOM	551	CG	HIS C 980	-1.892	102.959	46.997	1.00	84.15	C
ATOM	552	CD2	HIS C 980	-2.532	103.867	46.227	1.00	85.49	C
ATOM	553	ND1	HIS C 980	-1.043	103.678	47.815	1.00	85.84	N
ATOM	554	CE1	HIS C 980	-1.170	104.960	47.550	1.00	89.89	C
ATOM	555	NE2	HIS C 980	-2.067	105.111	46.591	1.00	88.60	N
ATOM	556	N	ARG C 981	-3.393	98.604	46.194	1.00	80.21	N
ATOM	557	CA	ARG C 981	-3.273	97.156	46.350	1.00	83.54	C
ATOM	558	C	ARG C 981	-3.079	96.385	45.028	1.00	81.92	C
ATOM	559	O	ARG C 981	-2.167	95.556	44.928	1.00	82.24	O
ATOM	560	CB	ARG C 981	-4.497	96.638	47.135	1.00	85.47	C
ATOM	561	CG	ARG C 981	-4.421	95.184	47.647	1.00	84.60	C
ATOM	562	CD	ARG C 981	-3.350	94.950	48.715	1.00	81.06	C
ATOM	563	NE	ARG C 981	-3.156	93.514	48.938	1.00	83.61	N
ATOM	564	CZ	ARG C 981	-2.444	92.979	49.927	1.00	82.35	C

ATOM	565	NH1	ARG	C	981	-1.841	93.759	50.811	1.00	80.71	N
ATOM	566	NH2	ARG	C	981	-2.345	91.657	50.034	1.00	79.63	N
ATOM	567	N	GLU	C	982	-3.914	96.656	44.022	1.00	80.43	N
ATOM	568	CA	GLU	C	982	-3.786	95.974	42.731	1.00	79.47	C
ATOM	569	C	GLU	C	982	-2.404	96.311	42.154	1.00	76.02	C
ATOM	570	O	GLU	C	982	-1.742	95.468	41.549	1.00	71.51	O
ATOM	571	CB	GLU	C	982	-4.898	96.413	41.748	1.00	80.96	C
ATOM	572	CG	GLU	C	982	-5.503	95.242	40.900	1.00	92.71	C
ATOM	573	CD	GLU	C	982	-6.581	95.659	39.837	1.00	100.52	C
ATOM	574	OE1	GLU	C	982	-7.568	96.362	40.206	1.00	102.24	O
ATOM	575	OE2	GLU	C	982	-6.445	95.262	38.642	1.00	95.96	O
ATOM	576	N	ILE	C	983	-1.949	97.532	42.392	1.00	70.78	N
ATOM	577	CA	ILE	C	983	-0.664	97.950	41.858	1.00	72.18	C
ATOM	578	C	ILE	C	983	0.518	97.342	42.579	1.00	74.15	C
ATOM	579	O	ILE	C	983	1.570	97.112	41.982	1.00	77.23	O
ATOM	580	CB	ILE	C	983	-0.499	99.493	41.882	1.00	70.97	C
ATOM	581	CG1	ILE	C	983	-1.659	100.156	41.129	1.00	66.21	C
ATOM	582	CG2	ILE	C	983	0.847	99.874	41.255	1.00	64.06	C
ATOM	583	CD1	ILE	C	983	-1.696	101.652	41.230	1.00	60.12	C
ATOM	584	N	GLU	C	984	0.365	97.091	43.868	1.00	77.02	N
ATOM	585	CA	GLU	C	984	1.468	96.517	44.618	1.00	79.38	C
ATOM	586	C	GLU	C	984	1.536	95.055	44.225	1.00	77.09	C
ATOM	587	O	GLU	C	984	2.611	94.471	44.090	1.00	74.08	O
ATOM	588	CB	GLU	C	984	1.222	96.681	46.119	1.00	88.11	C
ATOM	589	CG	GLU	C	984	2.184	97.655	46.801	1.00	99.14	C
ATOM	590	CD	GLU	C	984	1.475	98.580	47.793	1.00	109.11	C
ATOM	591	OE1	GLU	C	984	0.546	98.103	48.497	1.00	115.25	O
ATOM	592	OE2	GLU	C	984	1.856	99.777	47.871	1.00	110.47	O
ATOM	593	N	MET	C	985	0.361	94.481	44.016	1.00	73.92	N
ATOM	594	CA	MET	C	985	0.245	93.099	43.614	1.00	70.59	C
ATOM	595	C	MET	C	985	0.861	92.887	42.213	1.00	69.46	C
ATOM	596	O	MET	C	985	1.607	91.926	42.001	1.00	66.72	O
ATOM	597	CB	MET	C	985	-1.233	92.703	43.675	1.00	72.71	C
ATOM	598	CG	MET	C	985	-1.492	91.613	44.708	1.00	80.42	C
ATOM	599	SD	MET	C	985	-0.766	91.853	46.390	1.00	85.30	S
ATOM	600	CE	MET	C	985	1.105	91.464	46.198	1.00	82.08	C
ATOM	601	N	ALA	C	986	0.546	93.791	41.273	1.00	69.08	N
ATOM	602	CA	ALA	C	986	1.086	93.766	39.907	1.00	61.06	C
ATOM	603	C	ALA	C	986	2.615	93.820	39.977	1.00	61.60	C



ATOM	604	O	ALA	C	986	3.303	93.201	39.182	1.00	60.41	O
ATOM	605	CB	ALA	C	986	0.572	94.944	39.135	1.00	52.88	C
ATOM	606	N	GLN	C	987	3.150	94.579	40.923	1.00	64.40	N
ATOM	607	CA	GLN	C	987	4.599	94.650	41.083	1.00	69.94	C
ATOM	608	C	GLN	C	987	5.205	93.350	41.620	1.00	74.21	C
ATOM	609	O	GLN	C	987	6.300	92.942	41.218	1.00	74.81	O
ATOM	610	CB	GLN	C	987	4.983	95.727	42.075	1.00	73.29	C
ATOM	611	CG	GLN	C	987	4.787	97.131	41.646	1.00	74.46	C
ATOM	612	CD	GLN	C	987	5.230	98.082	42.734	1.00	74.15	C
ATOM	613	NE2	GLN	C	987	6.511	98.466	42.700	1.00	69.51	N
ATOM	614	OE1	GLN	C	987	4.443	98.447	43.616	1.00	71.07	O
ATOM	615	N	LYS	C	988	4.530	92.725	42.579	1.00	75.72	N
ATOM	616	CA	LYS	C	988	5.067	91.498	43.139	1.00	76.85	C
ATOM	617	C	LYS	C	988	5.101	90.456	42.035	1.00	74.61	C
ATOM	618	O	LYS	C	988	6.022	89.629	41.960	1.00	75.89	O
ATOM	619	CB	LYS	C	988	4.220	91.014	44.326	1.00	83.11	C
ATOM	620	CG	LYS	C	988	4.609	89.609	44.824	1.00	93.91	C
ATOM	621	CD	LYS	C	988	6.140	89.444	45.039	1.00	98.59	C
ATOM	622	CE	LYS	C	988	6.550	87.970	45.192	1.00	96.94	C
ATOM	623	NZ	LYS	C	988	7.178	87.683	46.513	1.00	101.06	N
ATOM	624	N	LEU	C	989	4.100	90.506	41.167	1.00	67.38	N
ATOM	625	CA	LEU	C	989	4.039	89.571	40.066	1.00	63.95	C
ATOM	626	C	LEU	C	989	5.287	89.710	39.200	1.00	63.62	C
ATOM	627	O	LEU	C	989	5.862	88.713	38.787	1.00	63.80	O
ATOM	628	CB	LEU	C	989	2.782	89.822	39.246	1.00	60.47	C
ATOM	629	CG	LEU	C	989	2.464	88.855	38.113	1.00	57.38	C
ATOM	630	CD1	LEU	C	989	2.515	87.434	38.615	1.00	56.34	C
ATOM	631	CD2	LEU	C	989	1.091	89.182	37.565	1.00	54.02	C
ATOM	632	N	LEU	C	990	5.711	90.940	38.928	1.00	63.58	N
ATOM	633	CA	LEU	C	990	6.906	91.159	38.119	1.00	63.56	C
ATOM	634	C	LEU	C	990	8.165	90.600	38.784	1.00	64.92	C
ATOM	635	O	LEU	C	990	9.055	90.093	38.096	1.00	62.19	O
ATOM	636	CB	LEU	C	990	7.084	92.645	37.830	1.00	61.74	C
ATOM	637	CG	LEU	C	990	6.074	93.214	36.848	1.00	60.69	C
ATOM	638	CD1	LEU	C	990	6.124	94.706	36.887	1.00	60.66	C
ATOM	639	CD2	LEU	C	990	6.384	92.706	35.467	1.00	63.00	C
ATOM	640	N	ASN	C	991	8.238	90.707	40.111	1.00	67.78	N
ATOM	641	CA	ASN	C	991	9.373	90.189	40.880	1.00	73.14	C
ATOM	642	C	ASN	C	991	9.567	88.705	40.638	1.00	73.68	C

ATOM	643	O	ASN	C	991	10.670	88.249	40.299	1.00	74.98	O
ATOM	644	CB	ASN	C	991	9.158	90.403	42.380	1.00	78.47	C
ATOM	645	CG	ASN	C	991	9.744	91.706	42.865	1.00	84.33	C
ATOM	646	ND2	ASN	C	991	8.906	92.539	43.479	1.00	87.31	N
ATOM	647	OD1	ASN	C	991	10.947	91.965	42.695	1.00	84.79	O
ATOM	648	N	SER	C	992	8.486	87.952	40.832	1.00	74.02	N
ATOM	649	CA	SER	C	992	8.518	86.516	40.634	1.00	72.44	C
ATOM	650	C	SER	C	992	8.788	86.152	39.168	1.00	70.80	C
ATOM	651	O	SER	C	992	9.392	85.115	38.911	1.00	71.78	O
ATOM	652	CB	SER	C	992	7.216	85.887	41.120	1.00	68.96	C
ATOM	653	OG	SER	C	992	6.140	86.325	40.325	1.00	75.27	O
ATOM	654	N	ASP	C	993	8.359	86.984	38.213	1.00	71.52	N
ATOM	655	CA	ASP	C	993	8.626	86.706	36.793	1.00	72.93	C
ATOM	656	C	ASP	C	993	10.134	86.756	36.544	1.00	75.63	C
ATOM	657	O	ASP	C	993	10.654	86.008	35.705	1.00	78.90	O
ATOM	658	CB	ASP	C	993	7.941	87.725	35.871	1.00	71.56	C
ATOM	659	CG	ASP	C	993	6.431	87.555	35.824	1.00	77.47	C
ATOM	660	OD1	ASP	C	993	5.900	86.632	36.481	1.00	82.03	O
ATOM	661	OD2	ASP	C	993	5.768	88.348	35.125	1.00	81.94	O
ATOM	662	N	LEU	C	994	10.823	87.653	37.259	1.00	74.25	N
ATOM	663	CA	LEU	C	994	12.268	87.804	37.142	1.00	73.89	C
ATOM	664	C	LEU	C	994	12.936	86.630	37.832	1.00	77.39	C
ATOM	665	O	LEU	C	994	14.002	86.163	37.408	1.00	77.56	O
ATOM	666	CB	LEU	C	994	12.743	89.084	37.805	1.00	73.64	C
ATOM	667	CG	LEU	C	994	14.220	89.291	37.510	1.00	71.58	C
ATOM	668	CD1	LEU	C	994	14.368	89.691	36.055	1.00	71.16	C
ATOM	669	CD2	LEU	C	994	14.777	90.357	38.418	1.00	74.31	C
ATOM	670	N	GLY	C	995	12.322	86.184	38.924	1.00	77.11	N
ATOM	671	CA	GLY	C	995	12.842	85.034	39.630	1.00	76.87	C
ATOM	672	C	GLY	C	995	12.807	83.852	38.671	1.00	76.99	C
ATOM	673	O	GLY	C	995	13.779	83.106	38.601	1.00	79.72	O
ATOM	674	N	GLU	C	996	11.710	83.681	37.926	1.00	74.12	N
ATOM	675	CA	GLU	C	996	11.604	82.574	36.970	1.00	75.44	C
ATOM	676	C	GLU	C	996	12.772	82.677	35.997	1.00	75.09	C
ATOM	677	O	GLU	C	996	13.544	81.740	35.846	1.00	73.31	O
ATOM	678	CB	GLU	C	996	10.274	82.632	36.199	1.00	73.95	C
ATOM	679	CG	GLU	C	996	9.818	81.301	35.556	1.00	73.82	C
ATOM	680	CD	GLU	C	996	8.433	81.395	34.888	1.00	77.98	C
ATOM	681	OE1	GLU	C	996	7.448	81.779	35.563	1.00	75.02	O

ATOM	682	OE2	GLU	C	996	8.325	81.077	33.680	1.00	77.06	O
ATOM	683	N	LEU	C	997	12.903	83.835	35.358	1.00	78.06	N
ATOM	684	CA	LEU	C	997	13.975	84.087	34.404	1.00	78.32	C
ATOM	685	C	LEU	C	997	15.374	83.765	34.937	1.00	78.80	C
ATOM	686	O	LEU	C	997	16.201	83.205	34.217	1.00	77.85	O
ATOM	687	CB	LEU	C	997	13.936	85.542	33.958	1.00	77.28	C
ATOM	688	CG	LEU	C	997	15.135	85.949	33.111	1.00	76.64	C
ATOM	689	CD1	LEU	C	997	15.128	85.187	31.794	1.00	73.66	C
ATOM	690	CD2	LEU	C	997	15.080	87.437	32.882	1.00	75.03	C
ATOM	691	N	ILE	C	998	15.641	84.120	36.189	1.00	77.25	N
ATOM	692	CA	ILE	C	998	16.947	83.856	36.778	1.00	80.31	C
ATOM	693	C	ILE	C	998	17.186	82.371	37.048	1.00	83.04	C
ATOM	694	O	ILE	C	998	18.311	81.881	36.886	1.00	84.10	O
ATOM	695	CB	ILE	C	998	17.140	84.687	38.064	1.00	79.40	C
ATOM	696	CG1	ILE	C	998	17.338	86.155	37.670	1.00	82.60	C
ATOM	697	CG2	ILE	C	998	18.340	84.181	38.859	1.00	77.20	C
ATOM	698	CD1	ILE	C	998	16.937	87.149	38.742	1.00	82.48	C
ATOM	699	N	ASN	C	999	16.130	81.663	37.448	1.00	83.79	N
ATOM	700	CA	ASN	C	999	16.215	80.231	37.715	1.00	80.31	C
ATOM	701	C	ASN	C	999	16.506	79.513	36.407	1.00	80.21	C
ATOM	702	O	ASN	C	999	17.221	78.514	36.394	1.00	79.90	O
ATOM	703	CB	ASN	C	999	14.897	79.681	38.276	1.00	81.63	C
ATOM	704	CG	ASN	C	999	14.604	80.160	39.685	1.00	83.96	C
ATOM	705	ND2	ASN	C	999	13.329	80.125	40.071	1.00	82.73	N
ATOM	706	OD1	ASN	C	999	15.513	80.536	40.426	1.00	87.64	O
ATOM	707	N	LYS	C1000		15.939	80.012	35.310	1.00	79.78	N
ATOM	708	CA	LYS	C1000		16.156	79.384	34.018	1.00	82.69	C
ATOM	709	C	LYS	C1000		17.539	79.701	33.523	1.00	87.29	C
ATOM	710	O	LYS	C1000		18.087	78.965	32.713	1.00	91.27	O
ATOM	711	CB	LYS	C1000		15.121	79.835	32.986	1.00	81.29	C
ATOM	712	CG	LYS	C1000		13.688	79.470	33.362	1.00	83.64	C
ATOM	713	CD	LYS	C1000		13.614	78.121	34.082	1.00	82.20	C
ATOM	714	CE	LYS	C1000		12.198	77.667	34.392	1.00	78.59	C
ATOM	715	NZ	LYS	C1000		12.266	76.569	35.393	1.00	79.19	N
ATOM	716	N	MET	C1001		18.111	80.801	34.001	1.00	90.75	N
ATOM	717	CA	MET	C1001		19.462	81.159	33.594	1.00	90.87	C
ATOM	718	C	MET	C1001		20.436	80.267	34.379	1.00	90.41	C
ATOM	719	O	MET	C1001		21.204	79.502	33.786	1.00	86.93	O
ATOM	720	CB	MET	C1001		19.746	82.633	33.887	1.00	91.75	C

ATOM	721	CG	MET	C1001	21.171	83.040	33.555	1.00	96.80	C
ATOM	722	SD	MET	C1001	21.772	84.462	34.507	1.00	104.71	S
ATOM	723	CE	MET	C1001	22.116	83.736	36.195	1.00	102.20	C
ATOM	724	N	LYS	C1002	20.397	80.370	35.709	1.00	87.99	N
ATOM	725	CA	LYS	C1002	21.254	79.563	36.573	1.00	89.70	C
ATOM	726	C	LYS	C1002	21.318	78.115	36.066	1.00	92.93	C
ATOM	727	O	LYS	C1002	22.354	77.457	36.171	1.00	96.73	O
ATOM	728	CB	LYS	C1002	20.728	79.572	38.015	1.00	87.91	C
ATOM	729	CG	LYS	C1002	21.259	80.674	38.936	1.00	88.01	C
ATOM	730	CD	LYS	C1002	20.895	80.339	40.397	1.00	93.03	C
ATOM	731	CE	LYS	C1002	21.721	81.109	41.441	1.00	97.29	C
ATOM	732	NZ	LYS	C1002	21.562	82.593	41.386	1.00	99.06	N
ATOM	733	N	LEU	C1003	20.206	77.622	35.522	1.00	95.37	N
ATOM	734	CA	LEU	C1003	20.147	76.259	34.994	1.00	96.66	C
ATOM	735	C	LEU	C1003	20.899	76.139	33.678	1.00	98.82	C
ATOM	736	O	LEU	C1003	21.751	75.275	33.542	1.00	101.68	O
ATOM	737	CB	LEU	C1003	18.698	75.791	34.775	1.00	95.97	C
ATOM	738	CG	LEU	C1003	17.827	75.312	35.947	1.00	93.54	C
ATOM	739	CD1	LEU	C1003	16.393	75.124	35.463	1.00	86.75	C
ATOM	740	CD2	LEU	C1003	18.380	74.017	36.524	1.00	89.52	C
ATOM	741	N	ALA	C1004	20.595	76.992	32.705	1.00	100.95	N
ATOM	742	CA	ALA	C1004	21.287	76.907	31.416	1.00	103.86	C
ATOM	743	C	ALA	C1004	22.817	77.076	31.577	1.00	105.77	C
ATOM	744	O	ALA	C1004	23.599	76.756	30.667	1.00	106.40	O
ATOM	745	CB	ALA	C1004	20.717	77.949	30.448	1.00	99.99	C
ATOM	746	N	GLN	C1005	23.230	77.565	32.746	1.00	104.01	N
ATOM	747	CA	GLN	C1005	24.641	77.766	33.051	1.00	101.96	C
ATOM	748	C	GLN	C1005	25.242	76.479	33.553	1.00	101.55	C
ATOM	749	O	GLN	C1005	26.385	76.148	33.251	1.00	103.75	O
ATOM	750	CB	GLN	C1005	24.813	78.829	34.124	1.00	101.05	C
ATOM	751	CG	GLN	C1005	24.698	80.210	33.593	1.00	104.56	C
ATOM	752	CD	GLN	C1005	25.625	81.136	34.306	1.00	106.03	C
ATOM	753	NE2	GLN	C1005	26.756	81.434	33.674	1.00	106.95	N
ATOM	754	OE1	GLN	C1005	25.346	81.575	35.425	1.00	107.39	O
ATOM	755	N	GLN	C1006	24.458	75.772	34.349	1.00	98.97	N
ATOM	756	CA	GLN	C1006	24.866	74.510	34.917	1.00	96.86	C
ATOM	757	C	GLN	C1006	24.851	73.431	33.834	1.00	96.20	C
ATOM	758	O	GLN	C1006	25.409	72.350	34.030	1.00	96.22	O
ATOM	759	CB	GLN	C1006	23.912	74.172	36.063	1.00	97.68	C

ATOM	760	CG	GLN	C1006	24.048	72.801	36.671	1.00102.93	C
ATOM	761	CD	GLN	C1006	23.163	72.647	37.901	1.00107.56	C
ATOM	762	NE2	GLN	C1006	23.495	71.685	38.754	1.00109.99	N
ATOM	763	OE1	GLN	C1006	22.186	73.382	38.076	1.00110.02	O
ATOM	764	N	TYR	C1007	24.228	73.730	32.693	1.00 96.63	N
ATOM	765	CA	TYR	C1007	24.142	72.762	31.599	1.00101.98	C
ATOM	766	C	TYR	C1007	24.628	73.311	30.265	1.00106.08	C
ATOM	767	O	TYR	C1007	23.866	73.388	29.297	1.00105.01	O
ATOM	768	CB	TYR	C1007	22.700	72.226	31.454	1.00102.62	C
ATOM	769	CG	TYR	C1007	22.205	71.480	32.678	1.00100.68	C
ATOM	770	CD1	TYR	C1007	21.822	72.170	33.824	1.00100.14	C
ATOM	771	CD2	TYR	C1007	22.223	70.087	32.729	1.00 99.33	C
ATOM	772	CE1	TYR	C1007	21.485	71.504	34.990	1.00 98.40	C
ATOM	773	CE2	TYR	C1007	21.887	69.408	33.900	1.00 99.82	C
ATOM	774	CZ	TYR	C1007	21.521	70.127	35.027	1.00 99.31	C
ATOM	775	OH	TYR	C1007	21.209	69.483	36.204	1.00 97.57	O
ATOM	776	N	VAL	C1008	25.908	73.689	30.226	1.00112.40	N
ATOM	777	CA	VAL	C1008	26.529	74.230	29.009	1.00115.62	C
ATOM	778	C	VAL	C1008	27.091	73.120	28.101	1.00118.68	C
ATOM	779	O	VAL	C1008	27.695	72.137	28.578	1.00117.20	O
ATOM	780	CB	VAL	C1008	27.686	75.220	29.327	1.00113.43	C
ATOM	781	CG1	VAL	C1008	27.885	76.188	28.144	1.00111.71	C
ATOM	782	CG2	VAL	C1008	27.398	75.965	30.605	1.00110.31	C
ATOM	783	N	MET	C1009	26.904	73.311	26.792	1.00119.55	N
ATOM	784	CA	MET	C1009	27.340	72.355	25.773	1.00120.49	C
ATOM	785	C	MET	C1009	26.614	71.033	26.043	1.00119.74	C
ATOM	786	O	MET	C1009	27.248	69.978	26.202	1.00119.45	O
ATOM	787	CB	MET	C1009	28.865	72.122	25.825	1.00122.89	C
ATOM	788	CG	MET	C1009	29.740	73.355	25.576	1.00121.78	C
ATOM	789	SD	MET	C1009	31.003	73.589	26.868	1.00126.30	S
ATOM	790	CE	MET	C1009	31.538	71.843	27.253	1.00121.09	C
ATOM	791	N	THR	C1010	25.283	71.103	26.109	1.00117.79	N
ATOM	792	CA	THR	C1010	24.447	69.925	26.363	1.00112.34	C
ATOM	793	C	THR	C1010	23.162	70.041	25.546	1.00109.06	C
ATOM	794	O	THR	C1010	22.902	71.063	24.904	1.00107.42	O
ATOM	795	CB	THR	C1010	24.040	69.810	27.873	1.00110.10	C
ATOM	796	CG2	THR	C1010	23.531	68.420	28.191	1.00110.33	C
ATOM	797	OG1	THR	C1010	25.175	70.047	28.712	1.00105.49	O
ATOM	798	N	SER	C1011	22.369	68.980	25.563	1.00106.23	N

ATOM	799	CA	SER C1011	21.088	68.985	24.876	1.00106.87	C
ATOM	800	C	SER C1011	20.139	69.820	25.756	1.00107.19	C
ATOM	801	O	SER C1011	19.082	70.297	25.308	1.00102.61	O
ATOM	802	CB	SER C1011	20.578	67.549	24.762	1.00107.83	C
ATOM	803	OG	SER C1011	20.787	66.826	25.974	1.00104.56	O
ATOM	804	N	LEU C1012	20.543	69.982	27.020	1.00107.60	N
ATOM	805	CA	LEU C1012	19.753	70.719	28.003	1.00107.90	C
ATOM	806	C	LEU C1012	19.973	72.207	27.945	1.00109.30	C
ATOM	807	O	LEU C1012	19.075	72.984	28.287	1.00110.31	O
ATOM	808	CB	LEU C1012	20.015	70.220	29.438	1.00104.23	C
ATOM	809	CG	LEU C1012	19.319	68.895	29.812	1.00103.41	C
ATOM	810	CD1	LEU C1012	19.096	68.867	31.327	1.00 99.74	C
ATOM	811	CD2	LEU C1012	17.969	68.739	29.062	1.00 97.65	C
ATOM	812	N	GLN C1013	21.164	72.600	27.505	1.00110.00	N
ATOM	813	CA	GLN C1013	21.506	74.009	27.394	1.00108.04	C
ATOM	814	C	GLN C1013	20.532	74.741	26.469	1.00104.48	C
ATOM	815	O	GLN C1013	20.138	75.874	26.739	1.00103.94	O
ATOM	816	CB	GLN C1013	22.928	74.158	26.862	1.00110.51	C
ATOM	817	CG	GLN C1013	23.373	75.603	26.716	1.00113.77	C
ATOM	818	CD	GLN C1013	24.452	75.747	25.670	1.00113.99	C
ATOM	819	NE2	GLN C1013	24.084	76.308	24.522	1.00112.15	N
ATOM	820	OE1	GLN C1013	25.600	75.339	25.876	1.00113.81	O
ATOM	821	N	GLN C1014	20.157	74.098	25.371	1.00102.14	N
ATOM	822	CA	GLN C1014	19.235	74.718	24.440	1.00100.91	C
ATOM	823	C	GLN C1014	17.838	74.778	25.043	1.00102.05	C
ATOM	824	O	GLN C1014	17.068	75.682	24.723	1.00104.42	O
ATOM	825	CB	GLN C1014	19.194	73.944	23.119	1.00102.30	C
ATOM	826	CG	GLN C1014	18.388	74.634	22.009	1.00110.82	C
ATOM	827	CD	GLN C1014	16.952	74.110	21.851	1.00115.56	C
ATOM	828	NE2	GLN C1014	16.046	74.585	22.709	1.00115.52	N
ATOM	829	OE1	GLN C1014	16.667	73.288	20.966	1.00116.95	O
ATOM	830	N	GLU C1015	17.510	73.830	25.926	1.00100.51	N
ATOM	831	CA	GLU C1015	16.178	73.788	26.534	1.00 95.53	C
ATOM	832	C	GLU C1015	15.959	74.945	27.489	1.00 90.60	C
ATOM	833	O	GLU C1015	15.087	75.788	27.249	1.00 84.83	O
ATOM	834	CB	GLU C1015	15.948	72.449	27.250	1.00 97.24	C
ATOM	835	CG	GLU C1015	14.516	72.235	27.763	1.00101.85	C
ATOM	836	CD	GLU C1015	13.407	72.502	26.710	1.00104.25	C
ATOM	837	OE1	GLU C1015	13.570	72.137	25.521	1.00100.17	O

ATOM	838	OE2	GLU	C1015	12.350	73.065	27.091	1.00103.74	O
ATOM	839	N	TYR	C1016	16.768	74.996	28.544	1.00 86.99	N
ATOM	840	CA	TYR	C1016	16.673	76.060	29.532	1.00 90.23	C
ATOM	841	C	TYR	C1016	16.819	77.464	28.935	1.00 91.23	C
ATOM	842	O	TYR	C1016	16.740	78.461	29.666	1.00 91.81	O
ATOM	843	CB	TYR	C1016	17.702	75.847	30.649	1.00 92.03	C
ATOM	844	CG	TYR	C1016	17.413	74.621	31.485	1.00 96.31	C
ATOM	845	CD1	TYR	C1016	16.145	74.410	32.027	1.00 95.33	C
ATOM	846	CD2	TYR	C1016	18.383	73.639	31.681	1.00 99.21	C
ATOM	847	CE1	TYR	C1016	15.844	73.247	32.736	1.00 97.48	C
ATOM	848	CE2	TYR	C1016	18.090	72.467	32.394	1.00 98.50	C
ATOM	849	CZ	TYR	C1016	16.817	72.282	32.915	1.00 96.64	C
ATOM	850	OH	TYR	C1016	16.513	71.138	33.617	1.00 95.40	O
ATOM	851	N	LYS	C1017	17.041	77.543	27.622	1.00 90.88	N
ATOM	852	CA	LYS	C1017	17.140	78.835	26.949	1.00 89.24	C
ATOM	853	C	LYS	C1017	15.755	79.157	26.417	1.00 85.90	C
ATOM	854	O	LYS	C1017	15.328	80.314	26.415	1.00 82.40	O
ATOM	855	CB	LYS	C1017	18.142	78.810	25.787	1.00 93.74	C
ATOM	856	CG	LYS	C1017	19.596	79.054	26.190	1.00 96.49	C
ATOM	857	CD	LYS	C1017	20.433	79.517	24.996	1.00 96.88	C
ATOM	858	CE	LYS	C1017	21.907	79.641	25.351	1.00 98.92	C
ATOM	859	NZ	LYS	C1017	22.677	80.119	24.171	1.00100.42	N
ATOM	860	N	LYS	C1018	15.055	78.131	25.949	1.00 83.14	N
ATOM	861	CA	LYS	C1018	13.708	78.342	25.457	1.00 87.47	C
ATOM	862	C	LYS	C1018	12.835	78.752	26.640	1.00 87.65	C
ATOM	863	O	LYS	C1018	11.830	79.466	26.483	1.00 84.27	O
ATOM	864	CB	LYS	C1018	13.169	77.070	24.822	1.00 89.97	C
ATOM	865	CG	LYS	C1018	13.613	76.895	23.399	1.00 96.20	C
ATOM	866	CD	LYS	C1018	12.885	75.739	22.745	1.00103.28	C
ATOM	867	CE	LYS	C1018	13.303	75.560	21.291	1.00104.51	C
ATOM	868	NZ	LYS	C1018	12.940	74.192	20.792	1.00103.98	N
ATOM	869	N	GLN	C1019	13.241	78.285	27.822	1.00 85.24	N
ATOM	870	CA	GLN	C1019	12.546	78.585	29.061	1.00 80.75	C
ATOM	871	C	GLN	C1019	12.922	79.979	29.522	1.00 82.79	C
ATOM	872	O	GLN	C1019	12.105	80.666	30.135	1.00 86.11	O
ATOM	873	CB	GLN	C1019	12.873	77.535	30.125	1.00 74.33	C
ATOM	874	CG	GLN	C1019	12.050	76.272	29.950	1.00 72.25	C
ATOM	875	CD	GLN	C1019	12.450	75.178	30.917	1.00 73.41	C
ATOM	876	NE2	GLN	C1019	12.486	73.935	30.434	1.00 77.00	N

ATOM	877	OE1	GLN	C1019	12.715	75.442	32.088	1.00	72.63	O
ATOM	878	N	MET	C1020	14.154	80.399	29.236	1.00	85.11	N
ATOM	879	CA	MET	C1020	14.577	81.749	29.591	1.00	84.66	C
ATOM	880	C	MET	C1020	13.717	82.684	28.746	1.00	83.25	C
ATOM	881	O	MET	C1020	13.164	83.656	29.247	1.00	83.62	O
ATOM	882	CB	MET	C1020	16.067	81.966	29.285	1.00	85.31	C
ATOM	883	CG	MET	C1020	16.959	81.858	30.524	1.00	90.41	C
ATOM	884	SD	MET	C1020	18.753	81.804	30.222	1.00	91.63	S
ATOM	885	CE	MET	C1020	19.239	83.527	30.360	1.00	88.91	C
ATOM	886	N	LEU	C1021	13.587	82.377	27.462	1.00	80.01	N
ATOM	887	CA	LEU	C1021	12.779	83.218	26.596	1.00	81.04	C
ATOM	888	C	LEU	C1021	11.353	83.338	27.097	1.00	81.68	C
ATOM	889	O	LEU	C1021	10.759	84.411	27.065	1.00	80.93	O
ATOM	890	CB	LEU	C1021	12.737	82.661	25.179	1.00	84.04	C
ATOM	891	CG	LEU	C1021	13.983	82.688	24.301	1.00	83.49	C
ATOM	892	CD1	LEU	C1021	13.507	83.028	22.895	1.00	80.96	C
ATOM	893	CD2	LEU	C1021	14.998	83.724	24.779	1.00	80.98	C
ATOM	894	N	THR	C1022	10.811	82.207	27.531	1.00	84.90	N
ATOM	895	CA	THR	C1022	9.446	82.110	28.037	1.00	85.69	C
ATOM	896	C	THR	C1022	9.251	83.048	29.208	1.00	83.51	C
ATOM	897	O	THR	C1022	8.390	83.934	29.197	1.00	80.07	O
ATOM	898	CB	THR	C1022	9.154	80.637	28.469	1.00	88.46	C
ATOM	899	CG2	THR	C1022	8.259	80.570	29.712	1.00	90.20	C
ATOM	900	OG1	THR	C1022	8.543	79.941	27.374	1.00	91.00	O
ATOM	901	N	ALA	C1023	10.092	82.826	30.208	1.00	81.70	N
ATOM	902	CA	ALA	C1023	10.094	83.586	31.436	1.00	83.77	C
ATOM	903	C	ALA	C1023	10.250	85.077	31.213	1.00	85.16	C
ATOM	904	O	ALA	C1023	9.714	85.859	31.998	1.00	89.04	O
ATOM	905	CB	ALA	C1023	11.210	83.085	32.352	1.00	83.59	C
ATOM	906	N	ALA	C1024	10.980	85.470	30.163	1.00	81.68	N
ATOM	907	CA	ALA	C1024	11.214	86.887	29.875	1.00	75.41	C
ATOM	908	C	ALA	C1024	10.025	87.513	29.145	1.00	73.27	C
ATOM	909	O	ALA	C1024	9.701	88.680	29.359	1.00	72.93	O
ATOM	910	CB	ALA	C1024	12.501	87.061	29.070	1.00	65.77	C
ATOM	911	N	HIS	C1025	9.369	86.740	28.290	1.00	68.05	N
ATOM	912	CA	HIS	C1025	8.209	87.249	27.576	1.00	68.21	C
ATOM	913	C	HIS	C1025	7.117	87.527	28.621	1.00	69.52	C
ATOM	914	O	HIS	C1025	6.305	88.444	28.459	1.00	65.51	O
ATOM	915	CB	HIS	C1025	7.727	86.206	26.551	1.00	71.98	C



ATOM	916	CG	HIS	C1025	6.534	86.631	25.743	1.00	78.78	C
ATOM	917	CD2	HIS	C1025	6.449	87.173	24.501	1.00	83.90	C
ATOM	918	ND1	HIS	C1025	5.237	86.520	26.198	1.00	84.22	N
ATOM	919	CE1	HIS	C1025	4.406	86.975	25.277	1.00	87.90	C
ATOM	920	NE2	HIS	C1025	5.113	87.378	24.237	1.00	86.95	N
ATOM	921	N	ALA	C1026	7.119	86.732	29.696	1.00	68.89	N
ATOM	922	CA	ALA	C1026	6.127	86.843	30.766	1.00	66.22	C
ATOM	923	C	ALA	C1026	6.342	88.146	31.470	1.00	67.21	C
ATOM	924	O	ALA	C1026	5.411	88.917	31.693	1.00	70.82	O
ATOM	925	CB	ALA	C1026	6.289	85.720	31.729	1.00	59.99	C
ATOM	926	N	LEU	C1027	7.594	88.373	31.826	1.00	65.47	N
ATOM	927	CA	LEU	C1027	7.994	89.597	32.467	1.00	63.68	C
ATOM	928	C	LEU	C1027	7.507	90.779	31.624	1.00	64.67	C
ATOM	929	O	LEU	C1027	7.048	91.774	32.164	1.00	70.41	O
ATOM	930	CB	LEU	C1027	9.516	89.625	32.591	1.00	60.17	C
ATOM	931	CG	LEU	C1027	10.140	90.845	33.254	1.00	61.80	C
ATOM	932	CD1	LEU	C1027	9.381	91.159	34.512	1.00	64.53	C
ATOM	933	CD2	LEU	C1027	11.599	90.582	33.579	1.00	66.87	C
ATOM	934	N	ALA	C1028	7.577	90.669	30.302	1.00	62.81	N
ATOM	935	CA	ALA	C1028	7.152	91.773	29.448	1.00	63.80	C
ATOM	936	C	ALA	C1028	5.645	91.975	29.356	1.00	64.53	C
ATOM	937	O	ALA	C1028	5.173	93.107	29.348	1.00	63.07	O
ATOM	938	CB	ALA	C1028	7.717	91.600	28.068	1.00	62.94	C
ATOM	939	N	VAL	C1029	4.890	90.887	29.265	1.00	66.59	N
ATOM	940	CA	VAL	C1029	3.439	90.986	29.172	1.00	67.48	C
ATOM	941	C	VAL	C1029	2.884	91.582	30.461	1.00	67.97	C
ATOM	942	O	VAL	C1029	1.915	92.351	30.448	1.00	65.88	O
ATOM	943	CB	VAL	C1029	2.824	89.607	28.930	1.00	66.88	C
ATOM	944	CG1	VAL	C1029	1.330	89.730	28.727	1.00	63.81	C
ATOM	945	CG2	VAL	C1029	3.472	88.985	27.709	1.00	66.42	C
ATOM	946	N	ASP	C1030	3.521	91.222	31.570	1.00	65.23	N
ATOM	947	CA	ASP	C1030	3.126	91.712	32.880	1.00	64.94	C
ATOM	948	C	ASP	C1030	3.488	93.173	33.094	1.00	62.44	C
ATOM	949	O	ASP	C1030	2.701	93.927	33.658	1.00	64.35	O
ATOM	950	CB	ASP	C1030	3.735	90.839	33.992	1.00	65.96	C
ATOM	951	CG	ASP	C1030	2.911	89.578	34.255	1.00	69.57	C
ATOM	952	OD1	ASP	C1030	1.701	89.591	33.944	1.00	67.28	O
ATOM	953	OD2	ASP	C1030	3.454	88.585	34.783	1.00	71.94	O
ATOM	954	N	ALA	C1031	4.668	93.576	32.643	1.00	59.88	N

ATOM	955	CA	ALA	C1031	5.072	94.959	32.796	1.00	57.53	C
ATOM	956	C	ALA	C1031	4.022	95.837	32.109	1.00	59.49	C
ATOM	957	O	ALA	C1031	3.706	96.935	32.579	1.00	58.64	O
ATOM	958	CB	ALA	C1031	6.428	95.162	32.176	1.00	51.37	C
ATOM	959	N	LYS	C1032	3.470	95.345	31.002	1.00	59.00	N
ATOM	960	CA	LYS	C1032	2.466	96.094	30.270	1.00	57.05	C
ATOM	961	C	LYS	C1032	1.148	96.057	31.023	1.00	60.38	C
ATOM	962	O	LYS	C1032	0.296	96.936	30.854	1.00	57.03	O
ATOM	963	CB	LYS	C1032	2.309	95.513	28.862	1.00	56.79	C
ATOM	964	CG	LYS	C1032	3.458	95.897	27.918	1.00	62.37	C
ATOM	965	CD	LYS	C1032	3.612	94.970	26.703	1.00	68.50	C
ATOM	966	CE	LYS	C1032	2.945	95.535	25.447	1.00	72.18	C
ATOM	967	NZ	LYS	C1032	3.085	94.605	24.287	1.00	75.66	N
ATOM	968	N	ASN	C1033	0.971	95.031	31.855	1.00	63.06	N
ATOM	969	CA	ASN	C1033	-0.264	94.919	32.623	1.00	62.59	C
ATOM	970	C	ASN	C1033	-0.163	95.835	33.817	1.00	59.41	C
ATOM	971	O	ASN	C1033	-1.151	96.441	34.210	1.00	57.40	O
ATOM	972	CB	ASN	C1033	-0.530	93.471	33.044	1.00	64.82	C
ATOM	973	CG	ASN	C1033	-1.004	92.614	31.880	1.00	74.38	C
ATOM	974	ND2	ASN	C1033	-1.214	93.253	30.728	1.00	79.97	N
ATOM	975	OD1	ASN	C1033	-1.185	91.398	32.009	1.00	78.02	O
ATOM	976	N	LEU	C1034	1.039	95.945	34.375	1.00	56.92	N
ATOM	977	CA	LEU	C1034	1.276	96.829	35.495	1.00	55.84	C
ATOM	978	C	LEU	C1034	0.805	98.193	35.032	1.00	59.67	C
ATOM	979	O	LEU	C1034	-0.033	98.835	35.671	1.00	65.25	O
ATOM	980	CB	LEU	C1034	2.760	96.887	35.807	1.00	56.08	C
ATOM	981	CG	LEU	C1034	3.112	97.924	36.866	1.00	64.48	C
ATOM	982	CD1	LEU	C1034	2.306	97.609	38.101	1.00	67.21	C
ATOM	983	CD2	LEU	C1034	4.603	97.907	37.181	1.00	64.72	C
ATOM	984	N	LEU	C1035	1.357	98.626	33.903	1.00	58.09	N
ATOM	985	CA	LEU	C1035	1.020	99.901	33.296	1.00	55.87	C
ATOM	986	C	LEU	C1035	-0.486	100.027	33.167	1.00	51.30	C
ATOM	987	O	LEU	C1035	-1.049	101.029	33.547	1.00	48.73	O
ATOM	988	CB	LEU	C1035	1.658	99.996	31.916	1.00	58.28	C
ATOM	989	CG	LEU	C1035	1.914	101.349	31.273	1.00	59.39	C
ATOM	990	CD1	LEU	C1035	2.086	101.110	29.799	1.00	59.31	C
ATOM	991	CD2	LEU	C1035	0.767	102.299	31.500	1.00	62.27	C
ATOM	992	N	ASP	C1036	-1.143	99.014	32.622	1.00	53.83	N
ATOM	993	CA	ASP	C1036	-2.592	99.079	32.488	1.00	58.81	C

ATOM	994	C	ASP	C1036	-3.343	99.361	33.809	1.00	60.83	C
ATOM	995	O	ASP	C1036	-4.246	100.197	33.825	1.00	58.01	O
ATOM	996	CB	ASP	C1036	-3.127	97.802	31.862	1.00	63.90	C
ATOM	997	CG	ASP	C1036	-4.650	97.795	31.771	1.00	75.23	C
ATOM	998	OD1	ASP	C1036	-5.274	96.953	32.452	1.00	86.78	O
ATOM	999	OD2	ASP	C1036	-5.224	98.627	31.032	1.00	80.05	O
ATOM	1000	N	VAL	C1037	-2.998	98.656	34.892	1.00	63.64	N
ATOM	1001	CA	VAL	C1037	-3.616	98.860	36.209	1.00	63.82	C
ATOM	1002	C	VAL	C1037	-3.492	100.351	36.588	1.00	65.23	C
ATOM	1003	O	VAL	C1037	-4.497	101.060	36.788	1.00	68.35	O
ATOM	1004	CB	VAL	C1037	-2.887	98.017	37.278	1.00	65.81	C
ATOM	1005	CG1	VAL	C1037	-3.460	98.265	38.655	1.00	63.68	C
ATOM	1006	CG2	VAL	C1037	-3.008	96.576	36.932	1.00	66.00	C
ATOM	1007	N	ILE	C1038	-2.254	100.830	36.684	1.00	56.67	N
ATOM	1008	CA	ILE	C1038	-1.988	102.232	37.008	1.00	52.09	C
ATOM	1009	C	ILE	C1038	-2.795	103.253	36.154	1.00	56.52	C
ATOM	1010	O	ILE	C1038	-3.207	104.319	36.643	1.00	61.00	O
ATOM	1011	CB	ILE	C1038	-0.506	102.495	36.857	1.00	40.92	C
ATOM	1012	CG1	ILE	C1038	0.251	101.813	37.991	1.00	40.83	C
ATOM	1013	CG2	ILE	C1038	-0.241	103.944	36.878	1.00	44.37	C
ATOM	1014	CD1	ILE	C1038	1.781	101.856	37.871	1.00	43.08	C
ATOM	1015	N	ASP	C1039	-3.016	102.951	34.880	1.00	58.87	N
ATOM	1016	CA	ASP	C1039	-3.788	103.863	34.044	1.00	63.24	C
ATOM	1017	C	ASP	C1039	-5.223	103.847	34.553	1.00	62.31	C
ATOM	1018	O	ASP	C1039	-5.846	104.903	34.639	1.00	61.21	O
ATOM	1019	CB	ASP	C1039	-3.712	103.478	32.540	1.00	64.64	C
ATOM	1020	CG	ASP	C1039	-2.406	103.983	31.850	1.00	70.50	C
ATOM	1021	OD1	ASP	C1039	-1.519	104.598	32.524	1.00	64.94	O
ATOM	1022	OD2	ASP	C1039	-2.283	103.749	30.621	1.00	73.26	O
ATOM	1023	N	GLN	C1040	-5.755	102.667	34.885	1.00	63.31	N
ATOM	1024	CA	GLN	C1040	-7.122	102.585	35.423	1.00	66.22	C
ATOM	1025	C	GLN	C1040	-7.111	103.430	36.720	1.00	65.53	C
ATOM	1026	O	GLN	C1040	-8.056	104.175	37.036	1.00	57.11	O
ATOM	1027	CB	GLN	C1040	-7.481	101.143	35.783	1.00	69.30	C
ATOM	1028	CG	GLN	C1040	-7.457	100.156	34.667	1.00	80.10	C
ATOM	1029	CD	GLN	C1040	-7.681	98.738	35.175	1.00	87.83	C
ATOM	1030	NE2	GLN	C1040	-6.715	97.844	34.925	1.00	91.51	N
ATOM	1031	OE1	GLN	C1040	-8.711	98.452	35.790	1.00	91.10	O
ATOM	1032	N	ALA	C1041	-6.022	103.283	37.469	1.00	62.66	N

ATOM	1033	CA	ALA	C1041	-5.853	104.025	38.698	1.00	62.47	C
ATOM	1034	C	ALA	C1041	-5.868	105.525	38.400	1.00	66.44	C
ATOM	1035	O	ALA	C1041	-6.569	106.275	39.088	1.00	69.97	O
ATOM	1036	CB	ALA	C1041	-4.539	103.635	39.384	1.00	59.49	C
ATOM	1037	N	ARG	C1042	-5.125	105.994	37.398	1.00	65.45	N
ATOM	1038	CA	ARG	C1042	-5.170	107.435	37.161	1.00	67.91	C
ATOM	1039	C	ARG	C1042	-6.545	107.875	36.667	1.00	68.21	C
ATOM	1040	O	ARG	C1042	-7.045	108.920	37.077	1.00	67.77	O
ATOM	1041	CB	ARG	C1042	-4.091	107.883	36.179	1.00	63.15	C
ATOM	1042	CG	ARG	C1042	-2.707	107.699	36.725	1.00	64.59	C
ATOM	1043	CD	ARG	C1042	-1.821	107.089	35.661	1.00	64.74	C
ATOM	1044	NE	ARG	C1042	-0.396	107.291	35.918	1.00	58.12	N
ATOM	1045	CZ	ARG	C1042	0.562	107.019	35.038	1.00	55.70	C
ATOM	1046	NH1	ARG	C1042	0.252	106.537	33.842	1.00	57.33	N
ATOM	1047	NH2	ARG	C1042	1.829	107.216	35.350	1.00	49.95	N
ATOM	1048	N	LEU	C1043	-7.161	107.079	35.801	1.00	68.03	N
ATOM	1049	CA	LEU	C1043	-8.468	107.436	35.285	1.00	73.06	C
ATOM	1050	C	LEU	C1043	-9.472	107.546	36.432	1.00	78.30	C
ATOM	1051	O	LEU	C1043	-10.299	108.463	36.451	1.00	77.88	O
ATOM	1052	CB	LEU	C1043	-8.927	106.404	34.246	1.00	69.68	C
ATOM	1053	CG	LEU	C1043	-8.057	106.338	32.978	1.00	69.22	C
ATOM	1054	CD1	LEU	C1043	-8.528	105.195	32.108	1.00	66.15	C
ATOM	1055	CD2	LEU	C1043	-8.101	107.653	32.205	1.00	62.85	C
ATOM	1056	N	LYS	C1044	-9.389	106.622	37.393	1.00	83.18	N
ATOM	1057	CA	LYS	C1044	-10.296	106.640	38.539	1.00	84.86	C
ATOM	1058	C	LYS	C1044	-10.144	107.999	39.194	1.00	85.31	C
ATOM	1059	O	LYS	C1044	-11.079	108.803	39.239	1.00	85.59	O
ATOM	1060	CB	LYS	C1044	-9.934	105.558	39.566	1.00	85.94	C
ATOM	1061	CG	LYS	C1044	-11.166	104.960	40.237	1.00	91.52	C
ATOM	1062	CD	LYS	C1044	-10.911	104.331	41.601	1.00	91.04	C
ATOM	1063	CE	LYS	C1044	-12.193	103.660	42.097	1.00	90.64	C
ATOM	1064	NZ	LYS	C1044	-12.051	103.064	43.449	1.00	91.14	N
ATOM	1065	N	MET	C1045	-8.939	108.256	39.681	1.00	82.94	N
ATOM	1066	CA	MET	C1045	-8.640	109.505	40.346	1.00	82.97	C
ATOM	1067	C	MET	C1045	-9.061	110.743	39.567	1.00	87.45	C
ATOM	1068	O	MET	C1045	-9.165	111.818	40.147	1.00	92.61	O
ATOM	1069	CB	MET	C1045	-7.155	109.588	40.649	1.00	79.19	C
ATOM	1070	CG	MET	C1045	-6.747	110.838	41.370	1.00	77.81	C
ATOM	1071	SD	MET	C1045	-4.965	110.819	41.573	1.00	91.61	S

ATOM	1072	CE	MET	C1045	-4.779	112.247	42.618	1.00	93.10	C
ATOM	1073	N	LEU	C1046	-9.283	110.618	38.261	1.00	89.77	N
ATOM	1074	CA	LEU	C1046	-9.693	111.779	37.467	1.00	92.15	C
ATOM	1075	C	LEU	C1046	-11.217	111.928	37.380	1.00	94.43	C
ATOM	1076	O	LEU	C1046	-11.732	113.043	37.230	1.00	93.71	O
ATOM	1077	CB	LEU	C1046	-9.086	111.717	36.056	1.00	88.87	C
ATOM	1078	CG	LEU	C1046	-7.660	112.254	35.905	1.00	87.24	C
ATOM	1079	CD1	LEU	C1046	-7.175	112.075	34.478	1.00	85.35	C
ATOM	1080	CD2	LEU	C1046	-7.641	113.718	36.283	1.00	85.90	C
ATOM	1081	N	GLY	C1047	-11.923	110.801	37.483	1.00	96.12	N
ATOM	1082	CA	GLY	C1047	-13.378	110.801	37.433	1.00	102.00	C
ATOM	1083	C	GLY	C1047	-14.033	110.519	38.786	1.00	106.82	C
ATOM	1084	O	GLY	C1047	-14.645	109.431	38.946	1.00	108.43	O
TER	1085		GLY	C1047						
ATOM	1055	N	THR	D 2	1.264	104.168	23.824	1.00	117.75	N
ATOM	1056	CA	THR	D 2	1.121	102.693	23.972	1.00	119.14	C
ATOM	1057	C	THR	D 2	0.948	102.019	22.616	1.00	120.27	C
ATOM	1058	O	THR	D 2	0.822	100.802	22.543	1.00	120.61	O
ATOM	1059	CB	THR	D 2	-0.072	102.329	24.931	1.00	119.19	C
ATOM	1060	CG2	THR	D 2	-0.381	100.832	24.916	1.00	114.83	C
ATOM	1061	OG1	THR	D 2	0.278	102.693	26.273	1.00	119.79	O
ATOM	1062	N	ARG	D 3	0.943	102.794	21.534	1.00	122.00	N
ATOM	1063	CA	ARG	D 3	0.821	102.183	20.212	1.00	122.43	C
ATOM	1064	C	ARG	D 3	2.247	101.762	19.825	1.00	121.24	C
ATOM	1065	O	ARG	D 3	2.438	100.766	19.122	1.00	120.23	O
ATOM	1066	CB	ARG	D 3	0.221	103.170	19.188	1.00	124.89	C
ATOM	1067	CG	ARG	D 3	-0.729	102.504	18.181	1.00	127.61	C
ATOM	1068	CD	ARG	D 3	-1.341	103.504	17.189	1.00	131.95	C
ATOM	1069	NE	ARG	D 3	-2.370	104.358	17.787	1.00	136.27	N
ATOM	1070	CZ	ARG	D 3	-3.151	105.196	17.101	1.00	137.27	C
ATOM	1071	NH1	ARG	D 3	-3.027	105.302	15.783	1.00	136.09	N
ATOM	1072	NH2	ARG	D 3	-4.065	105.926	17.729	1.00	137.17	N
ATOM	1073	N	GLU	D 4	3.236	102.515	20.322	1.00	119.46	N
ATOM	1074	CA	GLU	D 4	4.656	102.241	20.083	1.00	117.02	C
ATOM	1075	C	GLU	D 4	5.127	101.124	21.033	1.00	113.77	C
ATOM	1076	O	GLU	D 4	5.979	100.304	20.676	1.00	112.68	O
ATOM	1077	CB	GLU	D 4	5.479	103.524	20.283	1.00	120.10	C
ATOM	1078	CG	GLU	D 4	4.987	104.663	19.391	1.00	125.95	C
ATOM	1079	CD	GLU	D 4	6.071	105.680	19.009	1.00	129.44	C

ATOM	1080	OE1	GLU	D	4	6.490	106.502	19.860	1.00131.18	O
ATOM	1081	OE2	GLU	D	4	6.509	105.652	17.839	1.00131.54	O
ATOM	1082	N	LEU	D	5	4.576	101.115	22.247	1.00107.77	N
ATOM	1083	CA	LEU	D	5	4.866	100.080	23.238	1.00100.20	C
ATOM	1084	C	LEU	D	5	4.172	98.789	22.748	1.00101.89	C
ATOM	1085	O	LEU	D	5	4.540	97.680	23.140	1.00103.23	O
ATOM	1086	CB	LEU	D	5	4.292	100.486	24.607	1.00 89.57	C
ATOM	1087	CG	LEU	D	5	4.171	99.393	25.678	1.00 82.95	C
ATOM	1088	CD1	LEU	D	5	5.536	99.024	26.172	1.00 79.39	C
ATOM	1089	CD2	LEU	D	5	3.338	99.860	26.837	1.00 78.40	C
ATOM	1090	N	ASP	D	6	3.160	98.945	21.894	1.00103.15	N
ATOM	1091	CA	ASP	D	6	2.414	97.808	21.365	1.00104.18	C
ATOM	1092	C	ASP	D	6	3.096	97.197	20.153	1.00103.81	C
ATOM	1093	O	ASP	D	6	2.785	96.074	19.743	1.00102.97	O
ATOM	1094	CB	ASP	D	6	0.971	98.212	21.039	1.00108.00	C
ATOM	1095	CG	ASP	D	6	0.074	98.200	22.274	1.00112.58	C
ATOM	1096	OD1	ASP	D	6	0.237	97.269	23.096	1.00115.34	O
ATOM	1097	OD2	ASP	D	6	-0.785	99.100	22.417	1.00114.32	O
ATOM	1098	N	GLU	D	7	4.014	97.959	19.569	1.00104.18	N
ATOM	1099	CA	GLU	D	7	4.799	97.481	18.439	1.00104.53	C
ATOM	1100	C	GLU	D	7	5.713	96.462	19.118	1.00103.48	C
ATOM	1101	O	GLU	D	7	5.970	95.376	18.591	1.00102.50	O
ATOM	1102	CB	GLU	D	7	5.617	98.638	17.849	1.00106.95	C
ATOM	1103	CG	GLU	D	7	4.776	99.656	17.087	1.00110.40	C
ATOM	1104	CD	GLU	D	7	4.581	99.279	15.628	1.00113.03	C
ATOM	1105	OE1	GLU	D	7	5.459	99.643	14.813	1.00114.03	O
ATOM	1106	OE2	GLU	D	7	3.568	98.614	15.299	1.00113.25	O
ATOM	1107	N	LEU	D	8	6.176	96.835	20.311	1.00100.91	N
ATOM	1108	CA	LEU	D	8	7.043	95.997	21.135	1.00 96.57	C
ATOM	1109	C	LEU	D	8	6.300	94.770	21.645	1.00 98.57	C
ATOM	1110	O	LEU	D	8	6.724	93.638	21.424	1.00100.66	O
ATOM	1111	CB	LEU	D	8	7.542	96.766	22.354	1.00 89.15	C
ATOM	1112	CG	LEU	D	8	8.429	97.975	22.144	1.00 82.99	C
ATOM	1113	CD1	LEU	D	8	8.744	98.566	23.495	1.00 78.33	C
ATOM	1114	CD2	LEU	D	8	9.689	97.577	21.412	1.00 78.68	C
ATOM	1115	N	MET	D	9	5.207	94.995	22.364	1.00 98.60	N
ATOM	1116	CA	MET	D	9	4.448	93.877	22.891	1.00101.80	C
ATOM	1117	C	MET	D	9	4.186	92.858	21.787	1.00102.97	C
ATOM	1118	O	MET	D	9	4.132	91.649	22.040	1.00102.93	O

ATOM	1119	CB	MET	D	9	3.136	94.375	23.500	1.00104.99	C
ATOM	1120	CG	MET	D	9	3.338	95.015	24.860	1.00106.99	C
ATOM	1121	SD	MET	D	9	4.406	93.995	25.914	1.00107.55	S
ATOM	1122	CE	MET	D	9	3.273	92.744	26.447	1.00108.44	C
ATOM	1123	N	ALA	D	10	4.048	93.355	20.560	1.00102.71	N
ATOM	1124	CA	ALA	D	10	3.801	92.510	19.397	1.00102.15	C
ATOM	1125	C	ALA	D	10	5.039	91.707	18.967	1.00101.89	C
ATOM	1126	O	ALA	D	10	4.906	90.592	18.466	1.00102.04	O
ATOM	1127	CB	ALA	D	10	3.299	93.361	18.234	1.00 99.65	C
ATOM	1128	N	SER	D	11	6.234	92.268	19.161	1.00101.68	N
ATOM	1129	CA	SER	D	11	7.494	91.604	18.790	1.00100.63	C
ATOM	1130	C	SER	D	11	7.695	90.245	19.463	1.00104.57	C
ATOM	1131	O	SER	D	11	8.455	89.405	18.966	1.00104.79	O
ATOM	1132	CB	SER	D	11	8.697	92.485	19.141	1.00 96.62	C
ATOM	1133	OG	SER	D	11	8.655	93.731	18.478	1.00 92.87	O
ATOM	1134	N	LEU	D	12	7.033	90.037	20.598	1.00106.92	N
ATOM	1135	CA	LEU	D	12	7.154	88.781	21.337	1.00109.11	C
ATOM	1136	C	LEU	D	12	5.963	87.877	21.013	1.00112.49	C
ATOM	1137	O	LEU	D	12	5.917	86.712	21.421	1.00111.74	O
ATOM	1138	CB	LEU	D	12	7.196	89.075	22.837	1.00108.48	C
ATOM	1139	CG	LEU	D	12	8.137	90.203	23.254	1.00104.98	C
ATOM	1140	CD1	LEU	D	12	7.520	90.980	24.395	1.00100.51	C
ATOM	1141	CD2	LEU	D	12	9.489	89.632	23.634	1.00104.05	C
ATOM	1142	N	SER	D	13	5.009	88.448	20.276	1.00115.55	N
ATOM	1143	CA	SER	D	13	3.781	87.783	19.839	1.00119.71	C
ATOM	1144	C	SER	D	13	2.695	87.664	20.918	1.00122.54	C
ATOM	1145	O	SER	D	13	2.075	88.710	21.225	1.00123.57	O
ATOM	1146	CB	SER	D	13	4.112	86.401	19.257	1.00118.83	C
ATOM	1147	OG	SER	D	13	4.951	86.509	18.113	1.00118.69	O
ATOM	1148	OXT	SER	D	13	2.482	86.542	21.435	1.00124.00	O
TER	1149		SER	D	13					
ATOM	1086	N	THR	F	2	12.618	96.446	47.265	1.00167.72	N
ATOM	1087	CA	THR	F	2	13.892	96.405	46.489	1.00168.68	C
ATOM	1088	C	THR	F	2	14.921	95.534	47.201	1.00168.68	C
ATOM	1089	O	THR	F	2	15.977	95.221	46.647	1.00168.77	O
ATOM	1090	CB	THR	F	2	14.477	97.825	46.307	1.00169.03	C
ATOM	1091	CG2	THR	F	2	15.821	97.770	45.586	1.00169.26	C
ATOM	1092	OG1	THR	F	2	13.563	98.626	45.545	1.00170.92	O
ATOM	1093	N	ARG	F	3	14.607	95.142	48.431	1.00168.25	N

ATOM	1094	CA	ARG	F	3	15.506	94.304	49.213	1.00167.59	C
ATOM	1095	C	ARG	F	3	15.429	92.866	48.694	1.00168.72	C
ATOM	1096	O	ARG	F	3	16.417	92.131	48.745	1.00169.37	O
ATOM	1097	CB	ARG	F	3	15.122	94.374	50.695	1.00165.45	C
ATOM	1098	CG	ARG	F	3	16.317	94.416	51.642	1.00163.06	C
ATOM	1099	CD	ARG	F	3	15.889	94.705	53.078	1.00161.21	C
ATOM	1100	NE	ARG	F	3	15.607	96.119	53.329	1.00159.22	N
ATOM	1101	CZ	ARG	F	3	15.015	96.572	54.430	1.00158.39	C
ATOM	1102	NH1	ARG	F	3	14.639	95.720	55.375	1.00157.72	N
ATOM	1103	NH2	ARG	F	3	14.812	97.874	54.598	1.00157.85	N
ATOM	1104	N	GLU	F	4	14.255	92.484	48.184	1.00169.29	N
ATOM	1105	CA	GLU	F	4	14.025	91.146	47.628	1.00168.31	C
ATOM	1106	C	GLU	F	4	14.487	91.112	46.170	1.00167.94	C
ATOM	1107	O	GLU	F	4	14.764	90.045	45.609	1.00166.98	O
ATOM	1108	CB	GLU	F	4	12.540	90.787	47.687	1.00167.80	C
ATOM	1109	CG	GLU	F	4	11.896	90.899	49.060	1.00167.27	C
ATOM	1110	CD	GLU	F	4	10.579	90.140	49.139	1.00168.28	C
ATOM	1111	OE1	GLU	F	4	9.703	90.366	48.276	1.00167.92	O
ATOM	1112	OE2	GLU	F	4	10.420	89.316	50.065	1.00168.81	O
ATOM	1113	N	LEU	F	5	14.553	92.296	45.567	1.00167.58	N
ATOM	1114	CA	LEU	F	5	15.002	92.453	44.189	1.00167.99	C
ATOM	1115	C	LEU	F	5	16.537	92.441	44.166	1.00169.16	C
ATOM	1116	O	LEU	F	5	17.157	92.024	43.182	1.00168.77	O
ATOM	1117	CB	LEU	F	5	14.478	93.774	43.624	1.00166.25	C
ATOM	1118	CG	LEU	F	5	14.988	94.231	42.257	1.00165.05	C
ATOM	1119	CD1	LEU	F	5	14.468	93.324	41.150	1.00163.55	C
ATOM	1120	CD2	LEU	F	5	14.538	95.656	42.032	1.00164.01	C
ATOM	1121	N	ASP	F	6	17.140	92.897	45.263	1.00169.94	N
ATOM	1122	CA	ASP	F	6	18.595	92.933	45.391	1.00169.64	C
ATOM	1123	C	ASP	F	6	19.138	91.563	45.758	1.00169.28	C
ATOM	1124	O	ASP	F	6	20.317	91.278	45.546	1.00168.18	O
ATOM	1125	CB	ASP	F	6	19.023	93.965	46.434	1.00170.12	C
ATOM	1126	CG	ASP	F	6	18.893	95.385	45.925	1.00172.08	C
ATOM	1127	OD1	ASP	F	6	19.227	95.615	44.741	1.00172.61	O
ATOM	1128	OD2	ASP	F	6	18.470	96.269	46.701	1.00173.49	O
ATOM	1129	N	GLU	F	7	18.272	90.725	46.321	1.00169.63	N
ATOM	1130	CA	GLU	F	7	18.642	89.358	46.664	1.00169.36	C
ATOM	1131	C	GLU	F	7	18.916	88.778	45.282	1.00169.37	C
ATOM	1132	O	GLU	F	7	19.858	88.009	45.071	1.00169.25	O



ATOM	1133	CB	GLU	F	7	17.453	88.619	47.297	1.00169.43	C
ATOM	1134	CG	GLU	F	7	16.960	89.198	48.617	1.00168.79	C
ATOM	1135	CD	GLU	F	7	17.596	88.538	49.825	1.00168.60	C
ATOM	1136	OE1	GLU	F	7	17.092	87.480	50.260	1.00167.14	O
ATOM	1137	OE2	GLU	F	7	18.606	89.071	50.333	1.00168.56	O
ATOM	1138	N	LEU	F	8	18.069	89.199	44.345	1.00168.60	N
ATOM	1139	CA	LEU	F	8	18.125	88.783	42.951	1.00167.55	C
ATOM	1140	C	LEU	F	8	19.321	89.384	42.207	1.00168.46	C
ATOM	1141	O	LEU	F	8	20.059	88.662	41.530	1.00168.63	O
ATOM	1142	CB	LEU	F	8	16.817	89.177	42.252	1.00164.51	C
ATOM	1143	CG	LEU	F	8	15.527	88.563	42.814	1.00161.82	C
ATOM	1144	CD1	LEU	F	8	14.310	89.243	42.215	1.00160.14	C
ATOM	1145	CD2	LEU	F	8	15.500	87.079	42.514	1.00161.14	C
ATOM	1146	N	MET	F	9	19.517	90.696	42.341	1.00169.27	N
ATOM	1147	CA	MET	F	9	20.623	91.381	41.671	1.00170.34	C
ATOM	1148	C	MET	F	9	21.990	90.920	42.196	1.00170.50	C
ATOM	1149	O	MET	F	9	23.015	91.080	41.523	1.00170.08	O
ATOM	1150	CB	MET	F	9	20.474	92.903	41.821	1.00171.17	C
ATOM	1151	CG	MET	F	9	19.210	93.489	41.164	1.00172.23	C
ATOM	1152	SD	MET	F	9	18.947	93.057	39.408	1.00173.00	S
ATOM	1153	CE	MET	F	9	20.201	94.088	38.567	1.00172.02	C
ATOM	1154	N	ALA	F	10	21.988	90.333	43.391	1.00170.19	N
ATOM	1155	CA	ALA	F	10	23.204	89.820	44.021	1.00169.09	C
ATOM	1156	C	ALA	F	10	23.472	88.382	43.568	1.00168.90	C
ATOM	1157	O	ALA	F	10	24.601	87.896	43.636	1.00167.06	O
ATOM	1158	CB	ALA	F	10	23.064	89.874	45.540	1.00167.81	C
ATOM	1159	N	SER	F	11	22.421	87.707	43.109	1.00169.78	N
ATOM	1160	CA	SER	F	11	22.528	86.331	42.633	1.00169.93	C
ATOM	1161	C	SER	F	11	23.397	86.282	41.387	1.00171.22	C
ATOM	1162	O	SER	F	11	24.118	85.313	41.152	1.00170.34	O
ATOM	1163	CB	SER	F	11	21.141	85.771	42.307	1.00168.77	C
ATOM	1164	OG	SER	F	11	20.351	85.639	43.473	1.00167.98	O
ATOM	1165	N	LEU	F	12	23.313	87.341	40.589	1.00173.79	N
ATOM	1166	CA	LEU	F	12	24.082	87.455	39.358	1.00176.17	C
ATOM	1167	C	LEU	F	12	25.519	87.870	39.666	1.00178.24	C
ATOM	1168	O	LEU	F	12	26.379	87.870	38.784	1.00179.14	O
ATOM	1169	CB	LEU	F	12	23.418	88.481	38.435	1.00175.22	C
ATOM	1170	CG	LEU	F	12	21.974	88.127	38.071	1.00174.35	C
ATOM	1171	CD1	LEU	F	12	21.284	89.305	37.400	1.00173.85	C

ATOM	1172	CD2	LEU	F	12	21.982	86.906	37.169	1.00173.97	C
ATOM	1173	N	SER	F	13	25.764	88.221	40.927	1.00179.16	N
ATOM	1174	CA	SER	F	13	27.089	88.635	41.384	1.00178.97	C
ATOM	1175	C	SER	F	13	27.485	90.007	40.842	1.00178.68	C
ATOM	1176	O	SER	F	13	26.605	90.897	40.774	1.00178.20	O
ATOM	1177	CB	SER	F	13	28.139	87.596	40.975	1.00178.14	C
ATOM	1178	OG	SER	F	13	27.780	86.303	41.428	1.00177.41	O
ATOM	1179	OXT	SER	F	13	28.678	90.172	40.506	1.00178.07	O
TER	1180		SER	F	13					
HETATM	1	O	HOH	C	4	0.063	105.370	24.026	0.50 44.46	O
HETATM	2	O	HOH	C	6	4.059	85.123	29.006	1.00 68.21	O
HETATM	3	O	HOH	C	13	2.443	118.002	27.213	1.00 68.32	O
HETATM	4	O	HOH	C	15	-9.253	105.330	47.946	1.00 65.07	O
HETATM	5	O	HOH	C	17	5.281	111.016	36.277	1.00 75.53	O
HETATM	6	O	HOH	C	33	-6.271	97.901	44.910	1.00 66.09	O
HETATM	7	O	HOH	C	36	-12.626	115.981	38.240	1.00 66.58	O
HETATM	8	O	HOH	C	48	13.676	103.936	30.402	1.00 66.06	O
HETATM	9	O	HOH	C	50	-4.258	92.939	31.040	1.00 57.20	O
HETATM	10	O	HOH	C	79	5.798	82.614	25.107	1.00 72.80	O
HETATM	11	O	HOH	C	106	-7.939	111.090	44.635	1.00 54.84	O
HETATM	1150	O	HOH	D	37	2.384	105.217	19.682	1.00 71.42	O
HETATM	1151	O	HOH	D	111	10.178	87.969	17.399	1.00 73.03	O
HETATM	1181	O	HOH	F	105	11.710	93.548	46.450	1.00 87.72	O

END

## 2. The Augmented FAT/Paxillin Complex (§3.1.2 Structures):

ATOM	1	N	ILE	C	909	-7.120	90.264	27.594	1.00	84.95	N
ATOM	2	CA	ILE	C	909	-6.328	91.240	26.773	1.00	86.58	C
ATOM	3	C	ILE	C	909	-6.742	92.707	26.925	1.00	85.87	C
ATOM	4	O	ILE	C	909	-7.924	93.047	26.881	1.00	86.73	O
ATOM	5	CB	ILE	C	909	-6.375	90.883	25.252	1.00	85.93	C
ATOM	6	CG1	ILE	C	909	-5.547	91.908	24.460	1.00	84.17	C
ATOM	7	CG2	ILE	C	909	-7.829	90.811	24.763	1.00	79.59	C
ATOM	8	CD1	ILE	C	909	-5.233	91.508	23.026	1.00	82.55	C
ATOM	9	N	SER	C	910	-5.760	93.584	27.092	1.00	85.82	N
ATOM	10	CA	SER	C	910	-6.064	95.004	27.245	1.00	88.03	C
ATOM	11	C	SER	C	910	-6.002	95.773	25.931	1.00	87.92	C
ATOM	12	O	SER	C	910	-5.363	95.336	24.962	1.00	90.37	O
ATOM	13	CB	SER	C	910	-5.117	95.644	28.260	1.00	87.19	C
ATOM	14	OG	SER	C	910	-3.892	94.924	28.339	1.00	88.96	O
ATOM	15	N	PRO	C	911	-6.707	96.919	25.869	1.00	85.92	N
ATOM	16	CA	PRO	C	911	-6.692	97.727	24.649	1.00	82.06	C
ATOM	17	C	PRO	C	911	-5.458	98.621	24.779	1.00	76.36	C
ATOM	18	O	PRO	C	911	-4.891	98.763	25.878	1.00	72.62	O
ATOM	19	CB	PRO	C	911	-8.003	98.513	24.750	1.00	81.26	C
ATOM	20	CG	PRO	C	911	-8.052	98.813	26.204	1.00	83.81	C
ATOM	21	CD	PRO	C	911	-7.705	97.441	26.818	1.00	84.68	C
ATOM	22	N	PRO	C	912	-5.029	99.238	23.668	1.00	69.40	N
ATOM	23	CA	PRO	C	912	-3.851	100.103	23.695	1.00	63.70	C
ATOM	24	C	PRO	C	912	-3.917	101.091	24.857	1.00	60.56	C
ATOM	25	O	PRO	C	912	-4.996	101.538	25.235	1.00	61.26	O
ATOM	26	CB	PRO	C	912	-3.923	100.804	22.338	1.00	65.28	C
ATOM	27	CG	PRO	C	912	-4.655	99.848	21.490	1.00	64.22	C
ATOM	28	CD	PRO	C	912	-5.745	99.375	22.395	1.00	65.66	C
ATOM	29	N	PRO	C	913	-2.763	101.438	25.446	1.00	58.77	N
ATOM	30	CA	PRO	C	913	-2.797	102.386	26.571	1.00	61.24	C
ATOM	31	C	PRO	C	913	-3.755	103.530	26.256	1.00	63.36	C
ATOM	32	O	PRO	C	913	-3.840	103.956	25.109	1.00	67.19	O
ATOM	33	CB	PRO	C	913	-1.349	102.849	26.685	1.00	59.78	C
ATOM	34	CG	PRO	C	913	-0.577	101.661	26.222	1.00	59.63	C
ATOM	35	CD	PRO	C	913	-1.386	101.084	25.074	1.00	59.35	C
ATOM	36	N	THR	C	914	-4.458	104.042	27.266	1.00	65.08	N

ATOM	37	CA	THR	C	914	-5.436	105.093	27.011	1.00	69.04	C
ATOM	38	C	THR	C	914	-4.815	106.370	26.491	1.00	73.88	C
ATOM	39	O	THR	C	914	-3.717	106.786	26.919	1.00	72.02	O
ATOM	40	CB	THR	C	914	-6.315	105.419	28.250	1.00	69.24	C
ATOM	41	CG2	THR	C	914	-5.485	106.060	29.340	1.00	69.56	C
ATOM	42	OG1	THR	C	914	-7.361	106.329	27.874	1.00	67.64	O
ATOM	43	N	ALA	C	915	-5.531	106.964	25.535	1.00	76.34	N
ATOM	44	CA	ALA	C	915	-5.106	108.193	24.885	1.00	78.39	C
ATOM	45	C	ALA	C	915	-5.407	109.387	25.786	1.00	81.78	C
ATOM	46	O	ALA	C	915	-4.725	110.418	25.718	1.00	84.63	O
ATOM	47	CB	ALA	C	915	-5.821	108.341	23.538	1.00	73.31	C
ATOM	48	N	ASN	C	916	-6.399	109.226	26.660	1.00	82.80	N
ATOM	49	CA	ASN	C	916	-6.816	110.305	27.546	1.00	82.11	C
ATOM	50	C	ASN	C	916	-5.834	110.665	28.679	1.00	79.48	C
ATOM	51	O	ASN	C	916	-6.252	111.247	29.670	1.00	75.73	O
ATOM	52	CB	ASN	C	916	-8.204	109.979	28.131	1.00	88.81	C
ATOM	53	CG	ASN	C	916	-9.073	109.113	27.184	1.00	94.91	C
ATOM	54	ND2	ASN	C	916	-9.575	107.988	27.704	1.00	96.94	N
ATOM	55	OD1	ASN	C	916	-9.289	109.455	26.012	1.00	99.35	O
ATOM	56	N	LEU	C	917	-4.549	110.328	28.531	1.00	76.82	N
ATOM	57	CA	LEU	C	917	-3.513	110.651	29.529	1.00	76.15	C
ATOM	58	C	LEU	C	917	-2.212	111.089	28.847	1.00	76.67	C
ATOM	59	O	LEU	C	917	-1.728	110.419	27.941	1.00	78.80	O
ATOM	60	CB	LEU	C	917	-3.179	109.444	30.403	1.00	78.46	C
ATOM	61	CG	LEU	C	917	-4.159	108.769	31.351	1.00	80.00	C
ATOM	62	CD1	LEU	C	917	-3.506	107.526	31.939	1.00	78.87	C
ATOM	63	CD2	LEU	C	917	-4.546	109.731	32.447	1.00	85.50	C
ATOM	64	N	ASP	C	918	-1.611	112.173	29.311	1.00	78.12	N
ATOM	65	CA	ASP	C	918	-0.394	112.668	28.673	1.00	82.31	C
ATOM	66	C	ASP	C	918	0.858	111.919	29.108	1.00	81.67	C
ATOM	67	O	ASP	C	918	1.210	111.929	30.285	1.00	84.04	O
ATOM	68	CB	ASP	C	918	-0.238	114.174	28.947	1.00	88.22	C
ATOM	69	CG	ASP	C	918	1.043	114.760	28.347	1.00	94.03	C
ATOM	70	OD1	ASP	C	918	2.096	114.097	28.473	1.00	98.43	O
ATOM	71	OD2	ASP	C	918	1.002	115.882	27.776	1.00	97.26	
O1-											
ATOM	72	N	ARG	C	919	1.552	111.315	28.140	1.00	77.81	N
ATOM	73	CA	ARG	C	919	2.757	110.518	28.399	1.00	71.26	C
ATOM	74	C	ARG	C	919	4.063	111.292	28.346	1.00	73.28	C

ATOM	75	O	ARG C 919	5.138	110.691	28.354	1.00	77.64	O
ATOM	76	CB	ARG C 919	2.842	109.384	27.386	1.00	60.42	C
ATOM	77	CG	ARG C 919	1.550	108.657	27.167	1.00	57.11	C
ATOM	78	CD	ARG C 919	1.107	107.962	28.421	1.00	54.34	C
ATOM	79	NE	ARG C 919	-0.182	107.321	28.226	1.00	57.02	N
ATOM	80	CZ	ARG C 919	-0.705	106.445	29.072	1.00	55.74	C
ATOM	81	NH1	ARG C 919	-0.039	106.116	30.173	1.00	54.16	
N1+									
ATOM	82	NH2	ARG C 919	-1.874	105.878	28.794	1.00	54.13	N
ATOM	83	N	SER C 920	3.984	112.613	28.284	1.00	74.38	N
ATOM	84	CA	SER C 920	5.195	113.421	28.187	1.00	76.74	C
ATOM	85	C	SER C 920	6.091	113.252	29.365	1.00	75.30	C
ATOM	86	O	SER C 920	7.317	113.241	29.232	1.00	72.65	O
ATOM	87	CB	SER C 920	4.871	114.909	28.089	1.00	79.67	C
ATOM	88	OG	SER C 920	4.047	115.190	26.977	1.00	89.57	O
ATOM	89	N	ASN C 921	5.466	113.149	30.529	1.00	77.59	N
ATOM	90	CA	ASN C 921	6.220	113.042	31.761	1.00	80.00	C
ATOM	91	C	ASN C 921	5.910	111.775	32.547	1.00	79.61	C
ATOM	92	O	ASN C 921	6.108	111.720	33.763	1.00	83.99	O
ATOM	93	CB	ASN C 921	5.972	114.304	32.602	1.00	78.49	C
ATOM	94	CG	ASN C 921	6.493	115.567	31.912	1.00	79.04	C
ATOM	95	ND2	ASN C 921	5.604	116.532	31.661	1.00	74.33	N
ATOM	96	OD1	ASN C 921	7.684	115.660	31.596	1.00	79.77	O
ATOM	97	N	ASP C 922	5.440	110.756	31.831	1.00	73.79	N
ATOM	98	CA	ASP C 922	5.106	109.470	32.427	1.00	70.09	C
ATOM	99	C	ASP C 922	6.337	108.555	32.462	1.00	69.92	C
ATOM	100	O	ASP C 922	6.608	107.825	31.504	1.00	71.98	O
ATOM	101	CB	ASP C 922	3.996	108.781	31.630	1.00	65.82	C
ATOM	102	CG	ASP C 922	3.281	107.715	32.440	1.00	66.60	C
ATOM	103	OD1	ASP C 922	3.871	107.216	33.425	1.00	64.17	O
ATOM	104	OD2	ASP C 922	2.130	107.378	32.093	1.00	68.31	
O1-									
ATOM	105	N	LYS C 923	7.085	108.609	33.559	1.00	67.80	N
ATOM	106	CA	LYS C 923	8.267	107.779	33.713	1.00	66.08	C
ATOM	107	C	LYS C 923	7.884	106.297	33.809	1.00	62.54	C
ATOM	108	O	LYS C 923	8.695	105.440	33.505	1.00	65.36	O
ATOM	109	CB	LYS C 923	9.080	108.228	34.942	1.00	67.57	C
ATOM	110	CG	LYS C 923	10.228	109.196	34.620	1.00	73.58	C
ATOM	111	CD	LYS C 923	11.553	108.468	34.336	1.00	78.66	C

ATOM	112	CE	LYS C 923	12.152	107.810	35.606	1.00	85.47	C
ATOM	113	NZ	LYS C 923	13.465	107.085	35.397	1.00	79.94	
N1+									
ATOM	114	N	VAL C 924	6.661	105.978	34.222	1.00	57.97	N
ATOM	115	CA	VAL C 924	6.266	104.569	34.284	1.00	59.25	C
ATOM	116	C	VAL C 924	6.178	103.993	32.855	1.00	60.92	C
ATOM	117	O	VAL C 924	6.643	102.879	32.595	1.00	60.50	O
ATOM	118	CB	VAL C 924	4.903	104.386	35.012	1.00	59.50	C
ATOM	119	CG1	VAL C 924	4.414	102.937	34.899	1.00	51.04	C
ATOM	120	CG2	VAL C 924	5.065	104.748	36.465	1.00	55.92	C
ATOM	121	N	TYR C 925	5.578	104.768	31.947	1.00	59.17	N
ATOM	122	CA	TYR C 925	5.413	104.412	30.538	1.00	58.27	C
ATOM	123	C	TYR C 925	6.798	104.265	29.891	1.00	62.45	C
ATOM	124	O	TYR C 925	7.025	103.397	29.044	1.00	61.60	O
ATOM	125	CB	TYR C 925	4.613	105.514	29.839	1.00	54.96	C
ATOM	126	CG	TYR C 925	3.947	105.102	28.554	1.00	54.96	C
ATOM	127	CD1	TYR C 925	4.609	105.202	27.336	1.00	58.50	C
ATOM	128	CD2	TYR C 925	2.659	104.582	28.559	1.00	58.34	C
ATOM	129	CE1	TYR C 925	4.003	104.793	26.144	1.00	59.20	C
ATOM	130	CE2	TYR C 925	2.039	104.161	27.376	1.00	58.79	C
ATOM	131	CZ	TYR C 925	2.721	104.270	26.171	1.00	60.73	C
ATOM	132	OH	TYR C 925	2.130	103.849	25.001	1.00	57.74	O
ATOM	133	N	GLU C 926	7.725	105.123	30.299	1.00	65.25	N
ATOM	134	CA	GLU C 926	9.083	105.089	29.780	1.00	68.80	C
ATOM	135	C	GLU C 926	9.809	103.861	30.320	1.00	69.97	C
ATOM	136	O	GLU C 926	10.430	103.099	29.570	1.00	69.90	O
ATOM	137	CB	GLU C 926	9.820	106.358	30.202	1.00	75.59	C
ATOM	138	CG	GLU C 926	11.293	106.408	29.819	1.00	90.96	C
ATOM	139	CD	GLU C 926	11.965	107.723	30.223	1.00	101.09	C
ATOM	140	OE1	GLU C 926	11.383	108.464	31.050	1.00	109.17	O
ATOM	141	OE2	GLU C 926	13.079	108.010	29.724	1.00	106.84	
O1-									
ATOM	142	N	ASN C 927	9.717	103.666	31.629	1.00	68.66	N
ATOM	143	CA	ASN C 927	10.376	102.541	32.254	1.00	67.67	C
ATOM	144	C	ASN C 927	9.822	101.200	31.828	1.00	68.74	C
ATOM	145	O	ASN C 927	10.574	100.227	31.768	1.00	72.39	O
ATOM	146	CB	ASN C 927	10.352	102.684	33.773	1.00	68.05	C
ATOM	147	CG	ASN C 927	11.327	103.738	34.259	1.00	70.92	C
ATOM	148	ND2	ASN C 927	11.334	103.976	35.562	1.00	70.63	N

ATOM	149	OD1	ASN	C	927	12.072	104.335	33.465	1.00	69.96	O
ATOM	150	N	VAL	C	928	8.523	101.126	31.546	1.00	64.92	N
ATOM	151	CA	VAL	C	928	7.941	99.868	31.076	1.00	61.66	C
ATOM	152	C	VAL	C	928	8.547	99.631	29.700	1.00	60.07	C
ATOM	153	O	VAL	C	928	9.082	98.562	29.420	1.00	60.30	O
ATOM	154	CB	VAL	C	928	6.392	99.942	30.981	1.00	60.82	C
ATOM	155	CG1	VAL	C	928	5.872	98.889	30.022	1.00	60.29	C
ATOM	156	CG2	VAL	C	928	5.771	99.725	32.365	1.00	58.20	C
ATOM	157	N	THR	C	929	8.485	100.652	28.851	1.00	63.07	N
ATOM	158	CA	THR	C	929	9.054	100.578	27.512	1.00	61.40	C
ATOM	159	C	THR	C	929	10.504	100.131	27.584	1.00	62.87	C
ATOM	160	O	THR	C	929	10.971	99.358	26.749	1.00	63.14	O
ATOM	161	CB	THR	C	929	9.003	101.927	26.841	1.00	58.88	C
ATOM	162	CG2	THR	C	929	9.757	101.909	25.557	1.00	63.85	C
ATOM	163	OG1	THR	C	929	7.646	102.254	26.554	1.00	62.34	O
ATOM	164	N	GLY	C	930	11.216	100.623	28.589	1.00	64.51	N
ATOM	165	CA	GLY	C	930	12.602	100.244	28.739	1.00	64.78	C
ATOM	166	C	GLY	C	930	12.737	98.768	29.037	1.00	68.72	C
ATOM	167	O	GLY	C	930	13.534	98.079	28.411	1.00	73.17	O
ATOM	168	N	LEU	C	931	11.958	98.289	30.002	1.00	71.25	N
ATOM	169	CA	LEU	C	931	11.973	96.891	30.393	1.00	69.93	C
ATOM	170	C	LEU	C	931	11.542	96.037	29.233	1.00	66.95	C
ATOM	171	O	LEU	C	931	12.208	95.065	28.914	1.00	67.13	O
ATOM	172	CB	LEU	C	931	11.026	96.633	31.565	1.00	73.68	C
ATOM	173	CG	LEU	C	931	10.990	95.208	32.125	1.00	77.88	C
ATOM	174	CD1	LEU	C	931	12.404	94.755	32.513	1.00	77.15	C
ATOM	175	CD2	LEU	C	931	10.054	95.182	33.332	1.00	79.64	C
ATOM	176	N	VAL	C	932	10.424	96.365	28.603	1.00	65.09	N
ATOM	177	CA	VAL	C	932	10.009	95.537	27.488	1.00	69.46	C
ATOM	178	C	VAL	C	932	11.164	95.398	26.517	1.00	73.87	C
ATOM	179	O	VAL	C	932	11.497	94.297	26.098	1.00	72.32	O
ATOM	180	CB	VAL	C	932	8.820	96.110	26.756	1.00	63.05	C
ATOM	181	CG1	VAL	C	932	8.589	95.329	25.483	1.00	62.98	C
ATOM	182	CG2	VAL	C	932	7.609	96.025	27.642	1.00	59.58	C
ATOM	183	N	LYS	C	933	11.776	96.530	26.185	1.00	79.21	N
ATOM	184	CA	LYS	C	933	12.912	96.599	25.274	1.00	80.58	C
ATOM	185	C	LYS	C	933	14.141	95.773	25.707	1.00	83.29	C
ATOM	186	O	LYS	C	933	14.731	95.054	24.891	1.00	83.49	O
ATOM	187	CB	LYS	C	933	13.294	98.064	25.107	1.00	81.60	C

ATOM	188	CG	LYS	C	933	13.286	98.550	23.670	1.00	84.45	C
ATOM	189	CD	LYS	C	933	12.877	100.009	23.543	1.00	84.61	C
ATOM	190	CE	LYS	C	933	11.568	100.112	22.774	1.00	83.57	C
ATOM	191	NZ	LYS	C	933	11.236	101.508	22.371	1.00	88.80	
N1+											
ATOM	192	N	ALA	C	934	14.542	95.872	26.973	1.00	83.91	N
ATOM	193	CA	ALA	C	934	15.700	95.101	27.431	1.00	86.68	C
ATOM	194	C	ALA	C	934	15.429	93.604	27.294	1.00	88.36	C
ATOM	195	O	ALA	C	934	16.351	92.809	27.107	1.00	92.75	O
ATOM	196	CB	ALA	C	934	16.048	95.439	28.880	1.00	87.14	C
ATOM	197	N	VAL	C	935	14.159	93.227	27.407	1.00	85.45	N
ATOM	198	CA	VAL	C	935	13.733	91.839	27.268	1.00	81.49	C
ATOM	199	C	VAL	C	935	13.888	91.417	25.814	1.00	81.92	C
ATOM	200	O	VAL	C	935	14.375	90.328	25.520	1.00	83.58	O
ATOM	201	CB	VAL	C	935	12.247	91.673	27.699	1.00	79.53	C
ATOM	202	CG1	VAL	C	935	11.545	90.605	26.852	1.00	72.69	C
ATOM	203	CG2	VAL	C	935	12.184	91.310	29.164	1.00	75.15	C
ATOM	204	N	ILE	C	936	13.469	92.291	24.910	1.00	82.93	N
ATOM	205	CA	ILE	C	936	13.551	92.020	23.489	1.00	85.97	C
ATOM	206	C	ILE	C	936	15.010	91.975	23.021	1.00	92.14	C
ATOM	207	O	ILE	C	936	15.336	91.325	22.022	1.00	90.57	O
ATOM	208	CB	ILE	C	936	12.766	93.078	22.709	1.00	80.76	C
ATOM	209	CG1	ILE	C	936	11.295	93.014	23.104	1.00	78.23	C
ATOM	210	CG2	ILE	C	936	12.879	92.827	21.232	1.00	82.49	C
ATOM	211	CD1	ILE	C	936	10.444	94.028	22.396	1.00	76.28	C
ATOM	212	N	GLU	C	937	15.891	92.658	23.746	1.00	98.38	N
ATOM	213	CA	GLU	C	937	17.309	92.662	23.401	1.00	105.29	C
ATOM	214	C	GLU	C	937	17.875	91.261	23.702	1.00	106.70	C
ATOM	215	O	GLU	C	937	18.752	90.751	22.996	1.00	109.35	O
ATOM	216	CB	GLU	C	937	18.034	93.754	24.208	1.00	109.34	C
ATOM	217	CG	GLU	C	937	19.500	93.990	23.811	1.00	114.00	C
ATOM	218	CD	GLU	C	937	19.745	93.851	22.306	1.00	117.38	C
ATOM	219	OE1	GLU	C	937	18.904	94.339	21.512	1.00	115.32	O
ATOM	220	OE2	GLU	C	937	20.785	93.257	21.925	1.00	117.56	
O1-											
ATOM	221	N	MET	C	938	17.361	90.644	24.761	1.00	108.24	N
ATOM	222	CA	MET	C	938	17.762	89.296	25.136	1.00	107.56	C
ATOM	223	C	MET	C	938	16.978	88.301	24.275	1.00	108.86	C
ATOM	224	O	MET	C	938	17.521	87.303	23.809	1.00	107.20	O



ATOM	225	CB	MET C 938	17.444	89.039	26.605	1.00103.15	C
ATOM	226	CG	MET C 938	17.085	87.600	26.890	1.00100.99	C
ATOM	227	SD	MET C 938	16.864	87.280	28.638	1.00102.23	S
ATOM	228	CE	MET C 938	18.424	87.925	29.302	1.00 96.91	C
ATOM	229	N	SER C 939	15.696	88.584	24.061	1.00112.38	N
ATOM	230	CA	SER C 939	14.840	87.692	23.279	1.00117.67	C
ATOM	231	C	SER C 939	15.323	87.446	21.848	1.00119.77	C
ATOM	232	O	SER C 939	15.197	86.328	21.338	1.00118.72	O
ATOM	233	CB	SER C 939	13.392	88.216	23.235	1.00118.43	C
ATOM	234	OG	SER C 939	13.138	88.966	22.054	1.00120.19	O
ATOM	235	N	SER C 940	15.871	88.474	21.200	1.00122.53	N
ATOM	236	CA	SER C 940	16.335	88.328	19.820	1.00124.52	C
ATOM	237	C	SER C 940	17.828	88.067	19.662	1.00125.63	C
ATOM	238	O	SER C 940	18.302	87.764	18.559	1.00123.74	O
ATOM	239	CB	SER C 940	15.955	89.558	19.002	1.00124.34	C
ATOM	240	OG	SER C 940	16.234	89.323	17.633	1.00124.58	O
ATOM	241	N	LYS C 941	18.561	88.199	20.763	1.00127.31	N
ATOM	242	CA	LYS C 941	19.995	87.954	20.756	1.00130.31	C
ATOM	243	C	LYS C 941	20.260	86.516	21.259	1.00133.31	C
ATOM	244	O	LYS C 941	20.191	85.556	20.483	1.00134.26	O
ATOM	245	CB	LYS C 941	20.706	88.985	21.646	1.00129.68	C
ATOM	246	CG	LYS C 941	22.179	89.203	21.304	1.00133.13	C
ATOM	247	CD	LYS C 941	23.024	87.947	21.534	1.00136.10	C
ATOM	248	CE	LYS C 941	24.242	87.899	20.601	1.00136.33	C
ATOM	249	NZ	LYS C 941	25.034	89.168	20.595	1.00133.87	
N1+								
ATOM	250	N	ILE C 942	20.531	86.399	22.563	1.00135.72	N
ATOM	251	CA	ILE C 942	20.832	85.149	23.304	1.00135.88	C
ATOM	252	C	ILE C 942	20.989	83.747	22.671	1.00135.69	C
ATOM	253	O	ILE C 942	21.954	83.048	23.011	1.00136.41	O
ATOM	254	CB	ILE C 942	19.861	84.953	24.508	1.00135.80	C
ATOM	255	CG1	ILE C 942	20.569	84.151	25.618	1.00134.32	C
ATOM	256	CG2	ILE C 942	18.583	84.210	24.062	1.00133.16	C
ATOM	257	CD1	ILE C 942	19.708	83.865	26.818	1.00133.90	C
ATOM	258	N	GLN C 943	20.075	83.315	21.798	1.00134.34	N
ATOM	259	CA	GLN C 943	20.188	81.993	21.193	1.00132.88	C
ATOM	260	C	GLN C 943	21.674	81.652	21.016	1.00132.35	C
ATOM	261	O	GLN C 943	22.173	80.690	21.625	1.00132.00	O
ATOM	262	CB	GLN C 943	19.414	81.962	19.851	1.00132.04	C

ATOM	263	CG	GLN	C	943	17.982	81.446	20.006	1.00131.86	C
ATOM	264	CD	GLN	C	943	17.936	79.947	20.263	1.00131.58	C
ATOM	265	NE2	GLN	C	943	17.400	79.551	21.420	1.00128.52	N
ATOM	266	OE1	GLN	C	943	18.384	79.155	19.431	1.00131.63	O
ATOM	267	N	PRO	C	944	22.408	82.449	20.194	1.00131.19	N
ATOM	268	CA	PRO	C	944	23.835	82.210	19.966	1.00127.40	C
ATOM	269	C	PRO	C	944	24.699	82.162	21.238	1.00124.05	C
ATOM	270	O	PRO	C	944	25.070	81.116	21.760	1.00122.03	O
ATOM	271	CB	PRO	C	944	24.201	83.391	19.093	1.00128.29	C
ATOM	272	CG	PRO	C	944	23.087	83.384	18.151	1.00129.04	C
ATOM	273	CD	PRO	C	944	21.968	83.466	19.213	1.00130.52	C
ATOM	274	N	ALA	C	945	24.992	83.349	21.743	1.00122.53	N
ATOM	275	CA	ALA	C	945	25.806	83.568	22.946	1.00122.04	C
ATOM	276	C	ALA	C	945	25.841	82.540	24.075	1.00120.54	C
ATOM	277	O	ALA	C	945	24.840	81.906	24.400	1.00119.65	O
ATOM	278	CB	ALA	C	945	25.494	84.961	23.538	1.00121.84	C
ATOM	279	N	PRO	C	946	27.033	82.368	24.685	1.00120.48	N
ATOM	280	CA	PRO	C	946	27.308	81.442	25.797	1.00120.10	C
ATOM	281	C	PRO	C	946	27.088	82.176	27.137	1.00118.51	C
ATOM	282	O	PRO	C	946	26.599	83.308	27.138	1.00117.33	O
ATOM	283	CB	PRO	C	946	28.772	81.055	25.571	1.00121.49	C
ATOM	284	CG	PRO	C	946	29.366	82.309	24.986	1.00120.89	C
ATOM	285	CD	PRO	C	946	28.288	82.759	24.011	1.00120.40	C
ATOM	286	N	PRO	C	947	27.429	81.554	28.284	1.00118.59	N
ATOM	287	CA	PRO	C	947	27.252	82.190	29.601	1.00120.40	C
ATOM	288	C	PRO	C	947	28.096	83.451	29.875	1.00122.86	C
ATOM	289	O	PRO	C	947	27.870	84.150	30.863	1.00121.93	O
ATOM	290	CB	PRO	C	947	27.594	81.069	30.570	1.00119.50	C
ATOM	291	CG	PRO	C	947	27.130	79.871	29.861	1.00118.56	C
ATOM	292	CD	PRO	C	947	27.576	80.097	28.434	1.00118.85	C
ATOM	293	N	GLU	C	948	29.105	83.725	29.052	1.00126.09	N
ATOM	294	CA	GLU	C	948	29.921	84.935	29.256	1.00128.05	C
ATOM	295	C	GLU	C	948	29.179	86.102	28.618	1.00129.22	C
ATOM	296	O	GLU	C	948	29.651	87.246	28.633	1.00129.11	O
ATOM	297	CB	GLU	C	948	31.281	84.804	28.563	1.00128.79	C
ATOM	298	CG	GLU	C	948	32.407	84.236	29.412	1.00129.22	C
ATOM	299	CD	GLU	C	948	33.351	83.374	28.595	1.00129.49	C
ATOM	300	OE1	GLU	C	948	34.515	83.783	28.369	1.00127.95	O

ATOM	301	OE2	GLU	C	948	32.907	82.282	28.171	1.00130.34	
O1-										
ATOM	302	N	GLU	C	949	27.998	85.811	28.081	1.00130.67	N
ATOM	303	CA	GLU	C	949	27.249	86.828	27.372	1.00132.06	C
ATOM	304	C	GLU	C	949	25.753	87.036	27.699	1.00131.00	C
ATOM	305	O	GLU	C	949	25.239	88.139	27.493	1.00130.08	O
ATOM	306	CB	GLU	C	949	27.510	86.591	25.880	1.00134.83	C
ATOM	307	CG	GLU	C	949	29.022	86.702	25.559	1.00139.33	C
ATOM	308	CD	GLU	C	949	29.411	86.198	24.172	1.00142.36	C
ATOM	309	OE1	GLU	C	949	28.784	86.638	23.181	1.00144.45	O
ATOM	310	OE2	GLU	C	949	30.356	85.376	24.080	1.00140.95	
O1-										
ATOM	311	N	TYR	C	950	25.041	86.011	28.181	1.00129.73	N
ATOM	312	CA	TYR	C	950	23.648	86.241	28.575	1.00125.37	C
ATOM	313	C	TYR	C	950	23.553	86.517	30.088	1.00123.89	C
ATOM	314	O	TYR	C	950	22.607	87.168	30.529	1.00124.67	O
ATOM	315	CB	TYR	C	950	22.678	85.099	28.172	1.00124.27	C
ATOM	316	CG	TYR	C	950	23.065	83.664	28.475	1.00124.30	C
ATOM	317	CD1	TYR	C	950	23.439	83.256	29.757	1.00123.25	C
ATOM	318	CD2	TYR	C	950	22.993	82.694	27.471	1.00123.52	C
ATOM	319	CE1	TYR	C	950	23.729	81.904	30.027	1.00122.44	C
ATOM	320	CE2	TYR	C	950	23.276	81.354	27.728	1.00122.74	C
ATOM	321	CZ	TYR	C	950	23.645	80.961	29.000	1.00123.33	C
ATOM	322	OH	TYR	C	950	23.933	79.628	29.219	1.00122.73	O
ATOM	323	N	VAL	C	951	24.527	86.057	30.879	1.00121.89	N
ATOM	324	CA	VAL	C	951	24.483	86.321	32.314	1.00122.76	C
ATOM	325	C	VAL	C	951	24.330	87.824	32.567	1.00126.35	C
ATOM	326	O	VAL	C	951	23.721	88.226	33.566	1.00128.44	O
ATOM	327	CB	VAL	C	951	25.731	85.811	33.041	1.00121.55	C
ATOM	328	CG1	VAL	C	951	25.719	86.295	34.493	1.00119.27	C
ATOM	329	CG2	VAL	C	951	25.732	84.296	33.010	1.00122.16	C
ATOM	330	N	PRO	C	952	24.913	88.677	31.687	1.00127.99	N
ATOM	331	CA	PRO	C	952	24.782	90.131	31.868	1.00126.63	C
ATOM	332	C	PRO	C	952	23.495	90.571	31.136	1.00125.51	C
ATOM	333	O	PRO	C	952	22.759	91.421	31.623	1.00124.87	O
ATOM	334	CB	PRO	C	952	26.048	90.694	31.202	1.00126.03	C
ATOM	335	CG	PRO	C	952	27.016	89.550	31.238	1.00127.51	C
ATOM	336	CD	PRO	C	952	26.122	88.382	30.895	1.00128.76	C
ATOM	337	N	MET	C	953	23.236	89.989	29.960	1.00124.90	N

ATOM	338	CA	MET C 953	22.025	90.287	29.161	1.00124.90	C
ATOM	339	C	MET C 953	20.768	90.152	30.033	1.00123.24	C
ATOM	340	O	MET C 953	19.695	90.642	29.674	1.00123.57	O
ATOM	341	CB	MET C 953	21.900	89.307	27.982	1.00128.34	C
ATOM	342	CG	MET C 953	21.893	89.921	26.586	1.00132.89	C
ATOM	343	SD	MET C 953	21.585	88.654	25.299	1.00139.20	S
ATOM	344	CE	MET C 953	23.116	87.639	25.355	1.00133.99	C
ATOM	345	N	VAL C 954	20.914	89.433	31.149	1.00120.10	N
ATOM	346	CA	VAL C 954	19.851	89.218	32.134	1.00115.86	C
ATOM	347	C	VAL C 954	20.044	90.326	33.162	1.00114.76	C
ATOM	348	O	VAL C 954	19.100	91.026	33.523	1.00115.64	O
ATOM	349	CB	VAL C 954	19.980	87.827	32.841	1.00115.37	C
ATOM	350	CG1	VAL C 954	19.528	87.912	34.295	1.00114.62	C
ATOM	351	CG2	VAL C 954	19.132	86.800	32.120	1.00111.15	C
ATOM	352	N	LYS C 955	21.281	90.484	33.625	1.00112.03	N
ATOM	353	CA	LYS C 955	21.611	91.524	34.594	1.00110.08	C
ATOM	354	C	LYS C 955	20.988	92.853	34.129	1.00108.57	C
ATOM	355	O	LYS C 955	20.634	93.707	34.946	1.00107.99	O
ATOM	356	CB	LYS C 955	23.136	91.641	34.715	1.00109.26	C
ATOM	357	CG	LYS C 955	23.618	92.778	35.592	1.00112.85	C
ATOM	358	CD	LYS C 955	23.180	92.635	37.038	1.00113.69	C
ATOM	359	CE	LYS C 955	23.684	93.818	37.851	1.00117.31	C
ATOM	360	NZ	LYS C 955	23.412	93.674	39.305	1.00120.85	
N1+								
ATOM	361	N	GLU C 956	20.849	93.000	32.810	1.00106.12	N
ATOM	362	CA	GLU C 956	20.259	94.183	32.181	1.00104.23	C
ATOM	363	C	GLU C 956	18.766	94.254	32.481	1.00101.34	C
ATOM	364	O	GLU C 956	18.304	95.191	33.132	1.00101.80	O
ATOM	365	CB	GLU C 956	20.462	94.139	30.661	1.00107.40	C
ATOM	366	CG	GLU C 956	21.683	94.881	30.150	1.00115.30	C
ATOM	367	CD	GLU C 956	21.296	96.029	29.238	1.00120.67	C
ATOM	368	OE1	GLU C 956	20.256	95.899	28.554	1.00123.99	O
ATOM	369	OE2	GLU C 956	22.023	97.048	29.192	1.00123.79	
O1-								
ATOM	370	N	VAL C 957	18.018	93.275	31.974	1.00 97.84	N
ATOM	371	CA	VAL C 957	16.575	93.179	32.202	1.00 91.30	C
ATOM	372	C	VAL C 957	16.287	93.287	33.705	1.00 89.63	C
ATOM	373	O	VAL C 957	15.201	93.722	34.111	1.00 89.13	O
ATOM	374	CB	VAL C 957	16.024	91.823	31.670	1.00 86.99	C

ATOM	375	CG1	VAL	C	957	14.696	91.487	32.325	1.00	81.87	C
ATOM	376	CG2	VAL	C	957	15.859	91.885	30.162	1.00	83.49	C
ATOM	377	N	GLY	C	958	17.258	92.877	34.521	1.00	86.73	N
ATOM	378	CA	GLY	C	958	17.100	92.942	35.963	1.00	86.30	C
ATOM	379	C	GLY	C	958	17.253	94.357	36.489	1.00	87.09	C
ATOM	380	O	GLY	C	958	16.602	94.736	37.470	1.00	87.61	O
ATOM	381	N	LEU	C	959	18.122	95.134	35.836	1.00	88.08	N
ATOM	382	CA	LEU	C	959	18.390	96.533	36.203	1.00	87.22	C
ATOM	383	C	LEU	C	959	17.248	97.427	35.696	1.00	84.42	C
ATOM	384	O	LEU	C	959	16.860	98.399	36.361	1.00	81.73	O
ATOM	385	CB	LEU	C	959	19.752	96.998	35.617	1.00	90.23	C
ATOM	386	CG	LEU	C	959	21.069	96.402	36.183	1.00	94.61	C
ATOM	387	CD1	LEU	C	959	22.235	96.526	35.174	1.00	91.08	C
ATOM	388	CD2	LEU	C	959	21.416	97.110	37.493	1.00	96.47	C
ATOM	389	N	ALA	C	960	16.710	97.079	34.525	1.00	80.88	N
ATOM	390	CA	ALA	C	960	15.614	97.822	33.912	1.00	78.40	C
ATOM	391	C	ALA	C	960	14.308	97.632	34.678	1.00	77.74	C
ATOM	392	O	ALA	C	960	13.397	98.449	34.574	1.00	77.60	O
ATOM	393	CB	ALA	C	960	15.435	97.385	32.474	1.00	77.27	C
ATOM	394	N	LEU	C	961	14.216	96.536	35.424	1.00	77.06	N
ATOM	395	CA	LEU	C	961	13.037	96.242	36.225	1.00	75.44	C
ATOM	396	C	LEU	C	961	13.202	96.911	37.577	1.00	77.45	C
ATOM	397	O	LEU	C	961	12.229	97.333	38.204	1.00	76.85	O
ATOM	398	CB	LEU	C	961	12.883	94.737	36.432	1.00	73.48	C
ATOM	399	CG	LEU	C	961	11.791	94.360	37.440	1.00	72.22	C
ATOM	400	CD1	LEU	C	961	10.410	94.596	36.828	1.00	67.24	C
ATOM	401	CD2	LEU	C	961	11.961	92.903	37.858	1.00	73.06	C
ATOM	402	N	ARG	C	962	14.440	96.984	38.042	1.00	81.45	N
ATOM	403	CA	ARG	C	962	14.714	97.632	39.314	1.00	86.24	C
ATOM	404	C	ARG	C	962	14.209	99.069	39.193	1.00	83.35	C
ATOM	405	O	ARG	C	962	13.524	99.572	40.085	1.00	83.50	O
ATOM	406	CB	ARG	C	962	16.218	97.617	39.594	1.00	96.72	C
ATOM	407	CG	ARG	C	962	16.627	98.192	40.952	1.00	107.84	C
ATOM	408	CD	ARG	C	962	18.157	98.202	41.147	1.00	114.40	C
ATOM	409	NE	ARG	C	962	18.488	98.556	42.529	1.00	123.62	N
ATOM	410	CZ	ARG	C	962	19.715	98.810	42.983	1.00	127.32	C
ATOM	411	NH1	ARG	C	962	20.761	98.751	42.164	1.00	129.36	
N1+											
ATOM	412	NH2	ARG	C	962	19.890	99.139	44.262	1.00	127.50	N

ATOM	413	N	THR	C	963	14.550	99.700	38.066	1.00	81.04	N
ATOM	414	CA	THR	C	963	14.159	101.075	37.737	1.00	77.34	C
ATOM	415	C	THR	C	963	12.641	101.222	37.673	1.00	76.41	C
ATOM	416	O	THR	C	963	12.077	102.135	38.271	1.00	78.85	O
ATOM	417	CB	THR	C	963	14.703	101.532	36.342	1.00	77.75	C
ATOM	418	CG2	THR	C	963	14.212	102.939	36.011	1.00	73.04	C
ATOM	419	OG1	THR	C	963	16.136	101.527	36.336	1.00	76.39	O
ATOM	420	N	LEU	C	964	11.984	100.333	36.931	1.00	72.53	N
ATOM	421	CA	LEU	C	964	10.537	100.405	36.784	1.00	71.29	C
ATOM	422	C	LEU	C	964	9.855	100.296	38.114	1.00	71.98	C
ATOM	423	O	LEU	C	964	8.906	101.030	38.397	1.00	72.44	O
ATOM	424	CB	LEU	C	964	10.006	99.298	35.868	1.00	68.42	C
ATOM	425	CG	LEU	C	964	8.478	99.135	35.810	1.00	64.26	C
ATOM	426	CD1	LEU	C	964	7.791	100.441	35.463	1.00	57.94	C
ATOM	427	CD2	LEU	C	964	8.152	98.068	34.782	1.00	62.07	C
ATOM	428	N	LEU	C	965	10.341	99.370	38.931	1.00	74.48	N
ATOM	429	CA	LEU	C	965	9.764	99.152	40.246	1.00	75.89	C
ATOM	430	C	LEU	C	965	9.991	100.384	41.094	1.00	74.88	C
ATOM	431	O	LEU	C	965	9.085	100.824	41.815	1.00	73.74	O
ATOM	432	CB	LEU	C	965	10.368	97.896	40.879	1.00	76.31	C
ATOM	433	CG	LEU	C	965	9.876	96.665	40.106	1.00	76.66	C
ATOM	434	CD1	LEU	C	965	10.606	95.443	40.588	1.00	76.56	C
ATOM	435	CD2	LEU	C	965	8.357	96.507	40.275	1.00	75.94	C
ATOM	436	N	ALA	C	966	11.190	100.954	40.972	1.00	72.90	N
ATOM	437	CA	ALA	C	966	11.550	102.167	41.701	1.00	71.93	C
ATOM	438	C	ALA	C	966	10.582	103.315	41.362	1.00	70.46	C
ATOM	439	O	ALA	C	966	10.082	103.991	42.268	1.00	72.48	O
ATOM	440	CB	ALA	C	966	12.976	102.562	41.371	1.00	69.12	C
ATOM	441	N	THR	C	967	10.313	103.520	40.070	1.00	67.44	N
ATOM	442	CA	THR	C	967	9.398	104.565	39.627	1.00	63.01	C
ATOM	443	C	THR	C	967	7.976	104.304	40.072	1.00	64.40	C
ATOM	444	O	THR	C	967	7.271	105.235	40.454	1.00	65.31	O
ATOM	445	CB	THR	C	967	9.358	104.693	38.112	1.00	64.08	C
ATOM	446	CG2	THR	C	967	8.359	105.741	37.688	1.00	64.42	C
ATOM	447	OG1	THR	C	967	10.644	105.078	37.638	1.00	67.54	O
ATOM	448	N	VAL	C	968	7.524	103.056	40.012	1.00	63.53	N
ATOM	449	CA	VAL	C	968	6.156	102.809	40.440	1.00	65.67	C
ATOM	450	C	VAL	C	968	6.079	103.144	41.926	1.00	69.31	C
ATOM	451	O	VAL	C	968	5.044	103.603	42.400	1.00	68.50	O

ATOM	452	CB	VAL	C	968	5.682	101.338	40.194	1.00	64.11	C
ATOM	453	CG1	VAL	C	968	4.207	101.203	40.574	1.00	57.49	C
ATOM	454	CG2	VAL	C	968	5.860	100.949	38.731	1.00	60.33	C
ATOM	455	N	ASP	C	969	7.181	102.944	42.650	1.00	75.56	N
ATOM	456	CA	ASP	C	969	7.206	103.246	44.080	1.00	83.87	C
ATOM	457	C	ASP	C	969	7.015	104.739	44.334	1.00	87.31	C
ATOM	458	O	ASP	C	969	6.393	105.127	45.328	1.00	90.96	O
ATOM	459	CB	ASP	C	969	8.512	102.774	44.730	1.00	90.65	C
ATOM	460	CG	ASP	C	969	8.646	101.247	44.743	1.00	99.31	C
ATOM	461	OD1	ASP	C	969	7.585	100.569	44.687	1.00	99.15	O
ATOM	462	OD2	ASP	C	969	9.804	100.741	44.822	1.00	102.67	
O1-											
ATOM	463	N	GLU	C	970	7.551	105.579	43.451	1.00	87.78	N
ATOM	464	CA	GLU	C	970	7.383	107.025	43.592	1.00	87.87	C
ATOM	465	C	GLU	C	970	6.020	107.494	43.066	1.00	86.64	C
ATOM	466	O	GLU	C	970	5.565	108.587	43.390	1.00	89.18	O
ATOM	467	CB	GLU	C	970	8.467	107.757	42.828	1.00	87.52	C
ATOM	468	CG	GLU	C	970	9.852	107.398	43.245	1.00	98.17	C
ATOM	469	CD	GLU	C	970	10.886	108.142	42.426	1.00	107.97	C
ATOM	470	OE1	GLU	C	970	10.958	107.886	41.196	1.00	110.90	O
ATOM	471	OE2	GLU	C	970	11.615	108.980	43.015	1.00	110.97	
O1-											
ATOM	472	N	THR	C	971	5.355	106.657	42.284	1.00	82.40	N
ATOM	473	CA	THR	C	971	4.087	107.046	41.711	1.00	79.25	C
ATOM	474	C	THR	C	971	2.865	106.634	42.512	1.00	80.67	C
ATOM	475	O	THR	C	971	1.841	107.311	42.466	1.00	81.99	O
ATOM	476	CB	THR	C	971	3.993	106.485	40.276	1.00	79.59	C
ATOM	477	CG2	THR	C	971	2.685	106.873	39.595	1.00	75.08	C
ATOM	478	OG1	THR	C	971	5.091	106.996	39.512	1.00	72.72	O
ATOM	479	N	ILE	C	972	2.962	105.531	43.244	1.00	81.67	N
ATOM	480	CA	ILE	C	972	1.817	105.045	44.024	1.00	83.42	C
ATOM	481	C	ILE	C	972	1.269	106.051	45.048	1.00	80.81	C
ATOM	482	O	ILE	C	972	0.046	106.236	45.160	1.00	74.87	O
ATOM	483	CB	ILE	C	972	2.166	103.743	44.776	1.00	83.46	C
ATOM	484	CG1	ILE	C	972	2.802	102.745	43.820	1.00	84.93	C
ATOM	485	CG2	ILE	C	972	0.902	103.090	45.323	1.00	83.58	C
ATOM	486	CD1	ILE	C	972	3.825	101.854	44.487	1.00	89.93	C
ATOM	487	N	PRO	C	973	2.169	106.709	45.805	1.00	79.99	N
ATOM	488	CA	PRO	C	973	1.744	107.687	46.814	1.00	79.69	C

ATOM	489	C	PRO C 973	0.568	108.529	46.339	1.00	80.30	C
ATOM	490	O	PRO C 973	-0.466	108.639	47.004	1.00	81.02	O
ATOM	491	CB	PRO C 973	2.995	108.535	47.016	1.00	76.57	C
ATOM	492	CG	PRO C 973	4.097	107.565	46.802	1.00	75.19	C
ATOM	493	CD	PRO C 973	3.637	106.739	45.625	1.00	76.30	C
ATOM	494	N	LEU C 974	0.765	109.106	45.162	1.00	77.51	N
ATOM	495	CA	LEU C 974	-0.186	109.972	44.493	1.00	75.93	C
ATOM	496	C	LEU C 974	-1.568	109.412	44.101	1.00	74.44	C
ATOM	497	O	LEU C 974	-2.544	110.144	44.073	1.00	75.32	O
ATOM	498	CB	LEU C 974	0.491	110.533	43.243	1.00	76.44	C
ATOM	499	CG	LEU C 974	-0.441	111.137	42.189	1.00	80.68	C
ATOM	500	CD1	LEU C 974	-0.996	112.470	42.673	1.00	80.27	C
ATOM	501	CD2	LEU C 974	0.336	111.310	40.882	1.00	84.93	C
ATOM	502	N	LEU C 975	-1.675	108.129	43.801	1.00	73.62	N
ATOM	503	CA	LEU C 975	-2.967	107.620	43.354	1.00	75.01	C
ATOM	504	C	LEU C 975	-3.926	107.317	44.492	1.00	74.03	C
ATOM	505	O	LEU C 975	-3.518	107.273	45.653	1.00	75.19	O
ATOM	506	CB	LEU C 975	-2.734	106.391	42.475	1.00	75.34	C
ATOM	507	CG	LEU C 975	-1.607	106.735	41.489	1.00	78.17	C
ATOM	508	CD1	LEU C 975	-0.730	105.515	41.226	1.00	79.70	C
ATOM	509	CD2	LEU C 975	-2.208	107.321	40.208	1.00	79.20	C
ATOM	510	N	PRO C 976	-5.222	107.135	44.178	1.00	72.08	N
ATOM	511	CA	PRO C 976	-6.211	106.835	45.216	1.00	74.16	C
ATOM	512	C	PRO C 976	-5.691	105.762	46.154	1.00	75.80	C
ATOM	513	O	PRO C 976	-4.933	104.894	45.741	1.00	79.03	O
ATOM	514	CB	PRO C 976	-7.413	106.388	44.405	1.00	72.85	C
ATOM	515	CG	PRO C 976	-7.355	107.346	43.252	1.00	69.07	C
ATOM	516	CD	PRO C 976	-5.882	107.359	42.880	1.00	68.30	C
ATOM	517	N	ALA C 977	-6.082	105.823	47.421	1.00	80.66	N
ATOM	518	CA	ALA C 977	-5.611	104.827	48.381	1.00	80.60	C
ATOM	519	C	ALA C 977	-6.081	103.447	47.977	1.00	79.40	C
ATOM	520	O	ALA C 977	-5.274	102.504	47.939	1.00	78.47	O
ATOM	521	CB	ALA C 977	-6.120	105.152	49.803	1.00	79.02	C
ATOM	522	N	SER C 978	-7.378	103.357	47.658	1.00	77.53	N
ATOM	523	CA	SER C 978	-8.031	102.094	47.311	1.00	79.82	C
ATOM	524	C	SER C 978	-7.295	101.299	46.265	1.00	83.07	C
ATOM	525	O	SER C 978	-7.200	100.076	46.359	1.00	88.50	O
ATOM	526	CB	SER C 978	-9.484	102.323	46.851	1.00	77.34	C
ATOM	527	OG	SER C 978	-9.563	102.906	45.566	1.00	79.95	O



ATOM	528	N	THR	C	979	-6.742	101.997	45.285	1.00	82.72	N
ATOM	529	CA	THR	C	979	-6.036	101.333	44.206	1.00	77.91	C
ATOM	530	C	THR	C	979	-4.576	100.906	44.454	1.00	78.02	C
ATOM	531	O	THR	C	979	-3.975	100.280	43.582	1.00	79.71	O
ATOM	532	CB	THR	C	979	-6.049	102.220	42.970	1.00	74.94	C
ATOM	533	CG2	THR	C	979	-7.463	102.693	42.648	1.00	62.47	C
ATOM	534	OG1	THR	C	979	-5.230	103.361	43.230	1.00	75.64	O
ATOM	535	N	HIS	C	980	-3.995	101.207	45.610	1.00	77.48	N
ATOM	536	CA	HIS	C	980	-2.596	100.836	45.805	1.00	79.32	C
ATOM	537	C	HIS	C	980	-2.347	99.360	45.884	1.00	78.62	C
ATOM	538	O	HIS	C	980	-1.223	98.914	45.667	1.00	76.26	O
ATOM	539	CB	HIS	C	980	-2.002	101.472	47.063	1.00	82.98	C
ATOM	540	CG	HIS	C	980	-1.892	102.959	46.997	1.00	84.15	C
ATOM	541	CD2	HIS	C	980	-2.532	103.867	46.227	1.00	85.49	C
ATOM	542	ND1	HIS	C	980	-1.043	103.678	47.815	1.00	85.84	N
ATOM	543	CE1	HIS	C	980	-1.170	104.960	47.550	1.00	89.89	C
ATOM	544	NE2	HIS	C	980	-2.067	105.111	46.591	1.00	88.60	N
ATOM	545	N	ARG	C	981	-3.393	98.604	46.194	1.00	80.21	N
ATOM	546	CA	ARG	C	981	-3.273	97.156	46.350	1.00	83.54	C
ATOM	547	C	ARG	C	981	-3.079	96.385	45.028	1.00	81.92	C
ATOM	548	O	ARG	C	981	-2.167	95.556	44.928	1.00	82.24	O
ATOM	549	CB	ARG	C	981	-4.497	96.638	47.135	1.00	85.47	C
ATOM	550	CG	ARG	C	981	-4.421	95.184	47.647	1.00	84.60	C
ATOM	551	CD	ARG	C	981	-3.350	94.950	48.715	1.00	81.06	C
ATOM	552	NE	ARG	C	981	-3.156	93.514	48.938	1.00	83.61	N
ATOM	553	CZ	ARG	C	981	-2.444	92.979	49.927	1.00	82.35	C
ATOM	554	NH1	ARG	C	981	-1.841	93.759	50.811	1.00	80.71	
N1+											
ATOM	555	NH2	ARG	C	981	-2.345	91.657	50.034	1.00	79.63	N
ATOM	556	N	GLU	C	982	-3.914	96.656	44.022	1.00	80.43	N
ATOM	557	CA	GLU	C	982	-3.786	95.974	42.731	1.00	79.47	C
ATOM	558	C	GLU	C	982	-2.404	96.311	42.154	1.00	76.02	C
ATOM	559	O	GLU	C	982	-1.742	95.468	41.549	1.00	71.51	O
ATOM	560	CB	GLU	C	982	-4.898	96.413	41.748	1.00	80.96	C
ATOM	561	CG	GLU	C	982	-5.503	95.242	40.900	1.00	92.71	C
ATOM	562	CD	GLU	C	982	-6.581	95.659	39.837	1.00	100.52	C
ATOM	563	OE1	GLU	C	982	-7.568	96.362	40.206	1.00	102.24	O
ATOM	564	OE2	GLU	C	982	-6.445	95.262	38.642	1.00	95.96	
O1-											

ATOM	565	N	ILE	C	983	-1.949	97.532	42.392	1.00	70.78	N
ATOM	566	CA	ILE	C	983	-0.664	97.950	41.858	1.00	72.18	C
ATOM	567	C	ILE	C	983	0.518	97.342	42.579	1.00	74.15	C
ATOM	568	O	ILE	C	983	1.570	97.112	41.982	1.00	77.23	O
ATOM	569	CB	ILE	C	983	-0.499	99.493	41.882	1.00	70.97	C
ATOM	570	CG1	ILE	C	983	-1.659	100.156	41.129	1.00	66.21	C
ATOM	571	CG2	ILE	C	983	0.847	99.874	41.255	1.00	64.06	C
ATOM	572	CD1	ILE	C	983	-1.696	101.652	41.230	1.00	60.12	C
ATOM	573	N	GLU	C	984	0.365	97.091	43.868	1.00	77.02	N
ATOM	574	CA	GLU	C	984	1.468	96.517	44.618	1.00	79.38	C
ATOM	575	C	GLU	C	984	1.536	95.055	44.225	1.00	77.09	C
ATOM	576	O	GLU	C	984	2.611	94.471	44.090	1.00	74.08	O
ATOM	577	CB	GLU	C	984	1.222	96.681	46.119	1.00	88.11	C
ATOM	578	CG	GLU	C	984	2.184	97.655	46.801	1.00	99.14	C
ATOM	579	CD	GLU	C	984	1.475	98.580	47.793	1.00	109.11	C
ATOM	580	OE1	GLU	C	984	0.546	98.103	48.497	1.00	115.25	O
ATOM	581	OE2	GLU	C	984	1.856	99.777	47.871	1.00	110.47	
O1-											
ATOM	582	N	MET	C	985	0.361	94.481	44.016	1.00	73.92	N
ATOM	583	CA	MET	C	985	0.245	93.099	43.614	1.00	70.59	C
ATOM	584	C	MET	C	985	0.861	92.887	42.213	1.00	69.46	C
ATOM	585	O	MET	C	985	1.607	91.926	42.001	1.00	66.72	O
ATOM	586	CB	MET	C	985	-1.233	92.703	43.675	1.00	72.71	C
ATOM	587	CG	MET	C	985	-1.492	91.613	44.708	1.00	80.42	C
ATOM	588	SD	MET	C	985	-0.766	91.853	46.390	1.00	85.30	S
ATOM	589	CE	MET	C	985	1.105	91.464	46.198	1.00	82.08	C
ATOM	590	N	ALA	C	986	0.546	93.791	41.273	1.00	69.08	N
ATOM	591	CA	ALA	C	986	1.086	93.766	39.907	1.00	61.06	C
ATOM	592	C	ALA	C	986	2.615	93.820	39.977	1.00	61.60	C
ATOM	593	O	ALA	C	986	3.303	93.201	39.182	1.00	60.41	O
ATOM	594	CB	ALA	C	986	0.572	94.944	39.135	1.00	52.88	C
ATOM	595	N	GLN	C	987	3.150	94.579	40.923	1.00	64.40	N
ATOM	596	CA	GLN	C	987	4.599	94.650	41.083	1.00	69.94	C
ATOM	597	C	GLN	C	987	5.205	93.350	41.620	1.00	74.21	C
ATOM	598	O	GLN	C	987	6.300	92.942	41.218	1.00	74.81	O
ATOM	599	CB	GLN	C	987	4.983	95.727	42.075	1.00	73.29	C
ATOM	600	CG	GLN	C	987	4.787	97.131	41.646	1.00	74.46	C
ATOM	601	CD	GLN	C	987	5.230	98.082	42.734	1.00	74.15	C
ATOM	602	NE2	GLN	C	987	6.511	98.466	42.700	1.00	69.51	N

ATOM	603	OE1	GLN	C	987	4.443	98.447	43.616	1.00	71.07	O
ATOM	604	N	LYS	C	988	4.530	92.725	42.579	1.00	75.72	N
ATOM	605	CA	LYS	C	988	5.067	91.498	43.139	1.00	76.85	C
ATOM	606	C	LYS	C	988	5.101	90.456	42.035	1.00	74.61	C
ATOM	607	O	LYS	C	988	6.022	89.629	41.960	1.00	75.89	O
ATOM	608	CB	LYS	C	988	4.220	91.014	44.326	1.00	83.11	C
ATOM	609	CG	LYS	C	988	4.609	89.609	44.824	1.00	93.91	C
ATOM	610	CD	LYS	C	988	6.140	89.444	45.039	1.00	98.59	C
ATOM	611	CE	LYS	C	988	6.550	87.970	45.192	1.00	96.94	C
ATOM	612	NZ	LYS	C	988	7.178	87.683	46.513	1.00	101.06	
N1+											
ATOM	613	N	LEU	C	989	4.100	90.506	41.167	1.00	67.38	N
ATOM	614	CA	LEU	C	989	4.039	89.571	40.066	1.00	63.95	C
ATOM	615	C	LEU	C	989	5.287	89.710	39.200	1.00	63.62	C
ATOM	616	O	LEU	C	989	5.862	88.713	38.787	1.00	63.80	O
ATOM	617	CB	LEU	C	989	2.782	89.822	39.246	1.00	60.47	C
ATOM	618	CG	LEU	C	989	2.464	88.855	38.113	1.00	57.38	C
ATOM	619	CD1	LEU	C	989	2.515	87.434	38.615	1.00	56.34	C
ATOM	620	CD2	LEU	C	989	1.091	89.182	37.565	1.00	54.02	C
ATOM	621	N	LEU	C	990	5.711	90.940	38.928	1.00	63.58	N
ATOM	622	CA	LEU	C	990	6.906	91.159	38.119	1.00	63.56	C
ATOM	623	C	LEU	C	990	8.165	90.600	38.784	1.00	64.92	C
ATOM	624	O	LEU	C	990	9.055	90.093	38.096	1.00	62.19	O
ATOM	625	CB	LEU	C	990	7.084	92.645	37.830	1.00	61.74	C
ATOM	626	CG	LEU	C	990	6.074	93.214	36.848	1.00	60.69	C
ATOM	627	CD1	LEU	C	990	6.124	94.706	36.887	1.00	60.66	C
ATOM	628	CD2	LEU	C	990	6.384	92.706	35.467	1.00	63.00	C
ATOM	629	N	ASN	C	991	8.238	90.707	40.111	1.00	67.78	N
ATOM	630	CA	ASN	C	991	9.373	90.189	40.880	1.00	73.14	C
ATOM	631	C	ASN	C	991	9.567	88.705	40.638	1.00	73.68	C
ATOM	632	O	ASN	C	991	10.670	88.249	40.299	1.00	74.98	O
ATOM	633	CB	ASN	C	991	9.158	90.403	42.380	1.00	78.47	C
ATOM	634	CG	ASN	C	991	9.744	91.706	42.865	1.00	84.33	C
ATOM	635	ND2	ASN	C	991	8.906	92.539	43.479	1.00	87.31	N
ATOM	636	OD1	ASN	C	991	10.947	91.965	42.695	1.00	84.79	O
ATOM	637	N	SER	C	992	8.486	87.952	40.832	1.00	74.02	N
ATOM	638	CA	SER	C	992	8.518	86.516	40.634	1.00	72.44	C
ATOM	639	C	SER	C	992	8.788	86.152	39.168	1.00	70.80	C
ATOM	640	O	SER	C	992	9.392	85.115	38.911	1.00	71.78	O

ATOM	641	CB	SER C 992	7.216	85.887	41.120	1.00	68.96	C
ATOM	642	OG	SER C 992	6.140	86.325	40.325	1.00	75.27	O
ATOM	643	N	ASP C 993	8.359	86.984	38.213	1.00	71.52	N
ATOM	644	CA	ASP C 993	8.626	86.706	36.793	1.00	72.93	C
ATOM	645	C	ASP C 993	10.134	86.756	36.544	1.00	75.63	C
ATOM	646	O	ASP C 993	10.654	86.008	35.705	1.00	78.90	O
ATOM	647	CB	ASP C 993	7.941	87.725	35.871	1.00	71.56	C
ATOM	648	CG	ASP C 993	6.431	87.555	35.824	1.00	77.47	C
ATOM	649	OD1	ASP C 993	5.900	86.632	36.481	1.00	82.03	O
ATOM	650	OD2	ASP C 993	5.768	88.348	35.125	1.00	81.94	
O1-									
ATOM	651	N	LEU C 994	10.823	87.653	37.259	1.00	74.25	N
ATOM	652	CA	LEU C 994	12.268	87.804	37.142	1.00	73.89	C
ATOM	653	C	LEU C 994	12.936	86.630	37.832	1.00	77.39	C
ATOM	654	O	LEU C 994	14.002	86.163	37.408	1.00	77.56	O
ATOM	655	CB	LEU C 994	12.743	89.084	37.805	1.00	73.64	C
ATOM	656	CG	LEU C 994	14.220	89.291	37.510	1.00	71.58	C
ATOM	657	CD1	LEU C 994	14.368	89.691	36.055	1.00	71.16	C
ATOM	658	CD2	LEU C 994	14.777	90.357	38.418	1.00	74.31	C
ATOM	659	N	GLY C 995	12.322	86.184	38.924	1.00	77.11	N
ATOM	660	CA	GLY C 995	12.842	85.034	39.630	1.00	76.87	C
ATOM	661	C	GLY C 995	12.807	83.852	38.671	1.00	76.99	C
ATOM	662	O	GLY C 995	13.779	83.106	38.601	1.00	79.72	O
ATOM	663	N	GLU C 996	11.710	83.681	37.926	1.00	74.12	N
ATOM	664	CA	GLU C 996	11.604	82.574	36.970	1.00	75.44	C
ATOM	665	C	GLU C 996	12.772	82.677	35.997	1.00	75.09	C
ATOM	666	O	GLU C 996	13.544	81.740	35.846	1.00	73.31	O
ATOM	667	CB	GLU C 996	10.274	82.632	36.199	1.00	73.95	C
ATOM	668	CG	GLU C 996	9.818	81.301	35.556	1.00	73.82	C
ATOM	669	CD	GLU C 996	8.433	81.395	34.888	1.00	77.98	C
ATOM	670	OE1	GLU C 996	7.448	81.779	35.563	1.00	75.02	O
ATOM	671	OE2	GLU C 996	8.325	81.077	33.680	1.00	77.06	
O1-									
ATOM	672	N	LEU C 997	12.903	83.835	35.358	1.00	78.06	N
ATOM	673	CA	LEU C 997	13.975	84.087	34.404	1.00	78.32	C
ATOM	674	C	LEU C 997	15.374	83.765	34.937	1.00	78.80	C
ATOM	675	O	LEU C 997	16.201	83.205	34.217	1.00	77.85	O
ATOM	676	CB	LEU C 997	13.936	85.542	33.958	1.00	77.28	C
ATOM	677	CG	LEU C 997	15.135	85.949	33.111	1.00	76.64	C

ATOM	678	CD1	LEU	C	997	15.128	85.187	31.794	1.00	73.66	C
ATOM	679	CD2	LEU	C	997	15.080	87.437	32.882	1.00	75.03	C
ATOM	680	N	ILE	C	998	15.641	84.120	36.189	1.00	77.25	N
ATOM	681	CA	ILE	C	998	16.947	83.856	36.778	1.00	80.31	C
ATOM	682	C	ILE	C	998	17.186	82.371	37.048	1.00	83.04	C
ATOM	683	O	ILE	C	998	18.311	81.881	36.886	1.00	84.10	O
ATOM	684	CB	ILE	C	998	17.140	84.687	38.064	1.00	79.40	C
ATOM	685	CG1	ILE	C	998	17.338	86.155	37.670	1.00	82.60	C
ATOM	686	CG2	ILE	C	998	18.340	84.181	38.859	1.00	77.20	C
ATOM	687	CD1	ILE	C	998	16.937	87.149	38.742	1.00	82.48	C
ATOM	688	N	ASN	C	999	16.130	81.663	37.448	1.00	83.79	N
ATOM	689	CA	ASN	C	999	16.215	80.231	37.715	1.00	80.31	C
ATOM	690	C	ASN	C	999	16.506	79.513	36.407	1.00	80.21	C
ATOM	691	O	ASN	C	999	17.221	78.514	36.394	1.00	79.90	O
ATOM	692	CB	ASN	C	999	14.897	79.681	38.276	1.00	81.63	C
ATOM	693	CG	ASN	C	999	14.604	80.160	39.685	1.00	83.96	C
ATOM	694	ND2	ASN	C	999	13.329	80.125	40.071	1.00	82.73	N
ATOM	695	OD1	ASN	C	999	15.513	80.536	40.426	1.00	87.64	O
ATOM	696	N	LYS	C1000		15.939	80.012	35.310	1.00	79.78	N
ATOM	697	CA	LYS	C1000		16.156	79.384	34.018	1.00	82.69	C
ATOM	698	C	LYS	C1000		17.539	79.701	33.523	1.00	87.29	C
ATOM	699	O	LYS	C1000		18.087	78.965	32.713	1.00	91.27	O
ATOM	700	CB	LYS	C1000		15.121	79.835	32.986	1.00	81.29	C
ATOM	701	CG	LYS	C1000		13.688	79.470	33.362	1.00	83.64	C
ATOM	702	CD	LYS	C1000		13.614	78.121	34.082	1.00	82.20	C
ATOM	703	CE	LYS	C1000		12.198	77.667	34.392	1.00	78.59	C
ATOM	704	NZ	LYS	C1000		12.266	76.569	35.393	1.00	79.19	
N1+											
ATOM	705	N	MET	C1001		18.111	80.801	34.001	1.00	90.75	N
ATOM	706	CA	MET	C1001		19.462	81.159	33.594	1.00	90.87	C
ATOM	707	C	MET	C1001		20.436	80.267	34.379	1.00	90.41	C
ATOM	708	O	MET	C1001		21.204	79.502	33.786	1.00	86.93	O
ATOM	709	CB	MET	C1001		19.746	82.633	33.887	1.00	91.75	C
ATOM	710	CG	MET	C1001		21.171	83.040	33.555	1.00	96.80	C
ATOM	711	SD	MET	C1001		21.772	84.462	34.507	1.00	104.71	S
ATOM	712	CE	MET	C1001		22.116	83.736	36.195	1.00	102.20	C
ATOM	713	N	LYS	C1002		20.397	80.370	35.709	1.00	87.99	N
ATOM	714	CA	LYS	C1002		21.254	79.563	36.573	1.00	89.70	C
ATOM	715	C	LYS	C1002		21.318	78.115	36.066	1.00	92.93	C

ATOM	716	O	LYS C1002	22.354	77.457	36.171	1.00	96.73	O
ATOM	717	CB	LYS C1002	20.728	79.572	38.015	1.00	87.91	C
ATOM	718	CG	LYS C1002	21.259	80.674	38.936	1.00	88.01	C
ATOM	719	CD	LYS C1002	20.895	80.339	40.397	1.00	93.03	C
ATOM	720	CE	LYS C1002	21.721	81.109	41.441	1.00	97.29	C
ATOM	721	NZ	LYS C1002	21.562	82.593	41.386	1.00	99.06	
N1+									
ATOM	722	N	LEU C1003	20.206	77.622	35.522	1.00	95.37	N
ATOM	723	CA	LEU C1003	20.147	76.259	34.994	1.00	96.66	C
ATOM	724	C	LEU C1003	20.899	76.139	33.678	1.00	98.82	C
ATOM	725	O	LEU C1003	21.751	75.275	33.542	1.00	101.68	O
ATOM	726	CB	LEU C1003	18.698	75.791	34.775	1.00	95.97	C
ATOM	727	CG	LEU C1003	17.827	75.312	35.947	1.00	93.54	C
ATOM	728	CD1	LEU C1003	16.393	75.124	35.463	1.00	86.75	C
ATOM	729	CD2	LEU C1003	18.380	74.017	36.524	1.00	89.52	C
ATOM	730	N	ALA C1004	20.595	76.992	32.705	1.00	100.95	N
ATOM	731	CA	ALA C1004	21.287	76.907	31.416	1.00	103.86	C
ATOM	732	C	ALA C1004	22.817	77.076	31.577	1.00	105.77	C
ATOM	733	O	ALA C1004	23.599	76.756	30.667	1.00	106.40	O
ATOM	734	CB	ALA C1004	20.717	77.949	30.448	1.00	99.99	C
ATOM	735	N	GLN C1005	23.230	77.565	32.746	1.00	104.01	N
ATOM	736	CA	GLN C1005	24.641	77.766	33.051	1.00	101.96	C
ATOM	737	C	GLN C1005	25.242	76.479	33.553	1.00	101.55	C
ATOM	738	O	GLN C1005	26.385	76.148	33.251	1.00	103.75	O
ATOM	739	CB	GLN C1005	24.813	78.829	34.124	1.00	101.05	C
ATOM	740	CG	GLN C1005	24.698	80.210	33.593	1.00	104.56	C
ATOM	741	CD	GLN C1005	25.625	81.136	34.306	1.00	106.03	C
ATOM	742	NE2	GLN C1005	26.756	81.434	33.674	1.00	106.95	N
ATOM	743	OE1	GLN C1005	25.346	81.575	35.425	1.00	107.39	O
ATOM	744	N	GLN C1006	24.458	75.772	34.349	1.00	98.97	N
ATOM	745	CA	GLN C1006	24.866	74.510	34.917	1.00	96.86	C
ATOM	746	C	GLN C1006	24.851	73.431	33.834	1.00	96.20	C
ATOM	747	O	GLN C1006	25.409	72.350	34.030	1.00	96.22	O
ATOM	748	CB	GLN C1006	23.912	74.172	36.063	1.00	97.68	C
ATOM	749	CG	GLN C1006	24.048	72.801	36.671	1.00	102.93	C
ATOM	750	CD	GLN C1006	23.163	72.647	37.901	1.00	107.56	C
ATOM	751	NE2	GLN C1006	23.495	71.685	38.754	1.00	109.99	N
ATOM	752	OE1	GLN C1006	22.186	73.382	38.076	1.00	110.02	O
ATOM	753	N	TYR C1007	24.228	73.730	32.693	1.00	96.63	N

ATOM	754	CA	TYR	C1007	24.142	72.762	31.599	1.00101.98	C
ATOM	755	C	TYR	C1007	24.628	73.311	30.265	1.00106.08	C
ATOM	756	O	TYR	C1007	23.866	73.388	29.297	1.00105.01	O
ATOM	757	CB	TYR	C1007	22.700	72.226	31.454	1.00102.62	C
ATOM	758	CG	TYR	C1007	22.205	71.480	32.678	1.00100.68	C
ATOM	759	CD1	TYR	C1007	21.822	72.170	33.824	1.00100.14	C
ATOM	760	CD2	TYR	C1007	22.223	70.087	32.729	1.00 99.33	C
ATOM	761	CE1	TYR	C1007	21.485	71.504	34.990	1.00 98.40	C
ATOM	762	CE2	TYR	C1007	21.887	69.408	33.900	1.00 99.82	C
ATOM	763	CZ	TYR	C1007	21.521	70.127	35.027	1.00 99.31	C
ATOM	764	OH	TYR	C1007	21.209	69.483	36.204	1.00 97.57	O
ATOM	765	N	VAL	C1008	25.908	73.689	30.226	1.00112.40	N
ATOM	766	CA	VAL	C1008	26.529	74.230	29.009	1.00115.62	C
ATOM	767	C	VAL	C1008	27.091	73.120	28.101	1.00118.68	C
ATOM	768	O	VAL	C1008	27.695	72.137	28.578	1.00117.20	O
ATOM	769	CB	VAL	C1008	27.686	75.220	29.327	1.00113.43	C
ATOM	770	CG1	VAL	C1008	27.885	76.188	28.144	1.00111.71	C
ATOM	771	CG2	VAL	C1008	27.398	75.965	30.605	1.00110.31	C
ATOM	772	N	MET	C1009	26.904	73.311	26.792	1.00119.55	N
ATOM	773	CA	MET	C1009	27.340	72.355	25.773	1.00120.49	C
ATOM	774	C	MET	C1009	26.614	71.033	26.043	1.00119.74	C
ATOM	775	O	MET	C1009	27.248	69.978	26.202	1.00119.45	O
ATOM	776	CB	MET	C1009	28.865	72.122	25.825	1.00122.89	C
ATOM	777	CG	MET	C1009	29.740	73.355	25.576	1.00121.78	C
ATOM	778	SD	MET	C1009	31.003	73.589	26.868	1.00126.30	S
ATOM	779	CE	MET	C1009	31.538	71.843	27.253	1.00121.09	C
ATOM	780	N	THR	C1010	25.283	71.103	26.109	1.00117.79	N
ATOM	781	CA	THR	C1010	24.447	69.925	26.363	1.00112.34	C
ATOM	782	C	THR	C1010	23.162	70.041	25.546	1.00109.06	C
ATOM	783	O	THR	C1010	22.902	71.063	24.904	1.00107.42	O
ATOM	784	CB	THR	C1010	24.040	69.810	27.873	1.00110.10	C
ATOM	785	CG2	THR	C1010	23.531	68.420	28.191	1.00110.33	C
ATOM	786	OG1	THR	C1010	25.175	70.047	28.712	1.00105.49	O
ATOM	787	N	SER	C1011	22.369	68.980	25.563	1.00106.23	N
ATOM	788	CA	SER	C1011	21.088	68.985	24.876	1.00106.87	C
ATOM	789	C	SER	C1011	20.139	69.820	25.756	1.00107.19	C
ATOM	790	O	SER	C1011	19.082	70.297	25.308	1.00102.61	O
ATOM	791	CB	SER	C1011	20.578	67.549	24.762	1.00107.83	C
ATOM	792	OG	SER	C1011	20.787	66.826	25.974	1.00104.56	O

ATOM	793	N	LEU	C1012	20.543	69.982	27.020	1.00107.60	N
ATOM	794	CA	LEU	C1012	19.753	70.719	28.003	1.00107.90	C
ATOM	795	C	LEU	C1012	19.973	72.207	27.945	1.00109.30	C
ATOM	796	O	LEU	C1012	19.075	72.984	28.287	1.00110.31	O
ATOM	797	CB	LEU	C1012	20.015	70.220	29.438	1.00104.23	C
ATOM	798	CG	LEU	C1012	19.319	68.895	29.812	1.00103.41	C
ATOM	799	CD1	LEU	C1012	19.096	68.867	31.327	1.00 99.74	C
ATOM	800	CD2	LEU	C1012	17.969	68.739	29.062	1.00 97.65	C
ATOM	801	N	GLN	C1013	21.164	72.600	27.505	1.00110.00	N
ATOM	802	CA	GLN	C1013	21.506	74.009	27.394	1.00108.04	C
ATOM	803	C	GLN	C1013	20.532	74.741	26.469	1.00104.48	C
ATOM	804	O	GLN	C1013	20.138	75.874	26.739	1.00103.94	O
ATOM	805	CB	GLN	C1013	22.928	74.158	26.862	1.00110.51	C
ATOM	806	CG	GLN	C1013	23.373	75.603	26.716	1.00113.77	C
ATOM	807	CD	GLN	C1013	24.452	75.747	25.670	1.00113.99	C
ATOM	808	NE2	GLN	C1013	24.084	76.308	24.522	1.00112.15	N
ATOM	809	OE1	GLN	C1013	25.600	75.339	25.876	1.00113.81	O
ATOM	810	N	GLN	C1014	20.157	74.098	25.371	1.00102.14	N
ATOM	811	CA	GLN	C1014	19.235	74.718	24.440	1.00100.91	C
ATOM	812	C	GLN	C1014	17.838	74.778	25.043	1.00102.05	C
ATOM	813	O	GLN	C1014	17.068	75.682	24.723	1.00104.42	O
ATOM	814	CB	GLN	C1014	19.194	73.944	23.119	1.00102.30	C
ATOM	815	CG	GLN	C1014	18.388	74.634	22.009	1.00110.82	C
ATOM	816	CD	GLN	C1014	16.952	74.110	21.851	1.00115.56	C
ATOM	817	NE2	GLN	C1014	16.046	74.585	22.709	1.00115.52	N
ATOM	818	OE1	GLN	C1014	16.667	73.288	20.966	1.00116.95	O
ATOM	819	N	GLU	C1015	17.510	73.830	25.926	1.00100.51	N
ATOM	820	CA	GLU	C1015	16.178	73.788	26.534	1.00 95.53	C
ATOM	821	C	GLU	C1015	15.959	74.945	27.489	1.00 90.60	C
ATOM	822	O	GLU	C1015	15.087	75.788	27.249	1.00 84.83	O
ATOM	823	CB	GLU	C1015	15.948	72.449	27.250	1.00 97.24	C
ATOM	824	CG	GLU	C1015	14.516	72.235	27.763	1.00101.85	C
ATOM	825	CD	GLU	C1015	13.407	72.502	26.710	1.00104.25	C
ATOM	826	OE1	GLU	C1015	13.570	72.137	25.521	1.00100.17	O
ATOM	827	OE2	GLU	C1015	12.350	73.065	27.091	1.00103.74	
O1-									
ATOM	828	N	TYR	C1016	16.768	74.996	28.544	1.00 86.99	N
ATOM	829	CA	TYR	C1016	16.673	76.060	29.532	1.00 90.23	C
ATOM	830	C	TYR	C1016	16.819	77.464	28.935	1.00 91.23	C



ATOM	831	O	TYR C1016	16.740	78.461	29.666	1.00	91.81	O
ATOM	832	CB	TYR C1016	17.702	75.847	30.649	1.00	92.03	C
ATOM	833	CG	TYR C1016	17.413	74.621	31.485	1.00	96.31	C
ATOM	834	CD1	TYR C1016	16.145	74.410	32.027	1.00	95.33	C
ATOM	835	CD2	TYR C1016	18.383	73.639	31.681	1.00	99.21	C
ATOM	836	CE1	TYR C1016	15.844	73.247	32.736	1.00	97.48	C
ATOM	837	CE2	TYR C1016	18.090	72.467	32.394	1.00	98.50	C
ATOM	838	CZ	TYR C1016	16.817	72.282	32.915	1.00	96.64	C
ATOM	839	OH	TYR C1016	16.513	71.138	33.617	1.00	95.40	O
ATOM	840	N	LYS C1017	17.041	77.543	27.622	1.00	90.88	N
ATOM	841	CA	LYS C1017	17.140	78.835	26.949	1.00	89.24	C
ATOM	842	C	LYS C1017	15.755	79.157	26.417	1.00	85.90	C
ATOM	843	O	LYS C1017	15.328	80.314	26.415	1.00	82.40	O
ATOM	844	CB	LYS C1017	18.142	78.810	25.787	1.00	93.74	C
ATOM	845	CG	LYS C1017	19.596	79.054	26.190	1.00	96.49	C
ATOM	846	CD	LYS C1017	20.433	79.517	24.996	1.00	96.88	C
ATOM	847	CE	LYS C1017	21.907	79.641	25.351	1.00	98.92	C
ATOM	848	NZ	LYS C1017	22.677	80.119	24.171	1.00	100.42	
N1+									
ATOM	849	N	LYS C1018	15.055	78.131	25.949	1.00	83.14	N
ATOM	850	CA	LYS C1018	13.708	78.342	25.457	1.00	87.47	C
ATOM	851	C	LYS C1018	12.835	78.752	26.640	1.00	87.65	C
ATOM	852	O	LYS C1018	11.830	79.466	26.483	1.00	84.27	O
ATOM	853	CB	LYS C1018	13.169	77.070	24.822	1.00	89.97	C
ATOM	854	CG	LYS C1018	13.613	76.895	23.399	1.00	96.20	C
ATOM	855	CD	LYS C1018	12.885	75.739	22.745	1.00	103.28	C
ATOM	856	CE	LYS C1018	13.303	75.560	21.291	1.00	104.51	C
ATOM	857	NZ	LYS C1018	12.940	74.192	20.792	1.00	103.98	
N1+									
ATOM	858	N	GLN C1019	13.241	78.285	27.822	1.00	85.24	N
ATOM	859	CA	GLN C1019	12.546	78.585	29.061	1.00	80.75	C
ATOM	860	C	GLN C1019	12.922	79.979	29.522	1.00	82.79	C
ATOM	861	O	GLN C1019	12.105	80.666	30.135	1.00	86.11	O
ATOM	862	CB	GLN C1019	12.873	77.535	30.125	1.00	74.33	C
ATOM	863	CG	GLN C1019	12.050	76.272	29.950	1.00	72.25	C
ATOM	864	CD	GLN C1019	12.450	75.178	30.917	1.00	73.41	C
ATOM	865	NE2	GLN C1019	12.486	73.935	30.434	1.00	77.00	N
ATOM	866	OE1	GLN C1019	12.715	75.442	32.088	1.00	72.63	O
ATOM	867	N	MET C1020	14.154	80.399	29.236	1.00	85.11	N

ATOM	868	CA	MET	C1020	14.577	81.749	29.591	1.00	84.66	C
ATOM	869	C	MET	C1020	13.717	82.684	28.746	1.00	83.25	C
ATOM	870	O	MET	C1020	13.164	83.656	29.247	1.00	83.62	O
ATOM	871	CB	MET	C1020	16.067	81.966	29.285	1.00	85.31	C
ATOM	872	CG	MET	C1020	16.959	81.858	30.524	1.00	90.41	C
ATOM	873	SD	MET	C1020	18.753	81.804	30.222	1.00	91.63	S
ATOM	874	CE	MET	C1020	19.239	83.527	30.360	1.00	88.91	C
ATOM	875	N	LEU	C1021	13.587	82.377	27.462	1.00	80.01	N
ATOM	876	CA	LEU	C1021	12.779	83.218	26.596	1.00	81.04	C
ATOM	877	C	LEU	C1021	11.353	83.338	27.097	1.00	81.68	C
ATOM	878	O	LEU	C1021	10.759	84.411	27.065	1.00	80.93	O
ATOM	879	CB	LEU	C1021	12.737	82.661	25.179	1.00	84.04	C
ATOM	880	CG	LEU	C1021	13.983	82.688	24.301	1.00	83.49	C
ATOM	881	CD1	LEU	C1021	13.507	83.028	22.895	1.00	80.96	C
ATOM	882	CD2	LEU	C1021	14.998	83.724	24.779	1.00	80.98	C
ATOM	883	N	THR	C1022	10.811	82.207	27.531	1.00	84.90	N
ATOM	884	CA	THR	C1022	9.446	82.110	28.037	1.00	85.69	C
ATOM	885	C	THR	C1022	9.251	83.048	29.208	1.00	83.51	C
ATOM	886	O	THR	C1022	8.390	83.934	29.197	1.00	80.07	O
ATOM	887	CB	THR	C1022	9.154	80.637	28.469	1.00	88.46	C
ATOM	888	CG2	THR	C1022	8.259	80.570	29.712	1.00	90.20	C
ATOM	889	OG1	THR	C1022	8.543	79.941	27.374	1.00	91.00	O
ATOM	890	N	ALA	C1023	10.092	82.826	30.208	1.00	81.70	N
ATOM	891	CA	ALA	C1023	10.094	83.586	31.436	1.00	83.77	C
ATOM	892	C	ALA	C1023	10.250	85.077	31.213	1.00	85.16	C
ATOM	893	O	ALA	C1023	9.714	85.859	31.998	1.00	89.04	O
ATOM	894	CB	ALA	C1023	11.210	83.085	32.352	1.00	83.59	C
ATOM	895	N	ALA	C1024	10.980	85.470	30.163	1.00	81.68	N
ATOM	896	CA	ALA	C1024	11.214	86.887	29.875	1.00	75.41	C
ATOM	897	C	ALA	C1024	10.025	87.513	29.145	1.00	73.27	C
ATOM	898	O	ALA	C1024	9.701	88.680	29.359	1.00	72.93	O
ATOM	899	CB	ALA	C1024	12.501	87.061	29.070	1.00	65.77	C
ATOM	900	N	HIS	C1025	9.369	86.740	28.290	1.00	68.05	N
ATOM	901	CA	HIS	C1025	8.209	87.249	27.576	1.00	68.21	C
ATOM	902	C	HIS	C1025	7.117	87.527	28.621	1.00	69.52	C
ATOM	903	O	HIS	C1025	6.305	88.444	28.459	1.00	65.51	O
ATOM	904	CB	HIS	C1025	7.727	86.206	26.551	1.00	71.98	C
ATOM	905	CG	HIS	C1025	6.534	86.631	25.743	1.00	78.78	C
ATOM	906	CD2	HIS	C1025	6.449	87.173	24.501	1.00	83.90	C

ATOM	907	ND1	HIS	C1025	5.237	86.520	26.198	1.00	84.22	N
ATOM	908	CE1	HIS	C1025	4.406	86.975	25.277	1.00	87.90	C
ATOM	909	NE2	HIS	C1025	5.113	87.378	24.237	1.00	86.95	N
ATOM	910	N	ALA	C1026	7.119	86.732	29.696	1.00	68.89	N
ATOM	911	CA	ALA	C1026	6.127	86.843	30.766	1.00	66.22	C
ATOM	912	C	ALA	C1026	6.342	88.146	31.470	1.00	67.21	C
ATOM	913	O	ALA	C1026	5.411	88.917	31.693	1.00	70.82	O
ATOM	914	CB	ALA	C1026	6.289	85.720	31.729	1.00	59.99	C
ATOM	915	N	LEU	C1027	7.594	88.373	31.826	1.00	65.47	N
ATOM	916	CA	LEU	C1027	7.994	89.597	32.467	1.00	63.68	C
ATOM	917	C	LEU	C1027	7.507	90.779	31.624	1.00	64.67	C
ATOM	918	O	LEU	C1027	7.048	91.774	32.164	1.00	70.41	O
ATOM	919	CB	LEU	C1027	9.516	89.625	32.591	1.00	60.17	C
ATOM	920	CG	LEU	C1027	10.140	90.845	33.254	1.00	61.80	C
ATOM	921	CD1	LEU	C1027	9.381	91.159	34.512	1.00	64.53	C
ATOM	922	CD2	LEU	C1027	11.599	90.582	33.579	1.00	66.87	C
ATOM	923	N	ALA	C1028	7.577	90.669	30.302	1.00	62.81	N
ATOM	924	CA	ALA	C1028	7.152	91.773	29.448	1.00	63.80	C
ATOM	925	C	ALA	C1028	5.645	91.975	29.356	1.00	64.53	C
ATOM	926	O	ALA	C1028	5.173	93.107	29.348	1.00	63.07	O
ATOM	927	CB	ALA	C1028	7.717	91.600	28.068	1.00	62.94	C
ATOM	928	N	VAL	C1029	4.890	90.887	29.265	1.00	66.59	N
ATOM	929	CA	VAL	C1029	3.439	90.986	29.172	1.00	67.48	C
ATOM	930	C	VAL	C1029	2.884	91.582	30.461	1.00	67.97	C
ATOM	931	O	VAL	C1029	1.915	92.351	30.448	1.00	65.88	O
ATOM	932	CB	VAL	C1029	2.824	89.607	28.930	1.00	66.88	C
ATOM	933	CG1	VAL	C1029	1.330	89.730	28.727	1.00	63.81	C
ATOM	934	CG2	VAL	C1029	3.472	88.985	27.709	1.00	66.42	C
ATOM	935	N	ASP	C1030	3.521	91.222	31.570	1.00	65.23	N
ATOM	936	CA	ASP	C1030	3.126	91.712	32.880	1.00	64.94	C
ATOM	937	C	ASP	C1030	3.488	93.173	33.094	1.00	62.44	C
ATOM	938	O	ASP	C1030	2.701	93.927	33.658	1.00	64.35	O
ATOM	939	CB	ASP	C1030	3.735	90.839	33.992	1.00	65.96	C
ATOM	940	CG	ASP	C1030	2.911	89.578	34.255	1.00	69.57	C
ATOM	941	OD1	ASP	C1030	1.701	89.591	33.944	1.00	67.28	O
ATOM	942	OD2	ASP	C1030	3.454	88.585	34.783	1.00	71.94	
O1-										
ATOM	943	N	ALA	C1031	4.668	93.576	32.643	1.00	59.88	N
ATOM	944	CA	ALA	C1031	5.072	94.959	32.796	1.00	57.53	C

ATOM	945	C	ALA	C1031	4.022	95.837	32.109	1.00	59.49	C
ATOM	946	O	ALA	C1031	3.706	96.935	32.579	1.00	58.64	O
ATOM	947	CB	ALA	C1031	6.428	95.162	32.176	1.00	51.37	C
ATOM	948	N	LYS	C1032	3.470	95.345	31.002	1.00	59.00	N
ATOM	949	CA	LYS	C1032	2.466	96.094	30.270	1.00	57.05	C
ATOM	950	C	LYS	C1032	1.148	96.057	31.023	1.00	60.38	C
ATOM	951	O	LYS	C1032	0.296	96.936	30.854	1.00	57.03	O
ATOM	952	CB	LYS	C1032	2.309	95.513	28.862	1.00	56.79	C
ATOM	953	CG	LYS	C1032	3.458	95.897	27.918	1.00	62.37	C
ATOM	954	CD	LYS	C1032	3.612	94.970	26.703	1.00	68.50	C
ATOM	955	CE	LYS	C1032	2.945	95.535	25.447	1.00	72.18	C
ATOM	956	NZ	LYS	C1032	3.085	94.605	24.287	1.00	75.66	
N1+										
ATOM	957	N	ASN	C1033	0.971	95.031	31.855	1.00	63.06	N
ATOM	958	CA	ASN	C1033	-0.264	94.919	32.623	1.00	62.59	C
ATOM	959	C	ASN	C1033	-0.163	95.835	33.817	1.00	59.41	C
ATOM	960	O	ASN	C1033	-1.151	96.441	34.210	1.00	57.40	O
ATOM	961	CB	ASN	C1033	-0.530	93.471	33.044	1.00	64.82	C
ATOM	962	CG	ASN	C1033	-1.004	92.614	31.880	1.00	74.38	C
ATOM	963	ND2	ASN	C1033	-1.214	93.253	30.728	1.00	79.97	N
ATOM	964	OD1	ASN	C1033	-1.185	91.398	32.009	1.00	78.02	O
ATOM	965	N	LEU	C1034	1.039	95.945	34.375	1.00	56.92	N
ATOM	966	CA	LEU	C1034	1.276	96.829	35.495	1.00	55.84	C
ATOM	967	C	LEU	C1034	0.805	98.193	35.032	1.00	59.67	C
ATOM	968	O	LEU	C1034	-0.033	98.835	35.671	1.00	65.25	O
ATOM	969	CB	LEU	C1034	2.760	96.887	35.807	1.00	56.08	C
ATOM	970	CG	LEU	C1034	3.112	97.924	36.866	1.00	64.48	C
ATOM	971	CD1	LEU	C1034	2.306	97.609	38.101	1.00	67.21	C
ATOM	972	CD2	LEU	C1034	4.603	97.907	37.181	1.00	64.72	C
ATOM	973	N	LEU	C1035	1.357	98.626	33.903	1.00	58.09	N
ATOM	974	CA	LEU	C1035	1.020	99.901	33.296	1.00	55.87	C
ATOM	975	C	LEU	C1035	-0.486	100.027	33.167	1.00	51.30	C
ATOM	976	O	LEU	C1035	-1.049	101.029	33.547	1.00	48.73	O
ATOM	977	CB	LEU	C1035	1.658	99.996	31.916	1.00	58.28	C
ATOM	978	CG	LEU	C1035	1.914	101.349	31.273	1.00	59.39	C
ATOM	979	CD1	LEU	C1035	2.086	101.110	29.799	1.00	59.31	C
ATOM	980	CD2	LEU	C1035	0.767	102.299	31.500	1.00	62.27	C
ATOM	981	N	ASP	C1036	-1.143	99.014	32.622	1.00	53.83	N
ATOM	982	CA	ASP	C1036	-2.592	99.079	32.488	1.00	58.81	C

ATOM	983	C	ASP	C1036	-3.343	99.361	33.809	1.00	60.83	C
ATOM	984	O	ASP	C1036	-4.246	100.197	33.825	1.00	58.01	O
ATOM	985	CB	ASP	C1036	-3.127	97.802	31.862	1.00	63.90	C
ATOM	986	CG	ASP	C1036	-4.650	97.795	31.771	1.00	75.23	C
ATOM	987	OD1	ASP	C1036	-5.274	96.953	32.452	1.00	86.78	O
ATOM	988	OD2	ASP	C1036	-5.224	98.627	31.032	1.00	80.05	
O1-										
ATOM	989	N	VAL	C1037	-2.998	98.656	34.892	1.00	63.64	N
ATOM	990	CA	VAL	C1037	-3.616	98.860	36.209	1.00	63.82	C
ATOM	991	C	VAL	C1037	-3.492	100.351	36.588	1.00	65.23	C
ATOM	992	O	VAL	C1037	-4.497	101.060	36.788	1.00	68.35	O
ATOM	993	CB	VAL	C1037	-2.887	98.017	37.278	1.00	65.81	C
ATOM	994	CG1	VAL	C1037	-3.460	98.265	38.655	1.00	63.68	C
ATOM	995	CG2	VAL	C1037	-3.008	96.576	36.932	1.00	66.00	C
ATOM	996	N	ILE	C1038	-2.254	100.830	36.684	1.00	56.67	N
ATOM	997	CA	ILE	C1038	-1.988	102.232	37.008	1.00	52.09	C
ATOM	998	C	ILE	C1038	-2.795	103.253	36.154	1.00	56.52	C
ATOM	999	O	ILE	C1038	-3.207	104.319	36.643	1.00	61.00	O
ATOM	1000	CB	ILE	C1038	-0.506	102.495	36.857	1.00	40.92	C
ATOM	1001	CG1	ILE	C1038	0.251	101.813	37.991	1.00	40.83	C
ATOM	1002	CG2	ILE	C1038	-0.241	103.944	36.878	1.00	44.37	C
ATOM	1003	CD1	ILE	C1038	1.781	101.856	37.871	1.00	43.08	C
ATOM	1004	N	ASP	C1039	-3.016	102.951	34.880	1.00	58.87	N
ATOM	1005	CA	ASP	C1039	-3.788	103.863	34.044	1.00	63.24	C
ATOM	1006	C	ASP	C1039	-5.223	103.847	34.553	1.00	62.31	C
ATOM	1007	O	ASP	C1039	-5.846	104.903	34.639	1.00	61.21	O
ATOM	1008	CB	ASP	C1039	-3.712	103.478	32.540	1.00	64.64	C
ATOM	1009	CG	ASP	C1039	-2.406	103.983	31.850	1.00	70.50	C
ATOM	1010	OD1	ASP	C1039	-1.519	104.598	32.524	1.00	64.94	O
ATOM	1011	OD2	ASP	C1039	-2.283	103.749	30.621	1.00	73.26	
O1-										
ATOM	1012	N	GLN	C1040	-5.755	102.667	34.885	1.00	63.31	N
ATOM	1013	CA	GLN	C1040	-7.122	102.585	35.423	1.00	66.22	C
ATOM	1014	C	GLN	C1040	-7.111	103.430	36.720	1.00	65.53	C
ATOM	1015	O	GLN	C1040	-8.056	104.175	37.036	1.00	57.11	O
ATOM	1016	CB	GLN	C1040	-7.481	101.143	35.783	1.00	69.30	C
ATOM	1017	CG	GLN	C1040	-7.457	100.156	34.667	1.00	80.10	C
ATOM	1018	CD	GLN	C1040	-7.681	98.738	35.175	1.00	87.83	C
ATOM	1019	NE2	GLN	C1040	-6.715	97.844	34.925	1.00	91.51	N

ATOM	1020	OE1	GLN	C1040	-8.711	98.452	35.790	1.00	91.10	O
ATOM	1021	N	ALA	C1041	-6.022	103.283	37.469	1.00	62.66	N
ATOM	1022	CA	ALA	C1041	-5.853	104.025	38.698	1.00	62.47	C
ATOM	1023	C	ALA	C1041	-5.868	105.525	38.400	1.00	66.44	C
ATOM	1024	O	ALA	C1041	-6.569	106.275	39.088	1.00	69.97	O
ATOM	1025	CB	ALA	C1041	-4.539	103.635	39.384	1.00	59.49	C
ATOM	1026	N	ARG	C1042	-5.125	105.994	37.398	1.00	65.45	N
ATOM	1027	CA	ARG	C1042	-5.170	107.435	37.161	1.00	67.91	C
ATOM	1028	C	ARG	C1042	-6.545	107.875	36.667	1.00	68.21	C
ATOM	1029	O	ARG	C1042	-7.045	108.920	37.077	1.00	67.77	O
ATOM	1030	CB	ARG	C1042	-4.091	107.883	36.179	1.00	63.15	C
ATOM	1031	CG	ARG	C1042	-2.707	107.699	36.725	1.00	64.59	C
ATOM	1032	CD	ARG	C1042	-1.821	107.089	35.661	1.00	64.74	C
ATOM	1033	NE	ARG	C1042	-0.396	107.291	35.918	1.00	58.12	N
ATOM	1034	CZ	ARG	C1042	0.562	107.019	35.038	1.00	55.70	C
ATOM	1035	NH1	ARG	C1042	0.252	106.537	33.842	1.00	57.33	
N1+										
ATOM	1036	NH2	ARG	C1042	1.829	107.216	35.350	1.00	49.95	N
ATOM	1037	N	LEU	C1043	-7.161	107.079	35.801	1.00	68.03	N
ATOM	1038	CA	LEU	C1043	-8.468	107.436	35.285	1.00	73.06	C
ATOM	1039	C	LEU	C1043	-9.472	107.546	36.432	1.00	78.30	C
ATOM	1040	O	LEU	C1043	-10.299	108.463	36.451	1.00	77.88	O
ATOM	1041	CB	LEU	C1043	-8.927	106.404	34.246	1.00	69.68	C
ATOM	1042	CG	LEU	C1043	-8.057	106.338	32.978	1.00	69.22	C
ATOM	1043	CD1	LEU	C1043	-8.528	105.195	32.108	1.00	66.15	C
ATOM	1044	CD2	LEU	C1043	-8.101	107.653	32.205	1.00	62.85	C
ATOM	1045	N	LYS	C1044	-9.389	106.622	37.393	1.00	83.18	N
ATOM	1046	CA	LYS	C1044	-10.296	106.640	38.539	1.00	84.86	C
ATOM	1047	C	LYS	C1044	-10.144	107.999	39.194	1.00	85.31	C
ATOM	1048	O	LYS	C1044	-11.125	108.673	39.520	1.00	85.59	O
ATOM	1049	CB	LYS	C1044	-9.934	105.558	39.566	1.00	85.94	C
ATOM	1050	CG	LYS	C1044	-11.166	104.960	40.237	1.00	91.52	C
ATOM	1051	CD	LYS	C1044	-10.911	104.331	41.601	1.00	91.04	C
ATOM	1052	CE	LYS	C1044	-12.193	103.660	42.097	1.00	90.64	C
ATOM	1053	NZ	LYS	C1044	-12.051	103.064	43.449	1.00	91.14	
N1+										
ATOM	1054	N	MET	C1045	-8.795	108.526	39.447	1.00	0.00	N
ATOM	1055	CA	MET	C1045	-8.977	109.831	40.076	1.00	0.00	C
ATOM	1056	C	MET	C1045	-9.807	110.743	39.205	1.00	0.00	C

ATOM	1057	O	MET C1045	-9.606	110.845	37.985	1.00	0.00	O
ATOM	1058	CB	MET C1045	-7.592	110.466	40.382	1.00	0.00	C
ATOM	1059	CG	MET C1045	-6.702	109.693	41.379	1.00	0.00	C
ATOM	1060	SD	MET C1045	-5.283	110.701	41.838	1.00	0.00	S
ATOM	1061	CE	MET C1045	-4.298	109.426	42.635	1.00	0.00	C
ATOM	1062	H	MET C1045	-7.857	108.044	39.214	1.00	0.00	H
ATOM	1063	HA	MET C1045	-9.533	109.692	41.022	1.00	0.00	H
ATOM	1064	2HB	MET C1045	-7.739	111.487	40.784	1.00	0.00	H
ATOM	1065	3HB	MET C1045	-7.028	110.611	39.439	1.00	0.00	H
ATOM	1066	2HG	MET C1045	-6.348	108.751	40.919	1.00	0.00	H
ATOM	1067	3HG	MET C1045	-7.260	109.412	42.291	1.00	0.00	H
ATOM	1068	1HE	MET C1045	-4.864	108.940	43.450	1.00	0.00	H
ATOM	1069	2HE	MET C1045	-4.005	108.652	41.904	1.00	0.00	H
ATOM	1070	3HE	MET C1045	-3.377	109.860	43.063	1.00	0.00	H
ATOM	1071	N	LEU C1046	-10.884	111.532	39.820	1.00	0.00	N
ATOM	1072	CA	LEU C1046	-11.494	112.302	38.740	1.00	0.00	C
ATOM	1073	C	LEU C1046	-11.807	113.709	39.190	1.00	0.00	C
ATOM	1074	O	LEU C1046	-12.669	113.948	40.049	1.00	0.00	O
ATOM	1075	CB	LEU C1046	-12.774	111.589	38.217	1.00	0.00	C
ATOM	1076	CG	LEU C1046	-12.634	110.138	37.680	1.00	0.00	C
ATOM	1077	CD1	LEU C1046	-13.975	109.654	37.111	1.00	0.00	C
ATOM	1078	CD2	LEU C1046	-11.538	110.003	36.610	1.00	0.00	C
ATOM	1079	H	LEU C1046	-11.152	111.540	40.809	1.00	0.00	H
ATOM	1080	HA	LEU C1046	-10.761	112.395	37.919	1.00	0.00	H
ATOM	1081	2HB	LEU C1046	-13.221	112.212	37.418	1.00	0.00	H
ATOM	1082	3HB	LEU C1046	-13.533	111.585	39.024	1.00	0.00	H
ATOM	1083	HG	LEU C1046	-12.368	109.479	38.533	1.00	0.00	H
ATOM	1084	1HD1	LEU C1046	-14.782	109.696	37.867	1.00	0.00	H
ATOM	1085	2HD1	LEU C1046	-14.306	110.260	36.246	1.00	0.00	H
ATOM	1086	3HD1	LEU C1046	-13.917	108.604	36.770	1.00	0.00	H
ATOM	1087	1HD2	LEU C1046	-11.696	110.691	35.760	1.00	0.00	H
ATOM	1088	2HD2	LEU C1046	-10.538	110.223	37.030	1.00	0.00	H
ATOM	1089	3HD2	LEU C1046	-11.479	108.976	36.205	1.00	0.00	H
ATOM	1090	N	GLY C1047	-11.068	114.829	38.591	1.00	0.00	N
ATOM	1091	CA	GLY C1047	-11.584	116.042	39.218	1.00	0.00	C
ATOM	1092	C	GLY C1047	-12.201	116.961	38.191	1.00	0.00	C
ATOM	1093	O	GLY C1047	-13.305	117.486	38.363	1.00	0.00	O
ATOM	1094	H	GLY C1047	-10.296	114.767	37.838	1.00	0.00	H
ATOM	1095	3HA	GLY C1047	-10.786	116.535	39.690	0.00	0.00	H

ATOM	1096	HA	GLY C1047	-12.372	115.764	39.943	1.00	0.00	H
ATOM	1097	N	GLN C1048	-11.466	117.237	36.949	1.00	0.00	N
ATOM	1098	CA	GLN C1048	-12.304	118.142	36.169	1.00	0.00	C
ATOM	1099	C	GLN C1048	-13.667	117.540	35.920	1.00	0.00	C
ATOM	1100	O	GLN C1048	-13.807	116.372	35.565	1.00	0.00	O
ATOM	1101	CB	GLN C1048	-11.587	118.459	34.838	1.00	0.00	C
ATOM	1102	CG	GLN C1048	-12.317	119.458	33.881	1.00	0.00	C
ATOM	1103	CD	GLN C1048	-11.695	119.772	32.514	1.00	0.00	C
ATOM	1104	NE2	GLN C1048	-10.560	119.220	32.169	1.00	0.00	N
ATOM	1105	OE1	GLN C1048	-12.254	120.516	31.723	1.00	0.00	O
ATOM	1106	H	GLN C1048	-10.605	116.891	36.700	1.00	0.00	H
ATOM	1107	HA	GLN C1048	-12.451	119.075	36.745	1.00	0.00	H
ATOM	1108	2HB	GLN C1048	-11.411	117.506	34.297	1.00	0.00	H
ATOM	1109	3HB	GLN C1048	-10.578	118.858	35.060	1.00	0.00	H
ATOM	1110	2HG	GLN C1048	-12.489	120.421	34.396	1.00	0.00	H
ATOM	1111	3HG	GLN C1048	-13.332	119.090	33.643	1.00	0.00	H
ATOM	1112	1HE2	GLN C1048	-10.248	119.431	31.220	1.00	0.00	H
ATOM	1113	2HE2	GLN C1048	-10.180	118.556	32.846	1.00	0.00	H
ATOM	1114	N	MET C1049	-14.861	118.377	36.108	1.00	0.00	N
ATOM	1115	CA	MET C1049	-16.008	117.529	35.797	1.00	0.00	C
ATOM	1116	C	MET C1049	-17.045	118.288	35.005	1.00	0.00	C
ATOM	1117	O	MET C1049	-17.685	119.231	35.495	1.00	0.00	O
ATOM	1118	CB	MET C1049	-16.618	116.964	37.110	1.00	0.00	C
ATOM	1119	CG	MET C1049	-15.695	116.050	37.943	1.00	0.00	C
ATOM	1120	SD	MET C1049	-16.641	115.260	39.256	1.00	0.00	S
ATOM	1121	CE	MET C1049	-15.269	114.628	40.229	1.00	0.00	C
ATOM	1122	H	MET C1049	-14.885	119.412	36.415	1.00	0.00	H
ATOM	1123	HA	MET C1049	-15.665	116.690	35.163	1.00	0.00	H
ATOM	1124	2HB	MET C1049	-17.533	116.390	36.871	1.00	0.00	H
ATOM	1125	3HB	MET C1049	-16.967	117.798	37.752	1.00	0.00	H
ATOM	1126	2HG	MET C1049	-14.875	116.644	38.389	1.00	0.00	H
ATOM	1127	3HG	MET C1049	-15.219	115.272	37.318	1.00	0.00	H
ATOM	1128	1HE	MET C1049	-14.611	113.985	39.616	1.00	0.00	H
ATOM	1129	2HE	MET C1049	-14.666	115.461	40.631	1.00	0.00	H
ATOM	1130	3HE	MET C1049	-15.641	114.031	41.080	1.00	0.00	H
ATOM	1131	N	ARG C1050	-17.302	117.900	33.610	1.00	0.00	N
ATOM	1132	CA	ARG C1050	-18.338	118.804	33.118	1.00	0.00	C
ATOM	1133	C	ARG C1050	-19.573	118.038	32.708	1.00	0.00	C
ATOM	1134	O	ARG C1050	-19.576	117.273	31.746	1.00	0.00	O



ATOM	1135	CB	ARG	C1050	-17.762	119.628	31.932	1.00	0.00	C
ATOM	1136	CG	ARG	C1050	-18.633	120.829	31.466	1.00	0.00	C
ATOM	1137	CD	ARG	C1050	-18.009	121.565	30.269	1.00	0.00	C
ATOM	1138	NE	ARG	C1050	-18.876	122.716	29.881	1.00	0.00	N
ATOM	1139	CZ	ARG	C1050	-18.633	123.558	28.880	1.00	0.00	C
ATOM	1140	NH1	ARG	C1050	-17.592	123.472	28.101	1.00	0.00	
N1+										
ATOM	1141	NH2	ARG	C1050	-19.476	124.518	28.666	1.00	0.00	N
ATOM	1142	H	ARG	C1050	-16.845	117.145	33.087	1.00	0.00	H
ATOM	1143	HA	ARG	C1050	-18.623	119.480	33.947	1.00	0.00	H
ATOM	1144	2HB	ARG	C1050	-17.573	118.942	31.080	1.00	0.00	H
ATOM	1145	3HB	ARG	C1050	-16.756	120.007	32.207	1.00	0.00	H
ATOM	1146	2HG	ARG	C1050	-18.779	121.525	32.317	1.00	0.00	H
ATOM	1147	3HG	ARG	C1050	-19.648	120.477	31.190	1.00	0.00	H
ATOM	1148	2HD	ARG	C1050	-17.889	120.855	29.422	1.00	0.00	H
ATOM	1149	3HD	ARG	C1050	-16.987	121.909	30.537	1.00	0.00	H
ATOM	1150	HE	ARG	C1050	-19.739	122.924	30.393	1.00	0.00	H
ATOM	1151	1HH1	ARG	C1050	-16.968	122.693	28.323	1.00	0.00	H
ATOM	1152	2HH1	ARG	C1050	-17.476	124.159	27.354	1.00	0.00	H
ATOM	1153	1HH2	ARG	C1050	-20.287	124.569	29.286	1.00	0.00	H
ATOM	1154	2HH2	ARG	C1050	-19.272	125.155	27.894	1.00	0.00	H
ATOM	1155	N	PRO	C1051	-20.810	118.212	33.483	1.00	0.00	N
ATOM	1156	CA	PRO	C1051	-21.839	117.372	32.888	1.00	0.00	C
ATOM	1157	C	PRO	C1051	-21.398	116.818	31.523	1.00	0.00	C
ATOM	1158	O	PRO	C1051	-21.240	117.574	30.564	1.00	0.00	O
ATOM	1159	CB	PRO	C1051	-23.022	118.346	32.787	1.00	0.00	C
ATOM	1160	CG	PRO	C1051	-22.350	119.716	32.614	1.00	0.00	C
ATOM	1161	CD	PRO	C1051	-21.122	119.624	33.523	1.00	0.00	C
ATOM	1162	HA	PRO	C1051	-22.078	116.534	33.547	1.00	0.00	H
ATOM	1163	2HB	PRO	C1051	-23.575	118.333	33.729	1.00	0.00	H
ATOM	1164	3HB	PRO	C1051	-23.705	118.103	31.970	1.00	0.00	H
ATOM	1165	2HG	PRO	C1051	-23.007	120.544	32.892	1.00	0.00	H
ATOM	1166	3HG	PRO	C1051	-22.028	119.838	31.578	1.00	0.00	H
ATOM	1167	2HD	PRO	C1051	-21.369	119.915	34.546	1.00	0.00	H
ATOM	1168	3HD	PRO	C1051	-20.287	120.222	33.150	1.00	0.00	H
ATOM	1169	N	HIS	C1052	-21.164	115.375	31.362	1.00	0.00	N
ATOM	1170	CA	HIS	C1052	-20.764	115.178	29.971	1.00	0.00	C
ATOM	1171	C	HIS	C1052	-21.737	114.277	29.250	1.00	0.00	C
ATOM	1172	O	HIS	C1052	-22.730	113.795	29.816	1.00	0.00	O

ATOM	1173	CB	HIS	C1052	-19.367	114.536	30.011	1.00	0.00	C
ATOM	1174	CG	HIS	C1052	-18.330	115.386	29.337	1.00	0.00	C
ATOM	1175	CD2	HIS	C1052	-17.584	116.339	30.017	1.00	0.00	C
ATOM	1176	ND1	HIS	C1052	-17.985	115.337	27.988	1.00	0.00	N
ATOM	1177	CE1	HIS	C1052	-17.038	116.292	27.957	1.00	0.00	C
ATOM	1178	NE2	HIS	C1052	-16.737	116.934	29.118	1.00	0.00	N
ATOM	1179	H	HIS	C1052	-21.268	114.614	32.120	1.00	0.00	H
ATOM	1180	HA	HIS	C1052	-20.809	116.158	29.468	1.00	0.00	H
ATOM	1181	2HB	HIS	C1052	-19.368	113.544	29.517	1.00	0.00	H
ATOM	1182	3HB	HIS	C1052	-19.023	114.346	31.049	1.00	0.00	H
ATOM	1183	2HD	HIS	C1052	-17.679	116.553	31.078	1.00	0.00	H
ATOM	1184	1HE	HIS	C1052	-16.563	116.496	27.007	1.00	0.00	H
ATOM	1185	2HE	HIS	C1052	-16.049	117.682	29.288	1.00	0.00	H
TER	1186		HIS	C1052						
ATOM	1187	N	SER	D -3	-7.859	112.514	13.714	1.00	0.00	N
ATOM	1188	CA	SER	D -3	-7.673	111.506	14.754	1.00	0.00	C
ATOM	1189	C	SER	D -3	-6.214	111.371	15.121	1.00	0.00	C
ATOM	1190	O	SER	D -3	-5.330	111.314	14.267	1.00	0.00	O
ATOM	1191	CB	SER	D -3	-8.280	110.148	14.321	1.00	0.00	C
ATOM	1192	OG	SER	D -3	-7.550	109.526	13.258	1.00	0.00	O
ATOM	1193	H	SER	D -3	-7.031	113.064	13.294	1.00	0.00	H
ATOM	1194	HA	SER	D -3	-8.201	111.852	15.662	1.00	0.00	H
ATOM	1195	2HB	SER	D -3	-9.340	110.260	14.025	1.00	0.00	H
ATOM	1196	3HB	SER	D -3	-8.296	109.455	15.185	1.00	0.00	H
ATOM	1197	HG	SER	D -3	-7.607	110.105	12.494	1.00	0.00	H
ATOM	1198	N	ALA	D -2	-5.839	111.306	16.541	1.00	0.00	N
ATOM	1199	CA	ALA	D -2	-4.385	111.179	16.575	1.00	0.00	C
ATOM	1200	C	ALA	D -2	-3.954	110.189	17.630	1.00	0.00	C
ATOM	1201	O	ALA	D -2	-4.439	110.189	18.768	1.00	0.00	O
ATOM	1202	CB	ALA	D -2	-3.799	112.584	16.801	1.00	0.00	C
ATOM	1203	H	ALA	D -2	-6.506	111.345	17.390	1.00	0.00	H
ATOM	1204	HA	ALA	D -2	-4.041	110.790	15.599	1.00	0.00	H
ATOM	1205	1HB	ALA	D -2	-4.095	113.286	15.998	1.00	0.00	H
ATOM	1206	2HB	ALA	D -2	-4.136	113.027	17.758	1.00	0.00	H
ATOM	1207	3HB	ALA	D -2	-2.694	112.571	16.819	1.00	0.00	H
ATOM	1208	N	SER	D -1	-2.924	109.195	17.295	1.00	0.00	N
ATOM	1209	CA	SER	D -1	-2.723	108.392	18.498	1.00	0.00	C
ATOM	1210	C	SER	D -1	-1.257	108.102	18.716	1.00	0.00	C
ATOM	1211	O	SER	D -1	-0.521	107.740	17.799	1.00	0.00	O

ATOM	1212	CB	SER	D	-1	-3.559	107.089	18.438	1.00	0.00	C
ATOM	1213	OG	SER	D	-1	-3.079	106.165	17.456	1.00	0.00	O
ATOM	1214	H	SER	D	-1	-2.418	109.080	16.348	1.00	0.00	H
ATOM	1215	HA	SER	D	-1	-3.065	108.987	19.366	1.00	0.00	H
ATOM	1216	2HB	SER	D	-1	-4.627	107.307	18.248	1.00	0.00	H
ATOM	1217	3HB	SER	D	-1	-3.541	106.589	19.426	1.00	0.00	H
ATOM	1218	HG	SER	D	-1	-3.169	106.585	16.597	1.00	0.00	H
ATOM	1219	N	SER	D	0	-0.692	108.257	20.065	1.00	0.00	N
ATOM	1220	CA	SER	D	0	0.722	107.910	19.958	1.00	0.00	C
ATOM	1221	C	SER	D	0	1.168	107.088	21.145	1.00	0.00	C
ATOM	1222	O	SER	D	0	1.834	106.062	21.013	1.00	0.00	O
ATOM	1223	CB	SER	D	0	1.590	109.182	19.787	1.00	0.00	C
ATOM	1224	OG	SER	D	0	1.634	109.989	20.969	1.00	0.00	O
ATOM	1225	H	SER	D	0	-1.218	108.565	20.956	1.00	0.00	H
ATOM	1226	HA	SER	D	0	0.851	107.275	19.062	1.00	0.00	H
ATOM	1227	2HB	SER	D	0	1.239	109.794	18.935	1.00	0.00	H
ATOM	1228	3HB	SER	D	0	2.626	108.893	19.524	1.00	0.00	H
ATOM	1229	HG	SER	D	0	0.740	110.292	21.143	1.00	0.00	H
ATOM	1230	N	ALA	D	1	0.796	107.528	22.497	1.00	0.00	N
ATOM	1231	CA	ALA	D	1	1.363	106.546	23.417	1.00	0.00	C
ATOM	1232	C	ALA	D	1	0.867	105.156	23.096	1.00	0.00	C
ATOM	1233	O	ALA	D	1	0.093	104.936	22.157	1.00	0.00	O
ATOM	1234	CB	ALA	D	1	1.010	106.989	24.848	1.00	0.00	C
ATOM	1235	H	ALA	D	1	0.219	108.403	22.758	1.00	0.00	H
ATOM	1236	HA	ALA	D	1	2.462	106.540	23.294	1.00	0.00	H
ATOM	1237	1HB	ALA	D	1	1.413	107.994	25.077	1.00	0.00	H
ATOM	1238	2HB	ALA	D	1	-0.084	107.035	25.012	1.00	0.00	H
ATOM	1239	3HB	ALA	D	1	1.424	106.300	25.606	1.00	0.00	H
ATOM	1240	N	THR	D	2	1.264	104.168	23.824	1.00	117.75	N
ATOM	1241	CA	THR	D	2	1.121	102.693	23.972	1.00	119.14	C
ATOM	1242	C	THR	D	2	0.948	102.019	22.616	1.00	120.27	C
ATOM	1243	O	THR	D	2	0.822	100.802	22.543	1.00	120.61	O
ATOM	1244	CB	THR	D	2	-0.072	102.329	24.931	1.00	119.19	C
ATOM	1245	CG2	THR	D	2	-0.381	100.832	24.916	1.00	114.83	C
ATOM	1246	OG1	THR	D	2	0.278	102.693	26.273	1.00	119.79	O
ATOM	1247	N	ARG	D	3	0.943	102.794	21.534	1.00	122.00	N
ATOM	1248	CA	ARG	D	3	0.821	102.183	20.212	1.00	122.43	C
ATOM	1249	C	ARG	D	3	2.247	101.762	19.825	1.00	121.24	C
ATOM	1250	O	ARG	D	3	2.438	100.766	19.122	1.00	120.23	O

ATOM	1251	CB	ARG	D	3	0.221	103.170	19.188	1.00124.89	C
ATOM	1252	CG	ARG	D	3	-0.729	102.504	18.181	1.00127.61	C
ATOM	1253	CD	ARG	D	3	-1.341	103.504	17.189	1.00131.95	C
ATOM	1254	NE	ARG	D	3	-2.370	104.358	17.787	1.00136.27	N
ATOM	1255	CZ	ARG	D	3	-3.151	105.196	17.101	1.00137.27	C
ATOM	1256	NH1	ARG	D	3	-3.027	105.302	15.783	1.00136.09	
N1+										
ATOM	1257	NH2	ARG	D	3	-4.065	105.926	17.729	1.00137.17	N
ATOM	1258	N	GLU	D	4	3.236	102.515	20.322	1.00119.46	N
ATOM	1259	CA	GLU	D	4	4.656	102.241	20.083	1.00117.02	C
ATOM	1260	C	GLU	D	4	5.127	101.124	21.033	1.00113.77	C
ATOM	1261	O	GLU	D	4	5.979	100.304	20.676	1.00112.68	O
ATOM	1262	CB	GLU	D	4	5.479	103.524	20.283	1.00120.10	C
ATOM	1263	CG	GLU	D	4	4.987	104.663	19.391	1.00125.95	C
ATOM	1264	CD	GLU	D	4	6.071	105.680	19.009	1.00129.44	C
ATOM	1265	OE1	GLU	D	4	6.490	106.502	19.860	1.00131.18	O
ATOM	1266	OE2	GLU	D	4	6.509	105.652	17.839	1.00131.54	
O1-										
ATOM	1267	N	LEU	D	5	4.576	101.115	22.247	1.00107.77	N
ATOM	1268	CA	LEU	D	5	4.866	100.080	23.238	1.00100.20	C
ATOM	1269	C	LEU	D	5	4.172	98.789	22.748	1.00101.89	C
ATOM	1270	O	LEU	D	5	4.540	97.680	23.140	1.00103.23	O
ATOM	1271	CB	LEU	D	5	4.292	100.486	24.607	1.00 89.57	C
ATOM	1272	CG	LEU	D	5	4.171	99.393	25.678	1.00 82.95	C
ATOM	1273	CD1	LEU	D	5	5.536	99.024	26.172	1.00 79.39	C
ATOM	1274	CD2	LEU	D	5	3.338	99.860	26.837	1.00 78.40	C
ATOM	1275	N	ASP	D	6	3.160	98.945	21.894	1.00103.15	N
ATOM	1276	CA	ASP	D	6	2.414	97.808	21.365	1.00104.18	C
ATOM	1277	C	ASP	D	6	3.096	97.197	20.153	1.00103.81	C
ATOM	1278	O	ASP	D	6	2.785	96.074	19.743	1.00102.97	O
ATOM	1279	CB	ASP	D	6	0.971	98.212	21.039	1.00108.00	C
ATOM	1280	CG	ASP	D	6	0.074	98.200	22.274	1.00112.58	C
ATOM	1281	OD1	ASP	D	6	0.237	97.269	23.096	1.00115.34	O
ATOM	1282	OD2	ASP	D	6	-0.785	99.100	22.417	1.00114.32	
O1-										
ATOM	1283	N	GLU	D	7	4.014	97.959	19.569	1.00104.18	N
ATOM	1284	CA	GLU	D	7	4.799	97.481	18.439	1.00104.53	C
ATOM	1285	C	GLU	D	7	5.713	96.462	19.118	1.00103.48	C
ATOM	1286	O	GLU	D	7	5.970	95.376	18.591	1.00102.50	O

ATOM	1287	CB	GLU	D	7	5.617	98.638	17.849	1.00106.95	C
ATOM	1288	CG	GLU	D	7	4.776	99.656	17.087	1.00110.40	C
ATOM	1289	CD	GLU	D	7	4.581	99.279	15.628	1.00113.03	C
ATOM	1290	OE1	GLU	D	7	5.459	99.643	14.813	1.00114.03	O
ATOM	1291	OE2	GLU	D	7	3.568	98.614	15.299	1.00113.25	
O1-										
ATOM	1292	N	LEU	D	8	6.176	96.835	20.311	1.00100.91	N
ATOM	1293	CA	LEU	D	8	7.043	95.997	21.135	1.00 96.57	C
ATOM	1294	C	LEU	D	8	6.300	94.770	21.645	1.00 98.57	C
ATOM	1295	O	LEU	D	8	6.724	93.638	21.424	1.00100.66	O
ATOM	1296	CB	LEU	D	8	7.542	96.766	22.354	1.00 89.15	C
ATOM	1297	CG	LEU	D	8	8.429	97.975	22.144	1.00 82.99	C
ATOM	1298	CD1	LEU	D	8	8.744	98.566	23.495	1.00 78.33	C
ATOM	1299	CD2	LEU	D	8	9.689	97.577	21.412	1.00 78.68	C
ATOM	1300	N	MET	D	9	5.207	94.995	22.364	1.00 98.60	N
ATOM	1301	CA	MET	D	9	4.448	93.877	22.891	1.00101.80	C
ATOM	1302	C	MET	D	9	4.186	92.858	21.787	1.00102.97	C
ATOM	1303	O	MET	D	9	4.132	91.649	22.040	1.00102.93	O
ATOM	1304	CB	MET	D	9	3.136	94.375	23.500	1.00104.99	C
ATOM	1305	CG	MET	D	9	3.338	95.015	24.860	1.00106.99	C
ATOM	1306	SD	MET	D	9	4.406	93.995	25.914	1.00107.55	S
ATOM	1307	CE	MET	D	9	3.273	92.744	26.447	1.00108.44	C
ATOM	1308	N	ALA	D	10	4.048	93.355	20.560	1.00102.71	N
ATOM	1309	CA	ALA	D	10	3.801	92.510	19.397	1.00102.15	C
ATOM	1310	C	ALA	D	10	5.039	91.707	18.967	1.00101.89	C
ATOM	1311	O	ALA	D	10	4.906	90.592	18.466	1.00102.04	O
ATOM	1312	CB	ALA	D	10	3.299	93.361	18.234	1.00 99.65	C
ATOM	1313	N	SER	D	11	6.234	92.268	19.161	1.00101.68	N
ATOM	1314	CA	SER	D	11	7.494	91.604	18.790	1.00100.63	C
ATOM	1315	C	SER	D	11	7.695	90.245	19.463	1.00104.57	C
ATOM	1316	O	SER	D	11	8.455	89.405	18.966	1.00104.79	O
ATOM	1317	CB	SER	D	11	8.697	92.485	19.141	1.00 96.62	C
ATOM	1318	OG	SER	D	11	8.655	93.731	18.478	1.00 92.87	O
ATOM	1319	N	LEU	D	12	7.033	90.037	20.598	1.00106.92	N
ATOM	1320	CA	LEU	D	12	7.154	88.781	21.337	1.00109.11	C
ATOM	1321	C	LEU	D	12	5.963	87.877	21.013	1.00112.49	C
ATOM	1322	O	LEU	D	12	6.125	86.686	20.730	1.00111.74	O
ATOM	1323	CB	LEU	D	12	7.196	89.075	22.837	1.00108.48	C
ATOM	1324	CG	LEU	D	12	8.137	90.203	23.254	1.00104.98	C

ATOM	1325	CD1	LEU	D	12	7.520	90.980	24.395	1.00100.51	C
ATOM	1326	CD2	LEU	D	12	9.489	89.632	23.634	1.00104.05	C
ATOM	1327	N	SER	D	13	4.603	88.435	21.039	1.00 0.00	N
ATOM	1328	CA	SER	D	13	3.704	87.339	20.691	1.00 0.00	C
ATOM	1329	C	SER	D	13	4.069	86.745	19.351	1.00 0.00	C
ATOM	1330	O	SER	D	13	4.328	87.449	18.375	1.00 0.00	O
ATOM	1331	CB	SER	D	13	2.227	87.805	20.725	1.00 0.00	C
ATOM	1332	OG	SER	D	13	1.907	88.716	19.668	1.00 0.00	O
ATOM	1333	H	SER	D	13	4.325	89.453	21.269	1.00 0.00	H
ATOM	1334	HA	SER	D	13	3.836	86.539	21.442	1.00 0.00	H
ATOM	1335	2HB	SER	D	13	1.975	88.266	21.699	1.00 0.00	H
ATOM	1336	3HB	SER	D	13	1.557	86.927	20.644	1.00 0.00	H
ATOM	1337	HG	SER	D	13	2.442	89.503	19.795	1.00 0.00	H
ATOM	1338	N	ASP	D	14	4.115	85.283	19.207	1.00 0.00	N
ATOM	1339	CA	ASP	D	14	4.490	85.019	17.821	1.00 0.00	C
ATOM	1340	C	ASP	D	14	3.691	83.870	17.253	1.00 0.00	C
ATOM	1341	O	ASP	D	14	3.509	82.820	17.887	1.00 0.00	O
ATOM	1342	CB	ASP	D	14	6.015	84.743	17.711	1.00 0.00	C
ATOM	1343	CG	ASP	D	14	6.546	84.521	16.287	1.00 0.00	C
ATOM	1344	OD1	ASP	D	14	6.065	85.188	15.348	1.00 0.00	O
ATOM	1345	OD2	ASP	D	14	7.415	83.643	16.104	1.00 0.00	
O1-										
ATOM	1346	H	ASP	D	14	3.911	84.550	19.974	1.00 0.00	H
ATOM	1347	HA	ASP	D	14	4.247	85.916	17.220	1.00 0.00	H
ATOM	1348	2HB	ASP	D	14	6.283	83.855	18.313	1.00 0.00	H
ATOM	1349	3HB	ASP	D	14	6.595	85.577	18.138	1.00 0.00	H
ATOM	1350	N	PHE	D	15	3.112	84.001	15.909	1.00 0.00	N
ATOM	1351	CA	PHE	D	15	2.409	82.750	15.642	1.00 0.00	C
ATOM	1352	C	PHE	D	15	2.632	82.295	14.219	1.00 0.00	C
ATOM	1353	O	PHE	D	15	2.554	83.092	13.243	1.00 0.00	O
ATOM	1354	CB	PHE	D	15	0.879	82.935	15.876	1.00 0.00	C
ATOM	1355	CG	PHE	D	15	0.453	83.400	17.278	1.00 0.00	C
ATOM	1356	CD1	PHE	D	15	0.380	84.769	17.560	1.00 0.00	C
ATOM	1357	CD2	PHE	D	15	0.197	82.474	18.292	1.00 0.00	C
ATOM	1358	CE1	PHE	D	15	0.075	85.205	18.845	1.00 0.00	C
ATOM	1359	CE2	PHE	D	15	-0.120	82.911	19.575	1.00 0.00	C
ATOM	1360	CZ	PHE	D	15	-0.177	84.276	19.852	1.00 0.00	C
ATOM	1361	H	PHE	D	15	3.191	84.853	15.250	1.00 0.00	H
ATOM	1362	HA	PHE	D	15	2.802	81.966	16.318	1.00 0.00	H

ATOM	1363	2HB	PHE	D	15	0.354	81.987	15.648	1.00	0.00	H
ATOM	1364	3HB	PHE	D	15	0.471	83.643	15.126	1.00	0.00	H
ATOM	1365	1HD	PHE	D	15	0.606	85.495	16.791	1.00	0.00	H
ATOM	1366	2HD	PHE	D	15	0.261	81.413	18.090	1.00	0.00	H
ATOM	1367	1HE	PHE	D	15	0.052	86.263	19.060	1.00	0.00	H
ATOM	1368	2HE	PHE	D	15	-0.309	82.191	20.358	1.00	0.00	H
ATOM	1369	HZ	PHE	D	15	-0.409	84.617	20.849	1.00	0.00	H
ATOM	1370	N	LYS	D	16	2.950	80.883	13.963	1.00	0.00	N
ATOM	1371	CA	LYS	D	16	3.107	80.754	12.517	1.00	0.00	C
ATOM	1372	C	LYS	D	16	2.470	79.480	12.015	1.00	0.00	C
ATOM	1373	O	LYS	D	16	2.628	78.394	12.592	1.00	0.00	O
ATOM	1374	CB	LYS	D	16	4.617	80.799	12.156	1.00	0.00	C
ATOM	1375	CG	LYS	D	16	4.887	80.746	10.631	1.00	0.00	C
ATOM	1376	CD	LYS	D	16	6.368	80.723	10.240	1.00	0.00	C
ATOM	1377	CE	LYS	D	16	6.486	80.596	8.715	1.00	0.00	C
ATOM	1378	NZ	LYS	D	16	7.897	80.747	8.319	1.00	0.00	
N1+											
ATOM	1379	H	LYS	D	16	3.048	80.097	14.698	1.00	0.00	H
ATOM	1380	HA	LYS	D	16	2.586	81.600	12.033	1.00	0.00	H
ATOM	1381	2HB	LYS	D	16	5.147	79.966	12.662	1.00	0.00	H
ATOM	1382	3HB	LYS	D	16	5.073	81.720	12.572	1.00	0.00	H
ATOM	1383	2HG	LYS	D	16	4.379	81.595	10.134	1.00	0.00	H
ATOM	1384	3HG	LYS	D	16	4.436	79.835	10.195	1.00	0.00	H
ATOM	1385	2HD	LYS	D	16	6.874	79.869	10.735	1.00	0.00	H
ATOM	1386	3HD	LYS	D	16	6.867	81.638	10.610	1.00	0.00	H
ATOM	1387	2HE	LYS	D	16	5.872	81.365	8.201	1.00	0.00	H
ATOM	1388	3HE	LYS	D	16	6.091	79.616	8.375	1.00	0.00	H
ATOM	1389	1HZ	LYS	D	16	8.516	80.308	9.011	1.00	0.00	H
ATOM	1390	2HZ	LYS	D	16	8.087	80.277	7.428	1.00	0.00	H
ATOM	1391	3HZ	LYS	D	16	8.067	81.740	8.246	1.00	0.00	H
ATOM	1392	N	PHE	D	17	1.636	79.529	10.805	1.00	0.00	N
ATOM	1393	CA	PHE	D	17	1.168	78.166	10.575	1.00	0.00	C
ATOM	1394	C	PHE	D	17	1.211	77.819	9.106	1.00	0.00	C
ATOM	1395	O	PHE	D	17	0.791	78.614	8.219	1.00	0.00	O
ATOM	1396	CB	PHE	D	17	-0.297	78.010	11.086	1.00	0.00	C
ATOM	1397	CG	PHE	D	17	-0.541	78.323	12.571	1.00	0.00	C
ATOM	1398	CD1	PHE	D	17	-0.839	79.634	12.960	1.00	0.00	C
ATOM	1399	CD2	PHE	D	17	-0.408	77.329	13.543	1.00	0.00	C
ATOM	1400	CE1	PHE	D	17	-0.983	79.950	14.307	1.00	0.00	C

ATOM	1401	CE2	PHE	D	17	-0.563	77.644	14.891	1.00	0.00	C
ATOM	1402	CZ	PHE	D	17	-0.847	78.954	15.272	1.00	0.00	C
ATOM	1403	H	PHE	D	17	1.414	80.400	10.207	1.00	0.00	H
ATOM	1404	HA	PHE	D	17	1.832	77.463	11.113	1.00	0.00	H
ATOM	1405	2HB	PHE	D	17	-0.649	76.979	10.884	1.00	0.00	H
ATOM	1406	3HB	PHE	D	17	-0.974	78.638	10.472	1.00	0.00	H
ATOM	1407	1HD	PHE	D	17	-0.914	80.418	12.219	1.00	0.00	H
ATOM	1408	2HD	PHE	D	17	-0.166	76.315	13.256	1.00	0.00	H
ATOM	1409	1HE	PHE	D	17	-1.182	80.970	14.599	1.00	0.00	H
ATOM	1410	2HE	PHE	D	17	-0.451	76.874	15.640	1.00	0.00	H
ATOM	1411	HZ	PHE	D	17	-0.954	79.203	16.317	1.00	0.00	H
ATOM	1412	N	MET	D	18	1.758	76.518	8.696	1.00	0.00	N
ATOM	1413	CA	MET	D	18	1.666	76.475	7.239	1.00	0.00	C
ATOM	1414	C	MET	D	18	1.221	75.114	6.763	1.00	0.00	C
ATOM	1415	O	MET	D	18	0.979	74.189	7.554	1.00	0.00	O
ATOM	1416	CB	MET	D	18	3.035	76.861	6.614	1.00	0.00	C
ATOM	1417	CG	MET	D	18	3.535	78.291	6.914	1.00	0.00	C
ATOM	1418	SD	MET	D	18	4.966	78.665	5.889	1.00	0.00	S
ATOM	1419	CE	MET	D	18	5.514	80.156	6.732	1.00	0.00	C
ATOM	1420	H	MET	D	18	2.149	75.747	9.343	1.00	0.00	H
ATOM	1421	HA	MET	D	18	0.898	77.201	6.913	1.00	0.00	H
ATOM	1422	2HB	MET	D	18	2.980	76.748	5.514	1.00	0.00	H
ATOM	1423	3HB	MET	D	18	3.813	76.139	6.934	1.00	0.00	H
ATOM	1424	2HG	MET	D	18	3.815	78.379	7.981	1.00	0.00	H
ATOM	1425	3HG	MET	D	18	2.747	79.044	6.729	1.00	0.00	H
ATOM	1426	1HE	MET	D	18	4.706	80.907	6.774	1.00	0.00	H
ATOM	1427	2HE	MET	D	18	5.826	79.921	7.765	1.00	0.00	H
ATOM	1428	3HE	MET	D	18	6.376	80.602	6.206	1.00	0.00	H
TER	1429		MET	D	18						
HETATM	1430	O	HOH	D	37	2.384	105.217	19.682	1.00	71.42	O
HETATM	1431	O	HOH	D	111	10.178	87.969	17.399	1.00	73.03	O
ATOM	1432	N	SER	F	-3	3.544	97.175	60.553	1.00	0.00	N
ATOM	1433	CA	SER	F	-3	3.529	96.933	59.114	1.00	0.00	C
ATOM	1434	C	SER	F	-3	4.914	97.074	58.527	1.00	0.00	C
ATOM	1435	O	SER	F	-3	5.655	98.011	58.824	1.00	0.00	O
ATOM	1436	CB	SER	F	-3	2.513	97.867	58.409	1.00	0.00	C
ATOM	1437	OG	SER	F	-3	2.923	99.239	58.413	1.00	0.00	O
ATOM	1438	H	SER	F	-3	4.452	97.419	61.084	1.00	0.00	H
ATOM	1439	HA	SER	F	-3	3.215	95.886	58.947	1.00	0.00	H



ATOM	1440	2HB	SER	F	-3	1.508	97.781	58.863	1.00	0.00	H
ATOM	1441	3HB	SER	F	-3	2.380	97.547	57.357	1.00	0.00	H
ATOM	1442	HG	SER	F	-3	2.963	99.524	59.329	1.00	0.00	H
ATOM	1443	N	ALA	F	-2	5.331	96.187	57.689	1.00	0.00	N
ATOM	1444	CA	ALA	F	-2	6.677	96.376	57.155	1.00	0.00	C
ATOM	1445	C	ALA	F	-2	6.723	96.055	55.680	1.00	0.00	C
ATOM	1446	O	ALA	F	-2	6.554	94.907	55.252	1.00	0.00	O
ATOM	1447	CB	ALA	F	-2	7.635	95.503	57.984	1.00	0.00	C
ATOM	1448	H	ALA	F	-2	4.717	95.348	57.397	1.00	0.00	H
ATOM	1449	HA	ALA	F	-2	6.957	97.440	57.269	1.00	0.00	H
ATOM	1450	1HB	ALA	F	-2	7.615	95.777	59.057	1.00	0.00	H
ATOM	1451	2HB	ALA	F	-2	7.379	94.427	57.922	1.00	0.00	H
ATOM	1452	3HB	ALA	F	-2	8.683	95.608	57.649	1.00	0.00	H
ATOM	1453	N	SER	F	-1	6.977	97.142	54.723	1.00	0.00	N
ATOM	1454	CA	SER	F	-1	6.963	96.531	53.397	1.00	0.00	C
ATOM	1455	C	SER	F	-1	8.295	96.705	52.707	1.00	0.00	C
ATOM	1456	O	SER	F	-1	8.708	97.810	52.355	1.00	0.00	O
ATOM	1457	CB	SER	F	-1	5.800	97.095	52.542	1.00	0.00	C
ATOM	1458	OG	SER	F	-1	5.997	98.463	52.168	1.00	0.00	O
ATOM	1459	H	SER	F	-1	7.141	98.184	54.954	1.00	0.00	H
ATOM	1460	HA	SER	F	-1	6.808	95.443	53.524	1.00	0.00	H
ATOM	1461	2HB	SER	F	-1	4.831	96.991	53.066	1.00	0.00	H
ATOM	1462	3HB	SER	F	-1	5.691	96.493	51.619	1.00	0.00	H
ATOM	1463	HG	SER	F	-1	6.017	98.982	52.976	1.00	0.00	H
ATOM	1464	N	SER	F	0	9.022	95.664	52.479	1.00	0.00	N
ATOM	1465	CA	SER	F	0	10.311	95.829	51.812	1.00	0.00	C
ATOM	1466	C	SER	F	0	10.344	95.071	50.505	1.00	0.00	C
ATOM	1467	O	SER	F	0	9.925	93.918	50.409	1.00	0.00	O
ATOM	1468	CB	SER	F	0	11.473	95.406	52.745	1.00	0.00	C
ATOM	1469	OG	SER	F	0	11.510	93.995	52.983	1.00	0.00	O
ATOM	1470	H	SER	F	0	8.683	94.683	52.777	1.00	0.00	H
ATOM	1471	HA	SER	F	0	10.432	96.899	51.565	1.00	0.00	H
ATOM	1472	2HB	SER	F	0	11.425	95.942	53.712	1.00	0.00	H
ATOM	1473	3HB	SER	F	0	12.439	95.710	52.298	1.00	0.00	H
ATOM	1474	HG	SER	F	0	10.698	93.758	53.438	1.00	0.00	H
ATOM	1475	N	ALA	F	1	10.826	95.651	49.458	1.00	0.00	N
ATOM	1476	CA	ALA	F	1	10.832	94.870	48.224	1.00	0.00	C
ATOM	1477	C	ALA	F	1	12.118	95.077	47.461	1.00	0.00	C
ATOM	1478	O	ALA	F	1	12.764	94.131	46.995	1.00	0.00	O

ATOM	1479	CB	ALA	F	1	9.587	95.269	47.414	1.00	0.00	C
ATOM	1480	H	ALA	F	1	11.206	96.662	49.493	1.00	0.00	H
ATOM	1481	HA	ALA	F	1	10.774	93.797	48.485	1.00	0.00	H
ATOM	1482	1HB	ALA	F	1	8.653	95.075	47.975	1.00	0.00	H
ATOM	1483	2HB	ALA	F	1	9.588	96.344	47.150	1.00	0.00	H
ATOM	1484	3HB	ALA	F	1	9.512	94.702	46.468	1.00	0.00	H
ATOM	1485	N	THR	F	2	12.618	96.446	47.265	1.00	167.72	N
ATOM	1486	CA	THR	F	2	13.892	96.405	46.489	1.00	168.68	C
ATOM	1487	C	THR	F	2	14.921	95.534	47.201	1.00	168.68	C
ATOM	1488	O	THR	F	2	15.977	95.221	46.647	1.00	168.77	O
ATOM	1489	CB	THR	F	2	14.477	97.825	46.307	1.00	169.03	C
ATOM	1490	CG2	THR	F	2	15.821	97.770	45.586	1.00	169.26	C
ATOM	1491	OG1	THR	F	2	13.563	98.626	45.545	1.00	170.92	O
ATOM	1492	N	ARG	F	3	14.607	95.142	48.431	1.00	168.25	N
ATOM	1493	CA	ARG	F	3	15.506	94.304	49.213	1.00	167.59	C
ATOM	1494	C	ARG	F	3	15.429	92.866	48.694	1.00	168.72	C
ATOM	1495	O	ARG	F	3	16.417	92.131	48.745	1.00	169.37	O
ATOM	1496	CB	ARG	F	3	15.122	94.374	50.695	1.00	165.45	C
ATOM	1497	CG	ARG	F	3	16.317	94.416	51.642	1.00	163.06	C
ATOM	1498	CD	ARG	F	3	15.889	94.705	53.078	1.00	161.21	C
ATOM	1499	NE	ARG	F	3	15.607	96.119	53.329	1.00	159.22	N
ATOM	1500	CZ	ARG	F	3	15.015	96.572	54.430	1.00	158.39	C
ATOM	1501	NH1	ARG	F	3	14.639	95.720	55.375	1.00	157.72	
N1+											
ATOM	1502	NH2	ARG	F	3	14.812	97.874	54.598	1.00	157.85	N
ATOM	1503	N	GLU	F	4	14.255	92.484	48.184	1.00	169.29	N
ATOM	1504	CA	GLU	F	4	14.025	91.146	47.628	1.00	168.31	C
ATOM	1505	C	GLU	F	4	14.487	91.112	46.170	1.00	167.94	C
ATOM	1506	O	GLU	F	4	14.764	90.045	45.609	1.00	166.98	O
ATOM	1507	CB	GLU	F	4	12.540	90.787	47.687	1.00	167.80	C
ATOM	1508	CG	GLU	F	4	11.896	90.899	49.060	1.00	167.27	C
ATOM	1509	CD	GLU	F	4	10.579	90.140	49.139	1.00	168.28	C
ATOM	1510	OE1	GLU	F	4	9.703	90.366	48.276	1.00	167.92	O
ATOM	1511	OE2	GLU	F	4	10.420	89.316	50.065	1.00	168.81	
O1-											
ATOM	1512	N	LEU	F	5	14.553	92.296	45.567	1.00	167.58	N
ATOM	1513	CA	LEU	F	5	15.002	92.453	44.189	1.00	167.99	C
ATOM	1514	C	LEU	F	5	16.537	92.441	44.166	1.00	169.16	C
ATOM	1515	O	LEU	F	5	17.157	92.024	43.182	1.00	168.77	O

ATOM	1516	CB	LEU	F	5	14.478	93.774	43.624	1.00166.25	C
ATOM	1517	CG	LEU	F	5	14.988	94.231	42.257	1.00165.05	C
ATOM	1518	CD1	LEU	F	5	14.468	93.324	41.150	1.00163.55	C
ATOM	1519	CD2	LEU	F	5	14.538	95.656	42.032	1.00164.01	C
ATOM	1520	N	ASP	F	6	17.140	92.897	45.263	1.00169.94	N
ATOM	1521	CA	ASP	F	6	18.595	92.933	45.391	1.00169.64	C
ATOM	1522	C	ASP	F	6	19.138	91.563	45.758	1.00169.28	C
ATOM	1523	O	ASP	F	6	20.317	91.278	45.546	1.00168.18	O
ATOM	1524	CB	ASP	F	6	19.023	93.965	46.434	1.00170.12	C
ATOM	1525	CG	ASP	F	6	18.893	95.385	45.925	1.00172.08	C
ATOM	1526	OD1	ASP	F	6	19.227	95.615	44.741	1.00172.61	O
ATOM	1527	OD2	ASP	F	6	18.470	96.269	46.701	1.00173.49	
O1-										
ATOM	1528	N	GLU	F	7	18.272	90.725	46.321	1.00169.63	N
ATOM	1529	CA	GLU	F	7	18.642	89.358	46.664	1.00169.36	C
ATOM	1530	C	GLU	F	7	18.916	88.778	45.282	1.00169.37	C
ATOM	1531	O	GLU	F	7	19.858	88.009	45.071	1.00169.25	O
ATOM	1532	CB	GLU	F	7	17.453	88.619	47.297	1.00169.43	C
ATOM	1533	CG	GLU	F	7	16.960	89.198	48.617	1.00168.79	C
ATOM	1534	CD	GLU	F	7	17.596	88.538	49.825	1.00168.60	C
ATOM	1535	OE1	GLU	F	7	17.092	87.480	50.260	1.00167.14	O
ATOM	1536	OE2	GLU	F	7	18.606	89.071	50.333	1.00168.56	
O1-										
ATOM	1537	N	LEU	F	8	18.069	89.199	44.345	1.00168.60	N
ATOM	1538	CA	LEU	F	8	18.125	88.783	42.951	1.00167.55	C
ATOM	1539	C	LEU	F	8	19.321	89.384	42.207	1.00168.46	C
ATOM	1540	O	LEU	F	8	20.059	88.662	41.530	1.00168.63	O
ATOM	1541	CB	LEU	F	8	16.817	89.177	42.252	1.00164.51	C
ATOM	1542	CG	LEU	F	8	15.527	88.563	42.814	1.00161.82	C
ATOM	1543	CD1	LEU	F	8	14.310	89.243	42.215	1.00160.14	C
ATOM	1544	CD2	LEU	F	8	15.500	87.079	42.514	1.00161.14	C
ATOM	1545	N	MET	F	9	19.517	90.696	42.341	1.00169.27	N
ATOM	1546	CA	MET	F	9	20.623	91.381	41.671	1.00170.34	C
ATOM	1547	C	MET	F	9	21.990	90.920	42.196	1.00170.50	C
ATOM	1548	O	MET	F	9	23.015	91.080	41.523	1.00170.08	O
ATOM	1549	CB	MET	F	9	20.474	92.903	41.821	1.00171.17	C
ATOM	1550	CG	MET	F	9	19.210	93.489	41.164	1.00172.23	C
ATOM	1551	SD	MET	F	9	18.947	93.057	39.408	1.00173.00	S
ATOM	1552	CE	MET	F	9	20.201	94.088	38.567	1.00172.02	C

ATOM	1553	N	ALA	F	10	21.988	90.333	43.391	1.00170.19	N
ATOM	1554	CA	ALA	F	10	23.204	89.820	44.021	1.00169.09	C
ATOM	1555	C	ALA	F	10	23.472	88.382	43.568	1.00168.90	C
ATOM	1556	O	ALA	F	10	24.601	87.896	43.636	1.00167.06	O
ATOM	1557	CB	ALA	F	10	23.064	89.874	45.540	1.00167.81	C
ATOM	1558	N	SER	F	11	22.421	87.707	43.109	1.00169.78	N
ATOM	1559	CA	SER	F	11	22.528	86.331	42.633	1.00169.93	C
ATOM	1560	C	SER	F	11	23.397	86.282	41.387	1.00171.22	C
ATOM	1561	O	SER	F	11	24.118	85.313	41.152	1.00170.34	O
ATOM	1562	CB	SER	F	11	21.141	85.771	42.307	1.00168.77	C
ATOM	1563	OG	SER	F	11	20.351	85.639	43.473	1.00167.98	O
ATOM	1564	N	LEU	F	12	23.313	87.341	40.589	1.00173.79	N
ATOM	1565	CA	LEU	F	12	24.082	87.455	39.358	1.00176.17	C
ATOM	1566	C	LEU	F	12	25.519	87.870	39.666	1.00178.24	C
ATOM	1567	O	LEU	F	12	26.470	87.285	39.146	1.00179.14	O
ATOM	1568	CB	LEU	F	12	23.418	88.481	38.435	1.00175.22	C
ATOM	1569	CG	LEU	F	12	21.974	88.127	38.071	1.00174.35	C
ATOM	1570	CD1	LEU	F	12	21.284	89.305	37.400	1.00173.85	C
ATOM	1571	CD2	LEU	F	12	21.982	86.906	37.169	1.00173.97	C
ATOM	1572	N	SER	F	13	25.770	88.982	40.594	1.00 0.00	N
ATOM	1573	CA	SER	F	13	27.221	89.127	40.675	1.00 0.00	C
ATOM	1574	C	SER	F	13	27.870	87.837	41.117	1.00 0.00	C
ATOM	1575	O	SER	F	13	27.425	87.171	42.052	1.00 0.00	O
ATOM	1576	CB	SER	F	13	27.606	90.306	41.604	1.00 0.00	C
ATOM	1577	OG	SER	F	13	27.318	90.046	42.982	1.00 0.00	O
ATOM	1578	H	SER	F	13	25.030	89.573	41.112	1.00 0.00	H
ATOM	1579	HA	SER	F	13	27.599	89.344	39.659	1.00 0.00	H
ATOM	1580	2HB	SER	F	13	27.104	91.242	41.292	1.00 0.00	H
ATOM	1581	3HB	SER	F	13	28.689	90.518	41.507	1.00 0.00	H
ATOM	1582	HG	SER	F	13	26.368	89.937	43.062	1.00 0.00	H
ATOM	1583	N	ASP	F	14	29.068	87.362	40.410	1.00 0.00	N
ATOM	1584	CA	ASP	F	14	29.457	86.112	41.056	1.00 0.00	C
ATOM	1585	C	ASP	F	14	30.955	86.027	41.215	1.00 0.00	C
ATOM	1586	O	ASP	F	14	31.732	86.330	40.295	1.00 0.00	O
ATOM	1587	CB	ASP	F	14	28.913	84.893	40.259	1.00 0.00	C
ATOM	1588	CG	ASP	F	14	29.196	83.518	40.881	1.00 0.00	C
ATOM	1589	OD1	ASP	F	14	29.159	83.392	42.122	1.00 0.00	O
ATOM	1590	OD2	ASP	F	14	29.502	82.572	40.124	1.00 0.00	

O1-

ATOM	1591	H	ASP	F	14	29.562	87.843	39.579	1.00	0.00	H
ATOM	1592	HA	ASP	F	14	29.018	86.096	42.072	1.00	0.00	H
ATOM	1593	2HB	ASP	F	14	29.331	84.893	39.236	1.00	0.00	H
ATOM	1594	3HB	ASP	F	14	27.820	84.964	40.135	1.00	0.00	H
ATOM	1595	N	PHE	F	15	31.512	85.573	42.497	1.00	0.00	N
ATOM	1596	CA	PHE	F	15	32.964	85.597	42.345	1.00	0.00	C
ATOM	1597	C	PHE	F	15	33.596	84.385	42.986	1.00	0.00	C
ATOM	1598	O	PHE	F	15	33.578	84.204	44.236	1.00	0.00	O
ATOM	1599	CB	PHE	F	15	33.550	86.880	43.009	1.00	0.00	C
ATOM	1600	CG	PHE	F	15	33.022	88.225	42.485	1.00	0.00	C
ATOM	1601	CD1	PHE	F	15	31.875	88.788	43.058	1.00	0.00	C
ATOM	1602	CD2	PHE	F	15	33.634	88.861	41.403	1.00	0.00	C
ATOM	1603	CE1	PHE	F	15	31.338	89.962	42.542	1.00	0.00	C
ATOM	1604	CE2	PHE	F	15	33.102	90.043	40.894	1.00	0.00	C
ATOM	1605	CZ	PHE	F	15	31.953	90.591	41.462	1.00	0.00	C
ATOM	1606	H	PHE	F	15	30.958	85.281	43.376	1.00	0.00	H
ATOM	1607	HA	PHE	F	15	33.212	85.583	41.267	1.00	0.00	H
ATOM	1608	2HB	PHE	F	15	34.653	86.875	42.908	1.00	0.00	H
ATOM	1609	3HB	PHE	F	15	33.391	86.837	44.106	1.00	0.00	H
ATOM	1610	1HD	PHE	F	15	31.375	88.288	43.877	1.00	0.00	H
ATOM	1611	2HD	PHE	F	15	34.513	88.430	40.943	1.00	0.00	H
ATOM	1612	1HE	PHE	F	15	30.436	90.372	42.972	1.00	0.00	H
ATOM	1613	2HE	PHE	F	15	33.574	90.527	40.052	1.00	0.00	H
ATOM	1614	HZ	PHE	F	15	31.531	91.500	41.060	1.00	0.00	H
ATOM	1615	N	LYS	F	16	34.251	83.385	42.130	1.00	0.00	N
ATOM	1616	CA	LYS	F	16	34.758	82.349	43.025	1.00	0.00	C
ATOM	1617	C	LYS	F	16	36.261	82.233	42.923	1.00	0.00	C
ATOM	1618	O	LYS	F	16	36.820	81.827	41.894	1.00	0.00	O
ATOM	1619	CB	LYS	F	16	34.073	80.996	42.689	1.00	0.00	C
ATOM	1620	CG	LYS	F	16	34.489	79.843	43.636	1.00	0.00	C
ATOM	1621	CD	LYS	F	16	33.882	78.478	43.295	1.00	0.00	C
ATOM	1622	CE	LYS	F	16	34.433	77.424	44.263	1.00	0.00	C
ATOM	1623	NZ	LYS	F	16	33.727	76.148	44.052	1.00	0.00	
N1+											
ATOM	1624	H	LYS	F	16	34.340	83.413	41.054	1.00	0.00	H
ATOM	1625	HA	LYS	F	16	34.517	82.636	44.065	1.00	0.00	H
ATOM	1626	2HB	LYS	F	16	34.292	80.718	41.638	1.00	0.00	H
ATOM	1627	3HB	LYS	F	16	32.972	81.116	42.727	1.00	0.00	H
ATOM	1628	2HG	LYS	F	16	34.243	80.114	44.681	1.00	0.00	H

ATOM	1629	3HG	LYS	F	16	35.586	79.710	43.617	1.00	0.00	H
ATOM	1630	2HD	LYS	F	16	34.134	78.207	42.249	1.00	0.00	H
ATOM	1631	3HD	LYS	F	16	32.778	78.536	43.344	1.00	0.00	H
ATOM	1632	2HE	LYS	F	16	34.311	77.746	45.318	1.00	0.00	H
ATOM	1633	3HE	LYS	F	16	35.526	77.291	44.112	1.00	0.00	H
ATOM	1634	1HZ	LYS	F	16	33.526	76.006	43.055	1.00	0.00	H
ATOM	1635	2HZ	LYS	F	16	34.301	75.351	44.344	1.00	0.00	H
ATOM	1636	3HZ	LYS	F	16	32.878	76.199	44.597	1.00	0.00	H
ATOM	1637	N	PHE	F	17	37.085	82.614	44.079	1.00	0.00	N
ATOM	1638	CA	PHE	F	17	38.473	82.396	43.682	1.00	0.00	C
ATOM	1639	C	PHE	F	17	39.137	81.373	44.573	1.00	0.00	C
ATOM	1640	O	PHE	F	17	39.363	81.598	45.795	1.00	0.00	O
ATOM	1641	CB	PHE	F	17	39.270	83.733	43.770	1.00	0.00	C
ATOM	1642	CG	PHE	F	17	38.740	84.903	42.926	1.00	0.00	C
ATOM	1643	CD1	PHE	F	17	37.777	85.764	43.465	1.00	0.00	C
ATOM	1644	CD2	PHE	F	17	39.160	85.080	41.606	1.00	0.00	C
ATOM	1645	CE1	PHE	F	17	37.228	86.778	42.687	1.00	0.00	C
ATOM	1646	CE2	PHE	F	17	38.618	86.103	40.831	1.00	0.00	C
ATOM	1647	CZ	PHE	F	17	37.651	86.948	41.371	1.00	0.00	C
ATOM	1648	H	PHE	F	17	36.734	82.981	45.032	1.00	0.00	H
ATOM	1649	HA	PHE	F	17	38.493	82.012	42.645	1.00	0.00	H
ATOM	1650	2HB	PHE	F	17	40.326	83.551	43.489	1.00	0.00	H
ATOM	1651	3HB	PHE	F	17	39.337	84.058	44.829	1.00	0.00	H
ATOM	1652	1HD	PHE	F	17	37.422	85.617	44.476	1.00	0.00	H
ATOM	1653	2HD	PHE	F	17	39.894	84.415	41.173	1.00	0.00	H
ATOM	1654	1HE	PHE	F	17	36.464	87.417	43.103	1.00	0.00	H
ATOM	1655	2HE	PHE	F	17	38.941	86.232	39.808	1.00	0.00	H
ATOM	1656	HZ	PHE	F	17	37.219	87.733	40.767	1.00	0.00	H
ATOM	1657	N	MET	F	18	39.532	80.078	44.000	1.00	0.00	N
ATOM	1658	CA	MET	F	18	40.139	79.317	45.089	1.00	0.00	C
ATOM	1659	C	MET	F	18	41.576	78.977	44.777	1.00	0.00	C
ATOM	1660	O	MET	F	18	42.118	79.326	43.717	1.00	0.00	O
ATOM	1661	CB	MET	F	18	39.310	78.031	45.358	1.00	0.00	C
ATOM	1662	CG	MET	F	18	37.854	78.251	45.823	1.00	0.00	C
ATOM	1663	SD	MET	F	18	37.143	76.689	46.363	1.00	0.00	S
ATOM	1664	CE	MET	F	18	35.420	77.195	46.445	1.00	0.00	C
ATOM	1665	H	MET	F	18	39.401	79.755	42.978	1.00	0.00	H
ATOM	1666	HA	MET	F	18	40.144	79.946	45.999	1.00	0.00	H
ATOM	1667	2HB	MET	F	18	39.820	77.421	46.127	1.00	0.00	H

ATOM	1668	3HB	MET	F	18	39.300	77.393	44.451	1.00	0.00	H
ATOM	1669	2HG	MET	F	18	37.249	78.662	44.993	1.00	0.00	H
ATOM	1670	3HG	MET	F	18	37.798	78.983	46.650	1.00	0.00	H
ATOM	1671	1HE	MET	F	18	35.295	78.070	47.109	1.00	0.00	H
ATOM	1672	2HE	MET	F	18	35.050	77.465	45.440	1.00	0.00	H
ATOM	1673	3HE	MET	F	18	34.793	76.373	46.833	1.00	0.00	H
TER	1674		MET	F	18						
HETATM	1675	O	HOH	F	105	11.710	93.548	46.450	1.00	87.72	O
END											

## Appendix B. Mdp Simulation Files

### 1. Mdp file used for equilibrium simulations where P1/P2 unconstrained:

```
title          = MD production
; this is loosely based off of the VT pulling tutorial; heavily modified
; Run parameters
integrator      = md
dt              = 0.002
tinit          = 0
nsteps         = 5000000      ; 10 ns
; Output parameters
nstxout        = 1000        ; every 2 ps
nstvout        = 1000
nstfout        = 5000
nstxtcout      = 5000        ; every 1 ps
nstenergy      = 1000
; Bond parameters
constraint_algorithm = lincs
constraints     = hbonds
lincs_iter      = 1          ; accuracy of LINCS
lincs_order     = 4          ; also related to accuracy
; Single-range cutoff scheme
nstlist        = 5
ns_type        = grid
rlist          = 1.4
rcoulomb       = 1.4
rvdw           = 1.4
; PME electrostatics parameters
coulombtype    = PME
fourierspacing = 0.16
pme_order      = 4
ewald_rtol     = 1e-5
optimize_fft   = yes
; Berendsen temperature coupling is on in two groups
Tcoupl        = Nose-Hoover
tc_grps       = Protein Non-Protein
tau_t         = 0.2 0.2
ref_t         = 310 310
; Pressure coupling is on
Pcoupl        = Parrinello-Rahman
pcoupltype    = isotropic
tau_p         = 1.0
compressibility = 4.5e-5
ref_p         = 1.0
; Generate velocities is off
gen_vel       = no
; Periodic boundary conditions are on in all directions
pbc           = xyz
; Long-range dispersion correction
DispCorr      = EnerPres
; COM motion removal
```



```
; These options remove COM motion of the system
nstcomm      = 1
comm-mode     = Linear
comm-grps     = System
```

## 2. Mdp file used for equilibrium simulations where P1/P2 constrained:

```
title          = MD production
; this is loosely based off of the VT pulling tutorial; heavily modified
; Run parameters
integrator      = md
freezegrps     = freeze
freezedim      = Y Y Y
dt              = 0.002
tinit          = 0
nsteps         = 2500000      ; 5 ns
; Output parameters
nstxout         = 1000        ; every 2 ps
nstvout         = 1000
nstfout         = 5000
nstxtcout       = 5000        ; every 1 ps
nstenergy       = 1000
; Bond parameters
constraint_algorithm = lincs
constraints      = hbonds
lincs_iter      = 1           ; accuracy of LINCS
lincs_order     = 4           ; also related to accuracy
; Single-range cutoff scheme
nstlist         = 5
ns_type         = grid
rlist           = 1.4
rcoulomb        = 1.4
rvdw            = 1.4
; PME electrostatics parameters
coulombtype     = PME
fourierspacing  = 0.16
pme_order       = 4
ewald_rtol      = 1e-5
optimize_fft    = yes
; Berendsen temperature coupling is on in two groups
Tcoupl          = Nose-Hoover
tc_grps         = Protein Non-Protein
tau_t           = 0.2 0.2
ref_t           = 310 310
; Pressure coupling is on
Pcoupl          = Parrinello-Rahman
pcoupltype      = isotropic
tau_p           = 1.0
compressibility  = 4.5e-5
ref_p           = 1.0
; Generate velocities is ON
gen_vel         = yes
gen_temp        = 310
gen_seed        = -1
```

```

; Periodic boundary conditions are on in all directions
pbc          = xyz
; Long-range dispersion correction
DispCorr     = EnerPres
; COM motion removal
; These options remove COM motion of the system
nstcomm      = 1
comm-mode    = Linear
comm-grps    = System

```

### 3. Mdp file used for axial load scenario:

```

title        = smd_100 ; 100 pN
; this is loosely based off of the VT pulling tutorial; heavily modified
; Run parameters
integrator    = md
freezegrps   = freeze
freezedim    = Y Y Y
dt           = 0.002
tinit        = 0
nsteps       = 2500000 ; 5 ns
; Output parameters
nstxout       = 1000 ; every 2 ps
nstvout       = 1000
nstfout       = 5000
nstxtcout    = 5000 ; every ps
nstenergy     = 1000
; Bond parameters
constraint_algorithm = lincs
constraints   = hbonds
lincs_iter    = 1 ; accuracy of LINCS
lincs_order   = 4 ; also related to accuracy
; Single-range cutoff scheme
nstlist       = 5
ns_type       = grid
rlist         = 1.4
rcoulomb      = 1.4
rvdw          = 1.4
; PME electrostatics parameters
coulombtype   = PME
fourierspacing = 0.16
pme_order     = 4
ewald_rtol    = 1e-5
optimize_fft  = yes
; Berendsen temperature coupling is on in two groups
Tcoupl        = Nose-Hoover
tc_grps       = Protein Non-Protein
tau_t         = 0.2 0.2
ref_t         = 310 310
; Pressure coupling is on
Pcoupl        = Parrinello-Rahman
pcoupltype    = isotropic
tau_p         = 1.0
compressibility = 4.5e-5
ref_p         = 1.0

```

```

; Generate velocities is ON
gen_vel      = yes
gen_temp     = 310
gen_seed     = -1
; Periodic boundary conditions are on in all directions
pbc          = xyz
; Long-range dispersion correction
DispCorr     = EnerPres
; COM motion removal
; These options remove comm motion of the constraint / freeze group
nstcomm      = 1
comm_mode    = Linear
comm_grps    = System
; pull parameters
pull         = constant_force
pull_geometry = direction
pull_nstxout  = 500 ; will print the c.o.m. coordinates
pull_nstfout  = 500 ; forces on group
pull_ngroups  = 1
pull_group0   = Protein ;
pull_group1   = group_B ;
pull_pbcatom1 = 5 ; the CA of the 10th residue
pull_vec1     = 0.75 -1.19 -0.55 ; direction of pull, will be normalized
pull_k1       = 60.24 ; pull_k1*1.66 = 100 pN; units: [kJ / (mol * nm^2)]

```

#### 4. Mdp file used for perpendicular load scenario:

```

title        = smd_100 ; 100 pN
; this is loosely based off of the VT pulling tutorial; heavily modified
; Run parameters
integrator    = md
freezegrps   = freeze
freezedim    = Y Y Y
dt           = 0.002
tinit        = 0
nsteps       = 2500000 ; 5 ns
; Output parameters
nstxout       = 1000 ; every 2 ps
nstvout       = 1000
nstfout       = 5000
nstxtcout    = 5000 ; every ps
nstenergy     = 1000
; Bond parameters
constraint_algorithm = lincs
constraints    = hbonds
lincs_iter    = 1 ; accuracy of LINCS
lincs_order   = 4 ; also related to accuracy
; Single-range cutoff scheme
nstlist       = 5
ns_type       = grid
rlist         = 1.4
rcoulomb      = 1.4
rvdw          = 1.4
; PME electrostatics parameters

```

```

coulombtype = PME
fourierspacing = 0.16
pme_order = 4
ewald_rtol = 1e-5
optimize_fft = yes
; Berendsen temperature coupling is on in two groups
Tcoupl = Nose-Hoover
tc_grps = Protein Non-Protein
tau_t = 0.2 0.2
ref_t = 310 310
; Pressure coupling is on
Pcoupl = Parrinello-Rahman
pcoupltype = isotropic
tau_p = 1.0
compressibility = 4.5e-5
ref_p = 1.0
; Generate velocities is ON
gen_vel = yes
gen_temp = 310
gen_seed = -1

; Periodic boundary conditions are on in all directions
pbc = xyz
; Long-range dispersion correction
DispCorr = EnerPres
; COM motion removal
; These options remove comm motion of the constraint / freeze group
nstcomm = 1
comm_mode = Linear
comm_grps = System
; pull parameters
pull = constant_force
pull_geometry = direction
pull_nstxout = 500 ; will print the c.o.m. coordinates
pull_nstfout = 500 ; forces on group
pull_ngroups = 1
pull_group0 = Protein ;
pull_group1 = group_B ;
pull_pbcatom1 = 5 ; the CA of the 10th residue
pull_vec1 = 0.07 -0.31 0.92 ; direction of pull, will be normalized
pull_k1 = 60.24 ; pull_k1*1.66 = 100 pN; units: [kJ / (mol * nm^2)]

```

## Appendix C. MATLAB Codes

### 1. H1 Position MATLAB Code:

```
clear all;
close all;

% file name;
filename='xxxxxxx';

% Constants;
% -----
Average=10; % How many points you want to average (moving average)
N=2; % How many distance you want to calculate
R=36; % The row that you want readfile to start with
C=0; % The column that you want readfile to start with

% number of columns to compare
numcomp=1;

% For energy plots:
%-----
Xmin= 0;
Xmax= 1.5;
Ymin= 0;
Ymax= 1.5;
stepsize=0.01;

% load data for 1st file:
dat=dlmread([filename '.csv'], '\t',R,C);

% what the size of my matrix
sz=size(dat);
sz(1);
moving=sz(1)-Average+1;

% The calculation of the distances:
% -----
for i=1:sz(1);

    for L=1:1:N;
        p=2;
        x=dat(i,p)-0.5*(dat(i,p+6)+dat(i,p+12));
        y=dat(i,p+1)-0.5*(dat(i,p+7)+dat(i,p+13));
        z=dat(i,p+2)-0.5*(dat(i,p+8)+dat(i,p+14));
        Dtop(i,L)=sqrt(x^2+y^2+z^2);
```

```

        p=p+3;
        x=dat(i,p)-0.5*(dat(i,p+6)+dat(i,p+12));
        y=dat(i,p+1)-0.5*(dat(i,p+7)+dat(i,p+13));
        z=dat(i,p+2)-0.5*(dat(i,p+8)+dat(i,p+14));
        Dbottom(i,L)=sqrt(x^2+y^2+z^2);

    end
end

Dlave=zeros(moving,1);
D2ave=zeros(moving,1);

if Average>1;
    for i=1:moving;
        for c=0:1:Average-1;
            Dlave(i)=Dlave(i)+Dtop(i+c);
            D2ave(i)=D2ave(i)+Dbottom(i+c);
        end
        Dlave(i)=Dlave(i)/Average;
        D2ave(i)=D2ave(i)/Average;
    end
end

divsx=(-Xmin+Xmax)/stepsize;
divsy=(-Ymin+Ymax)/stepsize;

for i=1:divsx
    for j=1:divsy
        hist(i,j)=0;
    end
end

tot=0;

compmat=[1 2];

% loop through images (this part of script was taken from Steven script)
for n=1:moving

    % evaluate dat1; data in column specified by first entry of 'compmat'
    Dlave(n)
        x=round((Dlave(n)-Xmin)/stepsize);
    D2ave(n)
    % evaluate dat2; data in column specified by second entry of 'compmat'
        y=round((D2ave(n)-Ymin)/stepsize);

    % update histogram if within limits

        if ((x>0)&&(x<divsx))&&((y>0)&&(y<divsy))
            hist(x,y)=hist(x,y)+1;
            tot=tot+1;
        end
    end

end

% end loop over distances

```

```

pdf2d=hist/(tot-1);

% convert pdf2d to pmf2d
for i=1:divsx
    for j=1:divsy
        pmf2d(i,j)=-log(pdf2d(i,j));
    end
end

% create axis values

for i=1:divsx
    x_vals(i)=(Xmin+stepsize*i);
end

for i=1:divsy
    y_vals(i)=(Ymin+stepsize*i);
end

colstr1=num2str(compmat(1,1));
colstr2=num2str(compmat(1,2));
sxx=size(x_vals);
szy=size(y_vals);
szp=size(pmf2d);

figure (1)
h=surf(y_vals,x_vals,pmf2d);
title('xxxxxx','FontWeight','bold')
set(h,'EdgeColor','none')
axis([Ymin Ymax Xmin Xmax]);
xlabel('xxxxxx','FontSize', 8);
ylabel('xxxxxx','FontSize', 8);

```

## 2. Backbone Dihedral Angle $\psi$ MATLAB Code:

```

clear all;
close all;

% file names:
filename='xxxxxxxxx';

% Constants;
% -----
Average=10; % How many points you want to average (moving average)
N=5; % How many dihedral psi angle you want to calculate
R=66; % The row that you want readfile to start with
C=0; % The column that you want readfile to start with

% For energy plots:
%-----
Xmin= -180;
Xmax= 180;
stepsize=0.2;

```

```

% load data for 1st file:
dat=dlmread([filename '.csv'], '\t',R,C);

% what the size of my matrix
sz=size(dat);
sz(1);
moving=sz(1)-Average+1;

% The calculation of the dihedral angle:
% -----

for i=1:sz(1);
    j=1;
    p=2;
    for L=1:1:N;

        xba=dat(i,p+3)-dat(i,p);
        yba=dat(i,p+4)-dat(i,p+1);
        zba=dat(i,p+5)-dat(i,p+2);

        xcb=dat(i,p+6)-dat(i,p+3);
        ycb=dat(i,p+7)-dat(i,p+4);
        zcb=dat(i,p+8)-dat(i,p+5);

        xdc=dat(i,p+9)-dat(i,p+6);
        ydc=dat(i,p+10)-dat(i,p+7);
        zdc=dat(i,p+11)-dat(i,p+8);

        xt=yba*zcb-ycb*zba;
        yt=zba*xcb-zcb*xba;
        zt=xba*ycb-xcb*yba;

        xu=ycb*zdc-ydc*zcb;
        yu=zcb*xdc-zdc*xcb;
        zu=xcb*ydc-xdc*ycb;

        xtu=yt*zu-yu*zt;
        ytu=zt*xu-zu*xt;
        ztu=xt*yu-xu*yt;

        rt2=xt^2+yt^2+zt^2;
        ru2=xu^2+yu^2+zu^2;
        rtru=sqrt(rt2*ru2);

        rcb=sqrt(xcb^2+ycb^2+zcb^2);

        sign=(xcb*xtu+ycb*ytu+zcb*ztu)/(rcb*rtru);

        psi(i,j)=(sign/abs(sign))*180*acos((xt*xu+yt*yu+zt*zv)/rtru)/pi;

        j=j+1;
        p=p+9;
    end
end

```



```

psiave=zeros(moving,N);

if Average>1;
    for L=1:1:N;
        for i=1:moving;
            for c=0:1:Average-1;
                psiave(i,L)=psiave(i,L)+psi(i+c,L);
            end
            psiave(i,L)=psiave(i,L)/Average;
        end
    end
end

% the size of my matrix after doing the average:
szd=size(psi);
szdave=size(psiave);

divsx=(-Xmin+Xmax)/stepsize;

hist=zeros(divsx,N);

for u=1:1:N;

    tot=0;
    % initialize incidence counter
    for n=1:moving

        % evaluate dat1; data in column specified by first entry of 'compmat'
        psiave(n,u);
        x=round((psiave(n,u)-Xmin)/stepsize);

        % update histogram if within limits
        if ((x>0)&&(x<divsx))
            hist(x,u)=hist(x,u)+1;
            tot=tot+1;
        end
    end
end

pdf2d=hist/(tot-1);

% convert pdf2d to pmf2d
for i=1:divsx
    for j=1:N
        pmf2d(i,j)=-log(pdf2d(i,j));
    end
end

B=[1 1.9999 2 2.9999 3 3.9999 4 4.9999 5 5.9999];

```

```

for i=1:divsx
c=1;
    for j=1:N;
        pmf2B(i,c)=pmf2d(i,j);
        pmf2B(i,c+1)=pmf2d(i,j);
        c=c+2;
    end
end

% create axis values
for i=1:divsx
    x_val(i)=Xmin+stepsize*i;
end

pmf2B=transpose(pmf2B);
B=transpose(B);

figure (1);
h=surf(x_val,B, pmf2B);
title('xxxxxx','Fontweight','bold');
set(h,'EdgeColor','none')
axis([Xmin Xmax 1 N+1]);
xlabel('xxxxxxxxxxxx','FontSize',8);
ylabel('xxxxxxxxxxxx','FontSize',8);

```

### 3. Hydrogen Donor-Acceptor Pairs MATLAB Code:

```

clear all;
close all;

% file names:
filename='xxxxxxxxxx';

% Constants;
% -----
N=5;           % How many hydrogen donor acceptor pairs (residues) you want to
consider
R=88;         % The row that you want readfile to start with
C=1;          % The column that you want readfile to start with
ymin = 0;
ymax = 1;
xmin=0;
xmax=7;

% load data for 1st file:
dat=dlmread([filename '.csv'],'\t', R,C);

sz=size(dat);

sz(1);

T=4;          %the possible number of pairs with each residue
Htype=zeros(N,2*T);

```

```

p=1;
ss=0;

% The calculation of the hydrogen donor acceptor pairs:
% -----

for L=1:1:N;

    for i=1:sz(1);
        kk=0;
        v=0;
        m=zeros(T+4);

        for j=1:1:T;

            x1=dat(i,p)-dat(i,15+v+p);
            x2=dat(i,42+v+p)-dat(i,15+v+p);

            y1=dat(i,p+1)-dat(i,16+v+p);
            y2=dat(i,43+v+p)-dat(i,16+v+p);

            z1=dat(i,p+2)-dat(i,17+v+p);
            z2=dat(i,44+v+p)-dat(i,17+v+p);

            A=sqrt(x1^2+y1^2+z1^2);
            B=sqrt(x2^2+y2^2+z2^2);

            AB=A*B;
            AdotB=x1*x2+y1*y2+z1*z2;
            Hangle=180*acos(AdotB/AB)/pi;
            Hdis=10*A;

            if ( (Hangle<30) && (Hdis<3.5) );
                m(j)=1;
            end
            kk=kk+m(j);
            v=v+3;
        end
        m;
        kk;
        if kk==0;
            Htype(L,T+1)=Htype(L,T+1)+1;
        elseif kk==1;
            for j=1:1:T;
                Htype(L,j)=Htype(L,j)+m(j);
            end
        else
            for j=1:1:T;
                if ((m(j)==1) && (m(j+1)==1));
                    Htype(L,j+T+1)=Htype(L,j+T+1)+1;
                end
            end
        end
    end

    p=p+3;
end

```

```

for i=1:N;
    Htype1(i,1)=Htype(i,2);
    Htype1(i,2)=Htype(i,3);
    Htype1(i,3)=Htype(i,4);
    Htype1(i,4)=Htype(i,5);
    Htype1(i,5)=Htype(i,7);
    Htype1(i,6)=Htype(i,8);
end

Htype1=transpose(Htype1/sz(1));

Figure (1)
h=bar(Htype1);
title('xxxxxxxxxx','FontWeight','bold');
axis([xmin xmax ymin ymax]);
xlabel('xxxxxxxxxx','FontSize',8);
ylabel('xxxxxxxxxx','FontSize',8);

```

## 4. Salt Bridge's Calculation MATLAB Codes:

### a. Energy landscape plots:

```

clear all;
close all;

% file name;
filename1='xxxxxxxxxx';

% Constants;
% -----
Average=15; % How many points you want to average (moving average)
N=2; % How many distances you want to calculate
R=36; % The row that you want readfile to start with
C=0; % The column that you want readfile to start with

% number of columns to compare
numcomp=1;
compmat=[1 2];

% For energy plots:
%-----
Xmin= 0;
Xmax= 3;
Ymin= 0;
Ymax= 3;
stepsize=0.01;

% load data for 1st file:

```

```

dat=dlmread([filename '.csv'], '\t',R,C);

% what the size of my matrix
sz=size(dat);
sz(1);
moving=sz(1)-Average+1;

% The calculation of the distance:
% -----
for i=1:sz(1);
    p=2;
    for L=1:1:N;
        x=dat(i,p)-dat(i,p+3);
        y=dat(i,p+1)-dat(i,p+4);
        z=dat(i,p+2)-dat(i,p+5);
        D(i,L)=sqrt(x^2+y^2+z^2);
        p=p+6;
    end
end

Dave=zeros(moving,N);

if Average>1;
    for L=1:1:N;
        for i=1:moving;
            for c=0:1:Average-1;
                Dave(i,L)=Dave(i,L)+D(i+c,L);
            end
            Dave(i,L)=Dave(i,L)/Average;
        end
    end
end

% the size of my matrix after doing the average:
szd=size(D);
szdave=size(Dave);

divsx=(-Xmin+Xmax)/stepsize;
divsy=(-Ymin+Ymax)/stepsize;

for i=1:divsx
    for j=1:divsy
        hist(i,j)=0;
    end
end

tot=0;

% loop through images
for n=1:moving

    % evaluate dat1; data in column specified by first entry of 'compmat'
    x=round((Dave(n,1)-Xmin)/stepsize);

    % evaluate dat2; data in column specified by second entry of 'compmat'

```

```

        y=round((Dave(n,2)-Ymin)/stepsize);

        % update histogram if within limits
        if ((x>0)&&(x<divsx))&&((y>0)&&(y<divsy))
            hist(x,y)=hist(x,y)+1;
            tot=tot+1;
        end

    end

% end loop over distances

pdf2d=hist/(tot-1);

% convert pdf2d to pmf2d
for i=1:divsx
    for j=1:divsy
        pmf2d(i,j)=-log(pdf2d(i,j));
    end
end

% create axis values

for i=1:divsx
    x_vals(i)=(Xmin+stepsize*i);
end

for i=1:divsy
    y_vals(i)=(Ymin+stepsize*i);
end

colstr1=num2str(compmat(1,1));
colstr2=num2str(compmat(1,2));
sxx=size(x_vals);
szy=size(y_vals);
szp=size(pmf2d);

h=surf(y_vals,x_vals,pmf2d);
title('xxxxxxx','FontWeight','bold');
set(h,'EdgeColor','none');
axis([Ymin Ymax Xmin Xmax]);
xlabel('xxxxxxxxxxxxx','FontSize',8);
ylabel('xxxxxxxxxxxxx','FontSize',8);

```

## b. Cumulative probability plots:

```

clear all;
close all;

% file name;
filename='xxxxxxxxxxx';

% Constants;
% -----
Average=10; % How many points you want to average (moving average)
N=2;        % How many distance you want to calculate

```

```

R=30;          % The row that you want readfile to start with
C=0;          % The coluomn that you want readfile to start with
Xmin=0;
Xmax=3;
Ymin=0;
Ymax=1;
stepsize=0.01;

% load data for 1st file:
dat=dlmread([filename '.csv'], '\t',R,C);

sz=size(dat);
sz(1);
moving=sz(1)-Average+1;

% The calculation of the distance:
% -----

for i=1:sz(1);
    p=2;
    for L=1:1:N;
        x=dat(i,p)-dat(i,p+3);
        y=dat(i,p+1)-dat(i,p+4);
        z=dat(i,p+2)-dat(i,p+5);
        D(i,L)=sqrt(x^2+y^2+z^2);
        p=p+6;
    end
end

Dave=zeros(moving,N);

if Average>1;
    for L=1:1:N;
        for i=1:moving;
            for c=0:1:Average-1;
                Dave(i,L)=Dave(i,L)+D(i+c,L);
            end
            Dave(i,L)=Dave(i,L)/Average;
        end
    end
end

% the size of my matrix after doing the average:
szd=size(D);
szdave=size(Dave);

divsx=(-Xmin+Xmax)/stepsize;

hist=zeros(divsx,N);

totp=0;
for u=1:1:N;
    tot=totp;

```

```

% initialize incidence counter
for n=1:moving

% evaluate dat1; data in column specified by first entry of 'compmat'
    Dave(n,u);
    x=round((Dave(n,u)-Xmin)/stepsize);

% update histogram if within limits
    if ((x>0)&&(x<divsx))
        hist(x,u)=hist(x,u)+1;
        tot=tot+1;
    end

end

end
totp=tot;

for i=1:divsx
    x_vals(i)=Xmin+stepsize*i;
end

hist=hist/(tot-1);

szhist=size(hist);

cl=0;
bl=0;

for i=1:szhist(1);

    cl=cl+hist(i,1);
    bl=bl+hist(i,2);

    probhist(i,1)=cl;
    probhist(i,2)=bl;

end

plot(x_vals,probhist)
axis([Xmin Xmax Ymin Ymax]);
title('xxxxxxx','FontWeight','bold');
xlabel('xxxxxxx','FontSize',8);
ylabel('xxxxxxx','FontSize',8);
grid

```



## 5. H1/H4 Tail Interactions MATLAB Code:

```
clear all;
close all;

% file name;
filename='xxxxxxxxxxxx';

% Constants;
% -----
R=186;          % The row that you want readfile to start with
C=0;           % The column that you want readfile to start with
NO=4;
Prob=0.1;
Xmin= -0.5;
stepsize=1;
N=2;
Ymax=1;

% load data
dat=dlmread([filename '.csv'], '\t', R, C);

sz=size(dat);

% The calculation of the distance:
% -----

p=2;
v=0;
j=1;
for kk=1:1:13;

    w=137;
    for L=1:1:11;

        for i=1:sz(1);

            x=dat(i,p)-dat(i,w);
            y=dat(i,p+1)-dat(i,w+1);
            z=dat(i,p+2)-dat(i,w+2);
            DNO(i,j)=10*sqrt(x^2+y^2+z^2);

        end
        j=j+1;
        w=w+3;
    end
    p=p+3;

end

p=41;
v=0;
```

```

j=1;
for kk=1:1:19;

    w=98;
    for L=1:1:13;

        for i=1:sz(1);

            x=dat(i,p)-dat(i,w);
            y=dat(i,p+1)-dat(i,w+1);
            z=dat(i,p+2)-dat(i,w+2);
            DON(i,j)=10*sqrt(x^2+y^2+z^2);

        end
        j=j+1;
        w=w+3;
    end
    p=p+3;

end

szDNO=size(DNO);
szDON=size(DON);

DNOt(1:szDNO(2))=0;
DONt(1:szDON(2))=0;

for j=1:szDNO(2);

    for i=1:sz(1);

        if DNO(i,j)<=NO;
            DNOProb(i,j)=1;
            DNOt(j)=DNOt(j)+1;
        else
            DNOProb(i,j)=0;
        end

    end

end

for j=1:szDON(2);

    for i=1:sz(1);

        if DON(i,j)<=NO;
            DONProb(i,j)=1;
            DONt(j)=DONt(j)+1;
        else
            DONProb(i,j)=0;
        end

    end

end

DONt=DONt/sz(1);
DNOt=DNOt/sz(1);

```

```

szNON=szDON(2)+szDNO(2);

jj=1;
for j=1:szNON;
    if j<=szDNO(2);
        if DNOt(j)>=Prob;
            Final(jj,1)=j;
            Final(jj,2)=DNOt(j);
            jj=jj+1;
        end
    else
        if DONT(j-szDNO(2))>=Prob;
            Final(jj,1)=j;
            Final(jj,2)=DONT(j-szDNO(2));
            jj=jj+1;
        end
    end
end
Xmax=0;

for i=1:sz(1);
    interact=0;
    for j=1:szNON;
        if j<=szDNO(2);
            if DNOProb(i,j)==1;
                interact=interact+1;
            end
        else
            if DONProb(i,j-szDNO(2))==1;
                interact=interact+1;
            end
        end
    end
    inter(i,1)=interact;
    if Xmax<interact;
        Xmax=interact;
    end
end

Xmax=Xmax+0.5;

divsx=(-Xmin+Xmax)/stepsize;

hist=zeros(divsx,N);

for u=1:1:N;

% initialize incidence counter
tot=0;

    for n=1:sz(1);

        % evaluate dat1; data in column specified by first entry of 'compmat'
        inter(n,u);
        x=round((inter(n,u)-Xmin)/stepsize);

        % update histogram if within limits

```

```

        if ((x>0) && (x<divsx))
            hist(x,u)=hist(x,u)+1;
            tot=tot+1;
        end
    end
    hist(:,u)=hist(:,u)/tot;

end

bar(0:Xmax, hist)
axis([Xmin Xmax 0 Ymax]);
ylabel('xxxxxxx');
xlabel('xxxxxxx');

```

## 6. H1/H4 Tail Position MATLAB Code:

```

clear all;
close all;

% file name;
filename='xxxxxxx';

% Constants;
% -----
Average=15; % How many points you want to average (moving average)
N=2;        % How many torsion angle you want to calculate
R=42;       % The row that you want readfile to start with
C=0;        % The coluomn that you want readfile to start with

compmat=[1 2];

% number of columns to compare
numcomp=1;

% For energy plots:
%-----
Xmin= -180;
Xmax= 180;
Ymin= -180;
Ymax= 180;
stepsize=1;

% load data for 1st file:
dat=dlmread([filename '.csv'], '\t',R,C);

% what the size of my matrix
sz=size(dat);
sz(1);
moving=sz(1)-Average+1;

```

```

% The calculation of the torsion angle:
% -----
i=0;
p=2;
for i=1:sz(1);
    j=1;
    p=2;
    for L=1:1:N;

        xba=dat(i,p+3)-dat(i,p);
        yba=dat(i,p+4)-dat(i,p+1);
        zba=dat(i,p+5)-dat(i,p+2);

        xcb=dat(i,p+6)-dat(i,p+3);
        ycb=dat(i,p+7)-dat(i,p+4);
        zcb=dat(i,p+8)-dat(i,p+5);

        xdc=dat(i,p+9)-dat(i,p+6);
        ydc=dat(i,p+10)-dat(i,p+7);
        zdc=dat(i,p+11)-dat(i,p+8);

        xt=yba*zcb-ycb*zba;
        yt=zba*xcb-zcb*xba;
        zt=xba*ycb-xcb*yba;

        xu=ycb*zdc-ydc*zcb;
        yu=zcb*xdc-zdc*xcb;
        zu=xcb*ydc-xdc*ycb;

        xtu=yt*zu-yu*zt;
        ytu=zt*xu-zu*xt;
        ztu=xt*yu-xu*yt;

        rt2=xt^2+yt^2+zt^2;
        ru2=xu^2+yu^2+zu^2;
        rtru=sqrt(rt2*ru2);

        rcb=sqrt(xcb^2+ycb^2+zcb^2);

        sign=(xcb*xtu+ycb*ytu+zcb*ztu)/(rcb*rtru);

        psi(i,j)=(sign/abs(sign))*180*acos((xt*xu+yt*yu+zt*zu)/rtru)/pi;

        j=j+1;
        p=p+12;

    end
end

divsx=(-Xmin+Xmax)/stepsize;
divsy=(-Ymin+Ymax)/stepsize;

for i=1:divsx
    for j=1:divsy
        hist(i,j)=0;
    end
end

```

```

tot=0;

for p=1:numcomp(1)

    % loop through images
    for n=1:sz(1)

        % evaluate dat1; data in column specified by first entry of 'compmat'
        psi(n,compmat(p,1))
        x=round((psi(n,compmat(p,1))-Xmin)/stepsize);

        % evaluate dat2; data in column specified by second entry of 'compmat'
        y=round((psi(n,compmat(p,2))-Ymin)/stepsize);

        % update histogram if within limits
        if ((x>0)&&(x<divsx))&&((y>0)&&(y<divsy))
            hist(x,y)=hist(x,y)+1;
            tot=tot+1;
        end
    end
end

% end loop over distances
end

psi;
hist;
pdf2d=hist/tot;

% convert pdf2d to pmf2d
for i=1:divsx
    for j=1:divsy
        pmf2d(i,j)=-log(pdf2d(i,j));
    end
end

% create axis values
for i=1:divsx
    x_vals(i)=Xmin+stepsize*i;
end

for i=1:divsy
    y_vals(i)=Ymin+stepsize*i;
end

colstr1=num2str(compmat(1,1));
colstr2=num2str(compmat(1,2));
szx=size(x_vals);
szy=size(y_vals);
szp=size(pmf2d);

h=surf(y_vals,x_vals,pmf2d);
title('xxxxxxx','FontWeight','bold')
set(h,'EdgeColor','none')

```

```
axis([Ymin Ymax Xmin Xmax]);  
xlabel('xxxxxxxxx', 'Fontsize', 9);  
ylabel('xxxxxxxxx', 'Fontsize', 9);
```

## Appendix D. H1/H4 Tail Interaction Tables

### Equilibrium Simulations

1. Equilibrium simulations for augmented FAT/paxillin complex (with H4 tail and P1/P2 constrained):

**Table D-1: Electrostatic interactions found between H1/H4 tail that have a probability greater than 10% of 20 ns simulation time long. These runs belong to the equilibrium simulation of the FAT/paxillin complex (with H4 tail and P1/P2 constrained).**

Run#1			Run#2		
Electrostatic Interaction [atoms: residue #]		Probability	Electrostatic Interaction [atoms: residue #]		Probability
H1 tail	H4 tail		H1 tail	H4 tail	
O: 915	NE2: 1052	0.2215	There is no interaction has probability greater than 10%		
O: 916	NE2: 1052	0.2496			
OD1: 916	NE2: 1052	0.1651			
Run#3			Run#4		
Electrostatic Interaction [atoms: residue #]		Probability	Electrostatic Interaction [atoms: residue #]		Probability
H1 tail	H4 tail		H1 tail	H4 tail	
N: 918	O: 1047	0.5518	N: 916	OD1: 1048	0.1797
O: 916	N: 1047	0.3914	N: 918	O: 1048	0.1397
O: 916	N: 1050	0.1285	N: 918	O: 1049	0.5158
O: 918	N: 1049	0.3325	O: 910	NZ: 1044	0.1628
CG: 918	NE2: 1048	0.1849	O: 916	N: 1049	0.1699
			O: 916	N: 1050	0.2223
			O: 916	CZ: 1050	0.1936
			CG: 918	NE2: 1052	0.119



2. Equilibrium simulation for augmented FAT/paxillin with H4 tail and P1 constrained (without P2):

**Table D-2: Electrostatic interactions found between H1/H4 tail that have a probability greater than 10% of 20 ns simulation time long. These runs belong to the equilibration simulation of the augmented FAT/paxillin complex (with H4 tail and P1 constrained).**

Run#1			Run#2		
Electrostatic Interaction [atoms: residue #]		Probability	Electrostatic Interaction [atoms: residue #]		Probability
H1 tail	H4 tail		H1 tail	H4 tail	
N: 916	O: 1050	0.1127	OD1: 916	N: 1043	0.2407
N: 918	O: 1048	0.8887			
N: 919	O: 1048	0.1012			
O: 915	N: 1052	0.125			
O: 915	NE2: 1052	0.1143			
O: 916	N: 1050	0.9277			
O: 919	NE2: 1048	0.1262			
CG: 918	NE2: 1048	0.202			
CG: 918	NE2: 1052	0.2056			
OG: 920	NE2: 1048	0.1136			
Run#3			Run#4		
Electrostatic Interaction [atoms: residue #]		Probability	Electrostatic Interaction [atoms: residue #]		Probability
H1 tail	H4 tail		H1 tail	H4 tail	
O: 916	CZ: 1050	0.1267	N: 916	O: 1048	0.417
OG1: 914	NZ: 1044	0.1241	N: 916	O: 1050	0.129
OD1: 916	N: 1044	0.1891	N: 917	O: 1048	0.1771
OD1: 916	NZ: 1044	0.1826	N: 918	O: 1048	0.3751
			N: 918	OD1: 1048	0.5523
			ND2: 916	O: 1050	0.2855
			O: 916	N: 1049	0.2392
			O: 916	N: 1050	0.8814
			O: 917	NE2: 1052	0.1664
			CG: 918	NE2: 1052	0.1883

## Loaded Simulations

1. Axial load simulations for augmented FAT/paxillin complex (with H4 tail and P1/P2 constrained):

Typical behavior:

**Table D-3: Electrostatic interactions found between H1/H4 tail that have a probability greater than 10% of 20 ns simulation time long. These runs belong to the axial load simulations of the augmented FAT/paxillin complex (with H4 tail and P1 constrained). They represent the typical behavior of H1.**

Seed#1: Run#1			Seed#1: Run#2		
Electrostatic Interaction [atoms: residue #]		Probability	Electrostatic Interaction [atoms: residue #]		Probability
H1 tail	H4 tail		H1 tail	H4 tail	
N: 914	C: 1052	0.1959	N: 915	O: 1048	0.8813
N: 916	O: 1050	0.879	N: 917	O: 1045	0.5673
N: 918	O: 1048	0.8718	N: 917	O: 1046	0.1737
N: 920	O: 1046	0.254	O: 913	N: 1050	0.9012
CZ: 919	O: 1046	0.119	O: 915	N: 1047	0.5108
O: 914	N: 1052	0.6747	O: 915	N: 1048	0.7827
O: 916	N: 1050	0.9416	OG: 910	NE2: 1052	0.134
O: 918	N: 1047	0.2499	OD1: 916	N: 1047	0.6155
O: 918	N: 1048	0.6659			
CG: 918	NE2: 1052	0.1512			
Seed#2: Run#1			Seed#3: Run#1		
Electrostatic Interaction [atoms: residue #]		Probability	Electrostatic Interaction [atoms: residue #]		Probability
H1 tail	H4 tail		H1 tail	H4 tail	
N: 917	C: 1052	0.2389	N: 916	O: 1049	0.5874
N: 918	OD1: 1048	0.1182	N: 916	O: 1050	0.2203
N: 920	O: 1048	0.2079	N: 918	O: 1047	0.6823
ND2: 916	C: 1052	0.5857	N: 920	O: 1045	0.392
CZ: 919	O: 1049	0.1632	CZ: 919	O: 1043	0.2282
O: 915	N: 1052	0.1459	CZ: 919	O: 1046	0.1877
O: 917	N: 1052	0.408	O: 914	N: 1052	0.1997
O: 918	N: 1050	0.1058	O: 916	N: 1049	0.9249
OD1: 916	N: 1052	0.1746	O: 916	N: 1050	0.2801
			O: 918	N: 1047	0.629

**Table D-3: Continue ..**

<b>Seed#3: Run#2</b>			<b>Seed#4: Run#1</b>		
Electrostatic Interaction [atoms: residue #]		Probability	Electrostatic Interaction [atoms: residue #]		Probability
H1 tail	H4 tail		H1 tail	H4 tail	
N: 916	O: 1046	0.161	N: 916	O: 1047	0.1739
N: 917	O: 1046	0.1539	N: 916	OD1: 1048	0.1752
N: 917	O: 1049	0.3165	N: 917	O: 1049	0.1685
N: 918	O: 1046	0.347	N: 918	O: 1049	0.3927
N: 918	O: 1048	0.4454	N: 919	O: 1049	0.2362
N: 918	O: 1049	0.4482	N: 920	O: 1049	0.286
ND2: 916	O: 1048	0.2286	ND2: 916	O: 1049	0.1042
ND2: 916	O: 1049	0.1174	ND2: 921	C: 1052	0.2813
CZ: 919	O: 1043	0.1523	O: 914	NE2: 1048	0.1768
O: 916	N: 1048	0.836	O: 916	N: 1049	0.4676
O: 916	N: 1049	0.2705	O: 916	NE2: 1048	0.1534
O: 918	N: 1046	0.3182	O: 918	N: 1049	0.3347
O: 918	NE2: 1048	0.2907	OD1 921	N: 1052	0.3661
O: 921	NE2: 1048	0.3052			
OD1: 916	CZ: 1050	0.1412			
CG: 918	NE2: 1048	0.1664			
<b>Seed#4: Run#2</b>			<b>Seed#5: Run#2</b>		
Electrostatic Interaction [atoms: residue #]		Probability	Electrostatic Interaction [atoms: residue #]		Probability
H1 tail	H4 tail		H1 tail	H4 tail	
N: 916	O: 1047	0.1148	N: 920	OD1: 1048	0.1212
N: 918	O: 1049	0.2529			
N: 920	O: 1050	0.4338			
N: 921	C: 1052	0.1649			
CZ: 919	O: 1043	0.171			
ND2: 921	C: 1052	0.2518			
O: 916	N: 1049	0.2106			
O: 918	N: 1050	0.4007			
O: 919	N: 1052	0.1217			
OG: 920	N: 1052	0.1039			

Atypical behavior:

**Table D-4: Electrostatic interactions found between H1/H4 tail that have a probability greater than 10% of 20 ns simulation time long. These runs belong to the axial load simulations of the augmented FAT/paxillin complex (with H4 tail and P1 constrained). They represent the atypical behavior of H1.**

Seed#1: Run#1			Seed#2: Run#2		
Electrostatic Interaction [atoms: residue #]		Probability	Electrostatic Interaction [atoms: residue #]		Probability
H1 tail	H4 tail		H1 tail	H4 tail	
N: 916	O: 1050	0.406	There is no interaction has probability greater than 10%		
N: 918	O: 1048	0.9292			
ND2: 916	O: 1050	0.1429			
CZ: 919	O: 1046	0.1169			
O: 914	N: 1052	0.2661			
O: 915	N: 1052	0.2436			
O: 916	N: 1050	0.8778			
O: 918	N: 1048	0.8852			
CG: 918	NE2: 1052	0.5813			

2. Perpendicular load simulations for augmented FAT/paxillin complex (with H4 tail and P1 constrained):

Typical behavior:

**Table D-5: Electrostatic interactions found between H1/H4 tail that have a probability greater than 10% of 20 ns simulation time long. These runs belong to the perpendicular load simulations of the augmented FAT/paxillin complex (with H4 tail and P1 constrained). They represent the typical behavior of H1.**

Seed#1: Run#2			Seed#2: Run#2		
Electrostatic Interaction [atoms: residue #]		Probability	Electrostatic Interaction [atoms: residue #]		Probability
H1 tail	H4 tail		H1 tail	H4 tail	
N: 920	O: 1051	0.2253	N: 915	C: 1052	0.1028
O: 920	NE2: 1052	0.1299	N: 916	O: 1050	0.2593
O: 921	CZ: 1050	0.1732	N: 918	O: 1048	0.9866
OG: 920	CZ: 1050	0.1915	N: 920	O: 1046	0.3248
			N: 920	OD1: 1048	0.1113
			CZ: 919	O: 1043	0.3015
			CZ: 919	O: 1044	0.1023
			O: 914	N: 1052	0.1413
			O: 915	N: 1052	0.4923
			O: 916	N: 1050	0.9523
			O: 918	N: 1048	0.6669
			O: 919	NE2: 1048	0.1396
			OG1: 914	N: 1052	0.1708
			CG: 918	NE2: 1048	0.1329
			CG: 918	NE2: 1052	0.483
			OG: 920	NE2: 1048	0.1679
			OD1 921	NE2: 1048	0.1015
Seed#3: Run#1			Seed#3: Run#2		
Electrostatic Interaction [atoms: residue #]		Probability	Electrostatic Interaction [atoms: residue #]		Probability
H1 tail	H4 tail		H1 tail	H4 tail	
N: 914	C: 1052	0.1678	N: 918	O: 1049	0.1209
N: 916	O: 1050	0.4776	ND2: 921	OD1: 1048	0.1062
N: 918	O: 1048	0.9859			
N: 920	O: 1046	0.124			
CZ: 919	O: 1043	0.1696			
CZ: 919	O: 1044	0.2113			
CZ: 919	O: 1046	0.1067			
O: 914	N: 1052	0.3904			
O: 915	N: 1052	0.2933			
O: 916	N: 1050	0.9705			
O: 918	N: 1048	0.734			
O: 919	NE2: 1048	0.1337			
OG1: 914	N: 1052	0.1021			
CG: 918	NE2: 1048	0.1492			
CG: 918	NE2: 1052	0.3846			
OG: 920	NE2: 1048	0.1024			

**Table D-5: Continue ..**

Seed#4: Run#1			Seed#4: Run#2		
Electrostatic Interaction [atoms: residue #]		Probability	Electrostatic Interaction [atoms: residue #]		Probability
H1 tail	H4 tail		H1 tail	H4 tail	
N: 914	C: 1052	0.1146	N: 914	C: 1052	0.1578
N: 916	O: 1050	0.8907	N: 916	O: 1050	0.7926
N: 918	O: 1048	0.9765	N: 918	O: 1048	0.9798
N: 920	O: 1045	0.5482	N: 920	O: 1046	0.4227
ND2: 916	O: 1050	0.1313	O: 914	N: 1052	0.601
CZ: 919	O: 1046	0.1936	O: 916	N: 1050	0.9861
O: 914	N: 1052	0.6374	O: 918	N: 1048	0.6895
O: 916	N: 1050	0.9942	CG: 918	NE2: 1052	0.1819
O: 918	N: 1047	0.5003			
O: 918	N: 1048	0.7791			
O: 920	N: 1046	0.2738			
OD1: 916	NE2: 1052	0.1129			
CG: 918	NE2: 1048	0.1003			
CG: 918	NE2: 1052	0.1111			
OG: 920	NE2: 1048	0.1088			
Seed#5: Run#1			Seed#5: Run#2		
Electrostatic Interaction [atoms: residue #]		Probability	Electrostatic Interaction [atoms: residue #]		Probability
H1 tail	H4 tail		H1 tail	H4 tail	
N: 916	C: 1052	0.3008	N: 920	O: 1049	0.6024
N: 918	O: 1050	0.9319	CZ: 919	O: 1051	0.1285
N: 920	O: 1048	0.8746	O: 918	N: 1049	0.1382
O: 916	N: 1052	0.9408	CG: 918	N: 1049	0.1255
O: 918	N: 1050	0.8821	CG: 918	NE2: 1048	0.1572
O: 920	NE2: 1048	0.6003	OG: 920	N: 1049	0.1248
CG: 918	NE2: 1052	0.389	OG: 920	NE2: 1048	0.2407
			OD1 921	CZ: 1050	0.1402
Seed#6: Run#1					
Electrostatic Interaction [atoms: residue #]		Probability			
H1 tail	H4 tail				
There is no interaction has probability greater than 10%					

Atypical behavior:

**Table D-6: Electrostatic interactions found between H1/H4 tail that have a probability greater than 10% of 20 ns simulation time long. These runs belong to the perpendicular load simulations of the augmented FAT/paxillin complex (with H4 tail and P1 constrained). They represent the atypical behavior of H1.**

Seed#1: Run#1			Seed#2: Run#1		
Electrostatic Interaction [atoms: residue #]		Probability	Electrostatic Interaction [atoms: residue #]		Probability
H1 tail	H4 tail		H1 tail	H4 tail	
N: 920	O: 1051	0.2606	N: 914	C: 1052	0.2713
O: 918	CZ: 1050	0.1322	N: 916	O: 1050	0.8453
OG: 920	CZ: 1050	0.1113	N: 918	O: 1048	0.9947
			N: 920	O: 1045	0.2004
			N: 920	O: 1046	0.308
			CZ: 919	O: 1043	0.2924
			CZ: 919	O: 1044	0.1211
			CZ: 919	O: 1046	0.1833
			O: 914	N: 1052	0.743
			O: 916	N: 1050	0.9936
			O: 918	N: 1047	0.2627
			O: 918	N: 1048	0.7875
			CG: 918	NE2: 1048	0.1038
			CG: 918	NE2: 1052	0.3026
			OG: 920	NE2: 1048	0.1165
Seed#6: Run#2					
Electrostatic Interaction [atoms: residue #]		Probability			
H1 tail	H4 tail				
`There is no interaction has probability greater than 10%					

Repeatability of atypical behavior:

**Table D-7: Electrostatic interactions found between H1/H4 tail that have a probability greater than 10% of 20 ns simulation time long. These runs belong to the perpendicular load simulations of the augmented FAT/paxillin complex (with H4 tail and P1 constrained). They represent the repeatability of atypical behavior of H1.**

Seed#1: Run#3			Seed#1: Run#4		
Electrostatic Interaction [atoms: residue #]		Probability	Electrostatic Interaction [atoms: residue #]		Probability
H1 tail	H4 tail		H1 tail	H4 tail	
N: 917	C: 1052	0.2033	N: 914	O: 1050	0.2119
N: 918	O: 1049	0.1513	N: 915	O: 1048	0.2585
N: 918	C: 1052	0.128	N: 916	O: 1048	0.5311
ND2: 916	C: 1052	0.2254	N: 918	O: 1046	0.4265
			ND2: 916	O: 1046	0.1199
			O: 913	N: 1050	0.2539
			O: 913	NE2: 1052	0.1054
			O: 914	N: 1050	0.2598
			O: 914	CZ: 1050	0.1424
			O: 915	N: 1048	0.2192
			O: 916	N: 1047	0.1185
			O: 916	N: 1048	0.6149
			CG: 918	NE2: 1048	0.1683
Seed#1: Run#5			Seed#1: Run#6		
Electrostatic Interaction [atoms: residue #]		Probability	Electrostatic Interaction [atoms: residue #]		Probability
H1 tail	H4 tail		H1 tail	H4 tail	
There is no interaction has probability greater than 10%			N: 915	O: 1050	0.7948
			N: 917	O: 1048	0.8267
			ND2: 916	O: 1046	0.1007
			ND2: 916	O: 1048	0.1248
			CZ: 919	O: 1043	0.1396
			CZ: 919	O: 1046	0.2275
			CZ: 919	O: 1047	0.1311
			O: 913	N: 1052	0.4703
			O: 915	N: 1050	0.9408
			O: 917	N: 1048	0.1711
			O: 918	N: 1047	0.1105
			OD1: 916	N: 1048	0.2052
Seed#1: Run#7			Seed#1: Run#8		
Electrostatic Interaction [atoms: residue #]		Probability	Electrostatic Interaction [atoms: residue #]		Probability
H1 tail	H4 tail		H1 tail	H4 tail	
N: 920	O: 1051	0.1002	N: 918	OD1: 1048	0.2293
O: 921	CZ: 1050	0.1162	O: 916	NE2: 1048	0.4291
OG: 920	CZ: 1050	0.1466	O: 918	N: 1048	0.7627
			O: 918	N: 1049	0.7857
			O: 920	N: 1043	0.521
			CG: 918	N: 1048	0.2887
			CG: 918	NE2: 1048	0.4074



**Table D-7: Continue ..**

Seed#1: Run#9			Seed#1: Run#10		
Electrostatic Interaction [atoms: residue #]		Probability	Electrostatic Interaction [atoms: residue #]		Probability
H1 tail	H4 tail		H1 tail	H4 tail	
N: 914	C: 1052	0.1813	CZ: 919	O: 1043	0.1223
N: 916	O: 1050	0.7156	O: 918	N: 1048	0.1673
N: 917	O: 1050	0.1112			
N: 918	O: 1048	0.7587			
N: 920	O: 1046	0.1367			
CZ: 919	O: 1043	0.3087			
CZ: 919	O: 1046	0.2145			
O: 914	N: 1052	0.4565			
O: 916	N: 1050	0.8193			
O: 918	N: 1048	0.6148			
OD1: 916	N: 1052	0.1595			
CG: 918	NE2: 1052	0.2529			
OG: 920	NE2: 1048	0.1034			
Seed#1: Run#11					
Electrostatic Interaction [atoms: residue #]		Probability			
H1 tail	H4 tail				
There is no interaction has probability greater than 10%					

## References

1. Parsons, J.T., *Focal adhesion kinase: the first ten years*. Journal of Cell Science, 2003. **116**(8): p. 1409-1416.
2. van Nimwegen, M.J. and B. van de Water, *Focal adhesion kinase: A potential target in cancer therapy*. Biochemical Pharmacology, 2007. **73**(5): p. 597-609.
3. Owens, L.V., et al., *Overexpression of the Focal Adhesion Kinase (p125FAK) in Invasive Human Tumors*. Cancer Research, 1995. **55**(13): p. 2752-2755.
4. Mitra, S.K., et al., *Intrinsic FAK activity and Y925 phosphorylation facilitate an angiogenic switch in tumors*. Oncogene, 2006. **25**(44): p. 5969-5984.
5. Arold, S.T., M.K. Hoellerer, and M.E.M. Noble, *The Structural Basis of Localization and Signaling by the Focal Adhesion Targeting Domain*. Structure, 2002. **10**(3): p. 319-327.
6. Kuriyan, J. and D. Cowburn, *MODULAR PEPTIDE RECOGNITION DOMAINS IN EUKARYOTIC SIGNALING*. Annual Review of Biophysics and Biomolecular Structure, 1997. **26**(1): p. 259-288.
7. Mitra, S.K., D.A. Hanson, and D.D. Schlaepfer, *Focal adhesion kinase: in command and control of cell motility*. Nat Rev Mol Cell Biol, 2005. **6**(1): p. 56-68.
8. Cai, X., et al., *Spatial and Temporal Regulation of Focal Adhesion Kinase Activity in Living Cells*. Molecular and Cellular Biology, 2008. **28**(1): p. 201-214.
9. Hsia, D.A., et al., *Differential regulation of cell motility and invasion by FAK*. The Journal of Cell Biology, 2003. **160**(5): p. 753-767.
10. Lietha, D., et al., *Structural Basis for the Autoinhibition of Focal Adhesion Kinase*. Cell, 2007. **129**(6): p. 1177-1187.
11. Shi, Q. and D. Boettiger, *A Novel Mode for Integrin-mediated Signaling: Tethering Is Required for Phosphorylation of FAK Y397*. Molecular Biology of the Cell, 2003. **14**(10): p. 4306-4315.

12. Gao, G.H., et al., *NMR solution structure of the focal adhesion targeting domain of focal adhesion kinase in complex with a paxillin LD peptide - Evidence for a two-site binding model*. Journal of Biological Chemistry, 2004. **279**(9): p. 8441-8451.
13. Hayashi, I., K. Vuori, and R.C. Liddington, *The focal adhesion targeting (FAT) region of focal adhesion kinase is a four-helix bundle that binds paxillin*. Nat Struct Mol Biol, 2002. **9**(2): p. 101-106.
14. Hildebrand, J.D., M.D. Schaller, and J.T. Parsons, *Identification of sequences required for the efficient localization of the focal adhesion kinase, pp125FAK, to cellular focal adhesions*. The Journal of Cell Biology, 1993. **123**(4): p. 993-1005.
15. Schlaepfer, D.D. and T. Hunter, *Evidence for in vivo phosphorylation of the Grb2 SH2-domain binding site on focal adhesion kinase by Src-family protein-tyrosine kinases*. Mol Cell Biol, 1996. **16**(10): p. 5623-5633.
16. Prutzman, K.C., et al., *The Focal Adhesion Targeting Domain of Focal Adhesion Kinase Contains a Hinge Region that Modulates Tyrosine 926 Phosphorylation*. Structure, 2004. **12**(5): p. 881-891.
17. Schaller, M.D., *Paxillin: a focal adhesion-associated adaptor protein*. Oncogene, 2001. **20**(44): p. 6459.
18. Brown, M.C., M.S. Curtis, and C.E. Turner, *Paxillin LD motifs may define a new family of protein recognition domains*. Nat Struct Mol Biol, 1998. **5**(8): p. 677-678.
19. Brown, M.C., J.A. Perrotta, and C.E. Turner, *Identification of LIM3 as the principal determinant of paxillin focal adhesion localization and characterization of a novel motif on paxillin directing vinculin and focal adhesion kinase binding*. The Journal of Cell Biology, 1996. **135**(4): p. 1109-1123.
20. Dixon, R.D.S., et al., *New Insights into FAK Signaling and Localization Based on Detection of a FAT Domain Folding Intermediate*. Structure, 2004. **12**(12): p. 2161-2171.
21. Ding, F., et al., *Topological Determinants of Protein Domain Swapping*. Structure, 2006. **14**(1): p. 5-14.
22. Bakolitsa, C., et al., *Crystal Structure of the Vinculin Tail Suggests a Pathway for Activation*. Cell, 1999. **99**(6): p. 603-613.

23. Wilson, C., et al., *Three-dimensional structure of the LDL receptor-binding domain of human apolipoprotein E*. Science, 1991. **252**(5014): p. 1817-1822.
24. Rahuel, J., et al., *Structural basis for specificity of Grb2-SH2 revealed by a novel ligand binding mode*. Nature structural biology, 1996. **3**(7): p. 586-9.
25. Hess, B., et al., *GROMACS 4: Algorithms for Highly Efficient, Load-Balanced, and Scalable Molecular Simulation*. Journal of Chemical Theory and Computation, 2008. **4**(3): p. 435-447.
26. Van Der Spoel, D., et al., *GROMACS: Fast, flexible, and free*. Journal of Computational Chemistry, 2005. **26**(16): p. 1701-1718.
27. Hoellerer, M.K., et al., *Molecular Recognition of Paxillin LD Motifs by the Focal Adhesion Targeting Domain*. Structure, 2003. **11**(10): p. 1207-1217.
28. Webb, D.J., et al., *Paxillin phosphorylation sites mapped by mass spectrometry*. Journal of Cell Science, 2005. **118**(21): p. 4925-4929.
29. Oostenbrink, C., et al., *A biomolecular force field based on the free enthalpy of hydration and solvation: The GROMOS force-field parameter sets 53A5 and 53A6*. Journal of Computational Chemistry, 2004. **25**(13): p. 1656-1676.
30. Hess, B., *P-LINCS: A Parallel Linear Constraint Solver for Molecular Simulation*. Journal of Chemical Theory and Computation, 2007. **4**(1): p. 116-122.
31. Berendsen, H.J.C., et al., *Molecular dynamics with coupling to an external bath*. The Journal of Chemical Physics, 1984. **81**(8): p. 3684-3690.
32. Hoover, W.G., *Canonical dynamics: Equilibrium phase-space distributions*. Physical Review A, 1985. **31**(3): p. 1695-1697.
33. Nose, S., *A unified formulation of the constant temperature molecular dynamics methods*. The Journal of Chemical Physics, 1984. **81**(1): p. 511-519.
34. Parrinello, M. and A. Rahman, *Polymorphic transitions in single crystals: A new molecular dynamics method*. Journal of Applied Physics, 1981 **52**(12): p. 7182 - 7190